DOCTOR OF PHILOSOPHY

Cutaneous innervation of the hand

Sulaiman, Sara

Award date:
2014

DOCTOR OF PHILOSOPHY

Cutaneous innervation of the hand

Sara Sulaiman

2014

University of Dundee

College of Art, Science and Engineering
Centre for Anatomy and Human Identification

CUTANEOUS INNERVATION OF THE HAND

By:

MS. SARA SULAIMAN

Supervised by:

PROFESSOR ROGER SOAMES

DR CLARE LAMB

A thesis Submitted in fulfillment of the requirement of the degree

DOCTOR OF PHILOSOPHY IN SCIENCE IN HUMAN ANATOMY

March 2014

Table of Contents

Content **Page number**

List of Figures

List of Tables

List of Abbreviations

BSL	Bistyloid line
BR	Brachioradialis
CAHID	Centre for Anatomy and Human Identification
CB	Communicating branch
CDN	Common digital nerve
CT	Common trunk
DBUN	Dorsal branch of ulnar nerve
ECRL	Extensor carpi radialis longus
FCR	Flexor carpi radialis
FCU	Flexor carpi ulnaris
LABCN	Lateral antebrachial cutaneous nerve
LT	Lister's tubercle
MCP	Metacarpophalangeal joint
MN	Median nerve
n	Number
PCBMN	Palmar cutaneous branch of the median nerve
PCBUN	Palmar cutaneous branch of the ulnar nerve
PCL	Palmar carpal ligament
PDN	Proper digital nerve
PL	Palmaris longus
RMBMN	Recurrent motor branch of the median nerve
RN	Radial nerve
RSP	Radial styloid process
SBRN	Superficial branch of radial nerve
ST	Scaphoid tubercle
TCL	Transverse carpal ligament
UA	Ulnar artery
UD	Undetermined
UN	Ulnar nerve
USP	Ulnar styloid process
WC	Wrist Crease

Acknowledgments

This work will not have seen the light without the blessings of God to whom I give my ultimate thanks and gratitude. Moreover, I am grateful and indebted to many people who filled me with their kindness, support and guidance throughout the period of my project.

First of all, I would like to thank my principal supervisor Professor Roger Soames for his patience, guidance and the beautiful kind fatherly sprit he embraced upon me during my time being his student. Moreover, no amount of thanks can express my gratitude to my secondary supervisor, Dr. Clare lamb, who through her kindness, patience and immense knowledge provided continuous help, direction and support through various aspects of my project. I was lucky to have two supervisors who are approachable, encouraging and always concerned about my wellbeing in addition to how my research is developing. Who tolerated my crazy ideas, kept me focused and allowed me to create and thrive in my own pace.

Special thanks and appreciation to my Thesis Committee members, Professor Caroline Wilkinson and Professor Timothy Newman, who continuously gave invaluable suggestions and comments expressing a great spirit of adventure in regard to research.

A special note of thanks to all the teaching and support staff at the Center for Anatomy and Human Identification (CAHID) for providing a professional and stimulating environment to work. I was privileged to work among such a team with commitment, excitement and devotion to high standards of education. Special thanks to Dr. Catherine Carr, Dr. Paul Felts, Ms. Netta Gallazzi, Ms. Vivienne McGuire, and Ms. Gillian Malone.

My sincere gratitude goes to Dr. Stephen Hubbard, for all his help in the statistical aspect of this project. Despite his busy schedule, he still accommodated my questions and gave valuable suggestions. Special thanks go to Dr. Luca Albergante for his valuable suggestions and comments, his kindness and patience in explaining statistical tests for me. A note of thanks goes to Ms. Victoria Mcculloch for providing some of the visual illustrations in this project.

No amounts of thanks can describe my gratitude to my parents. Their unconditional love, continuous support and kindness made me the person I am today. While many doubted me

and my decision to go through this journey, their persistent encouragement and love allowed me to dream, be ambitious and dare to believe that this is achievable. To them, I am eternally grateful.

For a special, generous, forgiving, and supportive friend; Nasreen, thank you for being my safe haven where I was able to hide during my low and blue days.

Declaration

I hereby declare that this dissertation is a presentation of my original work conducted under the supervisor of Professor Roger Soames, Cox Professor of Anatomy, and Dr. Clare Lamb, Senior Lecturer in Anatomy at the Centre for Anatomy and Human Identification, University of Dundee. Contributions of others involved are clearly indicated. All references cited have been consulted by me. I certify that this work has never been accepted for the award of any other higher degree.

_____

Sarah Sulaiman

Summary

With the increase of hand pathologies in the last decade, the need to better understand the anatomy of the hand is becoming more vital. The cutaneous innervation of the hand is classically described to be supplied by palmar cutaneous branch of the median nerve (PCBMN), common digital nerves (CDNs), ulnar nerve (UN), palmar cutaneous branch of the ulnar nerve, dorsal branch of the ulnar nerve (DBUN), superficial branch of the radial nerve (SBRN) and occasionally the lateral antebrachial cutaneous nerve (LABCN). Although the sensory distribution of the hand has been described in the literature, reports have often shown contradicting views and occasionally different or incomplete descriptions. Furthermore, clinical procedures in the hand and wrist can result in painful and/or disabling postoperative complications. This thesis outlines, categorizes and describes the distribution and branching patterns of cutaneous branches supplying the palmar and dorsal surface of the hand and their relationship to the distal area of the forearm and wrist. It also investigates the palmar and dorsal communicating branches, their patterns and common locations. Moreover, the project discusses the impact of the distribution and branching patterns of the cutaneous nerves on surgical and diagnostic procedures performed in the hand, wrist and distal forearm. 160 cadaveric hands were dissected in the Centre for Anatomy and Human Identification (CAHID), University of Dundee. All cadavers were musculoskeletally mature adults with mean age of 82.5±9.4 (range: 53-101) years. Skin was removed from the distal half of the forearm to the metacarpophalangeal joints. Nerves under investigation were identified, dissected, and traced. Sketches, photographs, and measurements to predefined landmarks including the wrist crease (WC), bistyloid line (BSL) and the third metacarpophalangeal (MCP) joint were taken and results expressed as means, standard deviations and ranges. Patterns are classified and expressed with frequencies. The PCBMN was found to originate from the main trunk of the median nerve (MN) 54.1±15.7 mm proximal to the WC and course distally between flexor carpi radialis and palmaris longus (if present) to innervate the proximal palmar surface of the hand by branching into one of three types identified. Furthermore, two PCBMN were found in 8.9% of cases. The second, third, fourth CDNs were found to divide into proper digital nerves at a point located distal to the 70% of the distance between the third MCP joint and the BSL in 88% of cases. The cutaneous innervation of the palm was found to be relatively constant with the lateral 3½ digits being

supplied by the MN and the medial 1½ being supplied by the UN. A palmar CB was found between the third CDN-MN and fourth CDN-UN in 86.9% of the cases coursing in different patterns and changing the palmar sensory innervation of that previously described. The sensory innervation of the dorsum of the hand was variable. The most common pattern was being supplied by the SBRN innervating the lateral dorsal skin and the skin covering the lateral 2½ digits and the DBUN innervating the medial dorsal skin and the skin covering the medial 1½ digits found in 37.3%. All radial supply to the dorsum of the hand with the absence of the DBUN was found in 6.7%. The SBRN connected with the LABCN in 30.7% and with the DBUN in 26.4% complicating the sensory innervation in the dorsum of the hand. Understanding the cutaneous innervation of the hand, appreciation of the possible variations and presence of communicating branches will result in a better evaluation of signs and symptoms, establishing a proper therapeutic plan, avoiding iatrogenic injuries during surgical interventions, and properly diagnose postoperative complications leading to an increased quality of medical service and patient satisfaction.

1. Introduction

The human hand is a unique and complex structure. Hand injuries, trauma and pathology account for a considerable amount of health care problems. It is only natural that the hand has received a lot of attention in the literature as its relatively small size and high density of structures create delicate and close anatomical relationships (Figure 1.1). Understanding hand disease processes and treatment planning requires a detailed knowledge of hand anatomy and a high appreciation of the anatomical relationships between structures in the hand.

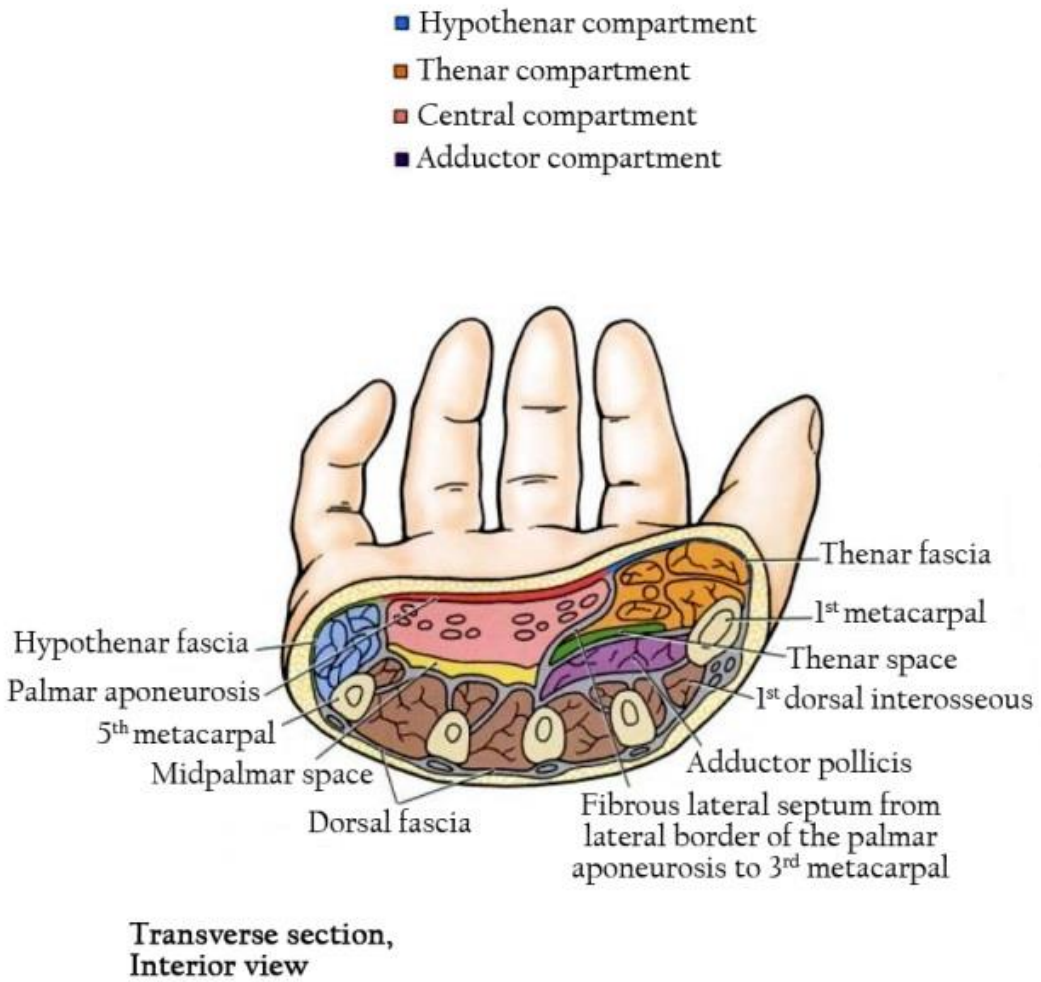

Figure 1.1: An illustration of a cross section of the hand at the carpal tunnel level showing the different compartments, spaces and fascia in the hand (Agur et al., 2008; figure 64, page 562).

Understanding the anatomy of the hand starts from the skin. Its dorsal and palmar superficial landmarks provide the basis for surgical planning and hand pathology assessment. In 1968, Kaplan introduced a unique system exploring the hand's superficial landmarks and their relationships to deeper structures. Kaplan's system is still used today and is considered a useful surgical map during surgical incision planning. Other bony landmarks, such as the ulnar and radial styloid processes, are used in clinical and research settings as they are easily palpable and relatively constant among different individuals. However, with so many landmarks in the hand and wrist area, how each affects anatomical morphometry is of interest.

The cutaneous innervation is an important aspect to consider during the planning of surgical approaches and anaesthesia. The literature describes the innervation of the hand to be by the median nerve (MN), ulnar nerve (UN), radial nerve (RN) and occasionally the lateral antebrachial cutaneous nerve (LABCN). The palmar cutaneous branch of the median nerve (PCBMN) innervates the proximal two-fifths of the midpalmar surface. It has received a lot of attention in the modern literature consistent with the evolution of surgical carpal tunnel release techniques. With relatively limited sample size anatomical studies, the course and branching patterns of the PCBMN have been outlined, with many recommendations for ideal incision sites to minimize postoperative complications. With many reports and different recommendations, a better understanding of the cutaneous innervation of the palm may increase patient's postoperative satisfaction and lead to fewer complications.

The digital nerves innervate the distal three-fifths of the palm and the palmar surface of the digits. The first, second and third common digital nerves (CDN) arise from the MN after it passes through the carpal tunnel, whereas the fourth CDN and the proper digital nerve (PDN) to the medial side of the little finger arise from the UN after it

passes through Guyon's canal (ulnar canal) extending from the proximal edge of the palmar carpal ligament to the fibrous arch of the hypothenar muscles in the medial side of the palm (Gross and Gelberman, 1985). The point of division of the CDN into PDNs has not been well investigated. Furthermore, the communicating branches (CB) between the MN and the UN can cause sensory alterations affecting the typical signs and symptoms of hand pathology; and when injured can complicate surgical procedures such as carpal tunnel and flexor tendon release. The literature has differing reports of the incidence rate of the CB and the most common branching patterns. Knowledge of the most common location and branching patterns of the CB will help to better plan therapeutic and diagnostic procedures to minimize iatrogenic injuries in the area.

The dorsum of the hand is supplied by the dorsal branch of the ulnar nerve (DBUN), the superficial branch of the radial nerve (SBRN) and occasionally the LABCN. The DBUN is classically described as innervating the medial dorsal skin of the hand and the skin covering the medial 1½ digits. The course of the DBUN puts it in risk during wrist arthroscopy and any procedure that requires a direct approach to the ulna such as open reduction and internal fixation, ulnar lengthening and shortening procedures, delayed union or non-union of ulnar fractures. It is also important to understand the course of the nerve to properly prepare and harvest neurocutaneous flaps.

The second nerve innervating the dorsum of the hand is the SBRN which supplies the laterodorsal surface of the hand and the skin covering the lateral 3½-2½ digits: it has many configurations. Due to its course in the distal forearm and wrist; and the variability of its position and branching patterns, it is vulnerable to injuries due to trauma or iatrogenesis. Many therapeutic and diagnostic procedures are conducted on the distal forearm and wrist area including fixation and reduction of distal radial

fractures, wrist arthroscopic procedures, de Quervain's syndrome release, radial artery harvest and cephalic vein cannulation. Understanding the anatomical course of the SBRN and its relationship to other structures in the distal forearm is not only important to ensure safe clinical practice; but also to create opportunities for the development of new medical techniques and applications.

Although described in the literature, the innervation territory and the pattern of distribution in the dorsum of the hand differ greatly among authors. Anatomical variations, communicating branches and most common patterns of distribution are not well described nor have the associations between the nerves or other anatomical structures in the dorsum of the hand been fully investigated. Furthermore, there are contradicting reports about the incidence of communicating branches between the nerves that supply the dorsum of the hand and their common locations. Description of the most common patterns of innervation and variations to these patterns in respect to well-known anatomical landmarks can greatly help in clinical settings. It will also aid in better evaluating electrophysiological studies, to properly diagnose and plan treatment, and safely intervene, if required.

The current study investigates the cutaneous innervation of the hand focusing on the PCBMN, CDNs, UN, SBRN, and DBUN. It describes their anatomical course, details their common patterns of distribution and discusses their significance in clinical settings. The study aims to fill the gap in the literature to better understand the cutaneous nerve supply to the hand and appreciate the relations between the nerves and other anatomical structures in the distal forearm and wrist.

1.1. The development of the sensory innervation pattern

The sensory innervation is organized segmentally where a region of skin (dermatome) is supplied by axons derived from a dorsal root ganglion and carried through one or more cutaneous nerves (Scott, 1992). The cutaneous fibres from each dorsal root ganglion grow precisely and accurately along marked pathways to their target region by receiving guidance from two sources: general and specific cues. The general cues channel general populations (different cells) down a common pathway; whereas, the specific cures are directed toward a particular population of cells directing them towards the appropriate target region (Tosney and Oakley, 1990; Scott, 1992). The following is an overview of the general and specific cues that direct the growth of dermatomes; however, as far as can be ascertained, the exact influences and processes of the development of the cutaneous innervation of the hand in humans (the nerves investigated in this study) were not fully investigated in the literature.

Tosney and Oakley (1990) reported that nerves avoid some regions and are attracted to others suggesting that the regions favourable for axonal growth are adjacent to relatively inhibitory regions. In the chick embryo, growing axons avoid perinotochordal mesenchyme and are attracted to the dorsal-anterior sclerotome establishing the dorsal-ventral position; they avoid the posterior sclerotome and are attracted to the anterior sclerotome establishing the anterior-posterior position of the spinal nerves; they avoid the growing pelvic girdle and are attracted to the plexus mesenchyme establishing the nerve trunk position (Tosney and Oakley, 1990; Scott, 1992). The inhibitory and/or permissive characteristic of a region is controlled by complex cellular interactions, phagocytosis, cell death with a molecular basis providing a relative balance of substances guiding the sensory neuron (Tosney and Landmesser, 1985; Goodman and Shatz, 1993; Kitsukawa et al., 1997).

Specific cues guiding the sensory peripheral fibres include the interactions between sensory axons and other sensory and motor axons. However; studies have also shown that cutaneous nerves were still able to grow in their approximate normal locations in chick embryos with motorneurons precursor removed (Scott, 1988). These results suggest that although motorneurons can provide cues to direct sensory axons, they are not essential (Scott, 1992).

Skin movement is also thought to affect the orientation and growth of sensory axons. Some studies suggest that axons from each dorsal root ganglion innervate skin embryologically derived from the same ganglion root. Scott (1982) suggested that sensory axons are specifically matched with the corresponding skin region creating dermatomes with specific boundaries and little overlap. However; the literature presents different dermatomal maps which can be attributed to the different methods used in different studies to define dermatomes being behaviour response or electrical neurophysiological response studies. Another reason for the inconsistency in dermatomes boundaries is the overlap of skin areas supplied by nerve fibres of adjacent dermatomes (Werner and Whitsel, 1967; Lee et al., 2008). Furthermore, as the skin and limb grow, nerve endings enlarge and grow, which can affect the orientation of the dermatome.

Attraction of axons to targeted epithelium is another mechanism where embryonic skin is thought to secrete neurotropic agents, other than nerve growth factor, that attracts cutaneous axons and thus acts like specific cues guiding cutaneous axons to their targeted region early in development (Lumsden and Davies, 1983). Skin epidermis has also shown inhibitory influences on axonal growth according to studies conducted on chick embryos (Scott, 1982; Martin et al., 1989).

Another specific cue is thought to be administered by the association between sensory axons and Merkel cells (Scott, 1992). Nerve growth factor is required for normal axonal growth and development: one source of nerve growth factor are Merkel cells. Merkel cells are thought to be a regulator of the density and distribution of nerve endings (Vos et al., 1991).

Although dermatomes are areas of skin innervated by one dorsal root ganglion, fibres can be carried through different nerve trunks. As the nerves enter the skin through different points, they can compete for skin via different mechanisms, and thus create different innervation patterns between individuals or even between the different sides of the same individual (Diamond, 1981; Scott, 1982; Scott, 1992).

Furthermore, the full growth and form of a human being is a result of different interactions between the developing individual, which is directed by genes, and its environment. In the early phase of development, the embryo's development and growth is sensitive to environmental cues that can modify, interfere or even disrupt its development (Gluckman et al., 2005). The effect of the environment is clearly evident in the different fingerprints between identical twins (siblings with exactly the same genotype), between the two hands of the same individual and even between the different fingers of the same hand. Such differences are obtained during the differentiation process of the skin and are caused by the different flow of the amniotic fluids around the fetus and its position in the uterus during differentiation of skin. However, fingerprints are expressed from the same gene therefore the resulting pattern will not be totally random but will retain some similarities (Jain et al., 2002). It is possible that environmental cues can influence the orientation and the distribution of nerves creating different patterns among individuals or even between the different sides of the same individual.

1.2. Peripheral nerves internal anatomy and injury

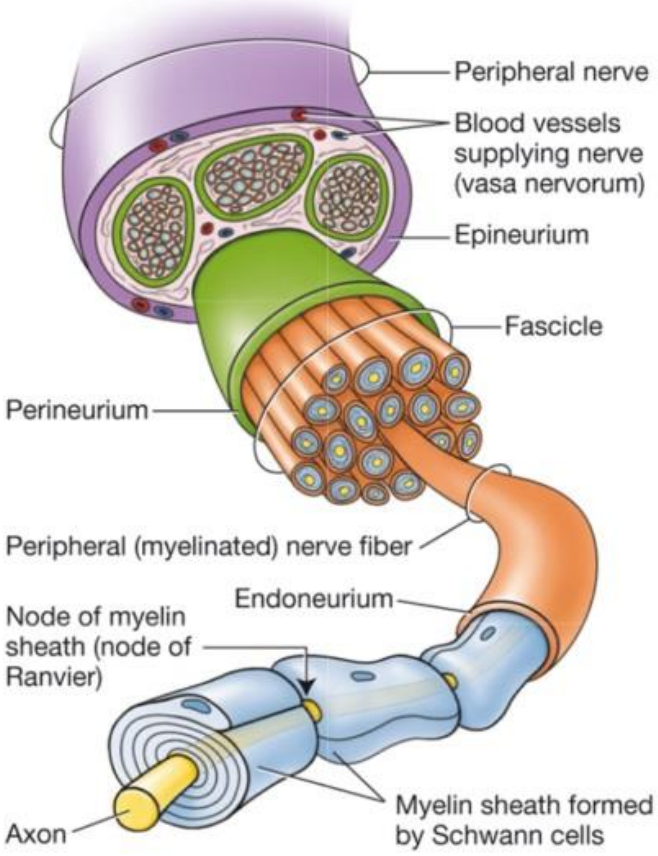

Figure 1.2: The internal organization of the peripheral nerve (Moore et al., 2011; figure 1.21, page 33).

Peripheral nerves connect the peripheral structures of the body to the brain and spinal cord (central nervous system) allowing for continuous reactions to the changes in the external and internal environments. With a variable mix of fibres being myelinated or unmyelinated, somatic or autonomic, the peripheral nerves are organized into bundles enclosed in three sheaths of connective tissue (Moore et al., 2011).

The nerve fibre consists of an axon, neurolemma and an endoneurium. An axon is a single process that carries impulse away from the neuron's cell body: it is surrounded by the cell membrane of Schwann cells, called neurolemma, separating it from other

axons. Myelinated nerve fibres have a myelin layer produced by a continuous series of Schwann cells enclosing and spiralling each individual axon. Each segment of myelin is about 1-2 mm long and is separated by gaps called nodes of Ranvier (Figure 1.2). Unmyelinated nerve fibres consist of several axons (up to 15) embedded separately in the cytoplasm of a non-myelin producing Schwann cell constituting a Remak fibre. About 75% of axons in cutaneous nerves and dorsal spinal roots are unmyelinated. Each nerve fibre is surrounded by a delicate connective tissue sheath called the endoneurium. It contains closely packed, fine, and mostly longitudinally arranged collagen fibres (Waxman et al., 1995; Wilkinson, 1998; Moore et al., 2011).

Several nerve fibres are grouped together to constitute a fascicle which varies in size between 0.04-3.5 mm. Each fascicle is enclosed by the perineurium, a relatively thin but dense and distinctive layer of fibrous tissue (Figure 1.2). The perineurium contains circular, longitudinal and oblique bundles of collagen fibres protecting and resisting tension to the nerve fibres, providing a barrier to prevent foreign substances from penetrating them, and maintaining homeostasis of the endoneurial fluid of the nerve fibres it encloses (Sunderland, 1965; Stewart, 2003; Moore et al., 2011).

A number of fascicles are embedded in connective tissue, called epifascular epineurium, separating and holding them loosely together; however, it thickens in its outer layers to form the epineurial epineurium. It contains collagen and elastic fibres that mostly run longitudinally, adipose tissue, blood vessels (vasa nervorum) and lymphatics. The epineurium varies in amount along the length of the nerve, between nerves, and between the same nerve at corresponding levels of the two sides. It protects the fascicles against deforming forces by providing a loose matrix which allows stretching of the nerve to accommodate the various moments of the joints without straining the

fascicle (Sunderland, 1965; Moore et al., 2011; Kiernan and Rajakumar, 2014) (Figure 1.2).

The blood supply to the nerve is arranged as a vascular plexus that penetrates all of the layers of the epineurium and perineurium. The vessels have a coiled configuration and approach the nerve trunk segmentally to ensure continuity of the vascular supply during the gliding of the nerves. The vessels cross into the endoneurium obliquely creating a possible valve mechanism (Rempel et al., 1999).

The longitudinal organization of the fascicles and their contents in the peripheral nerve is important in understanding the clinical signs and symptoms of different neuropathologies (Stewart, 2003). Historical studies have highlighted two theories: the first being that the fascicles are arranged like cables, where nerve fibres remain in the same discrete fascicle throughout the length of the nerve; while the second describes a plexiform internal pattern where the fascicles branch, split, join and intermingle throughout the length of the nerve (Figure 1.3) (Langley and Hashimoto, 1917; Jabaley et al., 1980; Stewart, 2003). The current view is that the fascicles are arranged like cables with each fascicle containing motor or sensory fibres specific to a certain region in the more distal regions of the nerve, such as the distal forearm or wrist. In proximal regions, the fascicles branch and intermingle in a plexiform pattern. The degree of intermingling differs between nerves; however, sensory or motor fibres to specific areas tend to remain grouped together as a fascicle or within fascicles throughout the nerve (Stewart, 2003). This view can explain the different and variable manifestations of neuropathies. Stewart (1987) studied the clinical manifestations of ulnar nerve neuropathies at the level of the elbow in 24 patients and reported that branches originating distal to the lesion can be involved or spared from any affect, indicating specific fascicle involvement. Muscles of the distal forearm were spared from any affect, while intrinsic

muscles of the hand were affected (Stewart, 1987). Such manifestations can easily confuse physicians into identifying the lesion to be at the wrist or hand rather than the elbow. Radial nerve lesions can also be manifested differently in Saturday-night palsy (radial nerve compression resulting from pressure against a firm object as seen after a deep sleep on the arm) (Trojaborg, 1970). One possible explanation is the differential involvement of fascicles within the radial nerve (Trojaborg, 1970; Stewart, 2003).

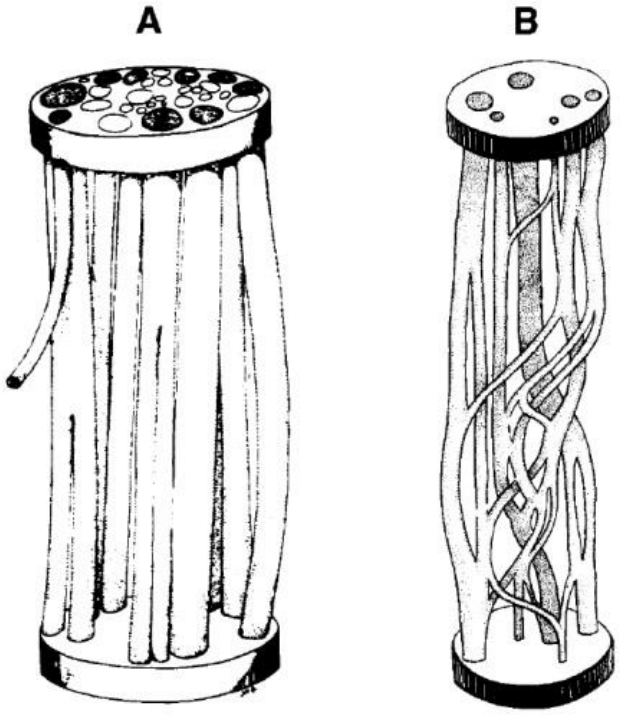

Figure 1.3: Illustrations of fascicular organization in the peripheral nerves. (A) The cable structure; (B) The plexiform structure (Stewart, 2003).

Selective fascicles could be injured due to their close proximity to bone where the potential for compression is greatest. During bone fractures, fascicles closer to the bone fragments could be injured. Moreover, fascicles which have less protective coverings are more vulnerable to injury. In addition, the vasa nervorum could be affected by changes in intraneural pressure leading to ischaemia. Based on the findings, Stewart (1987) suggested that the nerve fibres affected are those originating most distally from the

nerve as longer fibres are the more affected by the compromised axoplasmic flow. The longer fibres could be at more risk of damage, as seen in carpal tunnel syndrome where sensory disturbances are often reported in the most distal parts of the finger (Sunderland, 1965; Trojaborg, 1970; Stewart, 1987). It is important to appreciate the effect of the internal neural topography in hand neuropathologies.

Following injury to a peripheral nerve, complex but regulated events occur to restore function. Understanding the process is important to appreciate the signs and symptoms of different neuropathologies. Depending on the severity of injury, Seddon (1943) identified three types of nerve injuries and classified them into: neurapraxia, axonotmesis, and neurotmesis. Neurapraxia is the mildest form of nerve injury where nerve continuity is maintained, but the ion-induced conduction is blocked at the injury site leading to transient function loss as seen in compression injuries. Focal demylination and/or ischaemia are thought to be the causes of conduction block (Robinson, 2000). Axonotmesis occurs when the axons and the surrounding myelin sheaths are damaged, while the perineurium and the epineurium are still intact as seen in crush injuries, stretch injuries or percussion injuries. Axon and myelin degeneration distal to the site of injury occurs leading to complete denervation. Recovery is possible as the uninjured fibres sprout to reinnervate the target organ. Neurotmesis occurs after the nerve is severed where recovery is usually incomplete and can only be achieved with surgical intervention. It can be seen in sharp injuries, injection of noxious drugs, traction injuries or percussion injuries (Seddon, 1943; Wilkinson, 1998; Robinson, 2000; Burnett and Zager, 2004).

Sunderland (1951) further modified Seddon's classification of peripheral nerve injury, suggesting five categories based on the severity of the injury. A first degree injury corresponds to neurapraxia and a second degree to axonotmesis. Third degree injury

occurs where there is a partial injury to the endoneurium in addition to the axonal damage. This is a case between axonotmesis and neurotmesis. In Sunderland's classification, neurotmesis is further divided into a fourth degree injury, where all the components of the nerve are injured except the epineurium; and fifth degree injuries, where the nerve is completely severed (Figure 1.4) (Sunderland, 1951; Grant et al., 1999; Robinson, 2000; Burnett and Zager, 2004).

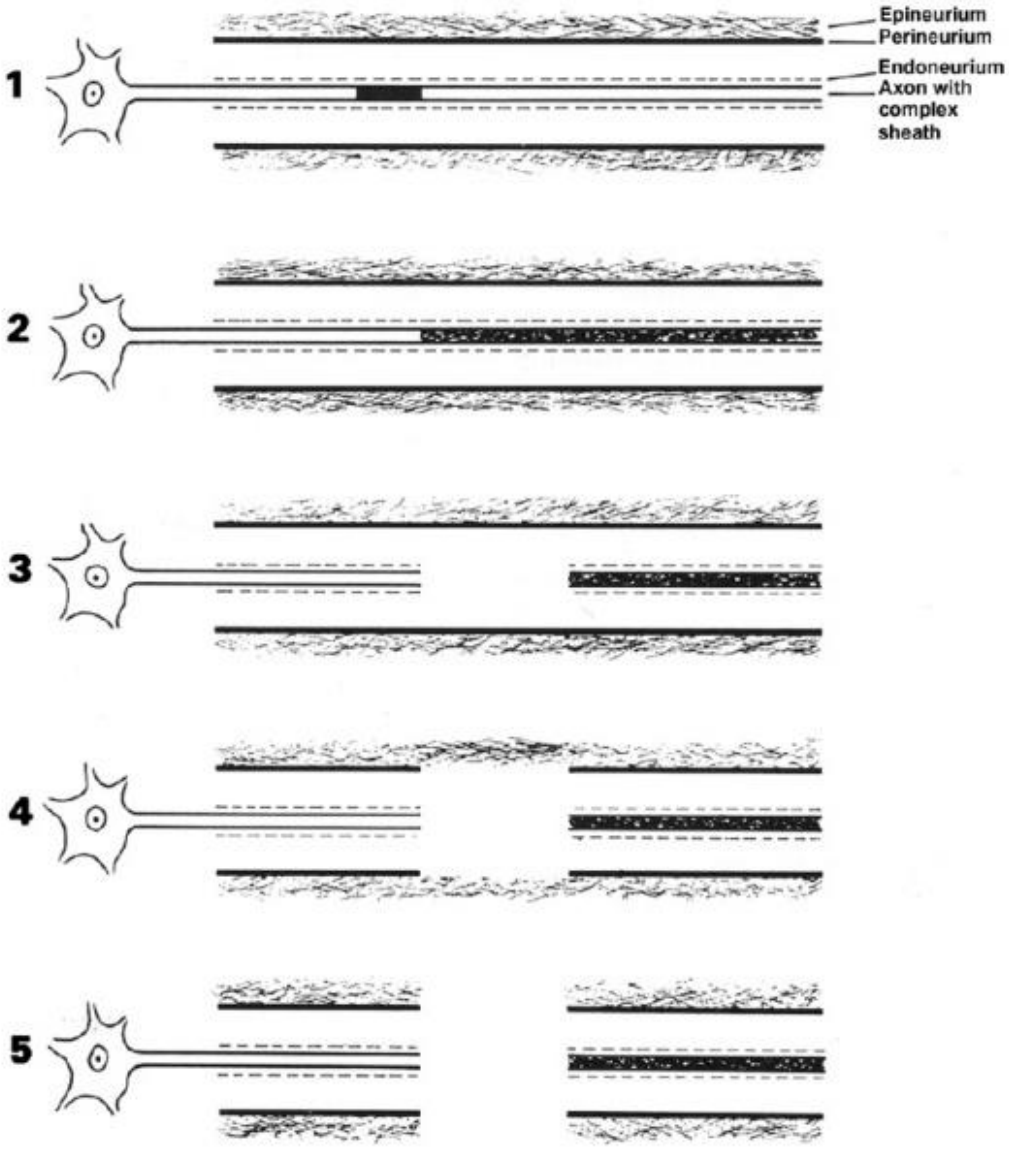

Figure 1.4: Diagrammatic illustration of the five degrees of nerve injuries as described by Sunderland. 1, first degree of injury; 2, second degree of injury; 3, third degree of injury; 4, fourth degree of injury; 5, fifth degree of injury (Campbell, 2008).

Neurapraxia (first degree injuries), no structural changes are noticed and thus no true degeneration or regeneration occurs. In axonotmesis (second degree injuries), a calcium-mediated process known as Wallerian degeneration occurs distal to the site of injury resulting in dissolution of the distal axon, remodelling of the nerve fibre components and regeneration by regrowth of new axons. Figure 1.5 shows the steps of Wallerian degeneration. Within hours of injury physical fragmentation of both axons and myelin occurs, neurotubules and neurofilaments becomes disorganized and irregular due to varicose swelling (Burnett and Zager, 2004). By 48 to 96 hours after injury, axonal continuity is lost and impulse conduction is not possible. Schwann cells become active within 24 hours of injury and divide rapidly to help in the degeneration and regeneration processes. Endoneural mast cells secret histamine and serotonin enhancing the permeability of the capillaries and facilitating the migration of macrophages to the site of injury. Schwann cells pass the degenerated axonal and myelin debris to macrophages that migrated to the site of injury through the permeable capillaries in the region. The process of cleaning and phagocytosis at the site of injury can extend from one week to several months (Campbell, 2008).

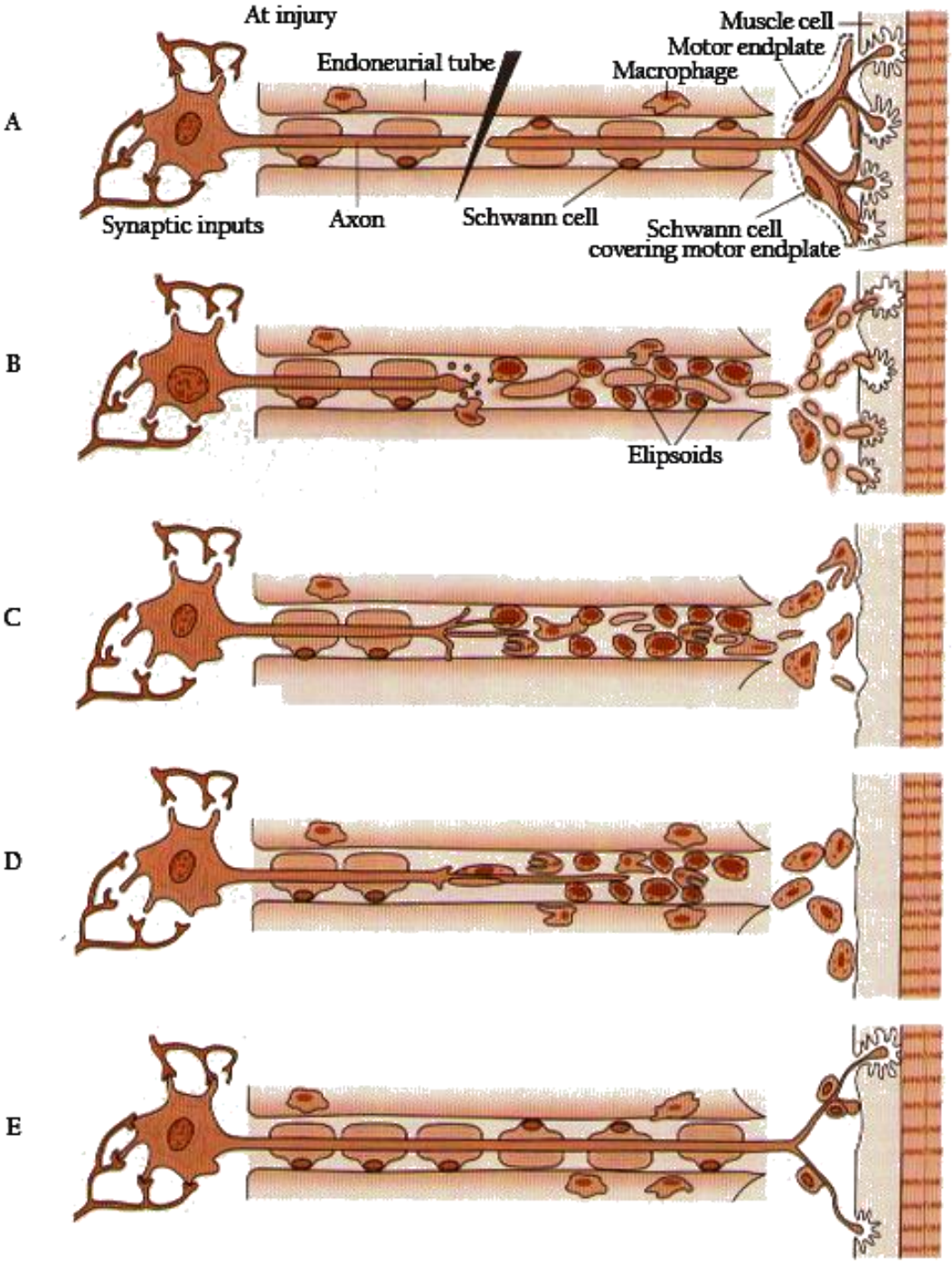

Figure 1.5: An illustration shows the process of Wallerian degeneration. (A) Injury occurs to the axon but the endoneurial tube is still intact; (B) Degeneration of axonal and myelin components of the distal segment. Elipsoids are formed by Schwann cells to facilitate phagocytosis by macrophages; (C) Degeneration and clearing of the distal segment are achieved. Regeneration of the axon begins guided by bands of Büngner (columns of Schwann cells); (D) regeneration continues in the endoneurial tube distal to the site of injury; (E) Full regrowth of axonal and associated myelin components (Nowak and Handford, 2003; figure 21.6, page 600).

In third degree injuries, retraction of the severed nerve occurs due to the elastic nature of the endoneurium. Capillaries are injured activating an inflammatory response at the site of injury. Fibroblasts rapidly increase in number and produce a dense fibrous scar swelling and often adhesions to the perineural tissue. In fourth and fifth degree injuries, severe trauma occurs to the endoneural tubes, fasciculi, and the epineurial membrane. Mast cells degranulate increasing the capillary permeability leading to edema and macrophage migration. The nerve ends becomes swollen containing disorganized Schwann cells, capillaries, fibroblast, macrophages, and collagen fibres. Regenerating axons attempt to penetrate the scar tissue but back into the proximal segment or into the surrounding tissue. Depending on the scar tissue formed and the severity of the injury, the regenerated axons can reach the distal segment.

Distal to the injured region, axonal and myelin components are cleared leaving endoneural tubes (Flores et al., 2000). The endoneural tubes are thickened due to the collage deposition on the outer surface of the Schwann cell basement membrane. If the tube does not receive a regenerating axon, it shrinks and fibroses. Stacks of Schwann cells, arranged in columns known as bands of Büngner, become visible late in the Wallerian degeneration process: they are thought to play a vital role in the process of regeneration where they guide axons into their target organs (Flores et al., 2000; Burnett and Zager, 2004).

Segments proximal to the injury site can also undergo Wallerian degeneration depending on the severity of the injury and the proximity of the injured site to the cell body. In the proximal segment near the site of injury, the axons and myelin reduce in diameter and Schwann cells degrade. The nerve cell body also reacts to injury in a process called chromatolysis. This includes nucleus migration to the periphery of the cell, degradation of Nissl granules and rough endoplasmic reticulum, and an increase in

the synthesis of RNA, protein components, lipids, and hydrolytic enzymes (Flores et al., 2000; Burnett and Zager, 2004). This process marks the shift of all function from impulse transmission to cellular repair, producing important materials for axonal regrowth during the regeneration phase (Waxman et al., 1995).

The regeneration process starts at the cell body with the reversal of chromatolysis. Materials are transported from the cell body to the site of axonal regeneration, and the regenerating axonal tip sprouts out. In severe injuries, scar tissue fills the gap between the severed nerve endings and resists the advancement of the regenerating axons. Furthermore, axons can grow and be misdirected into a functionally inappropriate endoneural tubes or even fail to re-enter the endoneural tube. The resistance that the regenerating axons receive at the site of injury leads to the creation of multiple smaller axon sprouts which do not all reach their target organ (Burnett and Zager, 2004; Campbell, 2008).

Axons entering the correct endoneural tube distal to the site of injury grow to reach the target organ. Sometimes, several sprouts may enter the endoneural tube, as a result the regenerated endoneural tube many contain more axons than the original. The specialized growth cone at the tip of the axon sprout contains multiple filopodia (cytoplasmic projections) that adhere to the basal lamina of Schwann cells and use it as a guide. If the axon tip is delayed in getting into the distal segment, the endoneural tube would have decreases in diameter and thus axonal regrowth is slowed (Fawett and Keynes, 1990; Campbell, 2008).

1.3. Hand Landmarks:

Understanding the surface anatomy of the hand is important in planning surgical procedures and the assessment of normal and abnormal function in the hand and wrist. The most important landmarks on the palmar surface of the hand are flexion creases, the pisiform, scaphoid tubercle, and hook of the hamate. On the dorsal surface of the hand are Lister's tubercle, the anatomic snuff box, the lunate fossa, and the radial and ulnar styloid processes.

1.3.1. Flexion creases:

The skin of the palm is firmly attached to the deep fascia by several relatively constant palmar creases. The palm creases are significant palmar landmarks because of their relationship to underlying structures. They also ensure stability of the skin during gripping and enable movement of the digits without impingement. Most creases do not correspond to their respective joints, however there are two prominent creases at the proximal interphalangeal joint, the proximal of which is usually used to determine the location of the underlying joint (Doyle and Botte, 2003). Appreciation of the relationship between the creases and the underlying osseous anatomy may be extremely useful in clinical and surgical settings such as tendon repairs, webbed fingers and Dupuytren's disease corrective procedures, trigger finger surgery and even carpal tunnel release. Creases can be grouped into four categories: the digital, palmar, thenar, and wrist skin creases (Figure 1.6).

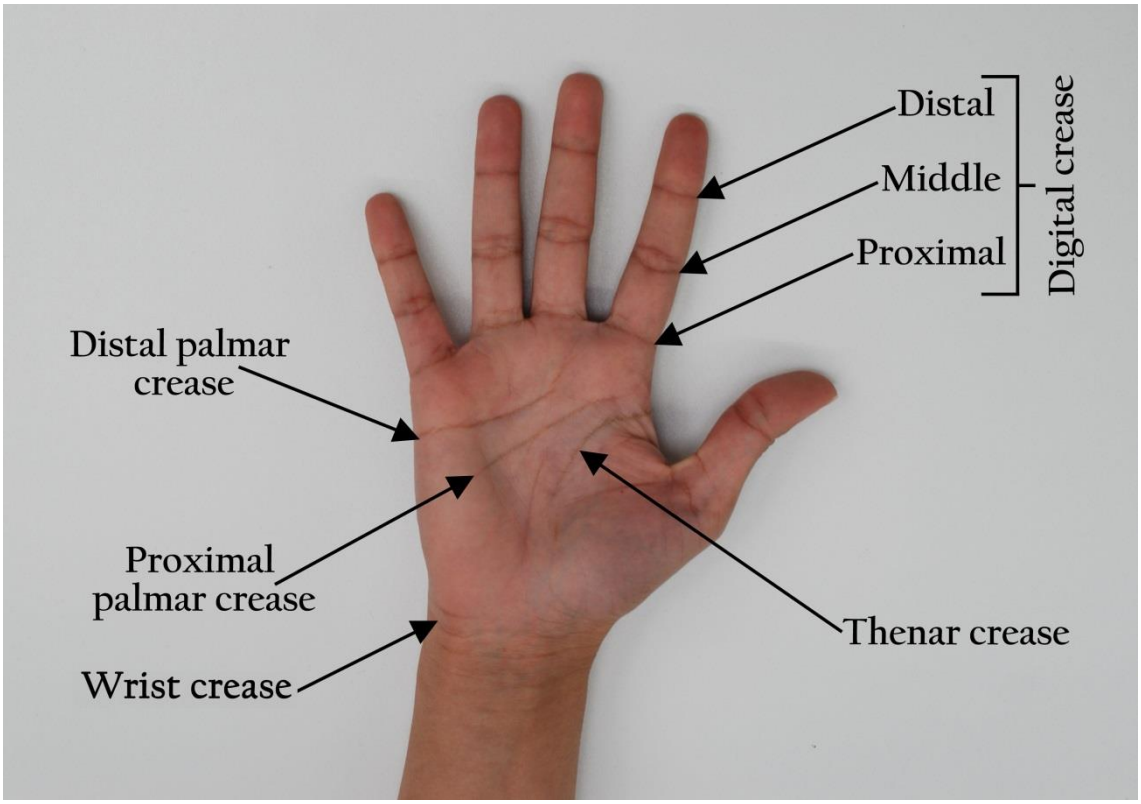

Figure 1.6: Hand flexion creases (Source: Author).

There are three horizontal digital creases: proximal, middle and distal digital creases in all fingers, except the thumb, which lie close to the metacarpophalangeal joint and the proximal and distal interphalangeal joints respectively. Bugbee and Botte (1993) reported that the distal digital skin creases, consisting of one or two closely placed lines, are always proximal to their associated distal interphalangeal joint by 7-7.8 mm. The middle digital creases are two separated lines, more oriented to their corresponding joint positions: they lie 1.6-2.6 mm proximal to the proximal interphalangeal joint. The proximal digital skin creases lie between 14.4-19.6 mm distal to their respective metacarpophalangeal joints and are usually two parallel lines separated by 3-4 mm. The metacarpophalangeal crease of the thumb is vertical rather than horizontal. The interphalangeal joint crease of the thumb is located 2.2 mm proximal to the interphalangeal joint whereas the proximal joint crease crosses

obliquely and directly over the metacarpophalangeal joint of the thumb (Kaplan, 1968; Bugbee and Botte, 1993).

Kaplan (1968) reported some interesting relations of the digital creases usually seen when the hand is placed on a flat surface:

- The distal digital crease of the index and ring fingers are on the same line and if extended align with tip of the little finger.
- The middle digital crease of the index and ring fingers and the distal digital crease of the little finger are on the same level.
- The second distal line of the proximal digital crease of the ring finger is in line with the middle digital crease of the little finger.

The palmar skin creases are associated with the metacarpophalangeal joints in the following manner: the distal palmar crease is located at a mean distance of 7.9 mm, 10.3 mm and 6.9 mm from the metacarpophalangeal joints of the little, ring, and middle finger respectively (Bugbee and Botte, 1993). The distal palmar crease can extend and reach the level of the metacarpophalangeal joint of the index finger in 18% of individuals (Chauhan et al., 2011). Moreover, the proximal palmar crease is located at a mean distance of 9.1 mm, 18.0 mm and 22.1 mm from the metacarpophalangeal joints of the index, middle and ring finger respectively (Bugbee and Botte, 1993; Doyle and Botte, 2003). In their study, Bugbee and Botte (1993) mentioned that a longitudinal line between the lateral border of the proximal palmar crease and the medial border of the distal palmar crease determines the location of the metacarpal neck in 73% of specimens. Other researchers, found the line to overlap with the head of the metacarpals in 38% and the metacarpal neck in 48% (Chauhan et al., 2011).

The thenar crease usually intersects the lateral side of the proximal palmar crease at its distal border and the distal wrist crease near the wrist centre at its proximal border. Bugbee and Botte (1993) reported that in 54% of specimens, the thenar crease lies directly over the metacarpal of the middle finger, being in line with the second web space in 38% and located within the third web space in 8%. In the proximal palm, the thenar crease crosses the capitate in approximately 50% of specimens. The thenar crease passes 22.6 mm to the centre of the trapeziometacarpal joint and 18.7 mm distal to the hook of the hamate on the medial side of the carpus (Bugbee and Botte, 1993). In another study investigating the palmar creases in an Indian population, Chauhan et al. (2011) reported that the thenar crease was located in the 2nd intermetacarpal space in 76% and crossed the scaphoid in 26% of individuals. Moreover, the thenar crease coursed 7.2 mm and 15.6 mm distal to the trapeziometacarpal joint and the hook of the hamate respectively. The study suggests that the difference in findings could be attributed to the racial differences due to North Americans possessing wider carpal regions than Indians.

There are three wrist creases, however only the distal wrist crease can be used as a reliable landmark. The distal wrist crease is located over the proximal carpal row. The centre of the lunate is located 9.2 mm proximal to the crease (Bugbee and Botte, 1993). In their study, Bugbee and Botte (1993) reported that the distal wrist crease crosses the scaphoid in 98% of individuals with the centre of the scaphoid waist laying 1 mm distal to it. Moreover, the study also reported that the midpoint of the trapeziometacarpal joint is located 19.4 mm distal to the crease. On the medial side, the pisiform lies directly on or slightly distal to the distal wrist crease, whereas the hook of the hamate is 12.6 mm distal to the crease. The crease is also located 11.7 mm distal to the base of the ulnar styloid process (Bugbee and Botte, 1993).

1.3.2. Bony landmarks:

There are many important bony landmarks in the hand. The pisiform, hook of the hamate, and the scaphoid tubercle are located in the palmar surface of the hand, whereas Lister's tubercle, the anatomic snuff-box, lunate fossa, and the radial and ulnar styloid processes are found in the dorsal aspect of the hand (Friedman, 2008).

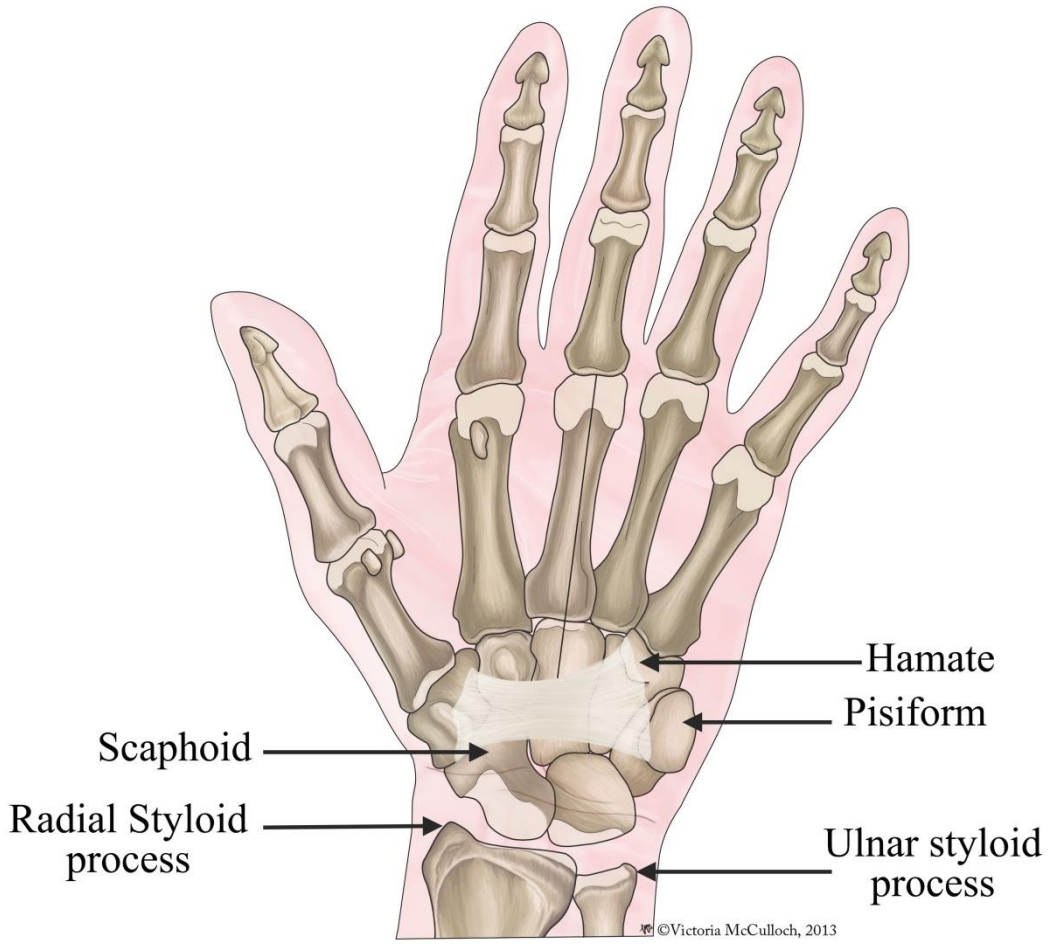

Figure 1.7: Important bony landmarks in the palmar surface of the hand.

The pisiform bone is a palpable landmark which lies on the medial palmar surface of the hand, on the distal wrist crease or slightly distal to it (Bugbee and Botte, 1993). It is used to identify the tendon of flexor carpi ulnaris, the neurovascular bundle and the

hook of the hamate (Doyle and Botte, 2003). The hook of the hamate is located on the medial palmar surface of the hand, some 10 mm lateral and distal to the pisiform: it may be difficult to palpate in some individuals because of its deep position. It is an important landmark to locate the ulnar artery and nerve and the medial border of the transverse carpal ligament (TCL) as it lies between the ulnar canal and the carpal tunnel. On the lateral side of the palm, the scaphoid tubercle projects to the distal lateral palm and almost always crosses the distal wrist crease (Figure 1.7).

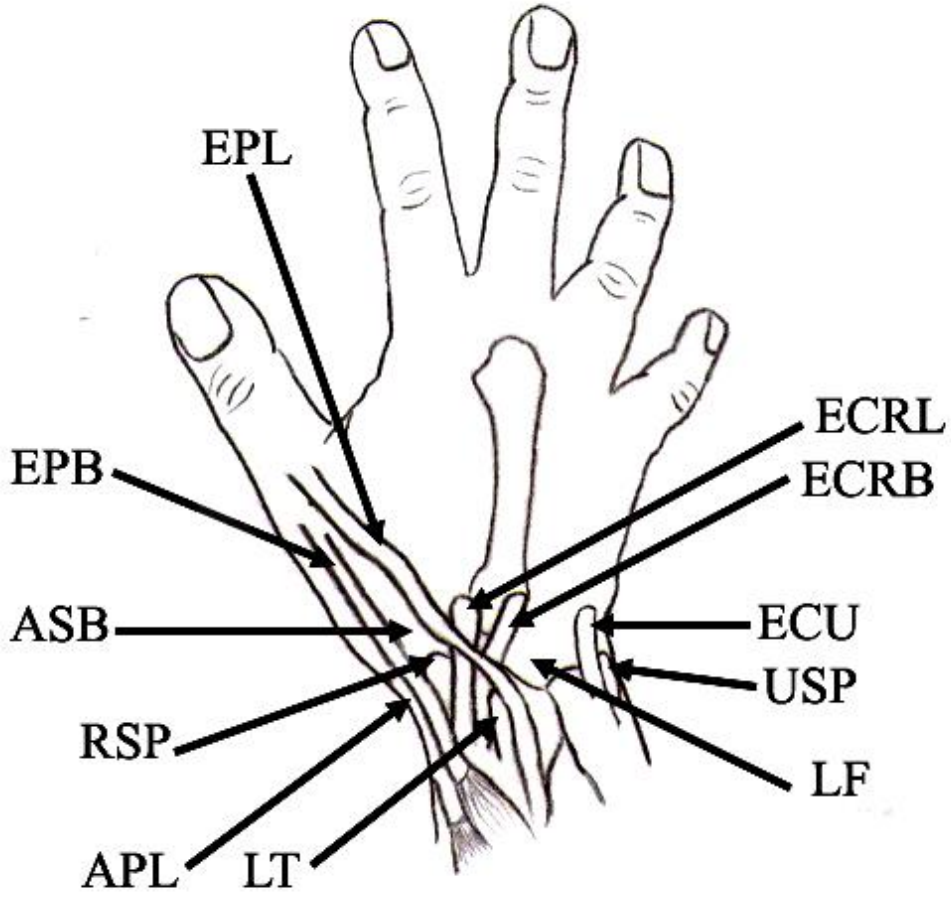

Figure 1.8: Important landmarks in the dorsum of the hand. LT, Lister's tubercle; APL, abductor pollicis longus; RSP, Radial styloid process; ASB, anatomical snuff box; EPB, extensor pollicis brevis; EPL, extensor pollicis longus; ECRL, extensor carpi radialis longus; ECRB, extensor carpi radialis brevis; ECU, extensor carpi ulnaris; USP, ulnar styloid process; LF, lunate fossa (Doyle and Botte, 2003; Figure 9.1, page 487).

A line on the dorsal surface of the hand crossing from the distal phalanx of the index to the dorsal wrist provides an important landmark. The line passes between the lunoscaphoid joint with the lunate positioned medial to it. Lister's tubercle, also medial to this line, can be palpated 5 mm proximal to the dorsal margin of the articular surface of the radius, in line with the cleft between the index and middle fingers. Extensor pollicis longus is located medial to the groove coursing laterally with extensor carpi radialis brevis passing lateral to it running medially (Figure 1.8) (Kaplan, 1968).

Another important landmark on the dorsum of the hand is the anatomic snuff box. It is a narrow triangle bounded medially by extensor pollicis longus, laterally by abductor pollicis longus and extensor pollicis brevis tendons, and proximally by the distal margin of the extensor retinaculum. The floor is formed mainly by the scaphoid and trapezium, with the radial styloid proximally and base of the first metacarpal distally. The radial artery passes through it. In the roof, the cephalic vein and several branches of the superficial branch of the radial nerve course subcutaneously. The tendon of extensor carpi radialis longus crosses its dorsomedial corner (Figure 1.8).

The lunate fossa is a depression located medial and distal to Lister's tubercle, in line with the longitudinal axis of the third metacarpal, distal to the distal radial margin: it corresponds to the location of the lunate (Figure 1.8). The radial styloid process is a distal projection on the lateral side of the distal margin of the radius. It can be palpated through the anatomic snuff box, just dorsal to the abductor pollicis longus and extensor pollicis brevis tendons that cross its apex. The ulnar styloid process is an expansion in the distal end of the ulna. It is mostly palpable when the forearm is supinated and is located about 10 mm proximal to the radial styloid process (Figure 1.7 and Figure 1.8) (Doyle and Botte, 2003).

1.3.3. Relationships of superficial landmarks to deeper structures of the hand:

Kaplan (1968) outlines a unique system of lines linking superficial landmarks of the hand to the deeper structures. Figure 1.9 illustrates the reference skin lines and their anatomical relationships.

The Kaplan system includes:

- Cardinal line (Figure 1.9: line A): drawn across the palm to connect between a point 20 mm distal to the pisiform and a point marked at the junction of the thumb proximal crease at the first interdigital fold. It approximately corresponds to the course of the deep motor branch of the ulnar nerve along with the deep palmar arch (Figure 1.9: 5).
- A vertical line from the lateral margin of the middle finger crossing the cardinal line in the palm (Figure 1.9: line C). The crossing point corresponds to the point at which the recurrent motor nerve penetrates the thenar eminence (Figure 1.9: 4).
- A vertical line from the medial margin of the ring finger crossing the cardinal line in the palm (Figure 1.9: line B). The crossing point corresponds to the hook of the hamate (Figure 1.9: 6), distal to which the bases of the 4^{th} and the 5^{th} metacarpals articulate.
- The middle of the medial third of the cardinal line, distal to pisiform and the hook of the hamate (Figure 1.9: dark star), corresponds to the division point of the ulnar nerve into deep and superficial branches.
- A line drawn connecting a point at the distal palmar crease along the course of the flexor tendons of the little finger and a point 20 mm distal to the tip of the trapezium tubercle (Figure1.9: line D). The proximal part of this line around the thenar eminence corresponds to the articular line between the trapezium and base of the first metacarpal.

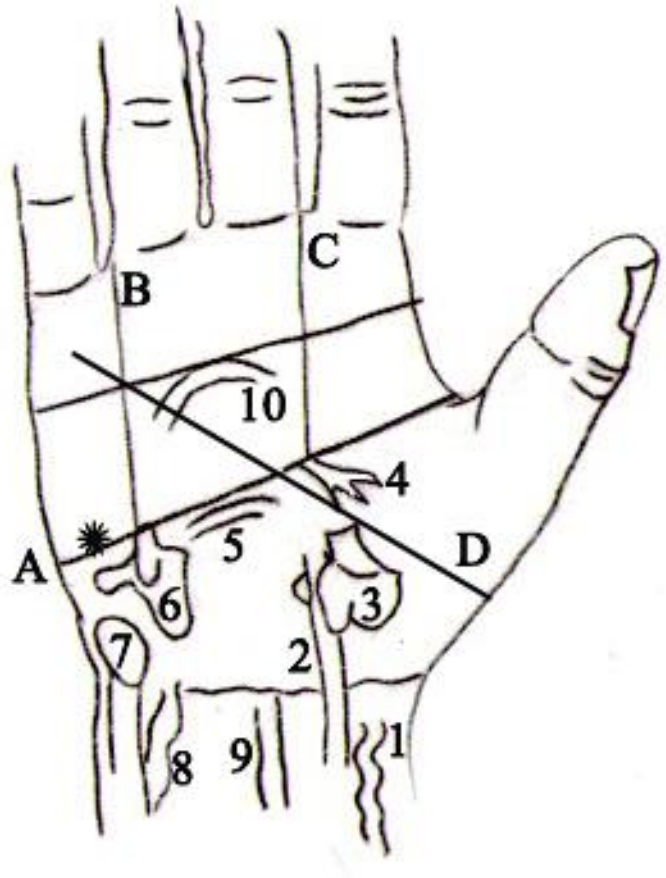

Figure 1.9: Kaplan system. (1) Radial artery; (2) Flexor carpi radialis tendon (3) trapezium; (4) recurrent motor branch of the median nerve; (5) deep palmar arch; (6) hamate; (7) pisiform; (8) ulnar artery; (9) median nerve; (10) superficial palmar arch; dark star, division point of the ulnar nerve into superficial and deep divisions; A, cardinal line; B, vertical line crosses the cardinal line at the hook of hamate; C, vertical line crosses the cardinal line at the point of the recurrent motor branch of the median nerve penetrating the thenar eminence; D, oblique line corresponds to the articular line between trapezium and the base of the first metacarpal at its proximal part at the base of the thenar eminence (Doyle and Botte, 2003; figure 10.3, page 535).

1.4. Palmar surface of the hand:

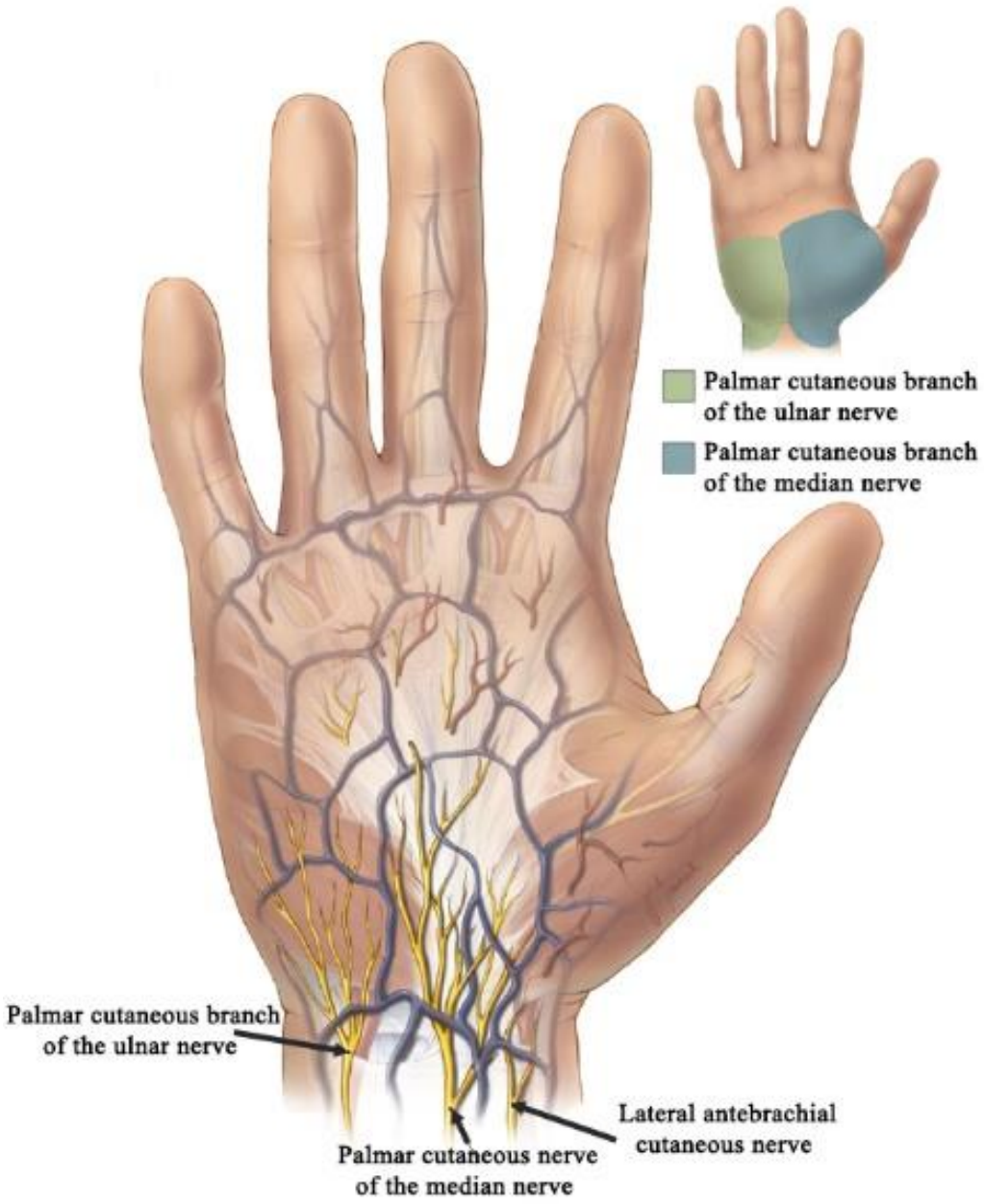

Figure 1.10: Palmar cutaneous branch of the median nerve and palmar cutaneous branch of the ulnar nerve innervation territory in the palm (Tubbs et al., 2011).

The palmar surface of the hand is innervated by two main nerves: the median and ulnar nerves. The median nerve gives the palmar cutaneous branch of the median nerve (PCBMN) in the distal forearm and supplies the proximal and lateral two fifths of the palm (Figure 1.10). After passing through the carpal tunnel, the median nerve gives the first three common digital nerves (CDN) that further divide into proper digital nerves (PDN) to supply the entire palmar surface of the lateral three and half digits and their dorsal surface to the distal interphalangeal joints.

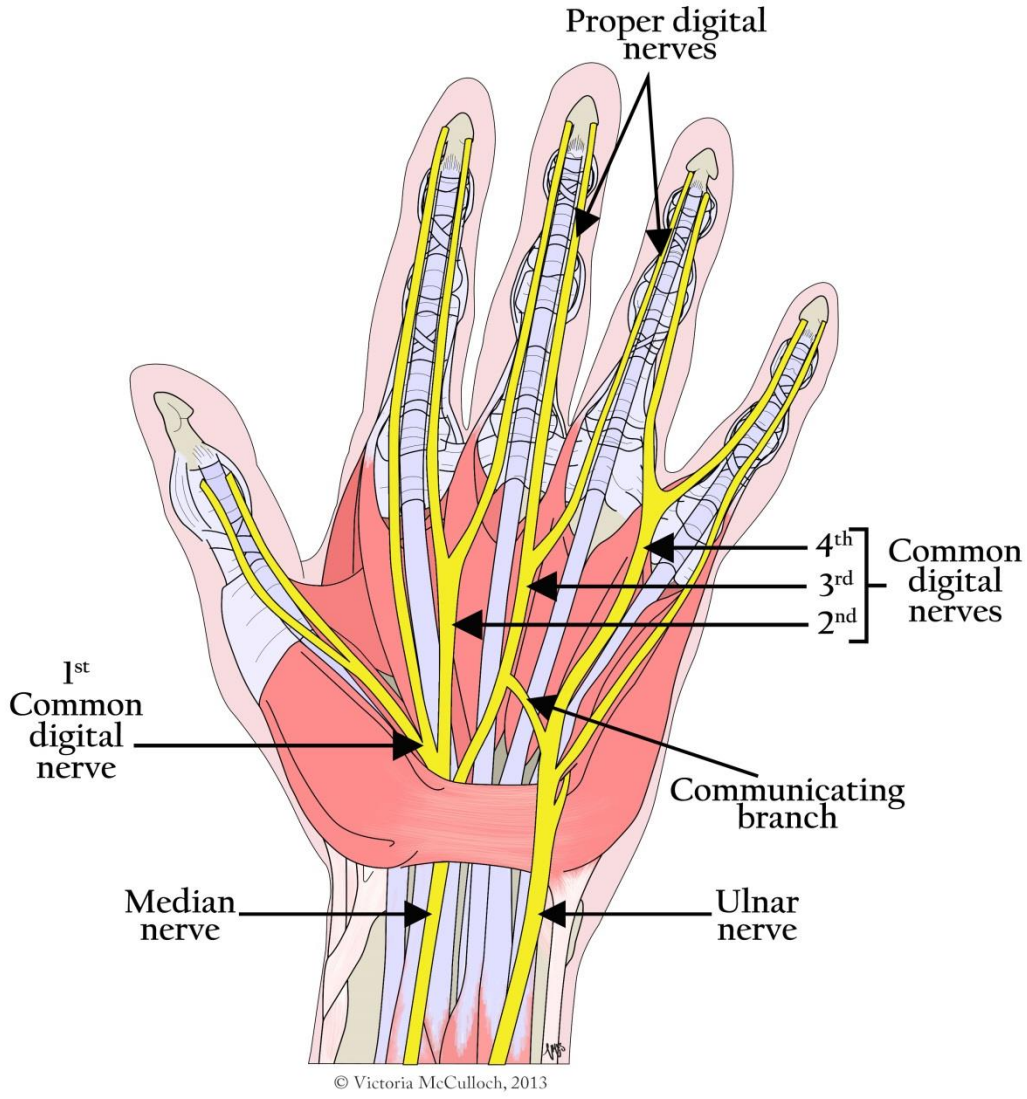

Figure 1.11: Sensory nerves supplying the palmar surface of the hand

Originating at various levels in the forearm, the palmar cutaneous branch of the ulnar nerve and the nerve of Henle supply the medial side of the palm (Figure 1.10). The ulnar nerve passes through the ulnar canal (Guyon's canal) and divides into a deep branch supplying motor innervation to most of the intrinsic muscles of the hand and a superficial branch that supplies sensory innervation to the medial one and half digits. Deep to the superficial palmar arch, a communicating branch may be present between the median and ulnar nerves. This communicating branch allows exchange of sensory fibres between the ulnar and median nerves (Ferrari and Gilbert, 1991; Don Griot et al., 2000; Griot et al., 2002; Loukas et al., 2007) (Figure 1.11).

The sensory distribution in the palm is fairly constant compared to that of the dorsal surface (Stappaerts et al., 1996; Laroy et al., 1998). Nevertheless, there are variations in reported boundaries of the innervation territory for each nerve. The median nerve is usually described as innervating the palmar surface of the lateral 3½ digits in anatomical charts and textbooks; however, according to Hoppenfeld (1976), as cited in Stappaerts et al. (1996), the sensory innervation to the ring finger as being entirely supplied by the ulnar nerve. Although less acknowledged by anatomists when describing the palmar sensory distribution, the medial side of the ring finger can be supplied by the ulnar nerve through fibres traveling in the palmar CB between the ulnar and median nerve. Investigating sensory disturbances in gunshot victims from World War I, Stopford (1918) reported that the ulnar nerve innervated the entire palmar surface of the ring and little fingers in 18% and extended to supply the medial side of the middle finger in 3% of the cases investigated. Investigating the median nerve supply to the palmar surface, the study reported that sensory disturbances were not noted on the radial side of the ring finger in 20%, nor was it found in the medial side of the middle finger in 4%. However, the median nerve supplied the entire ring finger in 4%.

The study also mentions that the sensory loss was not absolute in the lateral side of the ring finger suggesting a dual innervation of this area by the ulnar and median nerves (Stopford, 1918). Linell (1921) also reported some variation to the classical description of the nerve supply to the palmar surface from investigating 20 cases. In this study, the ulnar nerve innervated the palmar surface of the entire medial two digits in one case (5%) and innervated the medial side of the middle finger in three cases (15%) (Linell, 1921).

In velocity conduction studies the sensory distribution is remarkably constant. Laroy et al. (1998) investigated the palmar sensory distribution in 64 hands and reported that median nerve stimulation resulted in recordings obtained from the thumb, index, middle and ring fingers; whereas stimulation of the ulnar nerve resulted in recordings obtained from the little and ring fingers in all cases. The study also mentions that the ring finger receives equal contributions from the ulnar and median nerves (Laroy et al., 1998). Stappaerts et al. (1996) reported that median nerve stimulation resulted in recordings from the lateral 4 fingers in all cases except two where an additional recording was also obtained from the little finger. Furthermore, stimulation of the ulnar nerve resulted in recordings from the little and ring fingers in all cases except three where an additional recording was also obtained from the middle finger (Stappaerts et al., 1996). Such variation from the typical description can be attributed to the presence of a palmar CB allowing transfer of fibres between the two nerves. The innervation of the palmar surface can differ between the hands of the same individual. Although still high, symmetry was found in only 87% (Stappaerts et al., 1996).

1.4.1. Median nerve

In the axilla, anterior to the third portion of the axillary artery, the lateral and medial roots of the lateral and medial cords of the brachial plexus join to form the median nerve. Carrying fibres from the anterior rami of C5, C6, C7, C8 and T1, it supplies the majority of the flexor compartment of the forearm, some hand muscles and contributes to the cutaneous innervation of the hand. In the hand, the median nerve supplies the middle and lateral third of the palmar surface, the palmar surface covering the lateral 3½ digits and the dorsal skin covering the distal phalanges of the lateral 3½ digits by the palmar cutaneous branch of the median nerve and the common digital nerves.

1.4.1.1. Palmar Cutaneous Branch of the Median nerve

In the forearm, 50 to 70 mm proximal to the wrist crease, the median nerve gives off the palmar cutaneous branch of the median nerve (PCBMN). The nerve originates anterolaterally and continues with the main trunk epineurium for about 16-25 mm before it detaches coursing distally between palmaris longus and flexor carpi radialis. At the proximal edge of the TCL, the nerve takes a superficial course in line with the axis of the ring finger, entering its own fibrous tunnel in the ligament. However, the tunnel can be formed within the antebrachial fascia, the palmar carpal ligament (PCL), or the flexor retinaculum (Al-Qattan, 1997). The anterior compartment of the forearm is surrounded by the antebrachial fascia that thickens distally forming the PCL. Distal to the PCL and at deeper levels, the antebrachial fascia continues distally as the flexor retinaculum or the TCL (Moore et al., 2006). The nerve enters the tunnel 3 mm medial to the thenar crease and pierces the palmar aponeurosis 15 mm distal to the scaphoid tubercle (Naff et al., 1993; Matloub et al., 1998). It usually divides into a larger lateral and one or more medial branches that supply the lateral two-fifths of the palm and skin

over the thenar eminence (Taleisnik, 1973). The nerve continues to branch and penetrates the fascia and palmaris longus fibres blending with the palmar fascia. Table 1.1 summarizes the anatomical descriptions of the PCBMN in the literature. Das and Brown (1976) described the most common course of the PCBMN, after investigating 120 cases of carpal tunnel release, was to originate 30-60 mm proximal to the wrist, course deep to flexor digitorum superficialis, continue distally superficial to the TCL (flexor retinaculum) and distribute various branches in the mid-palm. However, the authors noted different patterns of the course of the nerve into the wrist where the PCBMN can course through or deep to the TCL rather than superficial to it before it became cutaneous (Das and Brown, 1976). In their study, Matloub et al. (1998) reported that the most common course of the PCBMN was through the TCL (flexor retinaculum) (37/40), where the nerve enters its tunnel between the superficial and the deep layers. However, in a minority of cases, the nerve coursed superficial to the TCL (flexor retinaculum) and no tunnel was found (3/40) (Matloub et al., 1998).

Table 1.1: Anatomical description of the palmar cutaneous branch of the median nerve as mentioned in the literature

Reference	No. Cadavers	Anatomical descriptions
Taleisnik (1973)	12 cadaveric hands	▪ Detailed description of the course and relationship to structures in the distal forearm. o Originated from the anterolateral side of the median nerve. o Palmar cutaneous branch of the median nerve (PCBMN) remains bound to the main trunk of the median nerve for 16-25 mm after its origin. o The PCBMN enters a 9-16 mm long tunnel between the superficial and deep layers of the transverse carpal ligament. o Divides into one larger lateral branch supplying the thenar aspect and smaller ulnar branches that perforate the transverse carpal ligament. ▪ Variations were found in 3/12.
Bezerra et al. (1986)	50 adult formalin fixed upper extremities	▪ Originated from the lateral side of the main trunk of the median nerve, 45.6±9.7 mm (range 24.6-66.8 mm) proximal to the wrist crease. ▪ It perforated the antebrachial fascia 7.9±3.2 mm (range 3.6-18.6 mm) proximal to the wrist crease. ▪ It emerged in the palm 7.6±3.2 mm (range 1.7-18.6 mm) distal to the wrist crease. ▪ The width of the nerve at the point of origin was 1.2±0.3 mm (range 0.7-2.1 mm). ▪ The length of the nerve from its point of origin to the point it gives its first branch was 52.4±16.2 (range 20.5-89.3 mm). ▪ Three types were reported based on the area innervated in the palm: o Type I: 29/50 (58%) PCBMN gave off one lateral branch innervating the thenar region and another intermediate supplying the intermediate region of the hand. o Type II: 17/50 (34%) PCBMN divided into three branches, lateral, intermediate and medial innervating the thenar, intermediate portion of the hand and the hypothenar region respectively. o Type III: 4/50 (8%) PCBMN gave off one intermediate branch innervating the intermediate portion of the hand, and another medial branch innervating the thenar region.

Reference	No. Cadavers	Anatomical descriptions
		▪ Variations to the three types were noted: o 6/50 (12%) presented a deep branch that connected with the digital nerve of the median nerve in 2 cases. o 2/50 (4%) palmar cutaneous nerve of the median nerve connected with the superficial branch of the radial nerve.
Hobbs et al. (1990)	25 fresh cadaveric upper extremities from 25 cadavers	▪ Originated from the lateral side of the main trunk of the median nerve in all cases. ▪ The nerve has an average length of 129 mm (range 70-265 mm). ▪ Originated 84 mm (range 30-215 mm) proximal to the wrist crease and travelled 45 mm (range 30-60 mm) distal to the wrist crease. ▪ Branches originated proximal to the wrist crease averaged 0.6 (range 0-2) and those originated distal to the wrist crease averaged 6 (range 3-12). ▪ Four branches (range 1-9) with length of 16 mm (range 9-40 mm) emerged from the lateral side of the PCBMN distal to the wrist crease. ▪ Two branches (range 0-5) with length of 4 mm (range 0-10 mm) emerged from the medial side of the PCBMN distal to the wrist crease. ▪ Communicated with the superficial branch of the radial nerve in 2 cases. ▪ Two PCBMNs originated from the median nerve at different levels were found in 4 cases all of which are from male hands.
Naff et al. (1993)	21 upper extremities from 12 fresh cadavers	▪ Originated from the radial side of the median nerve main trunk and coursed medially to the flexor carpi radialis (FCR). ▪ It entered the fascial sheath of the FCR 15 mm proximal to the scaphoid tubercle. ▪ It enters its tunnel at the level of the scaphoid tubercle. ▪ It pierced the palmar aponeurosis 15 mm distal to the scaphoid tubercle. ▪ Originated 57 mm proximal to the radial styloid process (greatest distance 110 mm).

Reference	No. Cadavers	Anatomical descriptions
Dowdy et al. (1994)	52 formalin fixed upper extremities (49 with PL)	▪ Originated 41 mm (range 20-70 mm) proximal to the distal wrist crease. ▪ Travelled through the tendon of palmaris longus in 2/49 specimens. o In the first case the nerve originated 30 mm proximal to the wrist crease and pierced the tendon 10 mm proximal to its insertion. o In the second case the nerve originated 45 mm proximal to the wrist crease and pierced the tendon 15 mm proximal to its insertion.
DaSilva et al. (1996)	12 fresh upper extremities from 9 cadavers	▪ Penetrated the antebrachial fascia 19 mm (range 14-26 mm) proximal to the wrist crease ▪ Penetrated the palmar aponeurosis 15 mm distal to the wrist crease. ▪ Gave branches proximal to the wrist crease in 3/12 specimens. ▪ Two types were reported: o Type A: the main trunk branches into 3 main branches; lateral, intermediate and ulnar (7/12). o Type B: The main trunk branches into many small non-distinct branches (5/12). ▪ Duplicate PCBMN that created a sensory loop and joined the palmar cutaneous branch of the median nerve by penetrating the lateral side of the transverse carpal ligament was noted in 1/12 specimens. ▪ Two PCBMNs with different origin points were noted in 1/12 specimens. ▪ Immunohistological studies showed unmyelinated fibres ending in the superficial layer of the TCL.
Martin et al. (1996)	25 fresh frozen cadaveric hands	▪ Originated from the radial side of the main trunk of the median nerve, 59 mm (range 41-78 mm) proximal to the wrist crease. ▪ Two PCBMNs were identified in two specimens.

Reference	No. Cadavers	Anatomical descriptions
Watchmaker et al. (1996)	25 fresh upper extremities	▪ Two nerves were identified in two specimens. ▪ Originated 41 mm proximal to the wrist crease (range 27-63 mm). ▪ Coursed 2 mm lateral to the thenar crease at the level of the wrist crease with a range of 6 mm lateral and medial of the thenar crease. ▪ It coursed 4-5.5 mm lateral to the inter-thenar depression. ▪ Coursed 9 mm (range 1-16 mm) lateral to the axis of the ring finger in extension; and coursed medial to the axis during flexion. ▪ The nerve overlapped with the medial antebrachial cutaneous nerve in one case (1/25). ▪ It could be traced 35-40 mm distal to the wrist crease by loupe magnification. ▪ No branching pattern and no communications with other cutaneous nerves were noted.
Matloub et al. (1998)	40 fresh-frozen upper extremities from 30 cadavers	▪ Originated from the lateral side of the main trunk of the median nerve, 44 mm proximal to the wrist crease. ▪ Two PCBMNs were found in 6/40 specimens. ▪ Average length of the tunnel is 8 mm (range 2-15 mm). ▪ PCBMN travelled superficial to the TCL (flexor retinaculum) in 3/40 specimens. ▪ PCBMN was partially covered by fibres of palmaris longus at its insertion point into the palmar aponeurosis in 3/40 specimens. ▪ Three distribution patterns were noted: o Type A: The nerve divided into one lateral and another medial branches that further divided into 1-5 branches to supply the skin (20/40). o Type B: Several lateral (three) and medial (two) branches come off the palmar cutaneous branch of the median nerve before it divides into medial and lateral branches (14/40). o Type C: Two palmar cutaneous branches of the median nerve originated from the main median nerve trunk and both gave smaller branches into the palm (6/40). ▪ The length of the PCBMN from the wrist crease to the most distal bifurcation point was 19 mm (range 10-25 mm).

Reference	No. Cadavers	Anatomical descriptions
		▪ The PCBMN passed 3 mm (range 0-7 mm) medial to the thenar crease. ▪ The angle between the terminal lateral and medial sub-branches was 60°. ▪ The most medial terminal branch was located 12 mm (range 4-21 mm) to the thenar crease and the most lateral terminal branch was located 5 mm (range 2-9 mm) to the thenar crease.
Chaynes et al. (2004)	35 hands from 25 cadavers	▪ Originated from the radial side of the main trunk of the median nerve in all cases, 44.3 mm (range 24.8-70.8 mm) proximal to the bistyloid line. ▪ Mean width 0.9±0.3 mm (range 0.4-1.9 mm). ▪ Two PCBMNs were found in one case. ▪ Became subcutaneous 5.7 mm proximal to the bistyloid line (15.3 mm proximal to 9.6 mm distal to the bistyloid line). ▪ Average length 54.6 mm (range 9.2-21.7 mm). ▪ One to three medial branches averaging 3.4 mm long and 1-7 lateral branches averaging 14.6 mm long were noted. ▪ Communicated with the superficial branch of the radial nerve in 5 cases. ▪ Two distribution patterns were reported: o Type A: The nerve divided into two branches (21/35). o Type B: The nerve divided into three branches (14/35).
Cheung et al. (2004)	120 upper extremities from 60 adult Chinese cadavers	▪ Originated from the lateral side of the median nerve in 88.3%, distance between palmaris longus and PCBMN at the level of distal wrist crease was 14 mm (range 6-37 mm). ▪ Originated from the medial side of the median nerve in 11.7%, distance between the palmaris longus and PCBMN at the level of the distal wrist crease was 3 mm (range 0-8 mm). ▪ Originated 32 mm (range 12-65 mm) proximal to the distal wrist crease.
Ozcanli et al. (2010)	16 fresh frozen and 14 formalin fixed cadaveric upper extremities	▪ Originated from the lateral side of the median nerve in 28/30. ▪ Originated 39.2±18.6 mm proximal to the distal wrist crease, and continued in the palm for 19.8±11.5 mm distal to the distal wrist crease.

One of the early descriptions of the pattern of distribution of the PCBMN was described by Taleisnik (1973). In this study of twelve hands the PCBMN usually divided into one large lateral branch supplying the thenar region and another smaller medial branch perforating the TCL and then continuing along the thenar crease supplying the midpalm (Taleisnik, 1973). After dissecting 50 adult hands, Bezerra et al. (1986) described three patterns of division: the most common type, found in 58% of specimens, included two branches one lateral innervating the thenar region and another intermediate coursing under the thenar crease and innervating the intermediate portion of the hand. In 34% of specimens, the PCBMN divided into lateral, intermediate and medial branches innervating the thenar, intermediate, and hypothenar regions of the hand respectively. The third type was reported in 8% of specimens where the PCBMN divided into intermediate and medial branches innervating the intermediate and thenar regions of the hand respectively (Bezerra et al., 1986). In their study, DaSilva et al. (1996) reported two patterns of division of the PCBMN. Pattern A (58.3%) with the main trunk of the nerve dividing into three terminal branches; lateral, medial and a longer intermediate one. Pattern B (41.7%) was identified with many non-distinct small branches from the main trunk penetrating the palmar aponeurosis (DaSilva et al., 1996). In another study, Chaynes et al. (2004) reported two types of pattern of the PCBMN: the nerve divided into two main branches in 21/35 (60%) cases and three branches in 14/35 (40%).

Many variations of the PCBMN have been reported in the literature. Two separate branches of the PCBMN originating at the same level or at different levels have been identified. It can have a more distal origin from the main trunk of the median nerve and originate at the level of the proximal edge of the TCL. The PCBMN can originate from the medial side of the main trunk of the median nerve rather than the commonly known

lateral origin; originate more proximally than usual or as high as the junction between the upper third and the middle third of the forearm (Das and Brown, 1976; Hobbs et al., 1990; Matloub et al., 1998). During localized anaesthesia to the region of the wrist or the thenar muscles, care must be taken to block the PCBMN along with the median nerve unless the block to the median nerve was made proximal to the origin of the PCBMN.

The PCBMN can also be absent, in which case its innervation area is taken over by the musculocutaneous nerve, the superficial branch of the radial nerve, the palmar cutaneous branch of the ulnar nerve or any combination of these nerves (Das and Brown, 1976; Born and Mahoney, 1995; Doyle and Botte, 2003). The PCBMN may communicate with the superficial branch of the radial nerve (SBRN). The connections between the two nerves were reported in 8% and could explain the sensory disturbances in the dorsum of the hand in patients who underwent wrist surgery (Hobbs et al., 1990). In a more recent study, Chaynes et al. (2004) reported a higher incidence rate of the connections (14.29%). According to Bezerra et al. (1986), both Kuhlmann and Meyer-Otetea (1976) and Kuhlmann et al. (1978) reported higher connection incidences between the PCBMN and the SBRN at 25% and 40% respectively. These connections may be at risk during surgical procedures to the lateral side of the wrist such as palmar wrist ganglion or procedures to the distal radius.

The PCBMN can also course deep to or through the fibres of the palmaris longus tendon. Dowdy et al. (1994) investigated 52 cadavers and reported 2 cases where the PCBMN passed through the fibres of palmaris longus tendon in its distal 20 mm endangering the nerve during palmaris longus tendon harvest. Matloub et al. (1998) also reported the PCBMN coursing deep to the terminal fibres of palmaris longus at its distal insertion into the palmar aponeurosis in 3/40 specimens. Therefore, during the harvest of palmaris longus tendon, it is recommended that the tendon be cut proximal

to the wrist crease with careful dissection of the lateral side where the PCBMN is most likely to course (Matloub et al., 1998).

Due to its course in the forearm, the PCBMN is at risk of injury during any surgical procedure along or adjacent to the ulnar side of flexor carpi radialis. A variation in the course of the nerve in relation to flexor carpi radialis has been reported. Nagle and Santiago (2008) noted that the PCBMN coursed superficial to the distal aspect of the flexor carpi radialis to terminate over the thenar eminence. Tendinitis in the region of the distal forearm, injury or inflammation that leads to soft tissue swelling, and scar formation after elective carpal tunnel release can lead to symptoms of PCBMN entrapment (Pardal-Fernández et al., 2011; Sierakowski et al., 2012). Patients would suffer from loss of sensibility in the proximal two-fifths of the palm and discomfort, but more importantly direct injury to the nerve can result in painful neuromas. The nerve can be also entrapped as it passes through its own fibrous tunnel. Naff et al. (1993) suggested that in cases where neuroma formation due to direct injury to the PCBMN cannot be validated; symptoms can be relieved by decompression of the nerve rather than completely sectioning it. Cases where PCBMN entrapment were identified were due to continuous pressure at the base of the wrist, an abnormal palmaris longus that causes pressure upon the nerve, the presence of cysts or ganglia (Buckmiller and Rickard, 1987; De Smet, 1998), or entrapment within the antebrachial fascia (Semer et al., 1996). Patients would suffer from symptoms including localized pain and numbness at the base of the thenar eminence (Nakamichi and Tachibana, 2000). Al-Qattan (1997) described six zones where the PCBMN is in danger of entrapment. It can be compressed at its origin from the main median nerve trunk by masses or anomalous tendons; by the flexor carpi superficialis fascia at the site it emerges at its lateral margin; at its course close to the medial margin of flexor carpi radialis tendon by

tendinitis or ganglia arising from the flexor carpi radialis sheath; at its tunnel by ganglia or an atypical palmaris longus; at the insertion of palmaris longus into the palmar fascia in cases where the nerve pierces the distal part of the muscle tendon and at the subcutaneous layer by fibrous and scar tissue formed after carpal tunnel release.

PCBMN entrapment can occur concomitant with compression of the main median nerve trunk in carpal tunnel syndrome. Due to the overlap between the sensory innervation of the PCBMN and the median nerve, it can be difficult to distinguish the abnormalities caused by PCBMN entrapment from that caused by median nerve compression in carpal tunnel syndrome (Wada et al., 2002; Imai et al., 2004). Imai et al. (2004) suggested that the PCBMN entrapment can be assessed objectively by analysing sensory nerve action potentials regardless of the presence of carpal tunnel syndrome. It is unclear however, if PCBMN entrapment in these cases is independent or linked to the median nerve neuropathy. Nonetheless, it is worthwhile evaluating for PCBMN entrapment in all cases of carpal tunnel syndrome.

The large nerve branches can be easily identified and retracted, but smaller branches will be difficult to preserve in open carpal tunnel release. In cases of a large branch injury, neuromas formed will present with easily recognizable symptoms. However, the smaller nerve branches can also be injured as they cross the TCL. Neuromas in this case will not be formed but the severed fibres could be trapped in the scarred tissue and cause unpleasant temporary or prolonged dysesthesia (Taleisnik, 1973). According to Ahčan et al. (2003) there are at least 2700 axons in the palmar triangle surrounding the incision used for carpal tunnel release, once injured can multiply by 10 folds creating 30,000 nerve sprouts. These nerve sprouts may be trapped within the scar tissue and cause scar discomfort and pain (Ahčan et al., 2003). After anatomic, histological and immunofluorescence studies, DaSilva et al. (1996) reported that the TCL is composed of

two layers. The superficial layer consists of loose connective tissue while the deep layer is composed of thick fibroblasts and collagen. The study demonstrated that only the superficial layer had unmyelinated nerve fibre endings whereas no fibres were detected in the deeper thick layers (DaSilva et al., 1996). Such studies suggest that small nerve endings will be injured during carpal tunnel release and will lead to inescapable postoperative pillar pain and scar discomfort (DaSilva et al., 1996; Martin et al., 1996; Ahčan et al., 2003). Moreover, in endoscopic release the main trunk of the PCBMN is in jeopardy at the proximal incision, smaller branches cannot be preserved as they pass through or superficial to the ligament and repeated passage of the endoscopic knife will further damage the small PCBMN branches. Postoperative pain may be explained by direct injury of the nerve fibres due to incisional trauma or indirectly by coagulation, suturing, or channel preparations during endoscopic procedures. Scar tenderness can be explained by nerve ending entrapment in scar tissue. The injured nerve endings develop sensitivity towards mechanical, thermal and chemical stimulation (Ahčan et al., 2002; Ahčan et al., 2003).

Since Phalen et al. (1950) described the diagnosis and the suggested sectioning of the TCL as a treatment; the surgical treatment of carpal tunnel syndrome has rapidly evolved to include many recommendations, techniques and approaches for placing the incision. Transverse incisions at the TCL can injure the main nerve trunk at the proximal wrist. Longitudinal incisions are advocated in many reports; however, there is debate where the incision should be placed (Table 1.2.). Gerritsen et al. (2001) reviewed fourteen studies to compare various surgical techniques in carpal tunnel release. The study reported that the standard open technique seems to offer better post-operative prognosis than endoscopic technique or open technique with a new incision.

Endoscopic carpal tunnel release had more neural complications but shorter recovery time (Gerritsen et al., 2001).

Table 1.2: Examples of different incision suggestions for the treatment of carpal tunnel syndrome as reported in the literature.

No	Reference	Method
1.	Phalen et al. (1950)	The first to suggest the surgical release of the transverse carpal ligament.
2.	Taleisnik (1973)	A longitudinal incision on the medial side of the axis of the ray of the ring finger.
3.	Ariyan and Watson (1977)	A longitudinal incision in the palm until the wrist crease.
4.	Engber and Gmeiner (1980)	A longitudinal incision in line with the ring finger ray axis.
5.	Chow (1989)	Endoscopic release of carpal tunnel syndrome.
6.	Hobbs et al. (1990)	A longitudinal incision 10 mm medial to the axis of the 3rd metacarpal (in line of the ring finger axis).
7.	Tsai et al. (1995)	One portal endoscopic technique with the aid of a custom-made glass tube and a meniscus knife.
8.	DaSilva et al. (1996)	A longitudinal incision along the axis of the ring finger.
9.	Watchmaker et al. (1996)	A longitudinal incision 5 mm ulnar to the interthenar depression.
10.	Serra et al. (1997)	Short incision 20 mm long in the midpalm in line with the third ray proximal to Kaplan's cardinal line.
11.	Matloub et al. (1998)	A longitudinal incision 10-15 mm medial and parallel to the thenar crease, stopping 15 mm distal to the wrist crease.
		Two small incisions: ▪ The first: 20 mm from the centre of the palm extending proximally and perpendicular to the wrist crease. ▪ The second: an incision on the medial side of palmaris longus tendon proximal to the wrist crease.

No	Reference	Method
12.	Avci and Sayli (2000)	Release by Knifelight inserted through a short 20 mm longitudinal incision in line with the ring finger and proximal to a transverse line crossing from the medial border of an abducted thumb.
13.	Cheung et al. (2004)	A longitudinal incision 10 mm medial to palmaris longus if present, if absent an incision as described by Taleisnik (1973) is used.
14.	Tubbs et al. (2005)	Dorsal incision between the proximal fourth and fifth metacarpals.
15.	Tubbs et al. (2011)	A longitudinal incision along a line through the middle of the ring finger.
16.	De la Fuente et al. (2013)	Sectioning the TCL by a "U"-shaped surgical probe and "V"-shaped scalpel with the aid of ultrasound. The probes are inserted through a 15 mm transverse incision starting at the palmaris longus tendon and coursing medially at the level of the distal wrist crease.

Many open techniques have been described to approach the carpal tunnel with minimal damage to the PCBMN. Taleisnik (1973) recommends the incision to be on the ulnar side of the axis of the ring finger at the level of the heel of the hand. However, such an approach will put the palmar branch of the ulnar nerve in danger of injury (Tubbs et al., 2011). Moreover, the study did not specify how the axis is determined. Watchmaker et al. (1996) were the first to show the variability of surface landmarks such as the ring finger axis ray and the palmar creases, in different anatomic positions of the hand. Their results confirmed that the axis of the ring finger differs significantly during flexion and extension. The PCBMN coursed 9 mm lateral to the axis in extension, whereas it coursed medial to the axis during flexion. Moreover, the axis of the ring finger varies depending on whether the fingers were adducted, abducted or held in-between (Watchmaker et al., 1996). Engber and Gmeiner (1980) investigated the palmar cutaneous branch of the ulnar nerve in 21 cadaveric hands and suggested that an

incision in line with the ring finger axis will limit injury to both the palmar cutaneous branch of the ulnar nerve and the PCBMN. Agreeing with Engber and Gmeiner (1980), Hobbs et al. (1990) also suggested that incisions are made 10 mm ulnar to the axis of the middle finger, which corresponds to an incision in line with the ring finger axis. Furthermore, Siegel et al. (1993) recommended the carpal tunnel release incision is in line with the axis of the ring finger avoiding injury to both PCBMN and the palmar cutaneous branch of the ulnar nerve. However, the authors emphasised that such an approach will preserve major neurovascular structures, but will not ensure complete avoidance of injury as there is no substitute for a wide meticulous exposure (Siegel et al., 1993). Martin et al. (1996) studied the cutaneous nerves in the palm of 25 fresh cadavers and reported that an incision in the line of the ring finger axis will injure the PCBMN in 3/25 cases and will injure cutaneous branches from the ulnar nerve in 16/25 cases. The tenderness often reported post-surgically by patients treated for carpal tunnel syndrome is most probably due to injury to small cutaneous nerves originating from the ulnar nerve rather than from PCBMN (Martin et al., 1996). However, Ahčan et al. (2003) investigated the subcutaneous nerve fibres crossing an incision line with the lateral border of the ring finger in 15 specimens and reported that fibres from the PCBMN are endangered in 10/15 specimens but did not mention the subcutaneous branches from the ulnar nerve.

DaSilva et al. (1996) studied the PCBMN in 12 fresh upper limbs and reported that in 7 cases the nerve divided into three branches as it passed into the proximal palm. The intermediate branch was found directly on the axis of the ring finger. Interestingly, the study also reported that the larger branches of the PCBMN are found superficial to the palmar aponeurosis and terminate in the skin and only the smaller deeper branches were found to terminate in the superficial layer of the carpal ligament (DaSilva et al.,

1996). Other studies suggested using the inter-thenar depression as a safe landmark for carpal tunnel release (Watchmaker et al., 1996). However, this approach will endanger the palmar cutaneous branch of the ulnar nerve. As the PCBMN enters its tunnel 3 mm medial to the thenar crease, a thenar incision would most likely injure the nerve or its branches (Ahčan et al., 2003). In an interesting Chinese study, Cheung et al. (2004) suggested using palmaris longus as a landmark for carpal tunnel release incision. The study recommends an incision 10 mm medial to the palmaris longus if present and making an incision on the ulnar side of the ring finger axis as described by Taleisnik (1973) if absent. Ozcanli et al. (2010) recommended the area between the superficial palmar arch and the distal region of the PCBMN that extends 39.2±18.6 mm distal to the distal WC as a safe zone for carpal tunnel release incision.

1.4.1.2. Digital nerves

The median nerve becomes superficial 50 mm proximal to the wrist. It courses deep to palmaris longus (if present), medial to flexor carpi radialis and flexor pollicis longus. It then enters the carpal tunnel superficial to flexor digitorm superficialis and deep to the TCL.

The carpal tunnel is a passageway between the forearm and wrist. Its roof is the TCL, the lateral wall contains the scaphoid and trapezium, the medial wall contains the hook of the hamate and pisiform, and its floor is formed by the palmar radiocarpal ligaments. The median nerve passes through the tunnel superficial to all the finger and thumb flexor tendons as one trunk immediately deep to the TCL.

Usually the recurrent motor branch of the median nerve leaves from the anterolateral surface at the distal margin of the TCL to supply the thenar muscles. After passing through the carpal tunnel, the median nerve gives three common digital nerves (CDN)

at the junction between the middle and distal third of the metacarpal shafts (Doyle and Botte, 2003).

The common digital nerves pass deep to the superficial palmar arch and the common digital arteries. Dividing into proper digital nerves (PDN) at the level of the metacarpal necks and continue superficial to the digital arteries. Bas and Kleinert (1999) investigated the branching point of the dorsal proper digital nerves and found them to be proximal to the A1 pulley zone (a zone spanning 20 mm proximal to the proximal digital crease to 10 mm distal to the proximal digital crease) in 62% of cases, which is more proximal than previously reported. The first common digital branch divides into three proper digital nerves after giving a motor branch to the first lumbrical. The first common digital nerve supplies the palmar surface of the thumb and lateral side of the index finger. The second common palmar digital nerve gives a motor branch to the second lumbrical before it courses distally and further divides to supply the medial side of the index finger and lateral side of the middle finger. The third common digital nerve can give a motor branch to the third lumbrical and continues distally to divide into proper digital nerves to the medial side of the middle finger and lateral side of the ring finger. It is not uncommon for the third common digital nerve to communicate with the fourth common digital nerve of the ulnar nerve (Figure 1.11).

Jolley et al. (1997) investigated the first common digital nerve in 79 adult cadaver hands and observed three patterns (Figure 1.12):

Type I: A PDN supplying the lateral side of the thumb and a CDN that further divides to supply the medial side of the thumb and lateral side of the index finger (Figure 1.12: A).

Type II: A trifurcation to produce three PDNs to supply the thumb and lateral side of the index finger (Figure 1.12: B).

Type III: A CDN that further divided to supply the medial and lateral sides of the thumb and a PDN that continued distally to supply the index finger (Figure 1.12: C).

These three types were found in 69%, 25%, and 6% of hands respectively (Jolley et al., 1997).

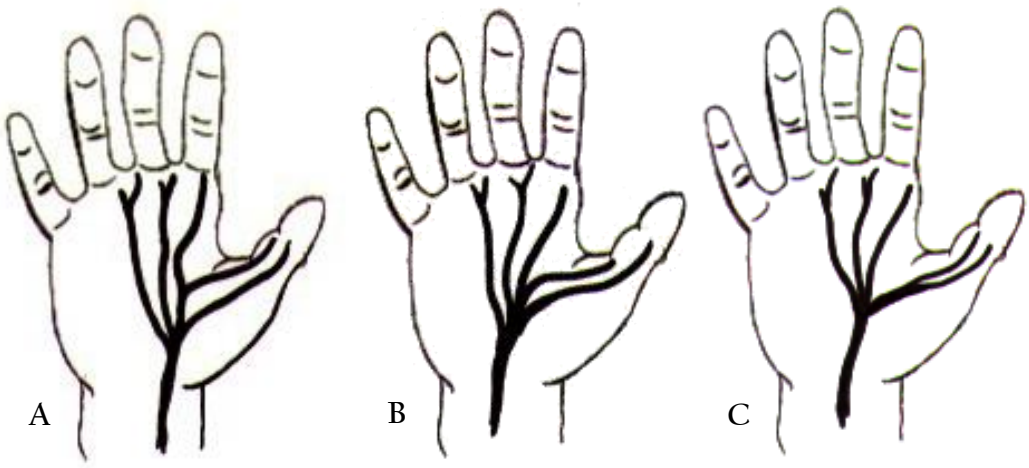

Figure 1.12: Schematic drawings of the branching patterns of the first common digital nerve. (A) Type I; (B) Type II; (C) Type III (Doyle and Botte, 2003; figure 10.3, page 571).

The median nerve can divide proximal to the distal edge of the carpal tunnel usually into a larger lateral and a smaller medial component in the forearm or at the level of the wrist (Eiken et al., 1971). Jeon et al. (2002) reported a case of high division of the third CDN at the level of the wrist crease discovered during endoscopic release of the carpal tunnel. Eiken et al. (1971) reported three cases of high division of the median nerve, as high as the level of the middle third of the forearm, and emphasized that care should be

taken when removing peritendinous tissue as it may mask the 2nd division of the median nerve. High bifurcation of the median nerve is usually accompanied by a median artery coursing between the two divisions. However, in their study, Berry et al. (2003) reported a high bifurcation of the median nerve with each division travelling in a separate compartment of the carpal tunnel. Such high division of the median nerve is considered a rare variation. Stančić et al. (1995) found it only once after exploring the median nerve in 100 cases. In a Korean study, Ahn et al. (2000) reported one case (0.3%) of high division of the median nerve after investigating 354 cases of elective carpal tunnel release. In another study conducted on 60 Iranian cadaveric hands, Alizadeh et al. (2006) reported high bifurcation of the median nerve in 5 cases (8.3%). Such variations can put the median nerve at risk of injury during carpal tunnel release, flexor tendosynovectomy or tendon repair in the carpal tunnel.

Common digital nerves can also divide into more than two proper digital nerves. Kuvat and Tagil (2009) reported a case of duplication of the proper digital nerves in the index finger. The patient had two medial and two lateral proper digital nerves on each side of the index finger (Kuvat and Tagil, 2009).

1.2.2. Ulnar nerve

The ulnar nerve originates from the medial cord of the brachial plexus carrying fibres from the anterior rami of C7, C8 and T1. It courses in the axilla medial to the axillary artery and continues distally in the arm to pierce the medial intramuscular septum 80 mm proximal to the medial epicondyle and passes to the posterior compartment of the arm. It enters the anterior compartment of the forearm by passing through the cubital tunnel where it usually gives three main branches: a motor branch to the medial part of

flexor digitorum profundus to the little and ring fingers, a palmar cutaneous branch and the dorsal branch of the ulnar nerve (Doyle and Botte, 2003).

At the level of the wrist, the ulnar nerve and artery pass through Guyon's canal, first described by Guyon in 1861. The canal is bounded between the pisiform and the hook of the hamate, proximally covered by the TCL and distally by palmaris brevis. The superficial branch of the ulnar nerve supplies the skin of the little finger and medial side of the ring finger. The artery usually passes lateral to the nerve and contributes to the formation of the superficial palmar arch. The ulnar nerve and artery pass lateral to the pisiform, superficial to the flexor retinaculum, and deep to the superficial carpal ligament. The canal is divided into three zones: Zone I of the ulnar tunnel (Guyon's canal) extends for about 30 mm from the transverse proximal edge of the TCL to the bifurcation of the nerve into deep and superficial branches about 10 mm distal to the pisiform, at about the level of the hamate. Zone II includes the motor division of the UN and Zone III contains the superficial branch of the UN distal to the UN bifurcation. Table 1.3 shows the boundaries and the content of each zone of Guyon's canal.

The superficial branch of the ulnar nerve courses distally over abductor and flexor digiti minimi, gives a motor branch to palmaris brevis, divides into a PDN to the medial side of the little finger and the fourth CDN that further divides at the level of the metacarpal shafts to supply the lateral side of the little finger and the medial side of the ring finger (Doyle and Botte, 2003). The superficial branch of the ulnar nerve was reported to supply the little finger and both sides of the ring finger in some cases (Bonnel and Vila, 1985). The superficial branch lies deep to the superficial palmar arch but superficial to the flexor tendons.

Table 1.3: Zones of Guyon's canal and their boundaries

	Zone I	**Zone II**	**Zone III**
Content	Ulnar nerve before bifurcation into deep and superficial branches	Deep motor division	Superficial division
Floor	Tendons of flexor digitorum profundus and medial portion of the transverse carpal ligament	Pisohamate and pisometacarpal ligament	Pisometacarpal ligament and capsule of the triquetrohamate joint and zone II
Lateral	Distal fibres of palmar carpal ligament merging with fibres of transverse carpal ligament	Transverse carpal ligament	Zone II
Medial	Pisiform and tendon of flexor carpi ulnaris	Abductor digiti minimi	Abductor digiti minimi
Roof	Palmaris brevis	Palmaris brevis and the superficial branch of the ulnar nerve	Palmaris brevis

Bonnel and Vila (1985) investigated the ulnar nerve in 50 adult cadaver hands and observed two patterns of division in Zone I.

Type A: The ulnar nerve bifurcated into one sensory branch and one motor branch.

Type B: The ulnar nerve trifurcated into two sensory branches and one motor branch.

Type A was found in 78% and type B in 22% of the cases investigated (Bonnel and Vila, 1985). Similarly, Lindsey and Watumull (1996) investigated the division patterns of the ulnar nerve at Guyon's canal in 31 fresh adult cadaver hands and reported comparable incidences for types A and B as 80.6% and 19.4% respectively.

Compression of the ulnar nerve in Guyon's canal can occur due to trauma, fractures, ulnar artery aneurysm, lipomas, ganglion formations and muscle variations. Injury to the ulnar nerve and artery can also occur during endoscopic decompression of the carpal tunnel.

Olave et al. (1997) described a variation of the ulnar nerve dividing into medial and lateral branches high in the forearm. The medial branch ran on the medial side of the artery and gave the deep division of the ulnar nerve and proper palmar digital nerve to the medial side of the little finger. The lateral branch rejoined the medial branch 35.0 mm distal to the wrist crease and gave off the palmar digital branch to the 4th interosseous space (Olave et al., 1997). Such a variation puts the lateral branch at risk during endoscopic carpal tunnel release.

Bozkurt et al. (2004) described another variation in the course of the ulnar nerve in the palm where the PDN to the medial side of the little finger was formed by two branches from the superficial division of the UN and a third branch from the deep motor branch piercing the abductor digiti minimi. Such a variation could lead to unexplained sensory disturbances to the medial side of the ring finger if the deep motor branch was compressed or injured (Bozkurt et al., 2004).

Kaplan (1963) was the first to describe a connection between the dorsal branch of the ulnar nerve (DBUN) and the superficial branch of the ulnar nerve: a similar case was reported by Bonnel and Vila (1985). Hoogbergen and Kauer (1992) reported a case of Kaplan anastomosis where the DBUN joined the deep branch of the ulnar nerve, whereas Paraskevas et al. (2008) reported another case where the DBUN connected to the main trunk of the ulnar nerve before its bifurcation.

McCarthy and Nalebuff (1980) reported a case where a branch from the DBUN innervated the little finger without joining the superficial branch of the ulnar nerve as described by Kaplan. Bozkurt et al. (2002) described a similar variation where the medial side of the little finger was innervated by the dorsal branch of the ulnar nerve, while the superficial branch of the ulnar nerve continued as a CDN to supply the fourth web-space. Similarly, Konig et al. (1994) described two cases of the 23 specimens investigated where the little finger was innervated by a branch from the DBUN without passing through Guyon's canal.

The Kaplan anastomosis and the DBUN branch to innervate the little finger are both at risk during surgical procedures on the ulnar side of the wrist, as in Guyon's canal exploration and flexor carpi ulnaris surgery, or in cases of pisiform fractures. Injury to the Kaplan anastomosis can lead to motor and sensory disturbances depending on the merger point of the nerve (PDN to the medial side of the little finger, superficial branch of the UN, motor division of the UN, main trunk of the UN). The presence of other innervation patterns can provide misleading physiological results and complicate surgical procedures.

1.4.2. Palmar communication between the median and the ulnar nerve

First described by Berrettini in 1741, the communicating branch between the ulnar and median nerves usually connects between the third and fourth CDNs and passes deep to the superficial palmar arch, distal to the TCL. It is also referred to as the ramus communicans, or ramus anastomoticus, or nerve of Berrettini. Reports differ in the incidence rate of communicating branches (CB) ranging between 4% and 100%. However, with incidence rates as high as 100% Bonnel and Vila (1985), 95% Ferrari and

Gilbert (1991), 94% Don Griot et al. (2000), and 80% Meals and Shaner (1983), the CB should be considered a normal anatomical finding rather than an anomaly.

Dogan et al. (2010) investigated the CB in the hands of 200 spontaneously aborted fetuses and found the CB in 29.5%. The authors explained the low incidence rate to be the result of racial differences and the gestational age as more than 80% of the CB were found in fetuses more than 20 weeks old (Dogan et al., 2010). Table 1.4 summarizes the major studies investigating the palmar CB between the MN and UN reported in the literature.

Table 1.4: The major anatomical studies investigating the incidence and pattern of the palmar communication branch between the median nerve and the ulnar nerve

NO.	Reference	No. Cadavers	Incidence	Classification	Pattern	
1.	Meals and Shaner, 1983	50 adult cadaver palms (35 frozen and 15 formalin fixed cadavers)	40 (80%)	Meals and Shaner	38 (95%)	The communication branch (CB) branched from the 4th common digital nerve (CDN) (ulnar) to the 3rd CDN (median) 23/38 fibres entered the lateral side of the ring finger 10/38 fibres entered the lateral side of the ring finger and medial side of the middle finger 5/38 final destination of the fibres could not be determined
					1 (2.5%)	The CB branched from the 3rd CDN (median) to the 4th CDN (ulnar)
					1 (2.5%)	Both 3rd and 4th CDN gave a CB that merged and continued in the midpalm
2.	Bonnel and Vila, 1985	50 formalin fixed adult cadaver hands	50 (100%)	Bonnel and Vila	46 (92%)	The CB branched from the 4th CDN (ulnar) to the 3rd CDN (median)
					4 (8%)	Both 3rd and 4th CDNs gave a CB that merged into a proper digital nerve (PDN) to the lateral side of the ring finger
3.	Ferrari and Gilbert, 1991	50 adult cadaver hands	45 (90%)	Ferrari and Gilbert	22 (48.9%)	The CB coursed obliquely from the 4th CDN (ulnar) to the 3rd CDN (median), the distance between the origin of the CB and the distal margin of the transverse carpal ligament was more than 4 mm and the origin angle is less than 54°.
					11 (24.4%)	The CB courses from the 4th CDN (ulnar) to the 3rd CDN (median) parallel to the distal margin of transverse carpal ligament, the distance between the origin of the CB and the distal margin of transverse carpal ligament was less than 4 mm with a right angle to the ulnar nerve.

NO.	Reference	No. Cadavers	Incidence	Classification	Pattern	
					10 (22.2%)	The CB coursed obliquely from the 4th CDN (ulnar) to the 3rd CDN (median), originated below the distal margin of the transverse carpal ligament, the origin angle is very acute.
					2 (4.4%)	The CB branched from the 3rd CDN (median) to the 4th CDN (ulnar)
4.	Bas and Kleinert, 1999	30 fresh adult cadaver palms	20 (67%)	Modified Meals and Shaner	11 (55%)	The CB branched from the 4th CDN (ulnar) to the 3rd CDN (median)
					4 (20%)	The CB branched from the 3rd CDN (median) to the 4th CDN (ulnar)
					5 (25%)	Multiple CBs coursing in both directions (diffuse interconnections)
5.	Stančić et al., 1999	100 fresh adult cadaver hands	81 (81%)	Ferrari and Gilbert	12 (14.8%)	The CB coursed obliquely from the 4th CDN (ulnar) to the 3rd CDN (median), the distance between the origin of the CB and the distal margin of the transverse carpal ligament was more than 4mm and the origin angle is less than 54°.
					16 (19.8%)	The CB courses from the 4th CDN (ulnar) to the 3rd CDN (median) parallel to the distal margin of the transverse carpal ligament, the distance between the origin of the CB and the distal margin of the transverse carpal ligament was less than 4 mm with a right angle to the ulnar nerve.
					53 (65.4%)	The CB coursed obliquely from the 4th CDN (ulnar) to the 3rd CDN (median), originated below the distal margin of the transverse carpal ligament, the origin angle is very acute.
					0 (0)	The CB branched from the 3rd CDN (median) to the 4th CDN (ulnar)
6.	Olave et al. 2001	56 formalin fixed adult Brazilian cadaveric hands	54 (96.4%)	No classification used, only observations were reported	45 (83.3%)	Originated from the 4^{th} CDN (ulnar) and inserted into the 3^{rd} CDN (median) distally
					8 (14.8%)	Originated from the 3^{rd} CDN (median) and inserted into the 4^{th} CDN (ulnar) distally

NO.	Reference	No. Cadavers	Incidence	Classification	Pattern	
					1 (1.9%)	Two branches one originated from the 4th CDN (ulnar) and inserted into the 3rd CDN (median) distally and the other originated from the 3rd CDN (median) and inserted into the 4th CDN (ulnar) distally crossing each other.
7.	Don Griot et al. 2000	53 formalin fixed from adult cadaver hands	50 (94%)	Modified Meals and Shaner	44 (88%)	The CB branched from the 4th CDN (ulnar) to the 3rd CDN (median)
					4 (8%)	The CB courses perpendicularly between the 3rd and 4th CDNs
					2 (4%)	The CB branched from the 3rd CDN (median) to the 4th CDN (ulnar)
8.	Griot et al. 2002	26 formalin fixed from adult cadaver palms purposely selected with CB	-	Modified Meals and Shaner	21 (80.8%)	The CB branched from the 4th CDN (ulnar) to the 3rd CDN (median) 11/21 fibres joined the lateral side of the ring finger 7/21 fibres entered the lateral side of the ring finger and medial side of the middle finger 3/21 final destination of the fibres could not be determined
					2 (7.7%)	The CB branched from the 3rd CDN (median) to the 4th CDN (ulnar) 1/2 fibres joined the medial side of the ring finger 1/2 fibres joined the medial side of the ring finger and lateral side of the little finger
					3 (11.5%)	The CB courses perpendicularly between 3rd and 4th CDNs 2/3 both 3rd and 4th CDN gave a CB that merged and continued in the midpalm 1/2 multiple CBs coursing in both directions (diffuse interconnections)

NO.	Reference	No. Cadavers	Incidence	Classification	Pattern	
9.	Kawashima et al, 2004	169 embalmed cadaveric hands	109 (74.5%)	Kawashima et al.	24 (14.2%)	Type A: CB branched from the 3rd CDN (median) to the 4th CDN (ulnar)
					5 (3%)	Type B: multiple CBs coursing in both directions (diffuse interconnections)
					60 (35.5%)	Type C: No CB
					1 (0.6%)	Type D: CB branched from 4th CDN (ulnar) to the lateral side of the ring finger
					79 (46.7%)	Type E: The CB branched from the 4th CDN (ulnar) to the 3rd CDN (median)
10.	Biafora & Gonzalez, (2007)	50 formalin fixed adult cadaveric hands	37 (74%)	Meals and Shaner	34 (91.9%)	The CB branches from the ulnar nerve and inserts into the median nerve distally 2/34 additional branch joining the proper digital nerve of the lateral side of the ring finger 1/34 a branch arose from the CB to join the proper digital branch to the ulnar side of the middle finger
					3 (8.1%)	The CB branches from the median nerve and attaches to the ulnar nerve distally
11.	Loukas et al., 2007	200 formalin fixed adult cadaveric hands	170 (85%)	Modified Meals and Shaner	143 (84.1%)	The CB branched from the 4th CDN (ulnar) to the 3rd CDN (median)
					12 (7.1%)	The CB branched from the 3rd CDN (median) to the 4th CDN (ulnar)
					6 (3.5%)	The CB courses perpendicularly between 3rd and 4th CDNs
					9 (5.3%)	Multiple CBs coursing in both directions (diffuse interconnections)

NO.	Reference	No. Cadavers	Incidence	Classification	Pattern	
12.	Tagil et al., 2007	30 embalmed adult cadavers palms	18 (60%)	Modified Meals and Shaner	12 (66.7%)	The CB branched from the 4th CDN (ulnar) to the 3rd CDN (median)
					1 (5.5%)	The CB branched from the 3rd CDN (median) to the 4th CDN (ulnar)
					2 (11.1%)	The CB courses perpendicularly between 3rd and 4th CDNs
					3 (16.7%)	Multiple CBs coursing in both directions (diffuse interconnections)
13.	Dogan et al., 2010	200 from spontaneously aborted fetuses	59 (29.5%)	Modified Kawashima et al. 2004, an additional type was added (type F)	10 (5%)	Type A: CB branched from the 3rd CDN (median) to the 4th CDN (ulnar)
					3 (1.5%)	Type B: multiple CBs coursing in both directions (diffuse interconnections)
					141 (70.5%)	Type C: No CB
					2 (1%)	Type D: CB branched from 4th CDN (ulnar) to the lateral side of the ring finger
					42 (21%)	Type E: CB branched from the 4th CDN (ulnar) to the 3rd CDN (median)
					2 (1%)	Type F: Both 3rd and 4th CDN gave a CB that merged and continued in the midpalm supplying the lateral ring finger

Many classification systems have been suggested in the literature. Meals and Shaner (1983) were the first to classify the communicating branch according to its origin and insertion point into three types:

Type I: The CB passed from the 4th CDN (ulnar) to the 3rd CDN (median).

Type II: The CB passed from the 3rd CDN (median) to the 4th CDN (ulnar).

Type III: Both the 3rd and 4th CDNs gave a branch that merged and continued in the midpalm.

They further subdivided Type I into three subtypes according to the final destination of the CB fibres (Meals and Shaner, 1983). However, they have not provided any morphometric data to localize the CB and this limits the surgical use of their results. Bonnel and Vila (1985) found the CB in all 50 cases investigated: they reported two types of CB previously described by Meals and Shaner (1983) (Table 1.4); however, they found that in the 4 cases of Type III, the fibres formed a PDN that supplied the lateral side of the ring finger. Bonnel and Vila (1985) were also the first to use morphometric data to localize the CB; however, their data was limited to the origin of the CB. Ferrari and Gilbert (1991) suggested another classification system based on the relationship of the CB to the TCL and angle of origin (Figure 1.13). Their four groups are:

Group I: The CB coursed obliquely from the 4th CDN (ulnar) to the 3rd CDN (median), the distance between the origin of the CB and the distal margin of the TCL was more than 4 mm and the origin angle less than 54° (Figure 1.13: 1).

Group II: The CB courses from the 4th CDN (ulnar) to the 3rd CDN (median) parallel to the distal margin of the TCL, the distance between the origin of the CB and the distal margin of the TCL was less than 4 mm with a right angle to the ulnar nerve (Figure 1.13: 2).

Group III: The CB coursed obliquely from the 4th CDN (ulnar) to the 3rd CDN (median), originated below the distal margin of the TCL, the origin angle is very acute (Figure 1.13: 3).

Group IV: The CB branched from the 3rd CDN (median) to the 4th CDN (ulnar) (Figure 1.13: 4).

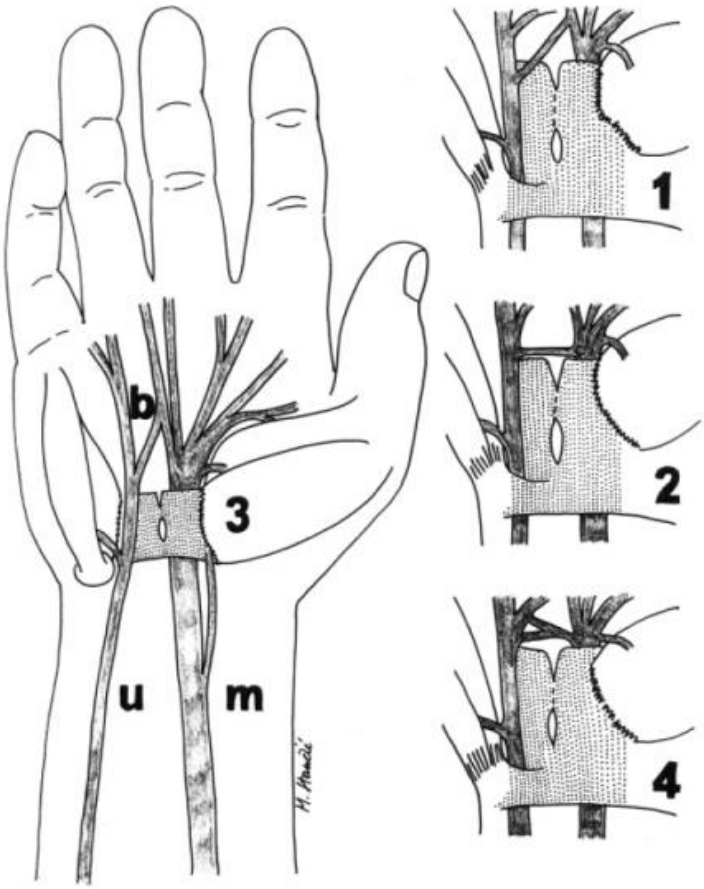

Figure 1.13: Schematic drawings of the branching patterns of the palmar communicating branch according to Ferrari and Gilbert classification. (1) Group I; (2) Group II; (3) Group III; (4) Group IV; u, ulnar nerve; m, median nerve; b, communicating branch (Stančić et al., 1999).

Ferrari and Gilbert (1991) also described a triangular zone in the palm where the CB is always found. This zone is bounded distally by the proximal transverse crease, laterally by the longitudinal crease between the thenar and hypothenar eminence and extends medially to the middle half of the hypothenar eminence (Ferrari and Gilbert, 1991). This area however, is not based on morphometric measurements, but rather on observation (Figure 1.14).

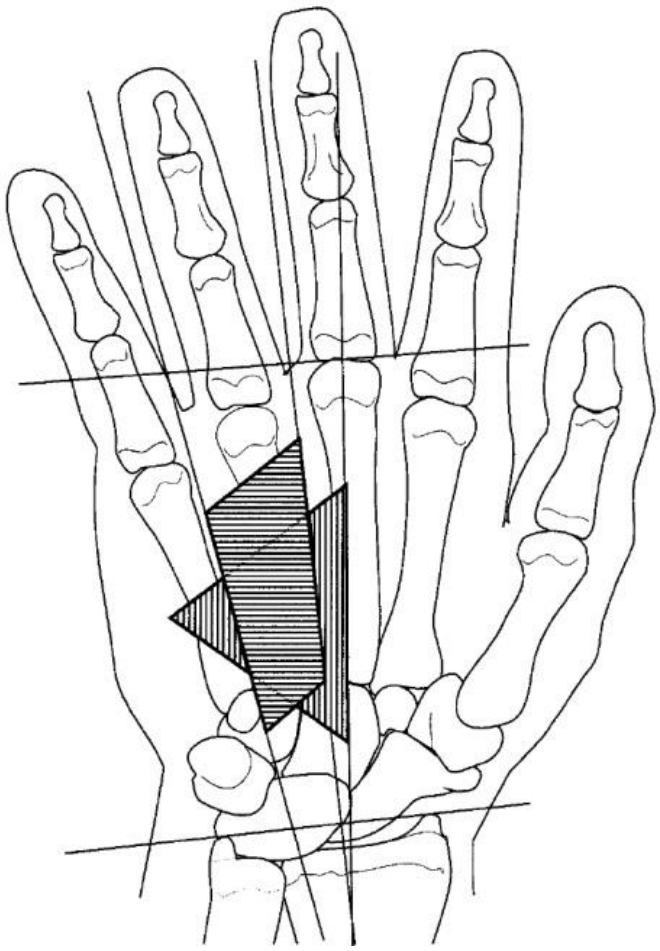

Figure 1.14: Risk area where the palmar communicating branch is most likely to be found as described by Ferrari and Gilbert (1991) (Triangular area) and Don Griot et al. (2000) (trapezoidal area) (Don Griot et al., 2000).

Although some might consider the Ferrari and Gilbert (1991) classification system to be arbitrary and confusing, Stančić et al. (1999) followed it in their investigation of 100 adult cadaver hands. Interestingly, they reported different distribution and incidence rates than did Ferrari and Gilbert (1991). (Table 1.4).

Bas and Kleinert (1999) published a detailed study of the nerve's distribution in the hand and digits. They modified the Meals and Shaner (1983) classification system by adding a new type where the palm has multiple CBs coursing in both directions between the MN and UN (diffuse interconnection) (Figure 1.15: 4). In 2000, Don Griot et al. described a new type where the CB travels perpendicularly between the 3rd and 4th CDNs (Figure 1.15: 3). Then in another study, they further investigated 26 of the palms with a CB and modified the Meals and Shaner (1983) classification system by adding several subtypes based on the final destination of the fibres in the CBs (Griot et al., 2002) (Table 1.4).

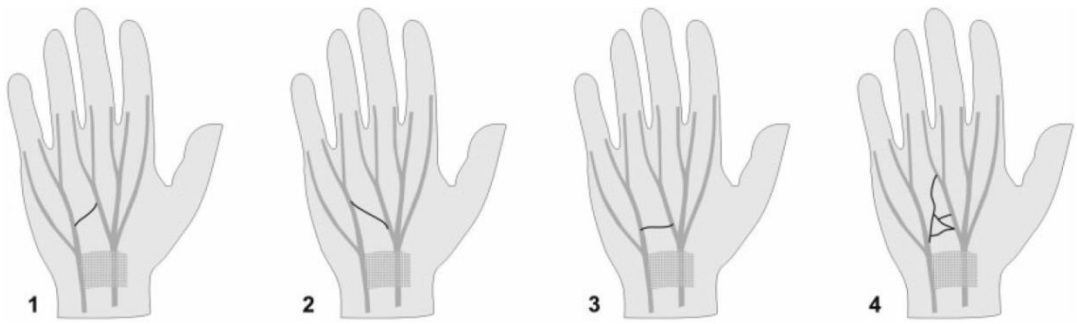

Figure 1.15: Schematic drawing of some of the branching patterns of the palmar communicating branch (CB) between the median and ulnar nerve as described in the literature. (1) The CB originate from the fourth common digital nerve (CDN) proximally and joins the third CDN distally; (2) the CB originates from the third CDN proximally and joins the fourth CDN distally; (3) The CB travels transversally between the third and fourth CDNs; (4) The CB is formed by multiple branches from both the third and fourth CDNs (Tagiel et al., 2007).

Don Griot et al. (2000) used morphometric measurements to localize the CB and described a rectangular risk zone where the CB would be in danger of injury during surgical procedures. Their risk zone corresponds to the morphometric parameters of the proximal origin and distal insertion of the CBs. The proximal origin of the CB was localized 22% to 69% of the distance between the BSL and the 3rd MCP joint, whereas the distal insertion was found 32% to 81% of the same distance (Don Griot et al., 2000). The previously indicated danger zone extends more distally and less medially and laterally compared to that described by Ferrari and Gilbert (1991) (Figure 1.14).

In another study conducted on 56 Brazilian cadaveric hands, Olave et al. (2001) mapped the location of the neurovascular structures in the palm in relation to the wrist crease and the TCL. The study found the palmar CB in 54 (96.4%) cases, in the majority of which (45/54, 83.3%) the CB originated from the 4th CDN (ulnar nerve) at a mean distance of 33.9±5.5 mm and 30.2±8.2 mm to the distal WC in right and left male hands respectively; while it emerged at 28.5±6.2 mm and 27.1.33 mm to the distal WC in right and left female hands respectively. The CB inserted into the 3rd CDN (median nerve) distally at 43.6±6.9 mm and 40.2±6.2 mm to the distal WC in right and left male hands respectively; while it joined at 40.7±7.8 mm and 34.4±1.6 mm to the distal WC in right and left female hands respectively. The study also reported that the CB was found 6.2±3.7 mm and 5.3±3.7 mm distal to the TCL at the axial line of the 4th metacarpal bone in male and female right hands respectively; while it was found 5.1±2.8 mm and 4.0±1.9 mm distal to the TCL at the axial line of the 4th metacarpal bone in male and female left hands respectively (Olave et al., 2001). Although the study presents significant results, the data does not account for the relative position of the CB but rather to the exact distances between structures.

Loukas et al. (2007) studied the palmar CB between the MN and UN in 200 adult cadavers and by using a modified Meals and Shaner (1983) classification system, were able to group the CB into four types and then further subdivide them into 15 subtypes. The authors described a risk area similar to the one suggested by Don Griot et al. (2000) (Figure 1.16). By using the midpoint of the CB as a reference point, they indicated that the danger zone extends between 35% and 62% of the distance between the BSL and the 3rd MCP joint, but also mention that the CB was found outside this zone in 27% of cases (Loukas et al., 2007).

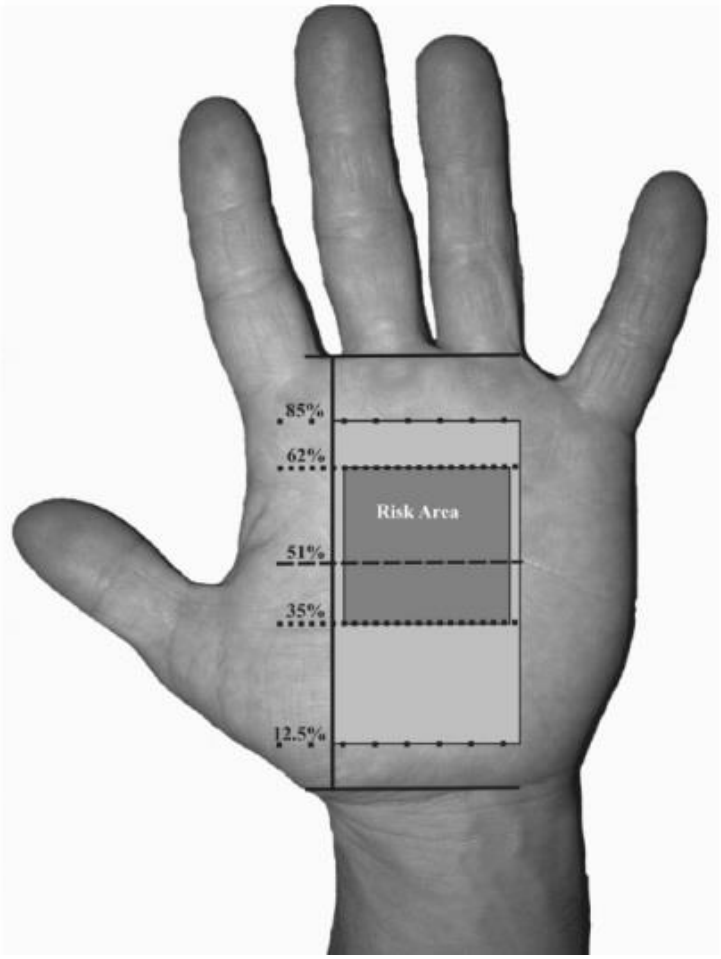

Figure 1.16: Risk area where the palmar communicating branch (CB) is most likely to be found as described by Loukas et al. (2007). Light grey area indicates the range where all palmar CBs were found; dark grey area indicates the area where the majority (83%) of the palmar CBs were found (Loukas et al., 2007).

In a study by Biafora and Gonzalez, (2007), morphometric data were collected from 50 adult cadaveric hands to map the CB between the MN and UN in the palm area using the distal wrist crease as a reference point. The CB was found to anastomose with the UN 31.68±7.50 mm (17-45 mm) distal to the distal WC and with the MN 39.03±7.32 mm (30-55 mm) distal to the distal WC. The study also defined the medial and lateral borders of where the CB is most likely to be found as the fifth ray and the third webspace respectively (Biafora and Gonzalez, 2007).

Investigating the palms of 169 adult cadavers Kawashima et al. (2004), later modified by Dogan et al. (2010), suggested a new classification system of six groups that includes the absence of the CB. The different types mentioned by Kawashima et al. (2004) and Dogan et al. (2010) were all previously described in the literature but categorized into more precise and logical systems.

The palmar CB between the MN and UN is clinically important because it alters the typical 3½ median-1½ ulnar sensory distribution of the digits thus potentially changing the clinical signs and symptoms and leading to errors in diagnosis. The size of the CB and location can vary among individuals. A case report by Rollins and Meals (1985) of laceration of the CB due to trauma found the CB to be equal in diameter to the 3rd CDN proximal to their merger indicating to them that almost half of the fibres of the 3rd CDN are from the ulnar nerve. Injury to this nerve could explain the sensory disturbances encountered in patients who underwent otherwise perfect wrist or hand surgery. Stančić et al. (1999) reported that the CB was located in the area of the distal incision of the two portal carpal release technique in 28% of cases investigated. Arner et al. (1994) reported 10 cases of sensory disturbances in the ring and the middle or little fingers after two portal endoscopic carpal tunnel release. The study also reported that a palmar CB was found in close proximity to the distal margin of the released TCL in two

patients and a neuroma was found in the CB in one patient (Arner et al., 1994). In another case report by May Jr and Rosen (1981) a large neuroma was found on the CB following a carpal tunnel release of a 34 year old patient. The neuroma caused sensory disturbances on the lateral side of the ring finger: symptoms were resolved once the neuroma was resected (May Jr and Rosen, 1981). Due to its close proximity to the distal margin of the TCL, the CB is at risk during surgical procedures to the hand and wrist in carpal tunnel release, ring finger flexor tendon surgery, Dupuytren's fasciectomy and during exploration of the ulnar side of the TCL and Guyon's canal (Rollins and Meals, 1985; Olave et al., 2001). Injury to the nerve causes tingling sensation or hyperesthesia in the digits depending on the topography of the injured branch in the affected patient (Loukas et al., 2007). Knowledge of the location and range of possible CBs will aid clinicians to better assess and diagnose cases pre-operatively, recognize and preserve CBs intra-operatively, and accurately evaluate complications post-operatively.

1.3. Dorsum of the hand:

The dorsum of the hand is supplied by the dorsal branch of the ulnar nerve (DBUN), the superficial branch of the radial nerve (SBRN) and occasionally the lateral antebrachial cutaneous nerve (LABCN). The DBUN originates about 80 mm proximal to the wrist crease and courses distally and dorsally to innervate the skin of the medial dorsal hand and the dorsal surface of the medial one and half digits (Figure 1.17) (Botte et al., 1990). The SBRN originates at the level of the lateral epicondyle and courses distally to become cutaneous by emerging between the tendons of brachioradialis and extensor carpi radialis longus. It supplies the dorsal skin of the hand and the dorsal skin of the lateral three and half digits as far as the distal interphalangeal joint. The DBUN and SBRN may communicate at the dorsum of the hand. The communicating branch allows exchange of sensory fibres between the two nerves.

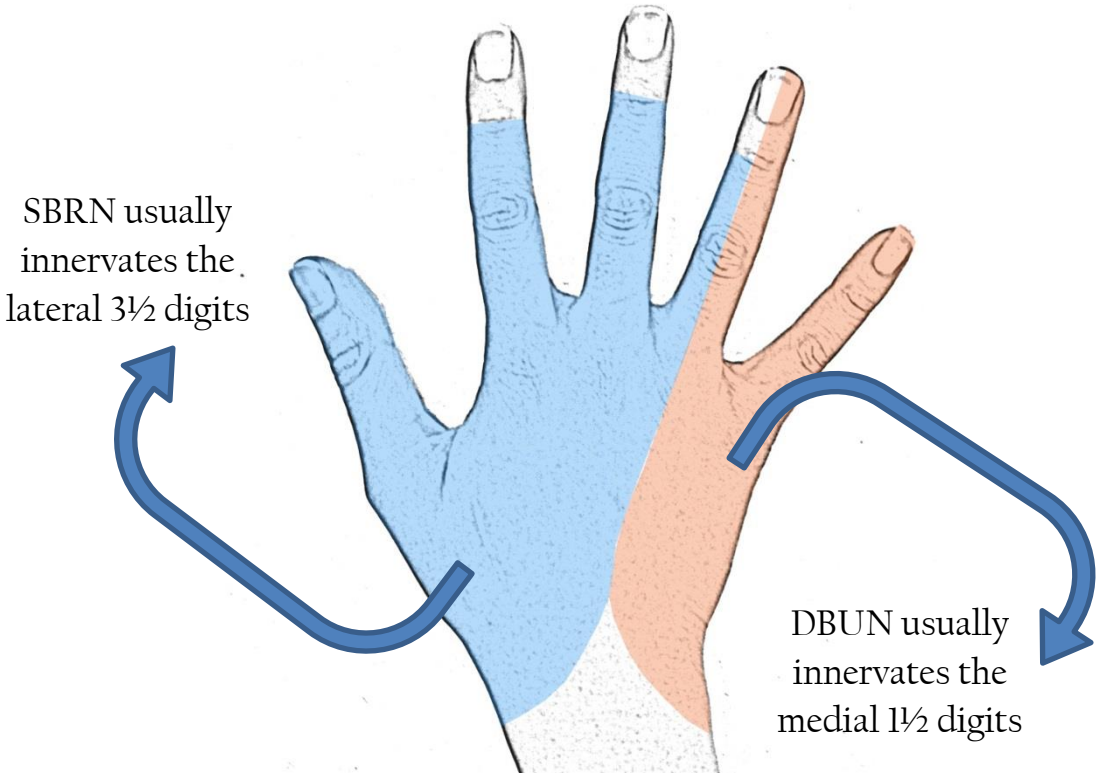

Figure 1.17: Schematic drawing showing the innervation territory classically described in the literature (Source: Author).

Knowledge of the sensory innervation of the dorsum of the hand is based generally on historical large studies examining the nerves of the dorsum of the hand. However, most studies agree that variations in the sensory innervation to the dorsum of the hand are not uncommon making the two nerves vulnerable to injury during arthroscopic and open surgeries performed in the dorsum of the hand (Cirpar et al., 2012). Stopford (1918) clinically examined more than 1000 gunshot patients from World War I and reported anaesthesia patterns following peripheral nerve injuries. The study reported that the DBUN was responsible for innervating the skin of the medial dorsal surface of the hand and the medial one and half digits in 79% (Stopford, 1918). Dissecting 16 cases, Linell (1921) found the DBUN to supply the dorsal surface of the medial one and half digits in only 2 cases (12.5%), the dorsal surface of the medial two digits in 2 cases (12.5%), the dorsal surface of the medial two and half digits in 11 cases (68.8%), and the dorsal surface of the medial three and half digits in one case (6.25%). The study

suggested that the seventh cervical nerve fibres, responsible for supplying the middle finger, travel in the DBUN from high connections at the level of the brachial plexus. Auerbach et al. (1994) investigated the SBRN in 20 cadaveric upper limbs and reported that the most common innervation pattern was the SBRN innervating the skin for over the lateral two and half digits noted in 45% of the cases, whereas it innervated the lateral three and half in 30%. The study also reported that the SBRN exceeded its innervation territory supplying the lateral four digits and the lateral four and half digits in one case each (Auerbach et al., 1994). In more recent studies, Mok et al (2006) investigated the dorsum of the hand in 30 cadaveric hands and reported that the most common pattern of distribution of the DBUN was innervation of the skin over the medial two and half digits, noted in 24/30 cases. The classical description of the medial one and half digits innervation was only present in 4/30 cases. The study also described the most common pattern of distribution for the SBRN, present in 16/30 cases, being innervation of the lateral two and half digits, whereas the classical description of the lateral three and half digits was only found in 9/30 cases. Moreover, dual innervation was noted in 10 cases where the two nerves innervated the medial side of the middle finger and/or the lateral side of the ring finger; however, no mention of communicating branches was made (Mok et al., 2006). In velocity conduction studies, a reduced or absent action potential response may result due to variations in the innervation territory. Authors have advocated that in cases of abnormal DBUN response, the SBRN should be stimulated to confirm pathology and exclude atypical sensory patterns (Dutra De Oliveira et al., 2000; Garibaldi and Nucci, 2000).

Communicating branches between the SBRN and the DBUN can alter the sensory innervation in the dorsum of the hand. The incidence rate of these communicating branches was reported as 4.2% by Botte et al. (1990), 15% by Auerbach et al. (1994), and

60% by Loukas et al. (2008). Such communication can explain the low, absent or/and atypical response in conduction velocity studies[1] (Garibaldi and Nucci, 2000).

An all radial supply to the dorsum of the hand has been mentioned in the literature with various incidence rates. In dissection based studies it was found in 4.2% as reported by Botte et al. (1990), 3.3% by Mok et al. (2006), 5.5% by Tiznado et al. (2012) and 8% by Robson et al. (2008). In velocity conduction studies it was reported in 19% by Pollak et al. (2013) and 12.9% by Stappaerts et al. (1996). In conduction velocity studies, small nerves cannot produce enough response to be detected due to their small diameter and/or the few number of axons present in that nerve. Examiners, studying the dorsum of the hand, would therefore interpret an absent or low amplitude as the nerve being absent and thus assume the dorsal surface of the hand to be solely supplied by the SBRN. This can explain the higher rates reported in conduction velocity studies compared to that reported in dissection based studies. Failure to recognise variations in the sensory innervation of the dorsum of the hand could lead to misdiagnosis of ulnar neuropathy in the forearm or at the elbow especially when there are more than two variations coexisting (Leis et al., 2010).

Interestingly, the pattern of the innervation in the dorsum of the hand is not only variable in general, but also variable between the two hands of the same individual. In a study conducted on cadavers, Huanmanop et al. (2007) reported asymmetry in the SBRN pattern in 17/79 cases (21.5%). In their study, Stappaerts et al. (1996) investigated the cutaneous nerve's action potential response from 31 subjects and reported that symmetry between the right and left hands was found in only 9/31 subjects (29%). Also Dutra de Oliveira et al. (2000) reported significant differences between right and left hand sides in 21% of their cases. In conduction velocity studies

[1] The communicating branch between the SBRN and DBUN is further explained in section 1.3.3.

where the healthy hand is used as a reference to compare the affected hand, it is important for clinicians interpreting the conduction velocity test results to be aware of possible variations and asymmetry. The other healthy hand should not be taken as an absolute reference.

Knowledge of the course and anatomical relations of the DBUN and the SBRN to other structures in the distal forearm and wrist is critical in clinical settings where diagnostic and therapeutic procedures can put them in danger of injury.

1.3.1. Superficial branch of the radial nerve

At the level of the elbow, the radial nerve divides into superficial and deep branches. The radial nerve can divide 20-50 mm proximal or distal to the radiocapitellar (humeroradial) joint. The superficial branch of the radial nerve (SBRN) courses superior to supinator and continues deep to brachioradialis. In the distal half of the forearm, the SBRN pierces the antebrachial fascia between the tendons of brachioradialis and extensor carpi radialis longus to become subcutaneous about 90 mm proximal to the wrist. In 10% of specimens, the nerve may become subcutaneous by piercing the tendon of brachioradialis (Doyle and Botte, 2003): a lower incidence was reported in a Thai cadaver study conducted by Huanmanop et al. (2007). The SBRN was noted to emerge between two parts of the brachioradialis tendon in 3.8% (Huanmanop et al., 2007). Such a variation might cause nerve entrapment.

The nerve continues distally and divides into two (91.67%) (one palmar and one dorsal) or three branches (8.33%) 51 mm proximal to the RSP (Ikiz and Üçerler, 2004). It is estimated that the nerve becomes subcutaneous and divides for the first time after it becomes subcutaneous in the distal 20-36% of the distance between the lateral humeral epicondyle and the RSP. All branches of the SBRN pass lateral to Lister's tubercle (LT),

with the closest branch to the first dorsal compartment passing within a mean distance of 4 mm. With various patterns and configurations, the palmar branch continues distally to supply the dorsolateral side of the thumb. It may divide into smaller branches that spread to supply the palmolateral side of the thenar eminence. It is not uncommon for the palmar branch to communicate with distal branches from the LABCN. The dorsal branch continues distally and further divides at the level of the RSP into two or three branches supplying the dorsomedial side of the thumb and the dorsolateral side of the index finger; the dorsomedial side of the index and the dorsolateral side of the middle finger; and the dorsomedial side of the middle finger and the dorsolateral side of the ring finger. The dorsomedial branch to the thumb and the dorsolateral branch to the index finger originated from the same main branch in 65% of the specimens (Doyle and Botte, 2003). The SBRN branches are numbered from dorsal to palmar and are called superficial radial 1 (SR1), SR2 and SR3 supplying the dorsal surface of the middle and lateral side of the ring finger, the index and medial side of the thumb, and the lateral side of the thumb respectively (Ikiz and Üçerler, 2004).

Knowledge of the branching patterns to the thumb and the digits may help prevent iatrogenic injuries of the nerve and its branches during various clinical procedures. Furthermore, understanding the patterns and the anatomical course can provide opportunities to modify or create new clinical applications for reconstructive hand surgeries. Various reverse neurofasciocutaneous flaps can be obtained from the SBRN branches with acceptable donor site morbidity (Tellioğlu et al., 2000). The pattern of distribution of the SBRN exhibited many configurations. Obtaining a classification system from those configurations is considered a challenge to anatomists. Table 1.5 describes the classification used in the literature and the incidence rate of each pattern.

Table 1.5: Patterns of distribution of the superficial branch of the radial nerve in the literature

NO	Reference	Sample size	Classification		Incidence
1	Ikiz and Üçerler, 2004	48 hands from 24 formalin fixed cadavers	Type I	Superficial branch of the radial nerve (SBRN) gives two branches: SR3 and a common medial trunk. The common medial trunk further divides into SR1 and SR2. ▪ SR1 coursed over the dorsal surface of the index finger ▪ SR2 coursed over the dorsal surface of the first metacarpal space ▪ SR3 coursed to the lateral side of the thumb	43 (89.53%)
			Type II	Trifurcation of the SBRN into three branches.	4 (8.33%)
			Type III	Similar to Type I with an extra branch medial to SR1 innervating the third metacarpal space is also present.	1 (2.08%)
2	Huanmanop et al., 2007	79 upper extremities from 40 formalin fixed Thai cadavers	Type I	SBRN gives two branches: SR3 and a common medial trunk. The common medial trunk further divides into SR1 and SR2. ▪ SR1 coursed over the dorsal surface of the index finger ▪ SR2 coursed over the dorsal surface of the first metacarpal space ▪ SR3 coursed to the lateral side of the thumb	64.60%
			Type II	Trifurcation of the SBRN into three branches	1.30%
			Type III	Similar to Type I with an extra branch medial to SR1 innervating the third metacarpal space is also present.	31.60%
			Type VI	SBRN gives SR1 and SR2 innervating the dorsal surface of the index finger and the first metacarpal space. SR3 is replaced by LABCN innervating the lateral side of the thumb.	2.50%

NO	Reference	Sample size	Classification		Incidence
3	Korcek and Wongworawat, 2011	40 upper extremities from 24 formalin fixed adult cadavers	Type I	SBRN divides into SR3 and a common medial trunk further dividing into SR1 and SR2.	34 (85.0%)
			Type II	SBRN divides into SR1 and a common lateral trunk that further divides into of SR2 and SR3.	4 (10.0%)
			Type III	SBRN divides into SR1 and SR2. SR3 is missing and replaced by LABCN.	2 (5.0%)
4	Gupta et al., 2012	60 upper extremities from 30 spontaneously aborted fetuses	Type I:	The SBRN innervated the lateral two and half digits	66.70%
				Ia: the main trunk bifurcated into SR3 and a medial common trunk that further divides into SR2 and SR1: ▪ SR 1 supplies the 2nd metacarpal space ▪ SR2 supplies the 2nd metacarpal space ▪ SR3 supplies the lateral side of the thumb	60%
				Ib: trifurcation of SBRN	6.70%
			Type II:	SBRN innervated the lateral 3 digits: SBRN divides into a medial common trunk supplying the middle, index finger and occasionally the medial side of the thumb; and SR3 branches supplying the thumb.	23.30%
				IIa: The SBRN bifurcated into SR3 and a medial common trunk that further divides into SR2 and SR1. SR3 supplies the lateral side of the thumb.	10%
				IIb: Trifurcation of the SBRN into 3 branches. SR3 innervates the entire thumb	10%
				IIc: The SBRN divides into 4 branches. SR3 innervates the lateral aspect of the thumb.	3.30%

NO	Reference	Sample size	Classification		Incidence
			Type III:	SBRN innervated the lateral 3 and half digits. The main trunk divided into a medial common trunk and SR3.	10%
				IIIa: The medial common branch divides into 4 branches innervating the lateral side of the ring, the entire middle and ring fingers. SR3 innervates the entire thumb.	6.67%
				IIIb: The medial common branch divides into 5 branches innervating the lateral side of the ring finger, the entire middle and index fingers, and the medial side of the thumb. SR3 innervates the lateral side of the thumb.	3.30%

Due to its location and close anatomic relations to other structures in the wrist and hand, the SBRN is at risk of direct or iatrogenic injury during distal radial fractures, fixation and reduction of the distal radial fractures, arthroscopic procedures to the wrist, cephalic vein cannulation, and first dorsal compartment release.

The SBRN is at risk of direct injury during distal radial fractures and indirectly during the treatment of those fractures. Compressive casts or fracture bracelets may cause nerve irritation and further complicate the injury (Ikiz and Üçerler, 2004). External fixator pins are used to stabilize distal radial fractures and have proven to give good clinical results. Anderson et al. (2004) investigated complications associated with using external fixation techniques in 24 patients and reported that 66.7% of patients developed different complications of which 21% were neuropathies involving the median nerve or the SBRN. The surgeon's technique in placing the pin influences the incidence of SBRN injury. An open technique can provide better visualisation and perseveration of the nerve. In Anderson et al. (2004) series 23 of the 24 patients had open technique. Moreover, Kirschner wire fixation is used to reduce and stabilize distal radial fractures. It is done through inserting the pins through the anatomic snuff box and through the RSP putting the branches of the SBRN that are passing close or over the region at risk of injury. Ikiz and Üçerler (2004) found a branch of the SBRN passing in the anatomic snuff box in 16.67% of specimens. Klitscher et al. (2007) reported that the closest branch to the RSP passed as close as 1 mm to the RSP. Steinberg et al., (1995) reported injury to the SBRN in 10% (2/20) and to the LABCN in 15% (3/20) of the specimens during percutaneous Kirschner wire fixation through the anatomic snuff box. The study also identified a safe zone of 68 mm^2 in the anatomic snuff box where injury to neurovascular structures could be avoided (Steinberg et al., 1995). However, individual anatomical variations in the anatomic snuff box eliminate the existence of a

true safe zone (Whipple and Poehling, 1996; Korcek and Wongworawat, 2011). Singh et al. (2005) investigated the incidence of SBRN injury due to radial Kirschner wire insertion through the styloid process and reported that damage was found in 20% (8/40) of cases investigated. The SBRN is not only at risk of injury during the insertion of the Kirschner wires, but also during removal and by the continuous friction with the bent or buried end of the wire (Singh et al., 2005; Sharma et al., 2006). Hochwald et al. (1997) compared the risk of inserting a Kirschner wire by an open technique and a limited open technique on the SBRN and noted that the SBRN was damaged in 7/22 (32%) in percutaneous insertion through the styloid process, while it was only injured in one case when the limited open technique was used. Many reports advocate placing the Kirschner wires into the distal radius by limited open incision with blunt dissection to the bone and using a soft tissue protector as it provides better visualization and allows identification and preservation of neurovascular structures (Hochwald et al., 1997; Singh et al., 2005).

Elastic intramedullary nailing is frequently used for displaced and unstable paediatric fractures in the forearm. It is a preferred technique as it limits soft tissue stripping, results in limited surgical scars, is minimally invasive and allows early postoperative movement (Klitscher et al., 2007; Cumming et al., 2008). Radial nailing is achieved about 20 mm proximal to the epiphysis (Garg et al., 2008). Although relatively infrequent, SBRN injury is one of the complications of this procedure (Cumming et al., 2008; Fernandez et al., 2010; Kang et al., 2011). Fernandez et al. (2010) reported that lesions of the SBRN may occur due to the primary fracture, insertion of the nails or at the time of material removal. Careful dissection and identification of the SBRN branches during the insertion of the nails can decrease the injury; however scar tissue

formation may hinder identification of the nerve and thus limit the possibility of preservation (Fernandez et al., 2010).

The SBRN and the cephalic vein have a close anatomical relationship making the nerve at risk during intravenous cannulation at the wrist (Boeson et al., 2000). Sawaizumi et al. (2003) reported 11 cases of injury to the SBRN due to intravenous injection into the cephalic vein at the wrist joint. Complete recovery was achieved within three months in 36.4% of cases; however complications persisted in the remaining 63.6% (Sawaizumi et al., 2003). The SBRN intersects the cephalic vein 54.3 mm proximal to the RSP; however the intersection point could be variable (Klitscher et al., 2007). Gupta et al. (2012) investigated the SBRN in 60 hands of spontaneously aborted fetuses and reported that the cephalic vein intersected the nerve at the level of the wrist or distal to it in all specimens. They also reported that the vein intersected the nerve once in 40% and twice in 80% of specimens (Gupta et al., 2012). Robson et al. (2008) indicated that the cephalic vein and the SBRN had a close association (<2 mm) in 80% of cases investigated. Boeson et al. (2000) recommends immediate withdrawal of the catheter if the patient complained of paresthesias or numbness, whereas Sawaizumi et al. (2003) believe that wrist venepuncture should only be performed when no other appropriate alternative is available. Klitscher et al. (2007) and Robson et al., (2008) recommend venepuncture to be performed prior to the nerve piercing the antebrachial fascia to avoid any crossing points of the SBRN with the cephalic vein.

Radial forearm fasciocutaneous free flaps are frequently used for the reconstruction of defects in the oral cavity, oropharyngeal cavity, upper limb, lower limb and genitalia (Emerick and Deschler, 2007). Damage to the SBRN is a common complication of the procedure. Radial nerve morbidity as a complication of radial fasciocutaneous free flap

harvest was reported as high as 54% (Lutz et al., 1999). Grinsell and Theile (2005) investigated radial nerve morbidity associated with radial artery free flap harvest in two techniques that depend on harvesting the venae commitantes or the cephalic vein with the flap. The study concluded that the incidence of damage to SBRN branches was 9% when harvesting the venae commitantes and doubled (18%) when the cephalic vein was involved (Grinsell and Theile, 2005). The doubling of nerve morbidity due to including the cephalic vein in the flap can be explained by the close anatomical association between the cephalic vein and the SBRN that puts the nerve in danger of injury during clinical procedures performed close to the cephalic vein (Robson et al., 2008).

The SBRN is an important structure to consider during clinical procedures to the radial artery. Robson et al., (2008) reported that the radial artery was closely associated with the SBRN at the level of the RSP in 12 (48%) of 25 specimens and to the LABCN in 6 (24%). The radial artery is harvested for coronary artery bypass surgery and is frequently used for arterial blood gas analysis. Percutaneous needle puncture is considerably painful and may provoke anxiety and discomfort in patients that require multiple arterial blood gas analysis (Tran et al., 2002). Several studies have concluded that the use of topical anesthetic gels did not contribute to the reduction of pain during radial artery puncture in comparison to local infiltrative anesthesia (Tran et al., 2002; Aaron et al., 2003; Robson et al., 2008). The pain might be induced as a result of irritation or injury to the SBRN branches or the LABCN which are closely associated to the radial artery. Robson et al. (2008) recommended approaching the artery from the ulnar side as they found no nerve branches passing on the ulnar aspect of the artery.

The radial artery is harvested for coronary artery bypass surgery: complications at the site of harvest have been reported in the literature. Greene and Malias (2001) reported sensory disturbances related to the SBRN and the LABCN in 36 arms (10.7%). A higher

incidence rate was reported by Siminelakis et al. (2004) after investigating 54 patients who underwent radial artery harvesting for coronary bypass surgery. Sensory disturbances were reported in 34.09% of which 31.28% were dorsal disturbances and 2.27% were palmar (Siminelakis et al., 2004). In another study investigating the complication of radial artery harvest in 560 patients, Denton et al. (2001) reported that dorsal sensation abnormalities were found in 13.8%, palmar abnormities were reported in 12.7% and decreased thumb function in 5.5% indicating the involvement of the median nerve and the SBRN. The study however, did not explore the possibility of involvement of LABCN injury and explains the neurological complications by direct injury to the SBRN and indirect median nerve ischemia due to loss of collateral radial blood supply (Denton et al., 2001). It is clear that the dorsal sensory abnormalities are caused by SBRN injury only; moreover the palmar abnormalities may be the result of injury to LABCN, SBRN branches, or both. Although endoscopic techniques use a small skin incision which minimizes wound infection and scarring leading to less postoperative recovery time and better cosmetic results, sensory disturbances have been reported in conventional and endoscopic radial artery harvest. The distribution of sensory disturbances indicates the involvement of both the SBRN and the LABCN in the conventional open method. Endoscopic harvest showed paresthesia in smaller areas confined to the SBRN sensory territory which suggests that only the SBRN is involved (Shapira et al., 2006). In another study neurological complications including a lesion in the radial artery and paraesthesia developed in 22 and 24 patients who underwent radial artery harvest by conventional open and endoscopic methods respectively (Bleiziffer et al., 2008).

Arthroscopy to the lateral area of the wrist or the dorsum of the hand can put the SBRN at risk of injury. Arthroscopy is a diagnostic and therapeutic tool used in many clinical

conditions including triangular fibrocartilage complex tears, carpal interosseous ligament injuries, reduction and fixation of distal radial fractures and resection of dorsal ganglia. The SBRN passes superficially to the arthroscopic portals. Kiliç et al. (2009) investigated the relation of wrist arthroscopy portals to the SBRN in 11 cadaveric hands. Due to the small area where arthroscopic portals can be positioned and the great number of individual anatomic variations, the authors stated that it was not possible to create guidelines to prevent SBRN injury and recommended making skin-only incisions and proceed by blunt dissection to establish portals and minimize the risk of injury to the SBRN (Kiliç et al., 2009). Ropars et al. (2010) investigated the portals used in carpometacarpal and metacarpophalangeal joints in thumb arthroscopy in 30 fresh cadaveric wrists and reported that SR2 and SR3 are at high risk of injury as they pass close to the portals.

Arthroplasty to the distal scaphoid joint is used to eliminate pain and restore strength and function in the wrist. The procedure includes a longitudinal 40 mm incision between the scaphoid and trapezium ending just distal to the RSP. Careful dissection and gentle retraction of the SBRN is essential to avoid injury to the nerves passing over the region (Wessels, 2004). Wessels (2004) investigated arthroplasty to the distal scaphoid joint in 63 patients and reported two cases of SBRN injuries. An interesting case was reported by Kuruvilla et al. (2002) of a patient complaining of sensory disturbances in the dorsomedial side of the hand after undergoing wrist arthroplasty even though the surgical incision did not pass over the DBUN. The SBRN innervated the entire dorsal surface of patient's hand, thus a lesion on the medial branches of the SBRN caused by the surgical incision resulted in sensory loss (Kuruvilla et al., 2002).

Extensive knowledge of the innervation of the wrist joint is essential in Wilhem's technique for wrist denervation. Careless dissection of the lateral side of the wrist over

the styloid process and the first dorsal compartment can injure sensory branches of the SBRN and/or cause neuromas (Ekerot et al., 1983). Paresthesia in the lateral region has been reported following the procedure indicating possible injury of the main nerve (Ferreres et al., 2002).

De Quervain's disease is an inflammatory disease of the first dorsal compartment. The surgical treatment of this condition includes the release of the first dorsal compartment to allow the inflammation to subside. Treatment varies from immobilization of the wrist to surgery according to the severity of the condition. Branches of the SBRN pass over the first compartment in 16.67% of cases (Ikiz and Üçerler, 2004). Investigating 40 Thai cadavers, Huanmanop et al. (2007) reported that the incidence of SBRN branches passing over the first dorsal compartment is double that mentioned by Ikiz and Üçerler (2004), being 38%. Klitscher et al. (2007) stated that the SBRN branches may pass as close as 2 mm to the middle of the first dorsal compartment. Many surgical techniques have been encouraged in the literature arguing their cosmetic outcome or reduced complications. According to Robson et al. (2008), the transverse incision or the z incision would have consistently crossed the SBRN branches in all cases investigated. The authors advocate the use of a longitudinal incision 25 mm proximal to the RSP as it avoided damaging any SBRN branches in 68%. The authors also stress the importance of careful dissection to help identify and preserve the nerve branches in the remaining 32% (Robson et al., 2008). Surgeons should be aware of the presence and close proximity of the nerve and should try to identify and preserve any nerve tissue to avoid postoperative complications.

Procedures done on the wrist or the dorsum of the hand such as nerve blocks through the anatomic snuff box or bone grafts taken from the distal radius between the first and second dorsal compartments can injure the nerve branches passing over the region. It is

reported that the SBRN passes over the anatomic snuff box in 16.67% of specimens (Ikiz and Üçerler, 2004); however Huanmanop et al. (2007) reported that SBRN branches passed over the anatomical snuff box in 64.6% in Thai cadavers.

It is important to anesthetize the main trunk prior to first branching to achieve total sensory blockade of the SBRN. Robson et al. (2008) recommend local anaesthetic infiltration to be administered when the SBRN becomes subcutaneous prior to giving its first branch between the distal 33% and 20% of the total length of the arm.

It is not uncommon for the SBRN to connect with the LABCN. Usually the LABCN connects with the palmar branch to supply the lateral side of the thenar eminence. Huanmanop et al. (2007) found the connections between the two nerves in 34 Thai cadaveric arms (43%), while Ikiz and Üçerler (2004) reported it in 20.83%. LABCN was found to extend over the anatomic snuff box in 52.5% and supply the same area as the SBRN in 10%. The LABCN was also reported to take over the innervation territory of SR3 (over the lateral and palmolateral side of the thenar eminence) in 5% (Korcek and Wongworawat, 2011). Mackinnon and Dellon (1985) reported a partial or complete overlap between the two nerves in 75% of cases and that injuries to SBRN will be associated with LABCN injuries. Due to the connections between the two nerves, sectioning SBRN alone to treat neuroma-related pain at the dorsolateral side of the wrist might not have effective outcomes (Mackinnon and Dellon, 1985; Robson et al., 2008). Knowledge of these connections is important in cases of denervation, wrist and thenar region local anaesthesia or nerve block. Table 1.6 outlines anatomic measurements of the SBRN described in the literature.

Table 1.6: Anatomic measurements of the superficial branch of the radial nerve (SBRN) to bony landmarks that are discussed in the literature

NO	Reference	No of Cadavers	1st branch	Closest branch to		Other findings
				Lister's tubercle	the centre of the 1st dorsal compartment	
1.	Abrams et al., 1992	20 fresh cadavers upper extremities	51±18 mm proximal to the RSP	16.0±0.5 mm	4.0±4.0 mm	▪ Becomes subcutaneous 90±14 mm proximal to the radial styloid process (RSP). ▪ Superficial branch of the radial nerve (SBRN) arose at the level of the lateral humeral epicondyle in 8/20 ▪ Within 21 mm of the lateral epicondyle in the 12/20 ▪ 2/20 the SBRN pierced the tendon of brachioradialis. ▪ Diameter when it pierced the fascia was 3±0.5 mm. ▪ Its first division included 3 branches in 3/20. ▪ SBRN became subcutaneous and first branched at the distal 36% and 20% of the distance from lateral epicondyle to the RSP respectively. ▪ At the level of the extensor retinaculum, the palmar and dorsal branch diameters were 2.0±0.4 and 2.0±0.2 respectively. ▪ Branch of SBRN lying over the centre of the first dorsal compartment in 35%. ▪ Connected with the lateral antebrachial cutaneous nerve (LCABN) in 7/20.
2.	Steinberg et al., 1995	20 fresh cadaver upper extremities	42 mm proximal to Lister's tubercle	-	-	▪ LABCN coursed through the anatomic snuff box in 9/20 (45%). ▪ The dorsal branch 2nd major division occurred 4 mm proximal to Lister's tubercle. ▪ S3 branch was on the border of the anatomic snuff box in all cases, 7.9±4.9 mm from the RSP.

NO	Reference	No of Cadavers	1st branch	Closest branch to		Other findings
				Lister's tubercle	the centre of the 1st dorsal compartment	
3.	Tellioğlu et al., 2000	8 cadaver upper extremities	46±5.7 mm	-	-	▪ The second major branching for the palmar branch occurred 4.8±2.1 mm; and the dorsal branch divided for the second time 16±2.3 mm distal to the RSP.
4.	Ikiz and Üçerler, 2004	48 hands from 24 formalin fixed cadavers	49±12 mm proximal to the RSP	15.8±1.2 mm	5.4±3 mm	▪ Becomes subcutaneous 92±14 mm proximal to the RSP ▪ The SBRN divided into three branches after it became subcutaneous in 4/48 (8.33%). ▪ SR2 coursed over the anatomical snuff box in 8/48 (16.67%). ▪ SR3 connected with the LABCN in 10/48 (20.83%). ▪ Branches passing over the 1st dorsal compartment in 8/48 (16.67%).
5.	Huanmanop et al., 2007	79 upper extremities from 40 formalin fixed Thai cadavers	46±1.5 mm	10±3.8 mm	38% has SBRN branches passing over the 1st dorsal compartment	▪ Becomes subcutaneous 73±1.5 mm to the RSP ▪ LABCN took over S3 in its absence in 2/43 female cadavers. ▪ Pierced the tendon of brachioradialis in 3.8%. ▪ Connected with the LABCN in 43%, of which 85.3% were with S3. ▪ Branches passed over the anatomic snuff box in 64.6%. ▪ Becomes subcutaneous 30% of the total length of the forearm (lateral epicondyle to the RSP). ▪ First major branch occurs in the distal 21% and 17% of the total forearm length in males and females respectively. ▪ The closest branch passed 2.9±1.8 mm from the RSP.

NO	Reference	No of Cadavers	1st branch	Closest branch to		Other findings
				Lister's tubercle	the centre of the 1st dorsal compartment	
6.	Klitscher et al., 2007	10 upper extremities from 5 embalmed cadavers	54.7±12.2 mm	16.4±3.7 mm	palmar 4.4±1.3 mm; dorsal 15.2±2.8 mm	▪ The second division of the SBRN occurred at the level of the RSP (0±5.7 mm) with a range of 10 mm proximal to the RSP to 10 mm distal to the RSP. ▪ The cephalic vein and the SBRN crossed at 54.3±7.6 mm proximal to the RSP (range:42-68 mm). ▪ Closest palmar and dorsal branches at the level of the RSP is 9.8±4.5 mm and 3.5±2.7 mm respectively.
7.	Robson et al., 2008	25 upper extremities from formalin fixed cadavers	49.2±14.4 mm	14.9±5.3 mm	dorsal 6.4±4.1 mm; palmar 4.9±3.0 mm	▪ Becomes subcutaneous 83.1±11.4 mm proximal to the RSP. ▪ The SBRN became substances in the distal 32.8±4.1% of the total length of the forearm. ▪ 25 mm incision from the RSP will avoid the nerves in 17/25 cases (68%) and in 8/25 (32%) the incision would at least partially cross the SBRN. ▪ Radial artery was closely associated with the SBRN in 12/25 (48%). ▪ SBRN was closely associated with the cephalic vein in 80%. Association with the cephalic vein was grouped into proximal and distal association in 16/25 (64%); 4/25(16%) proximal to the RSP; 3/25 (12%) distal to RSP; 2/25 (8%) no close association. ▪ An anomalous nerve distribution was noted in two hands.

NO	Reference	No of Cadavers	1st branch	Closest branch to		Other findings
				Lister's tubercle	the centre of the 1st dorsal compartment	
8.	Korcek and Wongworawat, 2011	40 upper extremities from 24 formalin fixed adult cadavers	31.46±10.73 mm to a line between RSP & LT.	-	S3 passed palmarly 1.37±2.73 mm; S2 passed dorsal 7.94±3.34 mm	▪ Second major branch was 4.18±10.23 mm proximal to a line between RSP & LT. ▪ LABCN was found distal to the RSP in 21/40 (52.5%); 17/40 (81.0%) were present palmar to SBRN; 4/40 (19.0%) supplied the same area as the SBRN. ▪ With the absence of S3, the LABCN took over supplying the area in 2/40 (5%).
9.	Samarakoon et al., 2011	25 upper extremities from formalin fixed Sri Lankan cadavers	55.7±14.3 mm	-	-	▪ Becomes subcutaneous 85.4±13.2 mm proximal to the RSP. ▪ SBRN divided into two branches in all specimens. ▪ The most medial and most lateral branches crossed the wrist joint 25.1±5.3 mm and 39.0±6.4 mm to Lister's tubercle respectively. ▪ The cephalic vein crossed the SBRN once in 68% and twice in 12%. ▪ The most distal crossing point between the cephalic vein and the SBRN was 51.0 mm distal to the RSP.

1.3.2. Dorsal branch of the ulnar nerve

Arising from the medial aspect of the main trunk of the ulnar nerve, the dorsal branch of the ulnar nerve (DBUN) supplies the dorsal surface of the medial 1½ digits. It originates 83 mm from the proximal border of the pisiform, courses distally and medially deep to flexor carpi ulnaris to become subcutaneous 50 mm proximal to the pisiform. Proximal to the wrist it gives two or three branches, one of which supplies the ulnocarpal joint capsule. The nerve can also divide before becoming subcutaneous (Mok et al., 2006). The course of the nerve differs slightly according to the anatomical position of the arm. The nerve passes close to the medial border of the widest diameter of the ulnar head when the arm is supinated; whereas it passes on the palmoulnar border of the ulna head when the arm is pronated (Botte et al., 1990). The nerve gives one or two branches in the hand to supply the little finger and medial side of the ring finger. The dorsal branches usually extend to the proximal interphalangeal joint. Table 1.7 shows the anatomic measurements for the point of origin and point of piercing the fascia for the DBUN as reported in the literature.

Table 1.7: Anatomic measurements and description for the dorsal branch of the ulnar nerve as described in the literature

No.	Reference	No. of cadavers	Anatomical descriptions
1.	Botte et al., 1990	24 fresh upper extremities from adult cadavers	▪ Originated 64±23 mm from the distal aspect of the head of the ulna and 83±24 mm from the proximal border of the pisiform. The origin point is located at the distal 26% of the total ulna length. ▪ At origin, the nerve had a slightly oval or round cross-section, 2.4 mm (1.6-3.5) in diameter. ▪ Pierces the fascia 50±18 mm proximal to the pisiform. ▪ The nerve gave 3-9 branches along its course with a diameter of 0.7-2.2 mm.

No.	Reference	No. of cadavers	Anatomical descriptions
			▪ The nerve was absent in one case and communicated with the superficial branch of the radial nerve (SBRN) in another
2.	Bertelli and Pagliei, 1998	35 upper extremities	▪ Originated 64.8 mm (50-160 mm) proximal to the pisiform. ▪ Measured 2.34 mm (1.2-3 mm) in diameter.
3.	Grossman et al., 1998	10 fresh upper extremities from adult cadavers and reported 6 cases of DBUN entrapment	▪ Originates 55 mm proximal to the head of ulna. ▪ The dorsal branch of the ulnar nerve (DBUN) reaches the dorsal aspect of the hand by crossing volar to the ulnar head. ▪ No communications were found between the DBUN and the SBRN.
4.	Casoli et al., 2004	22 fresh upper extremities from adult cadavers.	▪ Originated 80 mm (60-105 mm) proximal to the pisiform. ▪ Formed an angle of 30°-60° with the ulnar nerve coursing to the dorsum of the hand. ▪ The nerve divided into two terminal branches.
5.	Mok et al., 2006	30 formalin fixed upper extremities from adult cadavers	▪ Became subcutaneous 26 mm (6-41 mm) proximal to the ulna styloid process (USP). ▪ Divides for the first time 20 mm (-44-20 mm) distal to the USP. ▪ The second major division occurs 26 mm (-3-43 mm) distal to the USP.
6.	Tindall et al., 2006	10 left and 10 right upper extremities from 20 formalin fixed cadavers.	▪ The DBUN crossed a line between the USP and the fourth web space at an average of 24mm distal to the USP corresponding to the proximal 23% of the previously described distance. ▪ The DBUN coursed 14mm (10-19 mm) medially to the USP.
7.	Goto et al., 2010	30 formalin fixed upper extremities from adult cadavers	▪ Originated from the main trunk of the UN at 34±13 mm (7-61 mm) proximal to the USP. ▪ Two types were noted: o Proximal type: 21/30 o Distal type: 9/30

No.	Reference	No. of cadavers	Anatomical descriptions
8.	Puna and Poon, 2010	32 upper extremities from 19 soft embalmed cadavers	▪ Originated 51±14 mm (25-80 mm) proximal to the USP and 19±6 mm (10-30 mm) palmar and lateral to the subcutaneous border of the ulna. ▪ Crossed the subcutaneous border of the ulna from palmar to dorsal 2±11 mm (-25-25 mm) proximal to USP.
9.	Cavusoglu et al., 2011	14 formalin fixed upper extremities from 7 cadavers and 22 formalin-preserved upper extremities from 22 cadavers.	▪ Originates 180±2.9 mm distal to medial epicondyle and 83.6±2.4 mm proximal to the pisiform ▪ Pierces the fascia 54.7±1.5 mm to the pisiform. ▪ The DBUN bifurcated into two terminal branches. ▪ The DBUN diameter prior to its branching from the UN was 1.65±0.03 mm and at the dorsum of the hand was 1.6±0.03 mm.

Goto et al. (2010) classified the course of the DBUN based on its division pattern with respect to the ulnar styloid process into two groups:

Proximal type: The DBUN courses around the ulno-dorsal aspect of the hand proximal to the USP.

Distal type: The DBUN courses around the ulno-dorsal aspect of the hand distal to the USP.

The proximal type was found in 21/30 (70%), while the distal type was found in 9/30 specimens (30%) (Goto et al., 2010).

Variations in the anatomical course of the DBUN have been reported in the literature. The nerve can arise more proximally from the main trunk of the ulnar nerve even at the level of the elbow (Grossman et al., 1998). In a case report by Lama et al. (2009), the

DBUN originated from the main trunk of the UN at the level of the elbow near the cubital fossa and terminated by dividing into two lateral branches that supplied the dorsal medial half of the hand and the medial three digits, and a medial branch that connected with a branch from the superficial division of the ulnar nerve to supply the medial side of the little finger (Kaplan anastomosis). The nerve was found to be absent in some cases, during which the SBRN, the musculocutaneous nerve or the posterior cutaneous nerve of the forearm takes over supplying the region otherwise supplied by the DBUN.

Understanding the course and the relationships of the DBUN to the distal area of the forearm and the dorsal wrist and hand is important to avoid iatrogenic injuries to the nerve during diagnostic or therapeutic procedures such as wrist arthroscopy, electrodiagnostic studies, nerve block, carpal tunnel release, and harvesting ulnar nerve flaps. It can also be at risk during surgical procedures that require a direct approach to the subcutaneous border of the ulna as open reduction and internal fixation, ulnar lengthening and shortening procedures, delayed union or non-union of ulnar fracture treatments, ulna osteotomy and chronic osteomyelitis treatment (Puna and Poon, 2010). DBUN injury may present with numbness, dysesthesia, and pain due to neuroma formation. It is also important to appreciate its possible involvement in dorsal hand injuries or forearm pathologies as metacarpal bone fractures, extensor tendon injury, tenosynovitis of extensor carpi ulnaris, and puncture wounds (Grossman et al., 1998).

DBUN injury is one of the complications of wrist arthroscopy. Rodeo et al. (1993) mentioned that the low complications of wrist arthroscopy are due to the low frequency of the procedure and the knowledgeable and experienced surgeons performing it (Rodeo et al., 1993). For over 15 years, wrist arthroscopy is being used more frequently to treat various wrist and hand conditions including evaluation and

treatment of the triangular fibrocartilage complex, dorsal ganglion cysts, distal radial articular fractures, carpal fractures, carpal instability and inflammatory arthritis of the radiocarpal joint (Beredjiklian et al., 2004). As the nerve passes close to the 6th lateral portal used in wrist arthroscopy, it is in danger of injury during dissection or retraction; or strangulation between sutures. Beredjiklian et al. (2004) reported that complications occurred in 5.2% of patients who underwent wrist arthroscopy and that 1.9% of these cases were related to the DBUN or UN neurapraxia. Ahsan and Yao (2012), conducted a literature review on wrist arthroscopy complications and stated that they could be underestimated. Tsu-Hsin Chen et al. (2006) reported DBUN injury, whereas Nguyen et al. (2011) described cases where the ulnar nerve was sectioned during wrist arthroscopy to repair a triangular fibrocartilage complex. McAdams and Hentz (2002) investigated triangular fibrocartilage tear repair by using the inside-out technique in wrist arthroscopy and the effect on the DBUN. They reported that the nerve can pass as close as 0.4 mm to the surgical sutures (average, 1.9 mm) and was sandwiched between two sutures in 50% of specimens (McAdams and Hentz, 2002). Tindall et al. (2006) suggested the proximal fifth (19%) of the distance between the USP and the fourth web space as a safe zone where the 6R portal can be placed with no damage to the DBUN. Incising the skin and identifying the nerve before establishing arthroscopic portals or suture passage can prevent accidental sectioning or nerve strangulation (McAdams and Hentz, 2002; Tsu-Hsin Chen et al., 2006).

The DBUN is also used in preparing neurocutaneous flaps and as a donor site for nerve grafts. It provides more fascicles than other cutaneous nerves, less likelihood of developing neuromas, no sacrifice of major vascular axis and limited donor morbidity as the DBUN connects with the SBRN. It is relatively easy to dissect and provides up to 100 mm of nerve graft harvest (Bertelli and Pagliei, 1998; Casoli et al., 2004; Cavusoglu

et al., 2011). Detailed knowledge and appreciation of the anatomy, course and relations of the DBUN is important to properly design, harvest and apply neurocutaneous flaps.

1.3.3. Dorsal communication between the ulnar and radial nerve

It is not uncommon for the SBRN and the DBUN to communicate in the dorsum of the hand. However, the communicating branch between the ulnar and radial nerves has received limited attention in the literature. The presence of the communicating branch can alter the sensory innervation of the digits and complicate surgical procedures that have a dorsal approach to the hand or wrist (Loukas et al., 2011). Furthermore, the communicating branches in the dorsum of the hand may alter the response of conduction velocity tests and thus lead to misinterpretation of the results (Grinsell and Theile, 2005).

The incidence of the CB differs in the literature. Botte et al. (1990) found it in one specimen of 24 (4.16%), Auerbach et al. (1994) reported it in 15% of the 20 hands explored, while Loukas et al. (2008) investigated 200 formalin fixed adult cadaveric hands and reported the incidence of the communicating branch between the DBUN and the SBRN to be 60% (120/200). The communicating branch is classified according to its origin into 4 types:

Type I: the CB originated proximally from the radial nerve and joined the ulnar nerve distally.

Type II: the CB originated proximally from the ulnar nerve and joined the radial nerve distally.

Type III: the CB travelled perpendicularly between the radial and ulnar nerves.

Type IV: multiple CBs travelled between the two nerves.

The incidence rate of each type has been reported at 59.1%, 19.1%, 3.3% and 18.3% for type I, II, III, and IV respectively (Loukas et al., 2008).

Using the DBUN in nerve grafts is believed to cause limited donor site morbidity. This could be explained by the communicating branches in the dorsum of the hand and the overlap between the cutaneous nerves that would compensate the sensory loss (Bertelli and Pagliei, 1998; Cavusoglu et al., 2011). Tubbs et al. (2005) suggested releasing the TCL in carpal tunnel syndrome by a dorsal approach between the proximal fourth and fifth metacarpals. Such an approach may put the CB at risk of injury.

Using morphometric data, Loukas et al. (2008) were able to determine an area where the CB is at risk of injury during dorsal surgical approaches. The CB was found between 12% and 78% of the distance between the bistyloid line and the fourth MCP joint. Moreover, 85% of the CBs were found between 28% and 60% of the same distance outlining the high risk area (Figure 1.18). Mok et al. (2006) investigated the cutaneous innervation of the dorsum of the hand in 30 cadavers and outlined a safe-zone where surgical procedures can be performed with minimal risk to major nervous structures (Figure 1.19). The study, however did not mention the communicating branch between the ulnar and radial nerve and the proposed safe-zone corresponds exactly with the risk-zone proposed by Loukas et al. (2008).

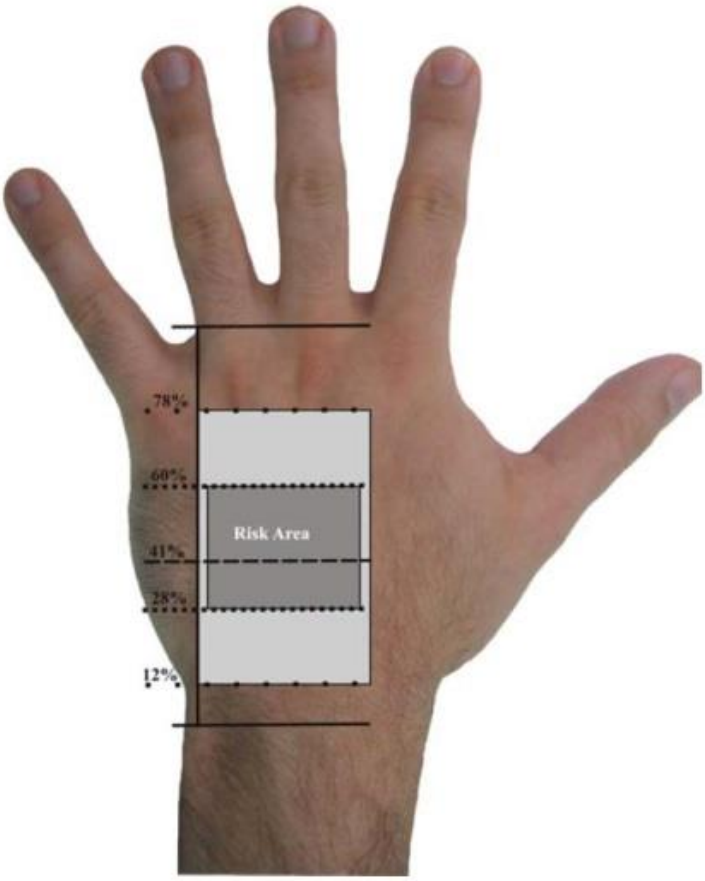

Figure 1.18: Risk area where the dorsal CB is most likely to be found as described by Loukas et al. (2008). Light grey area indicates the range where all dorsal CB were found; Dark grey area indicates where the majority (85%) of the dorsal CB were found; mean percentage is indicated by the dotted line at 41% (Loukas et al., 2008).

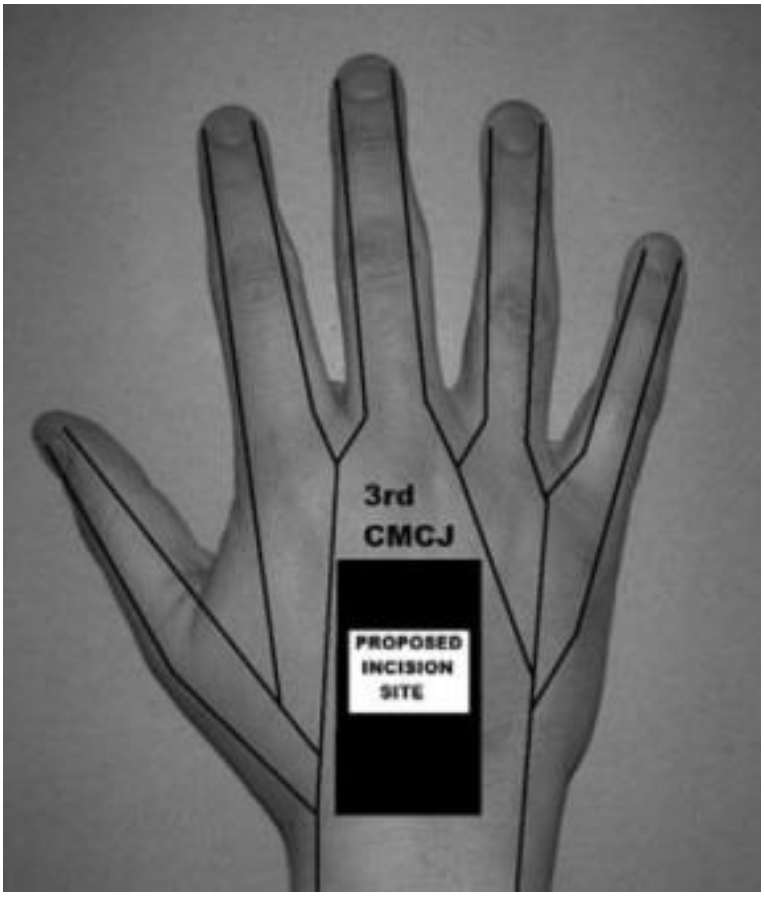

Figure 1.19: The suggested safe area where no major nerve passes as described by Mok et al. (2006). Dark lines outline the course of the SBRN supplying the lateral two and half digits and the DBUN supplying the medial two and half digits; CMCJ, metacarpophalangeal joint (Mok et al., 2006).

1.4. Project objectives:

Reducing postoperative complications and increasing patients satisfaction is a fundamental goal for hand surgeons. Understanding and appreciating the close and sensitive anatomical relationships in the hand is vital to achieving this goal. The literature often reports different descriptions with regard to the main nerves supplying the sensory innervation of the hand. This project will investigate the main nerves providing the cutaneous innervation to the hand: the PCBMN, CDNs, UN in the palm; and SBRN, DBUN and LABCN in the dorsum of the hand. It aims to describe their

common course and branching patterns, examine the prevalence of anatomic variations and their clinical significance. Furthermore, it aims to investigate possible CB, their prevalence and their impact in clinical settings. This project aims to achieve the following:

1. Outline the common course and the branching pattern of the cutaneous nerves that supply the hand and discuss possible variations in their course.
2. Categorize branching patterns and produce a classification system.
3. Investigate possible relations and associations between patterns of distributions.
4. Investigate dorsal-palmar communication between the nerves that supply the dorsal and palmar surfaces of the hand.
5. Describe the distribution and branching pattern of the SBRN, DBUN in the dorsum of the hand and their relationship to the wrist and distal area of the forearm.
6. Determine the incidence rate of the communicating branch(es) between the SBRN and DBUN, its/their pattern, and common locations.
7. Describe the distribution and branching pattern of the PCBMN in the palm and its relationship to the distal area of the forearm and wrist.
8. Describe the distribution and branching pattern of the MN and UN in the palm and their relationship to the wrist and distal area of the forearm.
9. Determine the incidence rate of the communicating branch(es) between the MN and UN in the hand, its/their pattern, and common location.
10. Discuss the impact of the distribution and branching patterns of the cutaneous nerves on surgical and diagnostic procedures.

2. Methods

2.1. Sample

All cadavers used for this study were obtained from the Centre for Anatomy and Human Identification (CAHID), University of Dundee. All dissections were carried out in CAHID's anatomy laboratory. The samples were collected during the period October 2011 to April 2013. All cadavers were musculoskeletally mature adults. Arms were not amputated and no signs of trauma or pathology were noticed. Measurements were taken for each dissection by one observer.

During the study period, measurements were obtained from 160 formalin-fixed cadavers. Table 2.1 summarizes the number of hands dissected during each academic year.

Table 2.1: Number of hands dissected during the study

Time Period	No. of hands		Total
	Males	Females	
October 2011- April 2012	29	48	77
October 2012-April 2013	41	42	83
Total	70	90	**160**

2.2. Anatomical Landmarks

Different landmarks were chosen for the palmar and dorsal surfaces of the hand. Landmarks were chosen because they are easily palpable and relatively constant among individuals. Furthermore, the landmarks were selected for their clinical relevance and significance. In the dorsum of the hand, the radial (RSP) and ulnar (USP) styloid processes, Lister's tubercle (LT), the third metacarpophalangeal (MCP) joint and the middle of the bistyloid line (BSL) were chosen. RSP was identified at the distal radial

end of the radius, palpitated through the anatomical snuff box. The USP was palpated at the distal medial end of the ulna. A horizontal line connecting between the RSP and USP was identified as the BSL. A thread was extended between the two styloid processes and then measured representing the length of the BSL. This measurement was used to determine the middle of the BSL. LT was identified as a bony palpable projection at the distal posterior surface of the radius (Figure 2.1).

Moreover, the distal wrist crease (WC), the distal margin of the TCL, the middle of the scaphoid tubercle, the proximal margin of the pisiform bone, the third MCP joint and the middle of the BSL were selected as landmarks for the palmar measurements (Figure 2.2). The scaphoid tubercle was palpated on the radial aspect of the base of the hand just distal to the distal WC, the middle of the scaphoid tubercle was estimated. The pisiform was identified on the medial base of the hand, palpitated just distal to the WC. The TCL was identified deep to the palmar aponeurosis making the roof of the carpal tunnel. The distal edge was determined at the level of the most proximal point at the distal margin. Table 2.2 lists the anatomical landmarks and their abbreviations used for this study.

Table 2.2: Summary of the anatomical landmarks used in this study

No.	Landmark	Abbreviation	Location
1.	Radial styloid process	RSP	Dorsal landmark
2.	Ulnar styloid processes	USP	Dorsal landmark
3.	Lister's tubercle	LT	Dorsal landmark
4.	The third metacarpophalangeal joint	3rd MCP joint	Dorsal & palmar landmark
5.	Middle of the bistyloid line	BSL	Dorsal & palmar landmark

No.	Landmark	Abbreviation	Location
6.	The distal wrist crease	WC	Palmar landmark
7.	The distal margin of the transverse carpal ligament	TCL	Palmar landmark
8.	The middle of the scaphoid tubercle	ST	Palmar landmark
9.	The proximal margin of the pisiform bone	PB	Palmar landmark

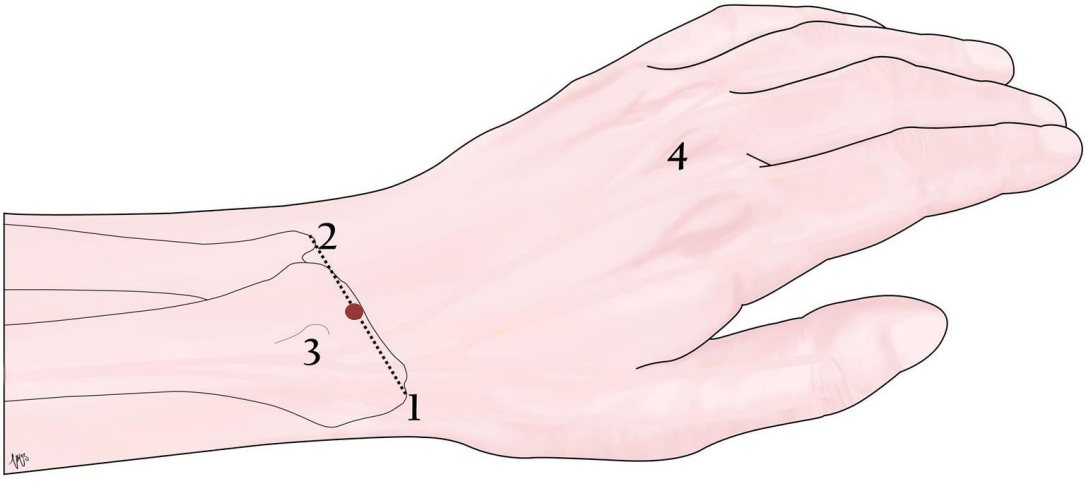

Figure 2.1: Dorsal landmarks used in this study. (1) Radial styloid process; (2) Ulnar styloid process; (3) Lister's tubercle; (4) The third metacarpophalangeal joint; dotted horizontal line connecting between the radial styloid process and the ulnar styloid process indicated the bistyloid line; Red dot indicates the middle of the bistyloid line.

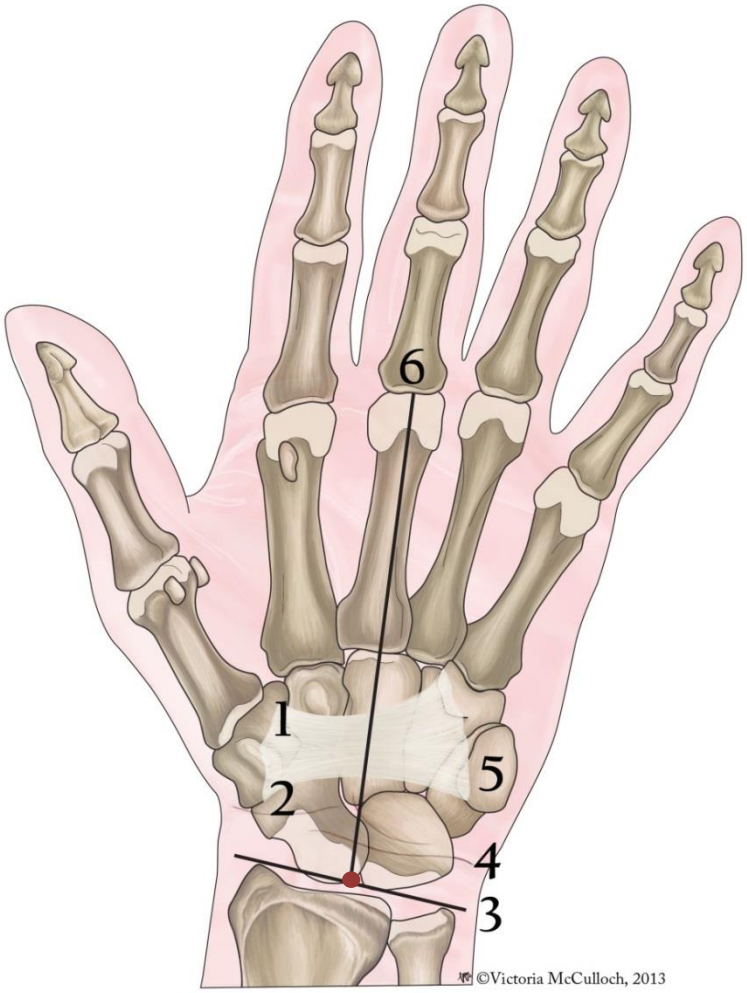

Figure 2.2: Palmar landmarks used in this study. (1) Transverse carpal ligament; (2) Scaphoid tubercle; (3) Bistyloid line; (4) Distal wrist crease; (5) Pisiform; (6) Third metacarpophalangeal joint; red dot indicates the middle of the bistyloid line.

2.3. Measurements

Measurements were taken by a single observer using digital calipers (Electronic Digital Caliper Model DC200-PW, Jade products) and recorded to the nearest 0.1 mm. Positive values are distal, negative values are proximal to the preselected landmarks. Results are expressed as means, standard deviations, maximum and minimum values.

Because of the embalming process used in this study, some pitfalls were noticed that might have affected the measurements obtained. Although the embalming fluid (formalin) does not have a significant effect on the length of the muscles while they are still fixed on the skeleton, it can still fixate the joints. With arthritic hands being common in the age group of the cadavers used in this study, full extension of the hands during measurement taking was not achieved without difficulty (Cutts, 1988; Waghmare and Sonar, 2012). It was also noted that once dissected, nerves can shrink as they are exposed to air and dry out slightly changing their position. Moreover, hand sizes differ between males and females. It also differs between individuals of the same gender. Measurements were expressed as relative values overcoming the possible influence of fixation solution on human tissue and the different body sizes in the studied sample except for some measurements taken for the UN, SBRN, and DBUN[1]. The distance between the third metacarpophalangeal joint and the middle of the BSL and WC were used as a reference, with measurements being expressed as a percentage of these distances.

Furthermore, because nerves were fully dissected from their surrounding fat and connective tissue, it is possible that the individual nerves may have changed in their position. However, care was taken to keep the nerves attached proximally to the

[1] Next section explain the measurements taken for each nerve in detail

antebrachial fascia where they became cutaneous or to the main trunk they originated from and distally to their respective final destination at the metacarpophalangeal joint level.

To test the intra-observer reliability, 16 samples were randomly selected from each phase were selected and measurements repeated (see Table 3.2). Differences between the original and repeated measurements were statistically tested by running Kruskal-Wallis test to check for the observer error. A result is considered statistically significant when $P<0.05$.

2.4. Dissection process

Skin was removed from the distal half of the forearm as far as the metacarpophalangeal joints. An incision was made on the lateral side of the distal forearm crossing the wrist area to the thumb; skin was dissected from proximal to distal (Figure 2.3 and 2.4). While cadavers were in the supine position, the MN was identified in the distal third of the forearm between the tendons of flexor carpi radialis and palmaris longus. The PCBMN was identified in the distal forearm by careful dissection around the main trunk of the median nerve (Figure 2.5 A). It was more difficult to identify the nerve in particularly wet specimens where the nerve and the surrounding fat seemed undistinguishable. In such cases, the distal forearm was packed with paper towels to absorb excess fluid.

Furthermore, the palmar aponeurosis was dissected and reflected, palmaris brevis resected, fascia and fat removed to visualize the superficial structures of the palm. The roof of Guyon's canal (palmaris brevis) was reflected medially or removed in some cases where it was less developed. The TCL was cut on its medial side if needed. Care was

taken not to damage the ulnar or median digital nerves and any possible communicating branches. The surplus fatty tissue was removed for better visualization of the nerves; however, the superficial palmar arch and the common digital arteries were kept and their relationship to the common digital nerves or any communicating branches noted (Figure 2.5 and 2.6).

In the dorsal surface of the hand, from the same incision previously made for the palmar surface, skin covering the dorsum of the hand to the metacarpophalangeal joints was removed. The cephalic vein was identified and marked. The rest of the dorsal veins were only removed to better visualize the nerves, otherwise they were preserved. The SBRN was identified as it became subcutaneous between the tendons of brachioradialis and extensor carpi radialis longus. Subcutaneous fatty tissue was removed and the nerve traced (Figure 2.7). DBUN, if present, was identified in the dorsum of the hand at the location where the SBRN nerve fibres stop. The DBUN, if present, was also identified, preserved and dissected in the dorsum of the hand.

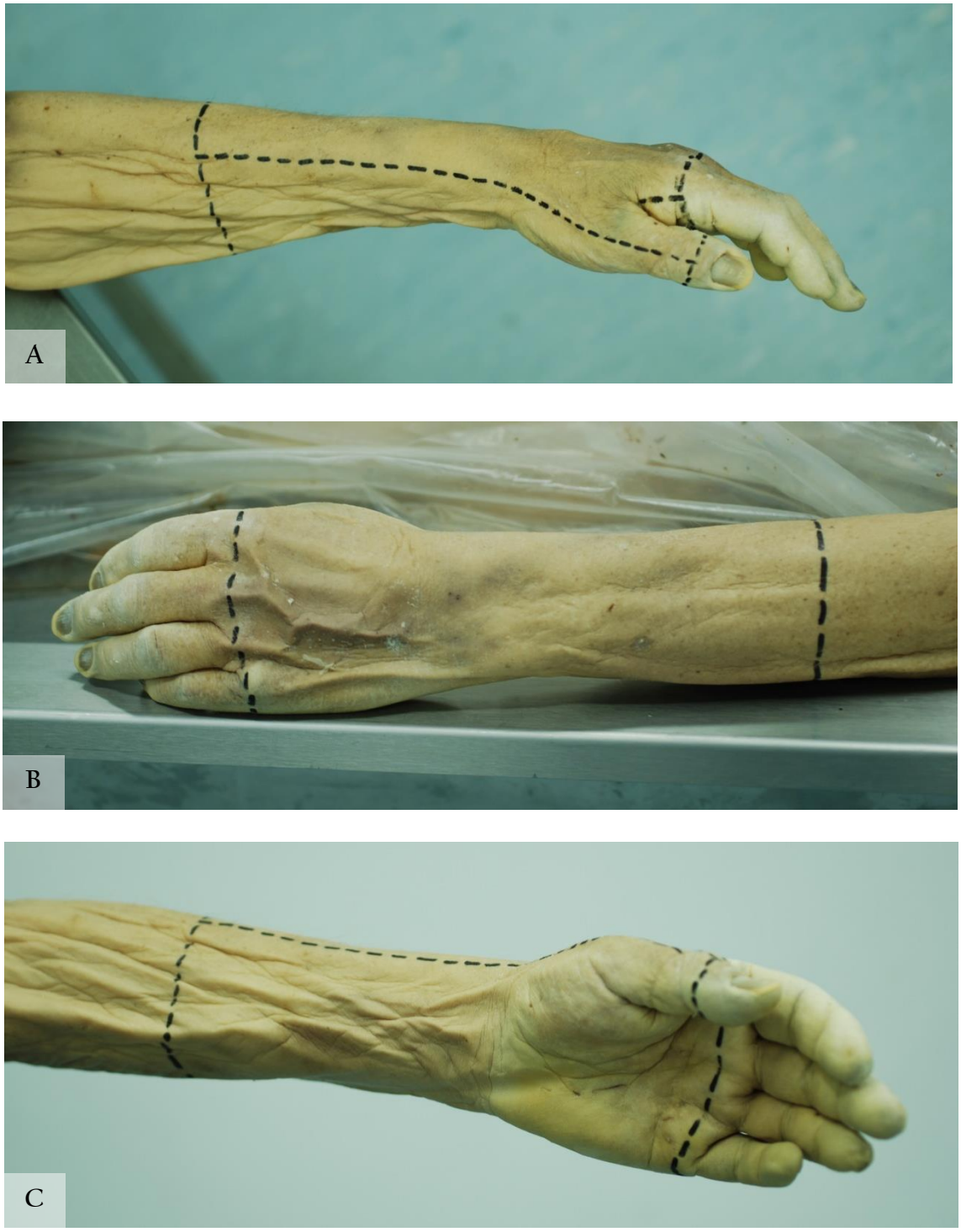

Figure 2.3: Skin incisions outlined in the distal forearm and hand. (A) Lateral hand view; (B) Posterior forearm and dorsal hand view; (C) Anterior forearm and palmar hand view.

Figure 2.4: Skin removed in the distal forearm and hand. (A) Lateral hand view; (B) Posterior forearm and dorsal hand view; (C) Anterior forearm and palmar hand view.

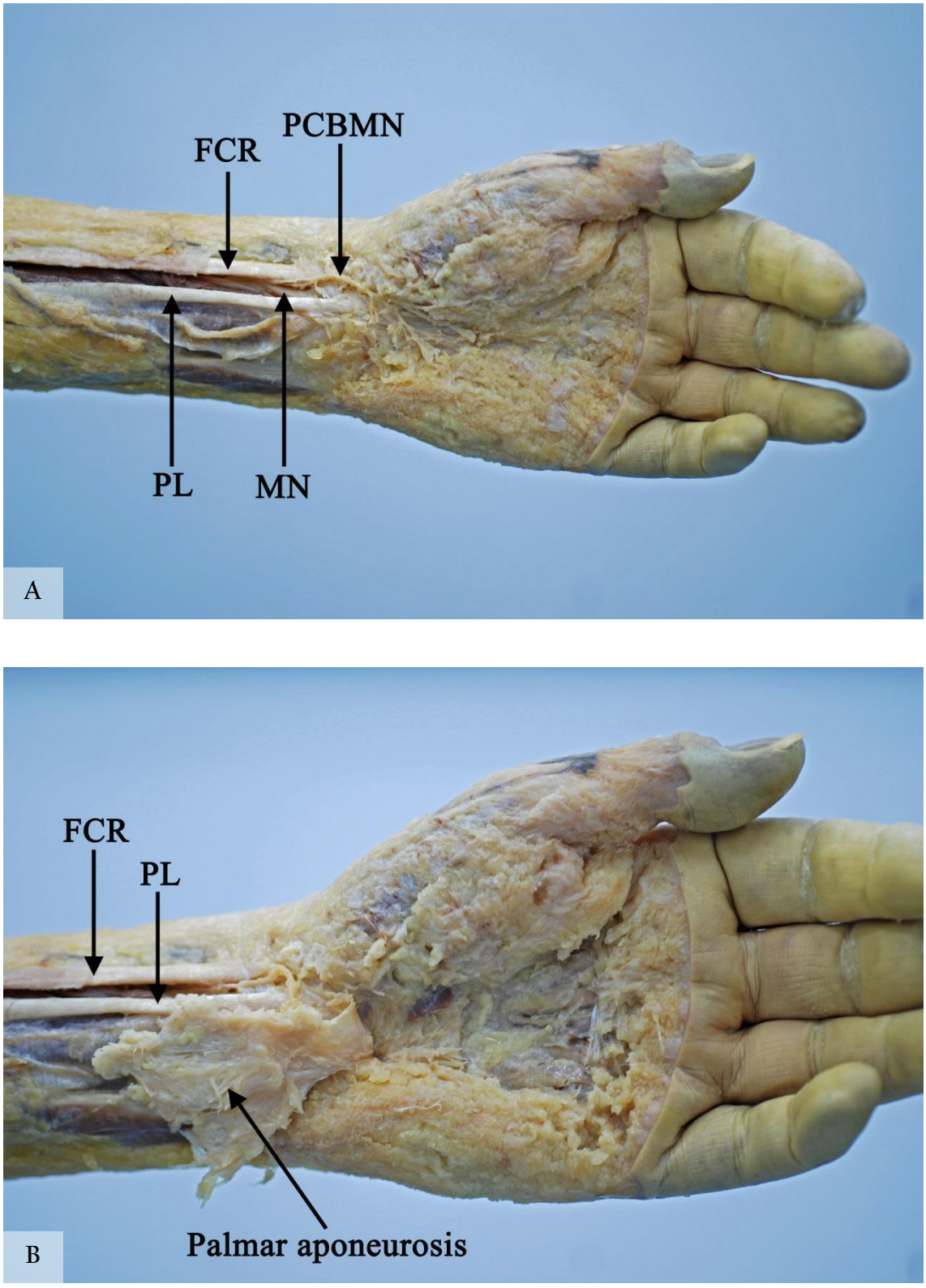

Figure 2.5: Dissection of the palmar surface of the hand. (A) Identifying the median nerve (MN) and the palmar cutaneous branch of the median nerve (PCBMN) at the distal forearm. (B) Reflecting the palmar aponeurosis. FCR, flexor carpi radialis; PL, palmaris longus.

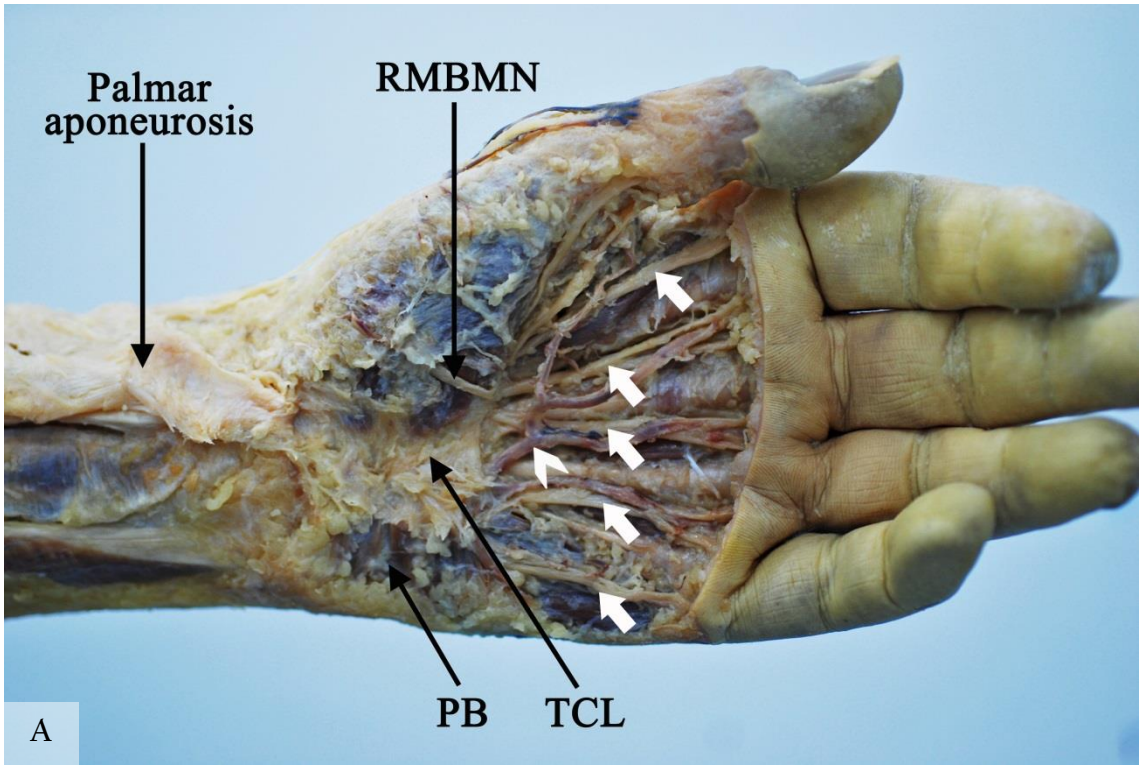

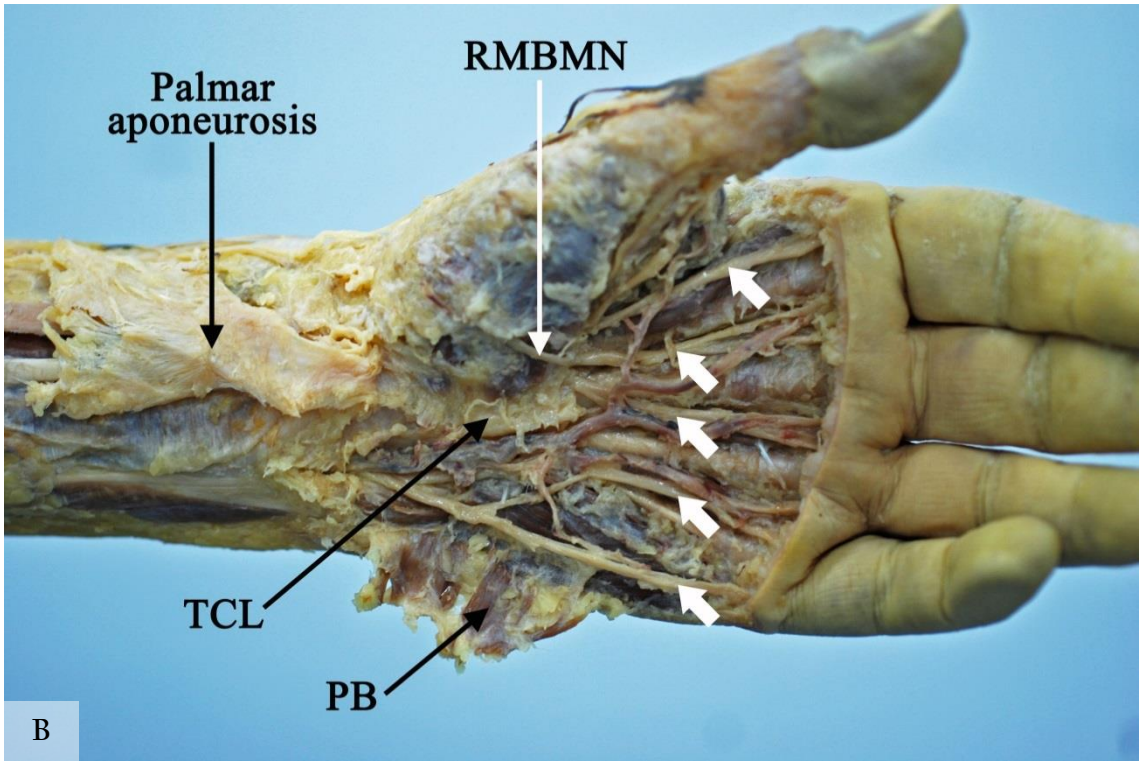

Figure 2.6: Dissection of the palmar surface of the hand. (A) Removing the surplus fascia and fat to view superficial palmar structures. (B) The palm after dissection and opening of Guyon's Canal. TCL, transverse carpal ligament; PB, palmaris brevis; RMBMN, recurrent motor branch of the median nerve; white bold arrows indicate the digital nerves; white arrow head indicates the superficial palmar arch.

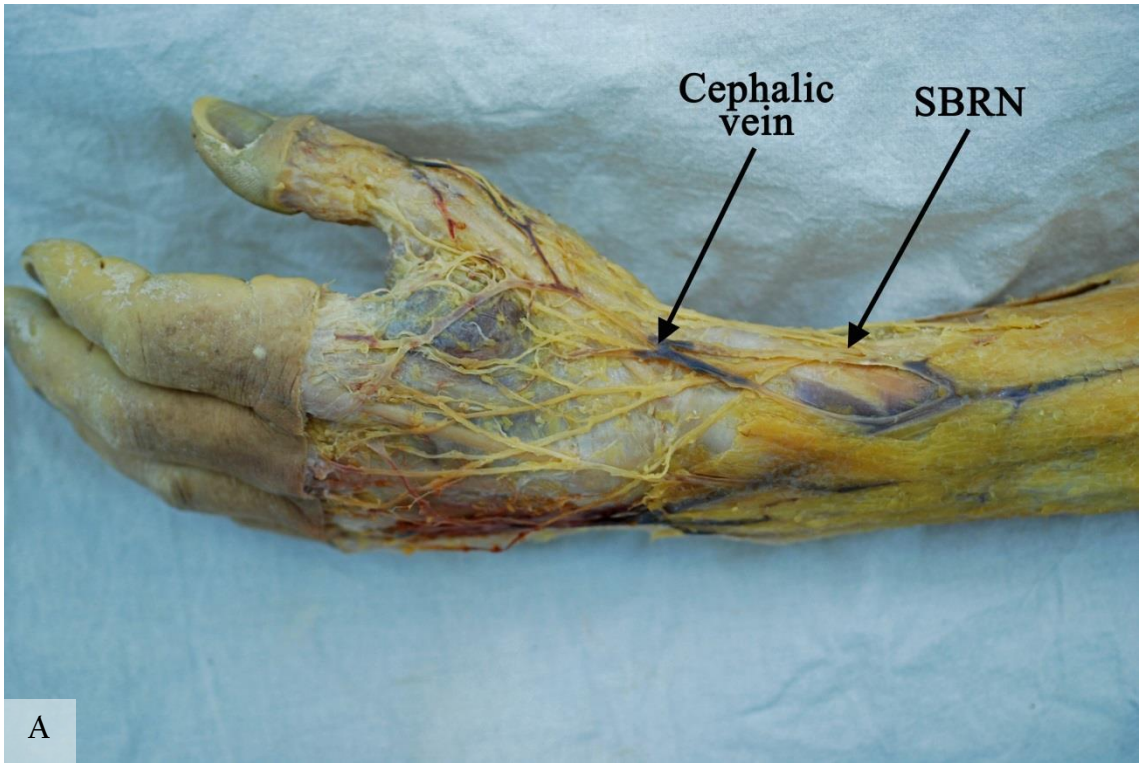

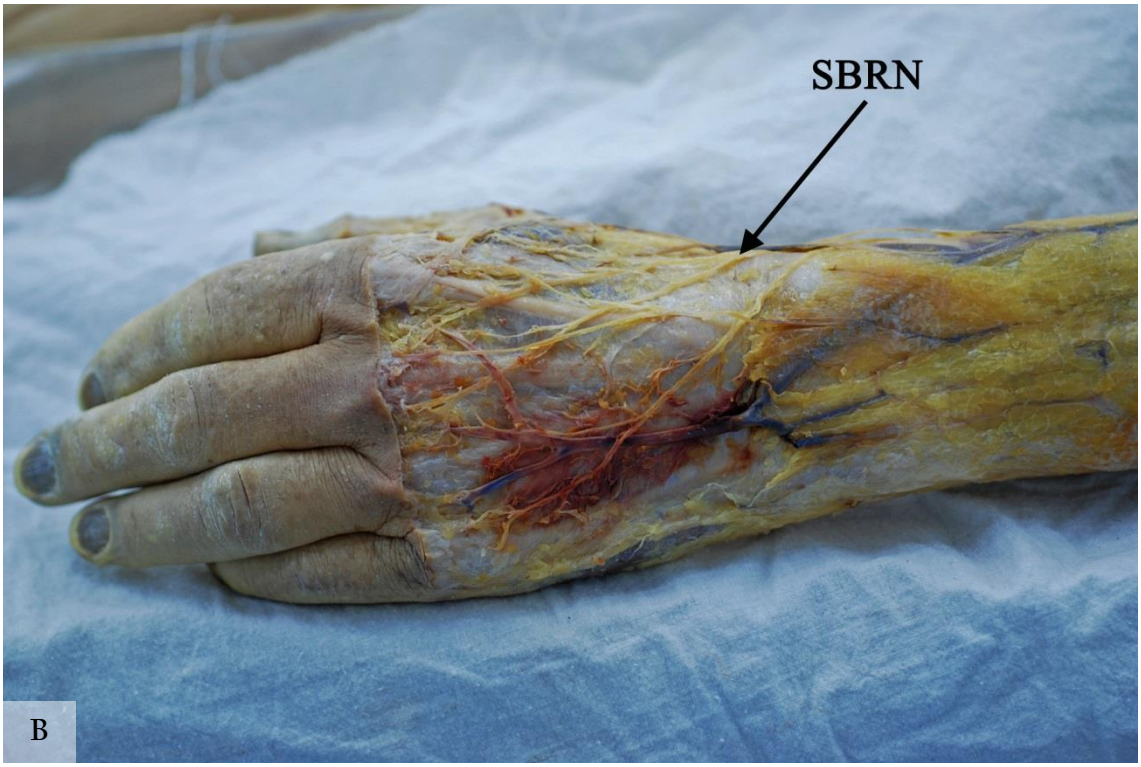

Figure 2.7: Dissection of the dorsal surface of the hand by removing the surplus fascia and fat to better view structures of interest. (A) Lateral hand view. (B) Dorsal hand view. SBRN, superficial branch of the radial nerve.

The origin of the PCBMN and the detachment point from the main trunk of the MN were marked and measurements were taken to the distal WC. The point of origin was defined as the point where the PCBMN could be seen as a separate nerve trunk but still coursing in the same neural sheath as the MN. The point of detachment was defined when the PCBMN separated from the MN neural sheath (Figure 2.8). The PCBMN was traced into the palm and small branches were preserved. The anatomical course of the nerve and its relationship to palmaris longus, flexor carpi radialis, and the PCL was noted. The nerve's tunnel was identified when the nerve coursed between the fibres of the PCL proximal to the WC (Figure 2.9). The distal end of the tunnel was identified as the nerve becomes subcutaneous between the fibres of the palmaris longus blending with the palmar aponeurosis. The length of the tunnel was measured. Branching patterns of the PCBMN were classified based on the number of sub-branches coming off the PCBMN and incidence rates were calculated.

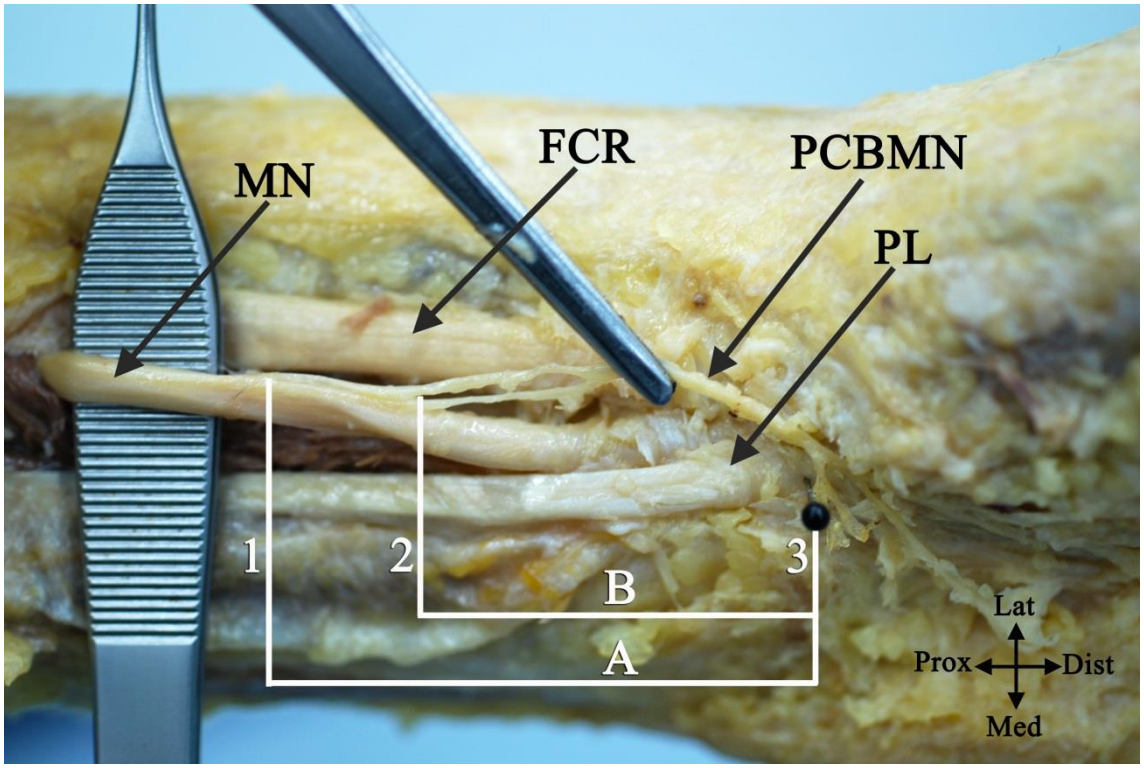

Figure 2.8: Distances measured of the palmar cutaneous branch of the median nerve (PCBMN). (1) Origin point of the PCBMN; (2) Detachment point of the PCBMN from the main trunk of the median nerve (MN); (3) Level of the wrist crease (WC) also indicated by the black pin; A, distance between the origin point and the WC; B, distance between the detachment point and the WC; PL, palmaris longus; FCR, flexor carpi radialis; Lat, lateral; Med, medial; Dist, distal; Prox, proximal.

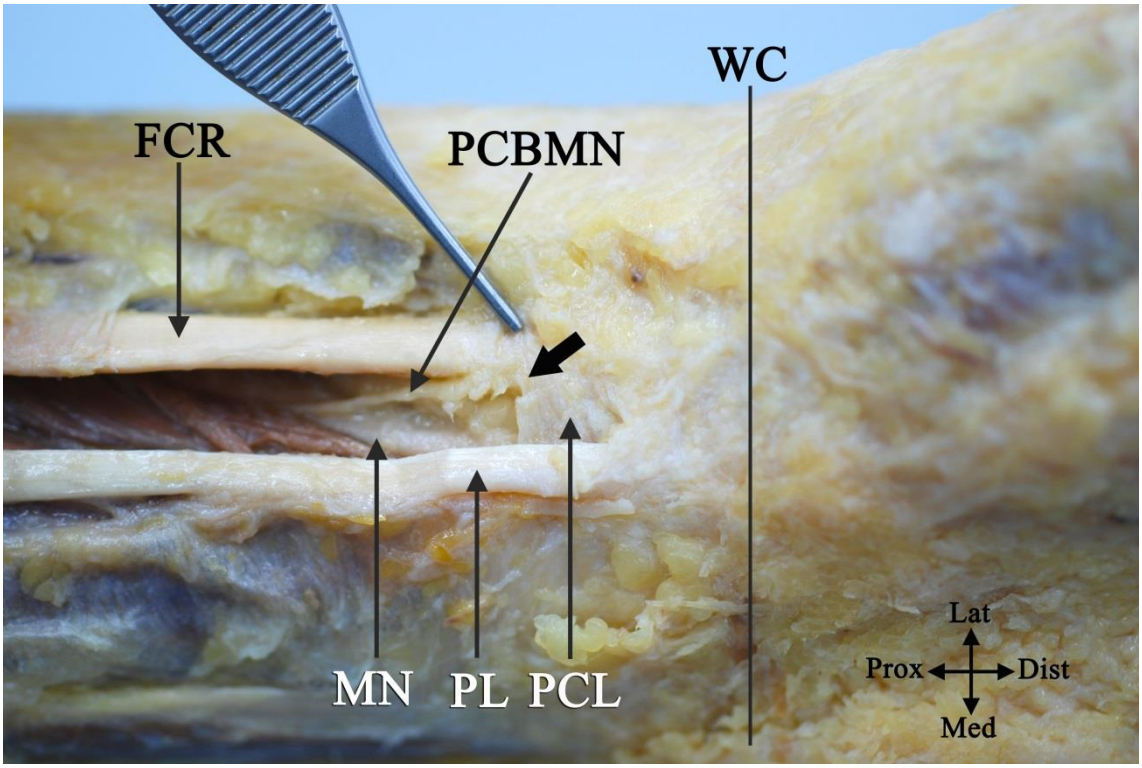

Figure 2.9: The palmar cutaneous branch of the median nerve (PCBMN) entering its tunnel indicated by the bold arrow through the fibres of the palmar carpal ligament (PCL). WC; wrist crease level; PL, palmaris longus; FCR, flexor carpi radialis; MN, median nerve; Lat, lateral; Med, medial; Dist, distal; Prox, proximal.

The first common digital nerve branching pattern was investigated. The point of CDNs division to PDNs was marked and distances perpendicular to the level of the scaphoid tubercle and the middle of the BSL measured. The distance between the branching point of the fourth CDN into the PDNs of the lateral side of the little finger and the medial side of the ring finger was perpendicular to the proximal edge of the pisiform and the middle of the BSL were also measured (Figure 2.10 and Figure 2.11).

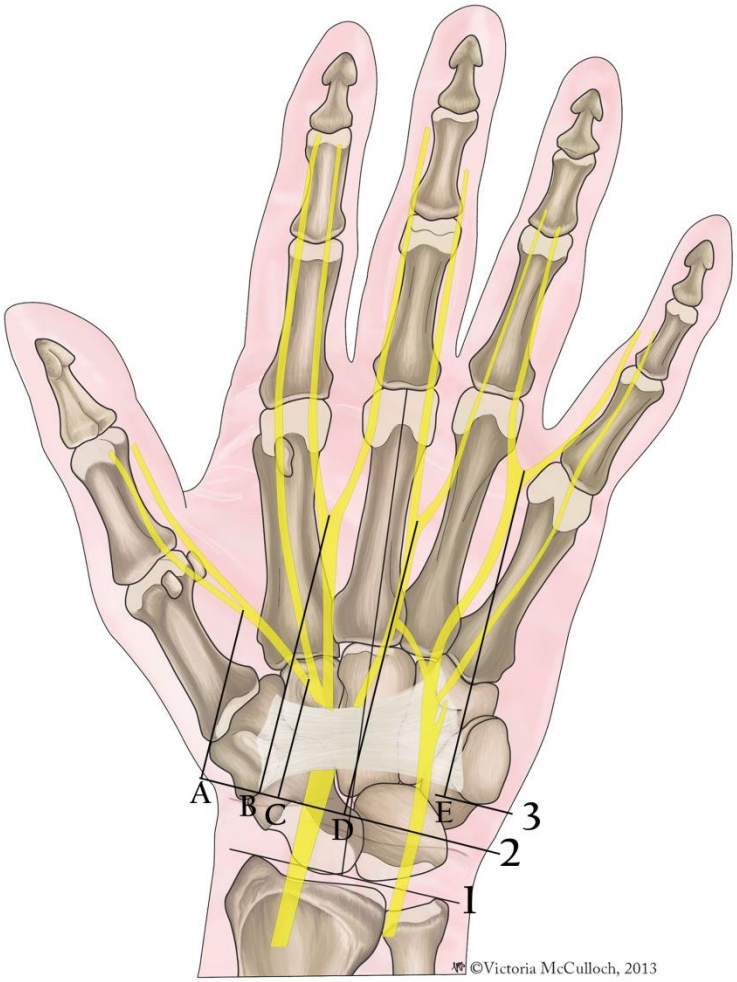

Figure 2.10: Distances measured of the common digital nerves (CDNs) division points into proper digital nerves. (1) Bistyloid line; (2) Scaphoid tubercle (ST) level; (3) Proximal edge of the pisiform; A, First CDN second division point to ST; B, Second CDN division point to ST; C, First CDN first division to ST; D, Third CDN division point to ST; E, Fourth CDN division point to distal edge of pisiform.

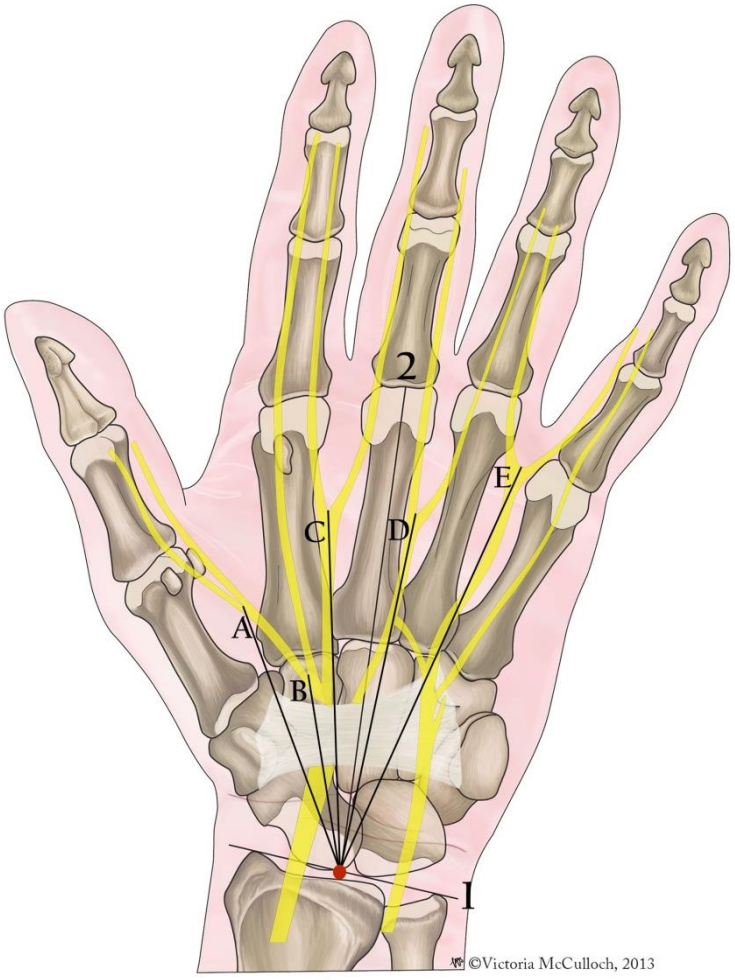

Figure 2.11: Distances measured of the common digital nerves (CDNs) division points into proper digital nerves. (1) Bistyloid line (BSL); (2) Third metacarpophalangeal joint; A, First CDN second division point to BSL; B, First CDN first division to BSL; C, Second CDN division point to BSL; D, Third CDN division point to BSL; E, Fourth CDN division point to BSL.

The ulnar nerve in Guyon's canal was also investigated. The UN point of division into deep and superficial branches was measured to the proximal margin of the pisiform (Figure 2.12). Communicating branches between the 4th CDN and the PDN to the little finger; the deep division of the ulnar nerve and the PDN to the little finger; and the DBUN and the UN or its branches were noted.

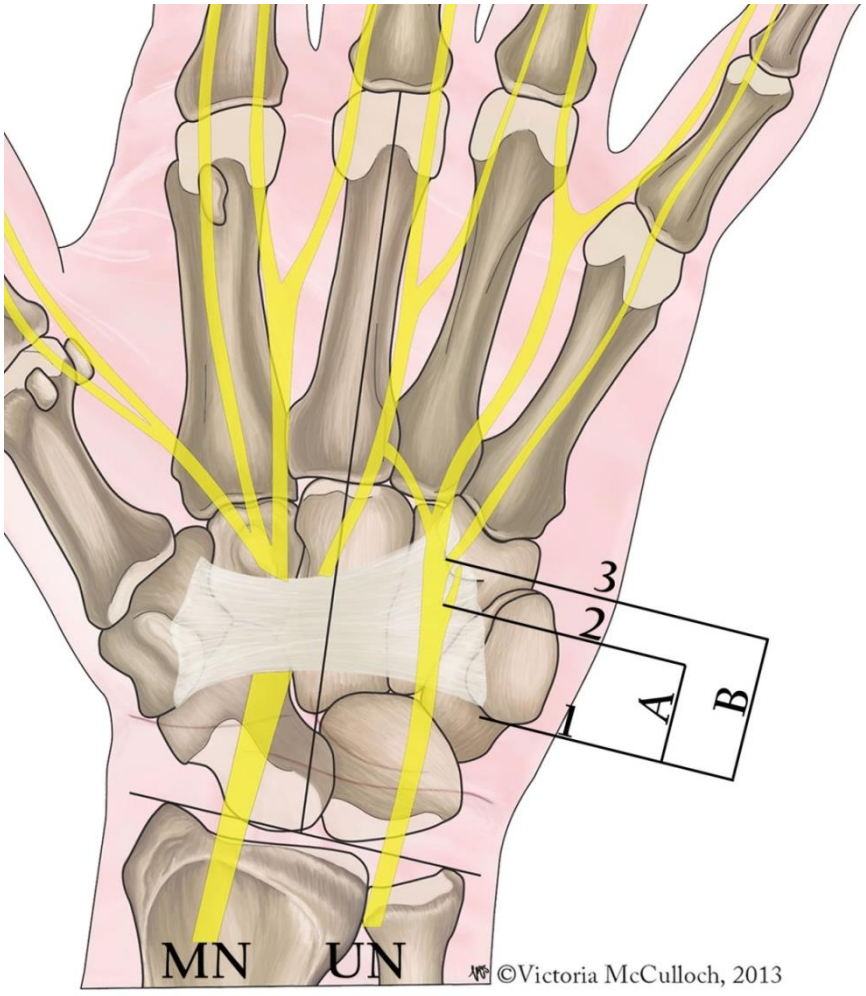

Figure 2.12: Distances measured of the ulnar nerve (UN) division points to the proximal edge of the pisiform. (1) The proximal edge of the pisiform; (2) The division point of the UN into deep and superficial branches; (3) The division point of the superficial branch into a proper digital nerve (PDN) to the medial side of the little finger and the fourth common digital nerve (CDN); A, The distance between the division point of the UN into deep and superficial divisions and the proximal edge of the pisiform; B, The distance between the division point of the superficial branch of the UN into a PDN to the medial side of the little finger and the fourth CDN to the proximal edge of the pisiform; MN, Median nerve; UN, Ulnar nerve.

When present, the communicating branch between the median and ulnar nerve was also investigated. The proximal and distal attachment points were marked and distances to the distal WC, distal margin of the TCL and the middle of the BSL measured (Figures 2.13-2.15). The angle at which the CB originated from the main trunk

and the CB length were measured. The angle was measured by using a protractor. The CBs were grouped and classified according to the proximal and distal attachment points. Distances from the third MCP joint to the WC and the middle of the BSL were measured. Results were expressed as relative values to the distances between the third MCP joint to the WC and the middle of the BSL. Based on the proximal and distal insertion points the CBs were plotted and a risk area where the CB is most commonly found was determined.

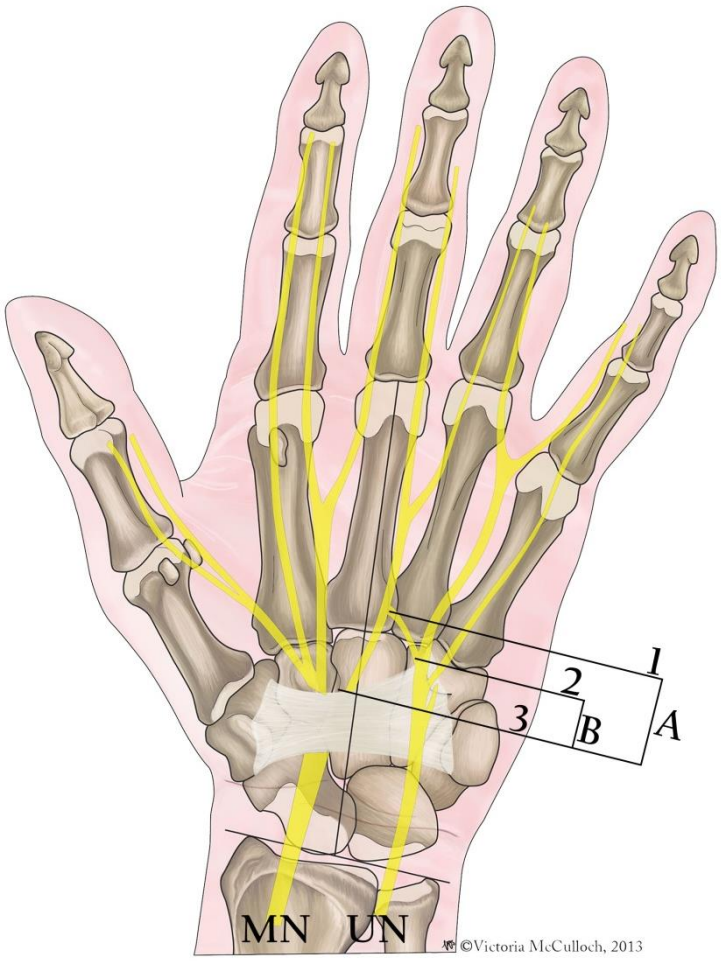

Figure 2.13: Distances measured of the palmar communicating branch (CB) with reference to the transverse carpal ligament (TCL). (1) Distal attachment point of the palmar CB; (2) Proximal attachment point of the palmar CB; (3) The distal margin of the TCL; A, distance between the distal attachment point and the TCL; B, distance between the proximal attachment point of the palmar CB and the TCL; MN, median nerve; UN, ulnar nerve.

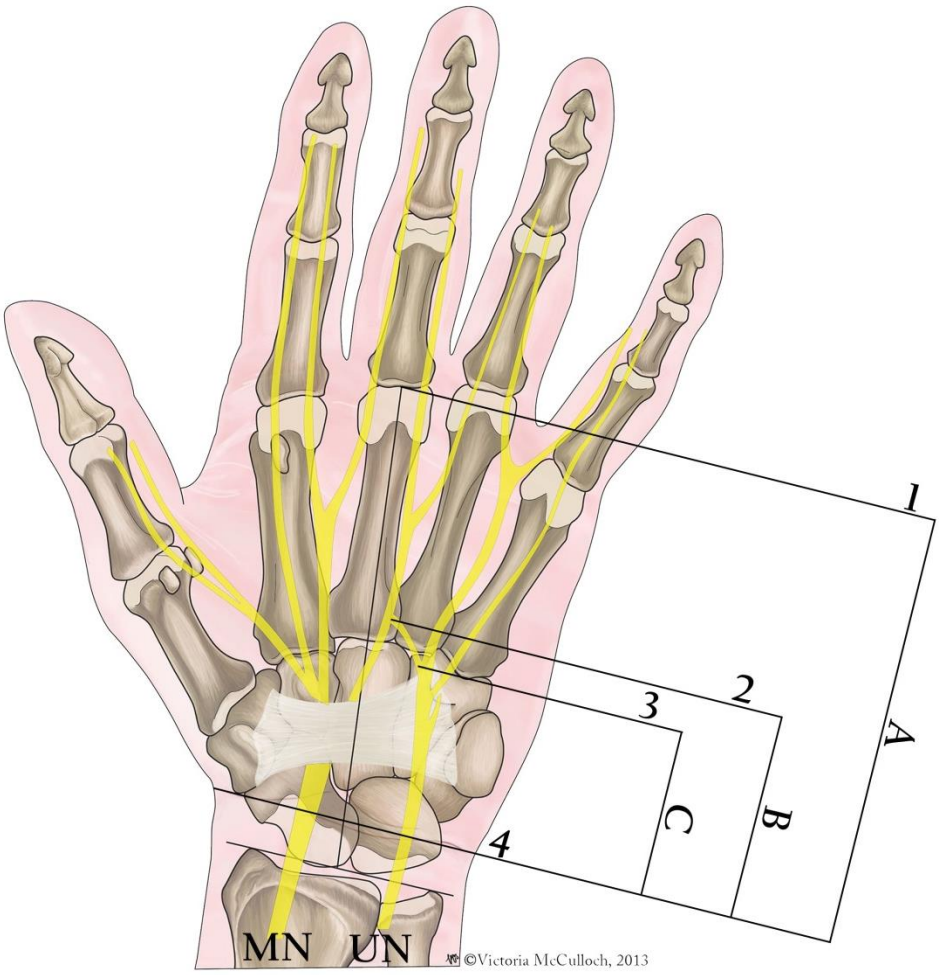

Figure 2.14: Distances measured of the palmar communicating branch (CB) with reference to the wrist crease (WC). (1) Third metacarpophalangeal joint; (2) Distal attachment point of the palmar CB; (3) Proximal attachment point of the palmar CB; (4) The WC; A, distance between the third MCP joint and the WC; B, distance between the distal attachment point and the WC; C, distance between the proximal attachment point of the palmar CB and the WC; MN, median nerve; UN, ulnar nerve.

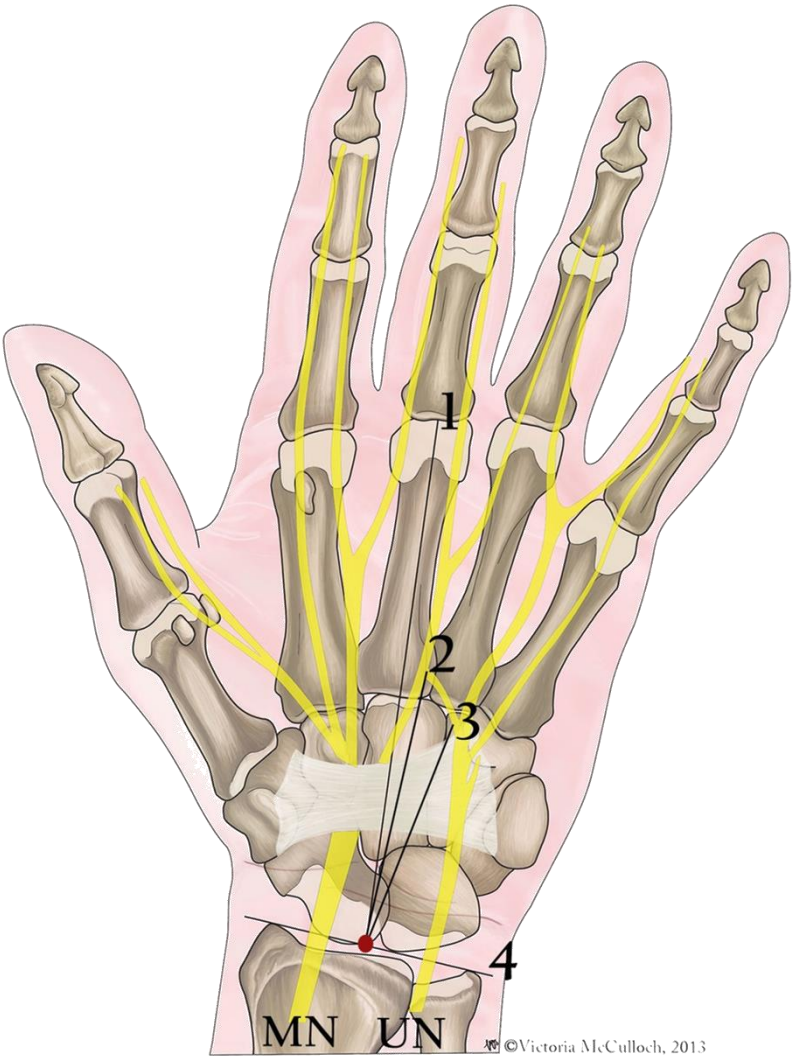

Figure 2.15: Distances measured of the palmar communicating branch (CB) with reference to the middle of the bistyloid line (BSL) (4). (1) The distance between the third MCP joint and the middle of the BSL; (2) The distance between the distal attachment point of the palmar CB and the middle of the BSL; (3) The distance between the proximal attachment point of the palmar CB and the middle of the BSL; red dot, middle of the BSL; MN, median nerve; UN, ulnar nerve.

In the dorsum of the hand, the SBRN and the DBUN were investigated. The point of piercing the antebrachial fascia and the first, second and third major branching points were noted and distances to the RSP were measured. Care was taken to preserve small branches and any connections between the SBRN and the DBUN and/or LABCN. The

total length of the radius was measured from the radial head to the RSP. The closest passing branch to LT was marked and the horizontal distance perpendicular to the long axis of the arm to the LT was measured (Figure 2.16). The distance between the middle of the closest palmar and dorsal branches to the RSP was measured. A point 25 mm distal to the RSP in line with the longitudinal margin of the lateral side of the index finger was marked and the distances to the closest palmar and dorsal branches documented to investigate a safe incision outline described by Robson et al. (2008). The relationship of the SBRN with the cephalic vein was noted (Figure 2.17). Branches passing over the anatomic snuff box were noted.

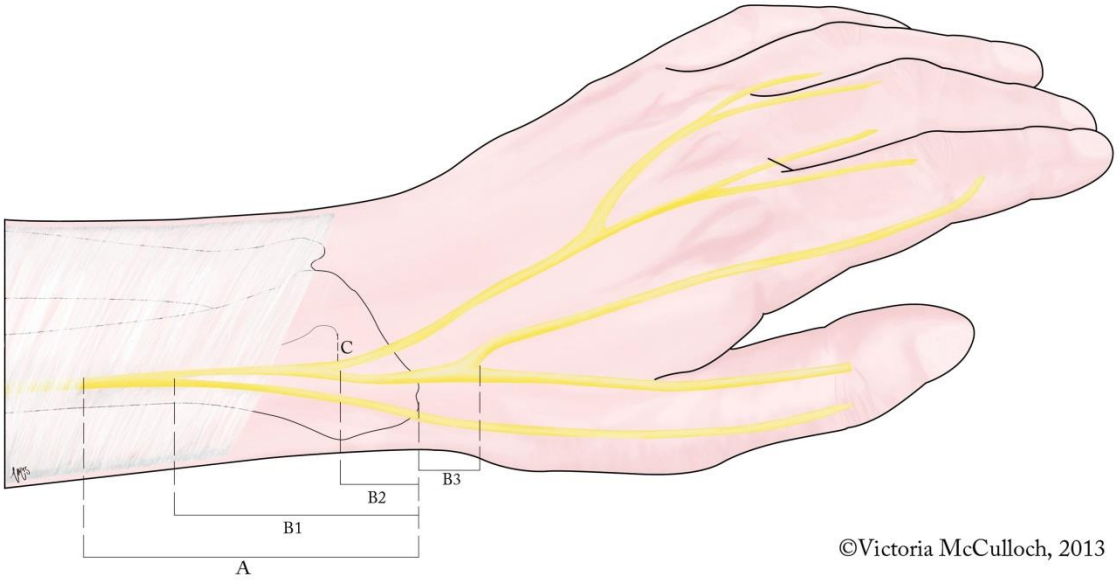

Figure 2.16: Anatomic measurements taken for the superficial branch of the radial nerve (SBRN). (A) Distance of the point of SBRN piercing the fascia to the radial styloid process (RSP); (B1) First, (B2) Second, (B3) Third major branching point to the RSP; (C) distance of the closest branch to Lister's tubercle.

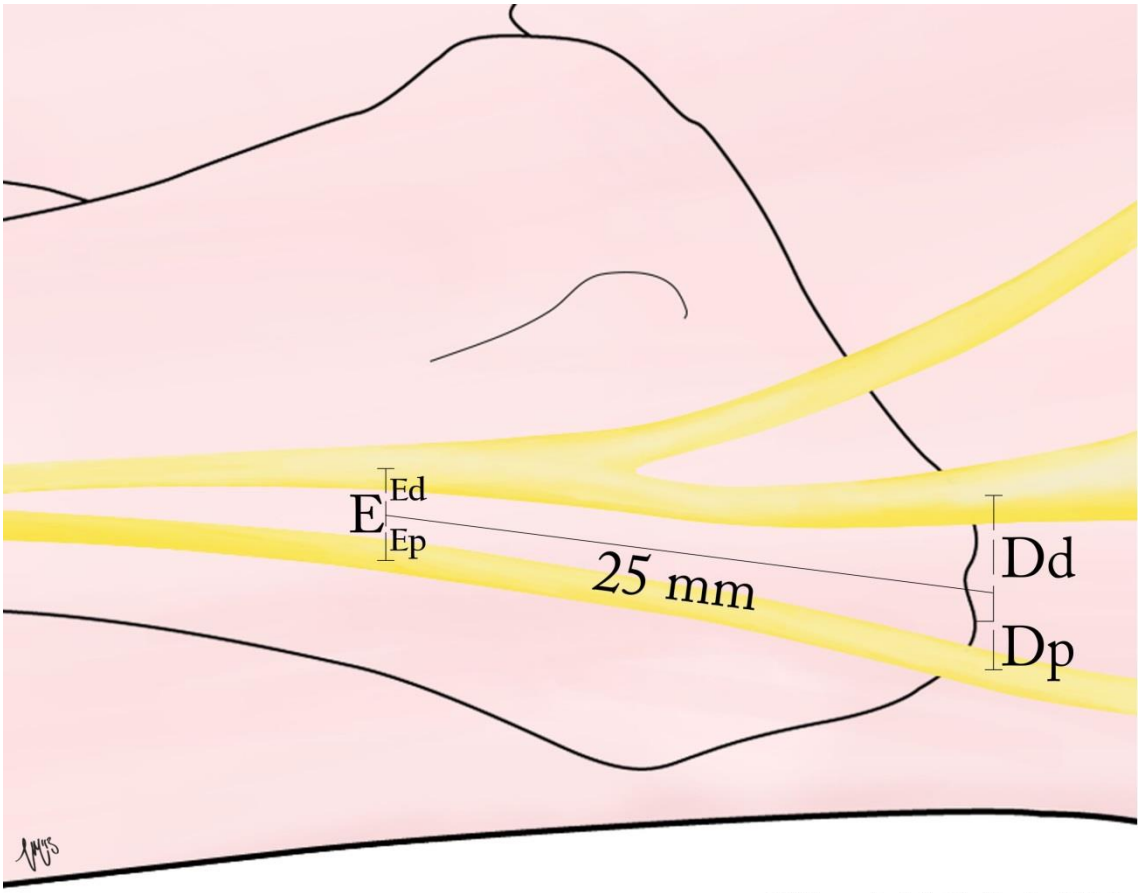

Figure 2.17: Anatomic measurements taken for the closest palmar and dorsal branches of the superficial branch of the radial nerve (SBRN). (Dp) The closest palmar branch to the radial styloid process (RSP); (Dd) The closest dorsal branch to the RSP; (E) A point 25 mm from the RSP; (Ep) The closest palmar branch to a point 25 mm to the RSP; (Ed) The closest dorsal branch to a point 25 mm to the RSP.

The DBUN was identified on the ulnar side of the wrist and traced proximally to the origin point from the main trunk of the ulnar nerve. The distance of the nerve's origin to the ulnar styloid process (USP) and the pisiform was measured. The nerve then was traced distally, patterns were preserved and first and second major branching points recorded to the USP (Figure 2.18). The point where the nerve pierced the fascia to become subcutaneous on the medial side of the wrist was noted and the distance to the USP measured. The total length of the ulna from the olecranon to the styloid process

was measured. The distance between the USP and the distal end of the fourth webspace between the medial side of the ring finger and the lateral side of the little finger was identified by a straight line and measured; the DBUN crosses this line in every hand. The distance between the USP and the point where the DBUN crossed the line was measured and expressed as a relative value of the distance between the USP and the distal end of the 4th webspace (Figure 2.19). The closest passing branch to the USP was identified and the horizontal distance measured (Figure 2.20).

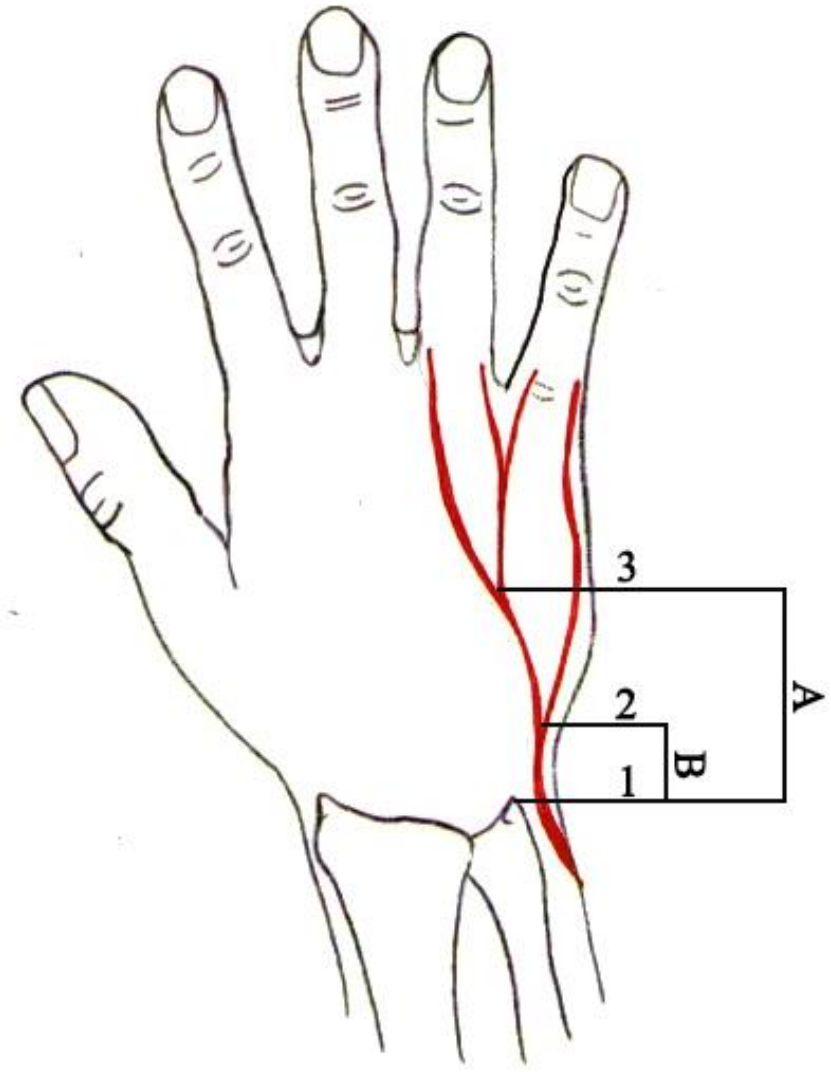

Figure 2.18: Anatomic measurements taken for the dorsal branch of the ulnar nerve. (1) Ulnar styloid process (USP); (2) First major branching point; (3) second major branching point; A, the distance between the second major branching point and the USP; B, the distance between the first major branching point and the USP.

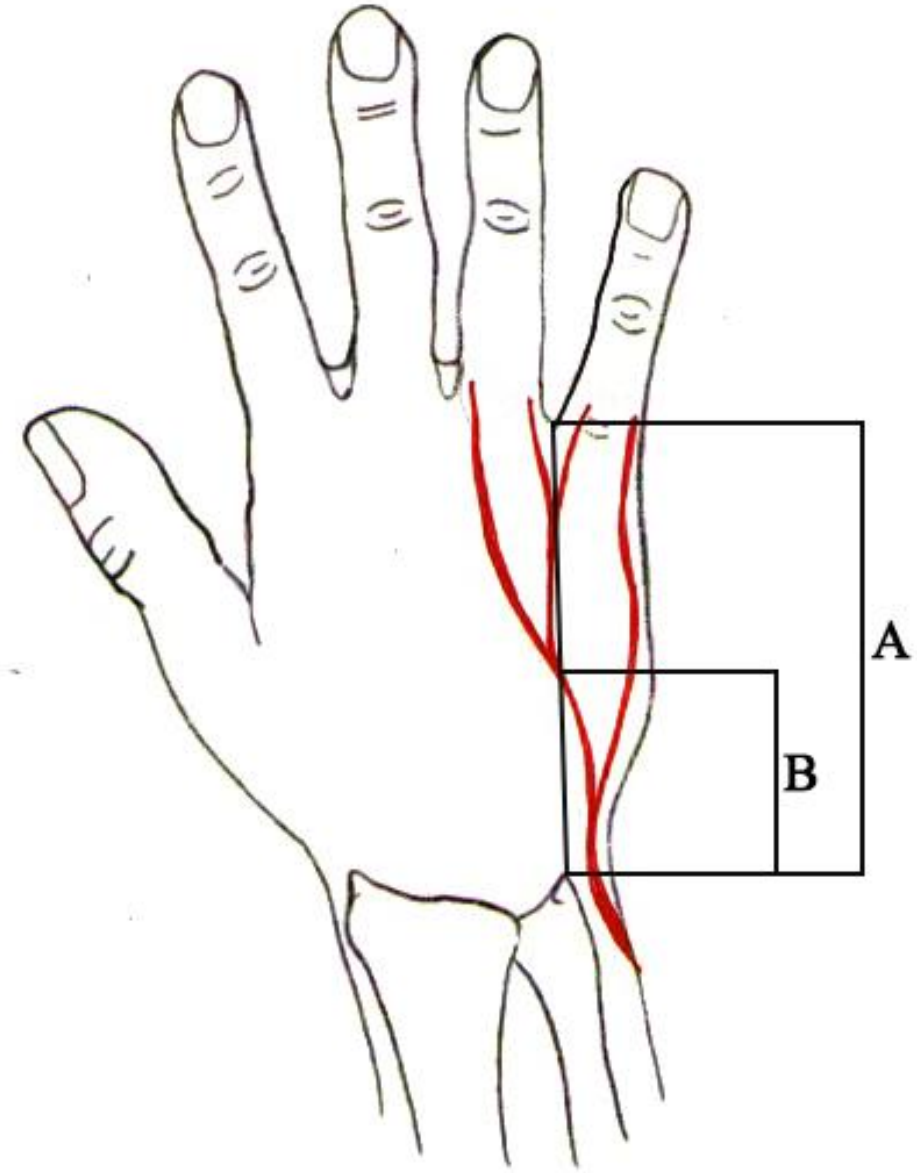

Figure 2.19: Anatomic measurements taken for the dorsal branch of the ulnar nerve (DBUN). (A) The distance between the ulnar styloid process (USP) and the fourth webspace; (B) The distance between the USP and the point where the DBUN crosses line A.

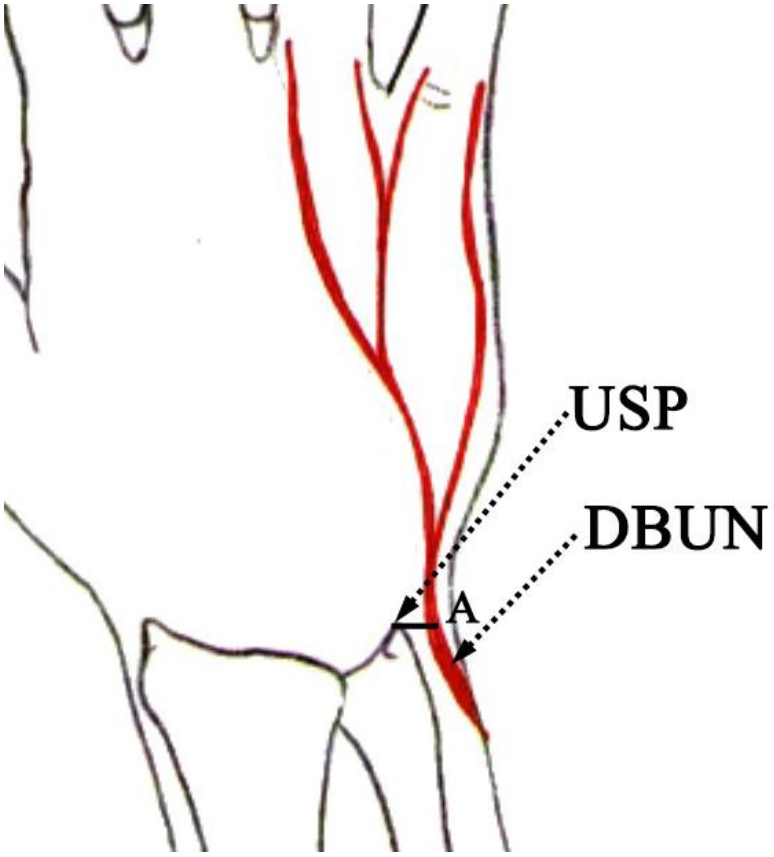

Figure 2.20: Anatomic measurements taken for the dorsal branch of the ulnar nerve (DBUN). (A) The horizontal distance between the ulnar styloid process (USP) and the closest branch of the DBUN.

Several measurements were taken to the SBRN and the DBUN communicating branch if present. The proximal and distal attachment points were marked and distances to the middle of the BSL measured. The angle of origin and the length of the communicating branch were recorded (Figure 2.21). The distance between the third MCP joint and the middle of the BSL was taken. The communicating branches was determined as relative values with reference to the BSL corresponding to the origin and insertion points and plotted to produce a risk area where the communicating branch is most likely to be encountered.

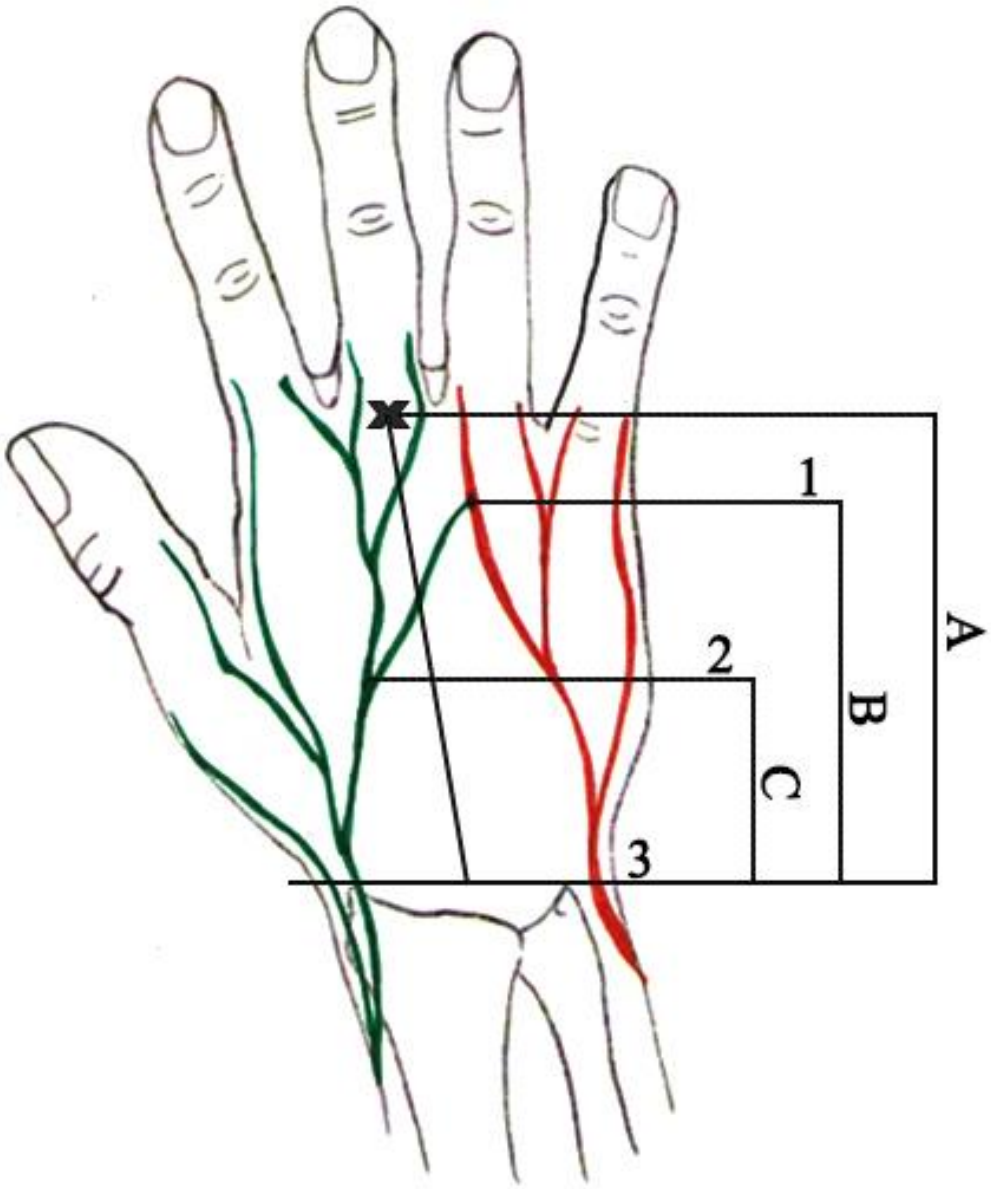

Figure 2.21: Distances measured of the dorsal communicating branch (CB) with reference to the bistyloid line (BSL). (1) Distal attachment point of the dorsal CB; (2) Proximal attachment point of the dorsal CB; (4) The BSL; (X) shows the location of the third metacarpophalangeal (MCP) joint. A, the distance between the third MCP joint and the BSL; B, distance between the distal attachment point and the BSL; C, distance between the proximal attachment point of the dorsal CB and the BSL.

Table 2.3 lists all the anatomic characteristics and measurements taken for the nerves of interest in this study.

Table 2.3: List of the anatomical measurements for each of the nerves investigated in the study

NO.	Anatomical characteristics and measurements
Palmar cutaneous branch of the median nerve (PCBMN)	
1.	Origin direction from the main trunk of the median nerve (MN)
2.	Distance from the point of origin to the wrist crease (WC)
3.	Distance from the point of detaching from the main trunk to the distal WC
4.	Anatomical relationship to palmaris longus
5.	Anatomical relationship to flexor carpi radialis
6.	Anatomical relationship to palmar carpal ligament
7.	Length of the PCBMN tunnel
8.	Branching pattern in the palm
9.	Angle between the lateral and medial branches in the palm
10.	Distance between the first branch coming off the PCBMN to the distal WC
Common digital nerves (CDN) -Median nerve (MN)	
11.	First CDN division point to the middle of the bistyloid line (BSL)
12.	First CDN division point to the scaphoid tubercle
13.	Second CDN division point to the middle of the BSL
14.	Second CDN division point to the scaphoid tubercle
15.	Third CDN division point to the middle of the BSL
16.	Third CDN division point to the scaphoid tubercle
17.	Third Metacarpophalangeal (MCP) joint to middle of the BSL
18.	Third MCP joint to scaphoid
19.	Third MCP joint to the middle of the BSL
Ulnar nerve (UN)	
20.	The point of division of the UN into superficial and deep branches to the proximal edge of the pisiform
21.	Fourth CDN division point to the middle of the BSL
22.	Fourth CDN division point to the proximal edge of the pisiform
The palmar communicating branch (CB) between the UN and MN	
23.	Distance between the proximal insertion point to the distal WC
24.	Distance between the proximal insertion point to distal edge of TCL
25.	Distance between the proximal insertion point to middle of the BSL
26.	Distance between the distal insertion point to distal WC
27.	Distance between the distal insertion point to distal edge of the TCL
28.	Distance between the distal insertion point to middle of the BSL

NO.	Anatomical characteristics and measurements
29.	The length of the communicating branch
30.	The angle at which the proximal attachment leaves the CDN
31.	The distance between the third MCP joint to the distal WC
32.	The distance between the third MCP joint to the middle of the BSL
Superficial branch of the radial nerve (SBRN)	
33.	Point of piercing the antebrachial fascia to the radial styloid process (RSP)
34.	The first major branching point to the RSP
35.	The second major branching point to the RSP
36.	The third major branching point to the RSP
37.	The closest branch to Lister's tubercle
38.	The distances to the closest palmar and dorsal branches to a point 25 mm distal to the RSP
39.	The distances to the closest palmar and dorsal branches to the RSP
40.	The first crossing point with the cephalic vein after the SBRN became subcutaneous
41.	The diameter of the nerve prior to its first major branching point
Dorsal branch of the ulnar nerve (DBUN)	
42.	The point of origin to the ulnar styloid process (USP)
43.	The point of origin to the proximal edge of the pisiform
44.	The first major branching point to the USP
45.	The second major branching point to the USP
46.	The diameter of the nerve prior to its first major branching point
47.	The distance between the USP and the fourth webspace
48.	The distance between the USP and the point where the DBUN crosses a line between the USP and the fourth webspace
The dorsal communicating branch between the DBUN and SBRN	
49.	The proximal attachment point to the middle of the BSL
50.	The distal attachment point to the middle of the BSL
51.	The length of the communicating branch
52.	The angle at which the proximal attachment leaves DBUN/SBRN
53.	The distances from the third MCP joint to the middle of the BSL

2.5. Photographs and visual illustrations

Photographs were taken for all samples by digital cameras (Pentex Optio WG-1 GPS and Nikon D40 with Macro sigma lens). Pictures were edited in Adobe Photoshop CS5.1 image manipulation software. Editing of pictures only included changes in

contrast, brightness, highlights and shadow intensity to better visualize the nerves and other structures. No alteration of the content of each image was performed including addition, deletion, or substitution that would change the shape or location of the structures. Some visual illustrations were created to support this document by Ms. Victoria McCulloch, medical artist, University of Dundee and some were produced by the author.

2.6. Statistics

Data has been manipulated and summarized by: descriptive statistics and univariant analysis. Means, standard deviations, maximum and minimum values were calculated. Patterns were described in terms of frequencies and percentages. Pearson's chi-square test was used to investigate the relationships between categorical dependent variables. All statistical calculations were conducted using IBM Statistical Program for Social Sciences (SPSS) version 21. A result is considered statistically significant when $P<0.05$.

3. Results

A total of 160 cadaveric hands from 81 adult cadavers were investigated in this study. However, the number of samples investigated differs for each nerve. The maximum number of samples studied for any nerve was 155. Some samples were excluded because the nerve under investigation was destroyed or/and its branching point was manipulated during previous dissection making it difficult to produce accurate measurements. Table 3.1 shows the number of samples investigated for each nerve.

Table 3.1: Number of samples investigated for each nerve

No.	Nerve under investigation	No. of samples
1.	Palmar cutaneous branch of the median nerve (PCBMN)	123
2.	Common digital nerves (CDNs)-Median nerve (MN)	155
3.	Ulnar nerve (UN)	144
4.	Communicating branch between median nerve & ulnar nerve	98
5.	Superficial branch of the radial nerve (SBRN)	150
6.	Dorsal branch of the ulnar nerve (DBUN)	139
7.	Communicating branch between the superficial branch of the radial nerve and the dorsal branch of the ulnar nerve	37

3.1. Intra-observer results

Repeated measures of 16 random cases (10% of the total samples) were collected to test the intra-observer error. The Kruskal-Wallis gave a high P-values (>0.05) for all the variables tested. Therefore, the null hypothesis stating that there are no statistical difference between the two measurements is retained (Table 3.2). The intra-observer error is within the acceptable range (5%) indicating that the measurements and statistical comparisons are reliable and precise.

Table 3.2: Chi-Square results for repeated measures

Variable measured	Chi-Square	df	Sig.	Retain the null Hypothesis
Palmar Communicating branch between the median and the ulnar nerves				
Proximal attachment to TCL	.240	1	.624	Yes
Distal attachment to TCL	.364	1	.546	Yes
Angle of origin	.353	1	.553	Yes
MCPJ to WC	1.740	1	.187	Yes
Proximal to WC	3.273	1	.070	Yes
Distal to WC	1.322	1	.250	Yes
Length	.205	1	.651	Yes
BSL	.023	1	.880	Yes
Common digital nerves (CDN)				
First CDN first branching point to the BSL	.051	1	.821	Yes
First CDN second branching point to the BSL	1.534	1	.215	Yes
First CDN first branching point to scaphoid	.009	1	.925	Yes
First CDN second branching point to scaphoid	.658	1	.417	Yes
Second CDN division into PDN to the BSL	1.890	1	.169	Yes
Second CDN division into PDN to scaphoid	1.144	1	.285	Yes
Third CDN division into PDN to the BSL	.003	1	.955	Yes
Third CDN division into PDN to scaphoid	1.069	1	.301	Yes
Ulnar nerve (UN)				
Branching point of the Deep branch of the UN to the pisiform	.005	1	.945	Yes
Branching point of the superficial branch of the UN to the pisiform	.000	1	1.000	Yes

3.2.Palmar cutaneous branch of the median nerve

The PCBMN was investigated in 123 cadaveric hands: 50 (40.7%) were male and 73 (59.3%) female. Mean age was 82.6 ±9.8 years (range: 53-98). The PCBMN was found in all hands studied; however, two PCBMNs were identified in 11 cases (8.9%) originating at the same or different levels from the main trunk of the median nerve.

The PCBMN originated from the lateral side of the main trunk in the majority of cases (115/123, 93.5%). However, it was also found to originate from the posterolateral, medial and anterior side of the main trunk of the median nerve in 1.6% (2/123), 1.6% (2/123) and 3.3% (4/123) of hands respectively (Figure 3.1).

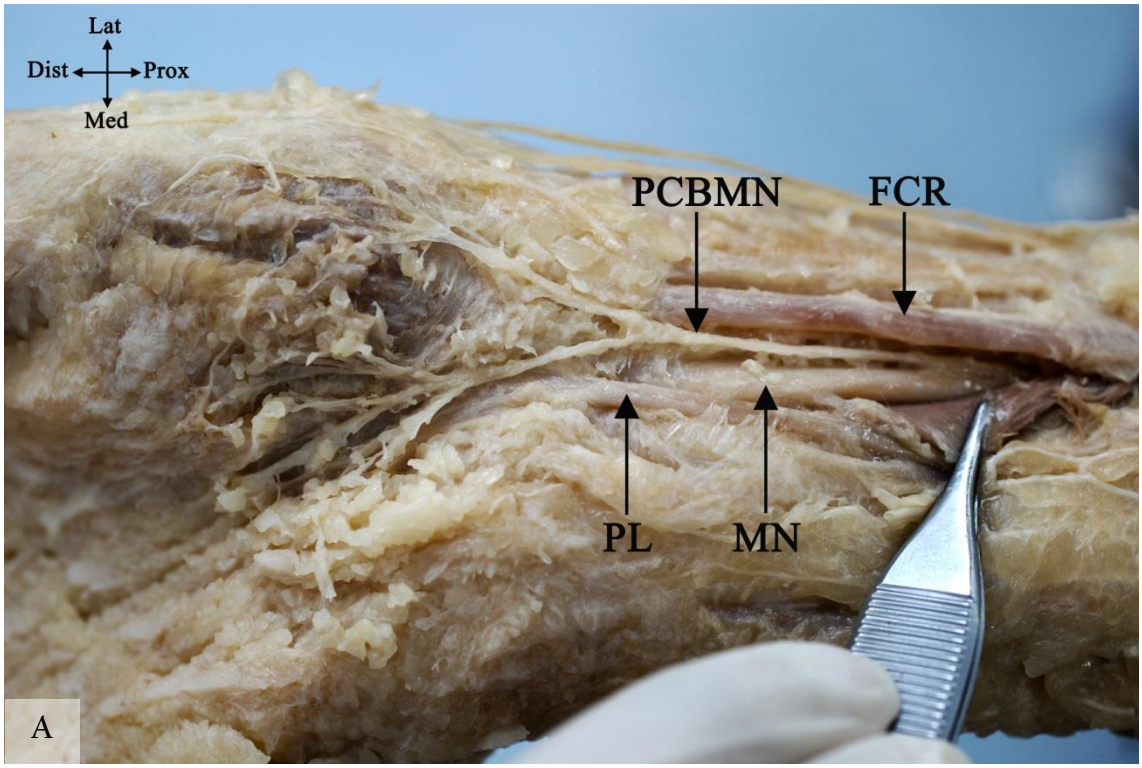

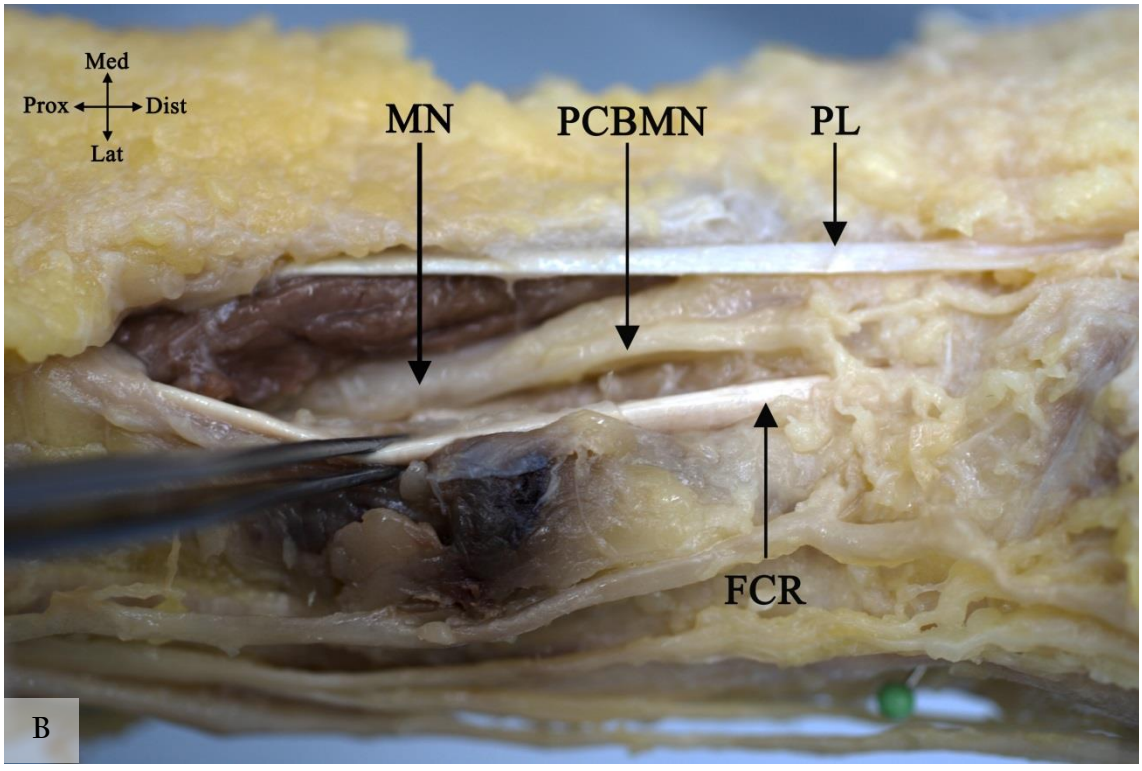

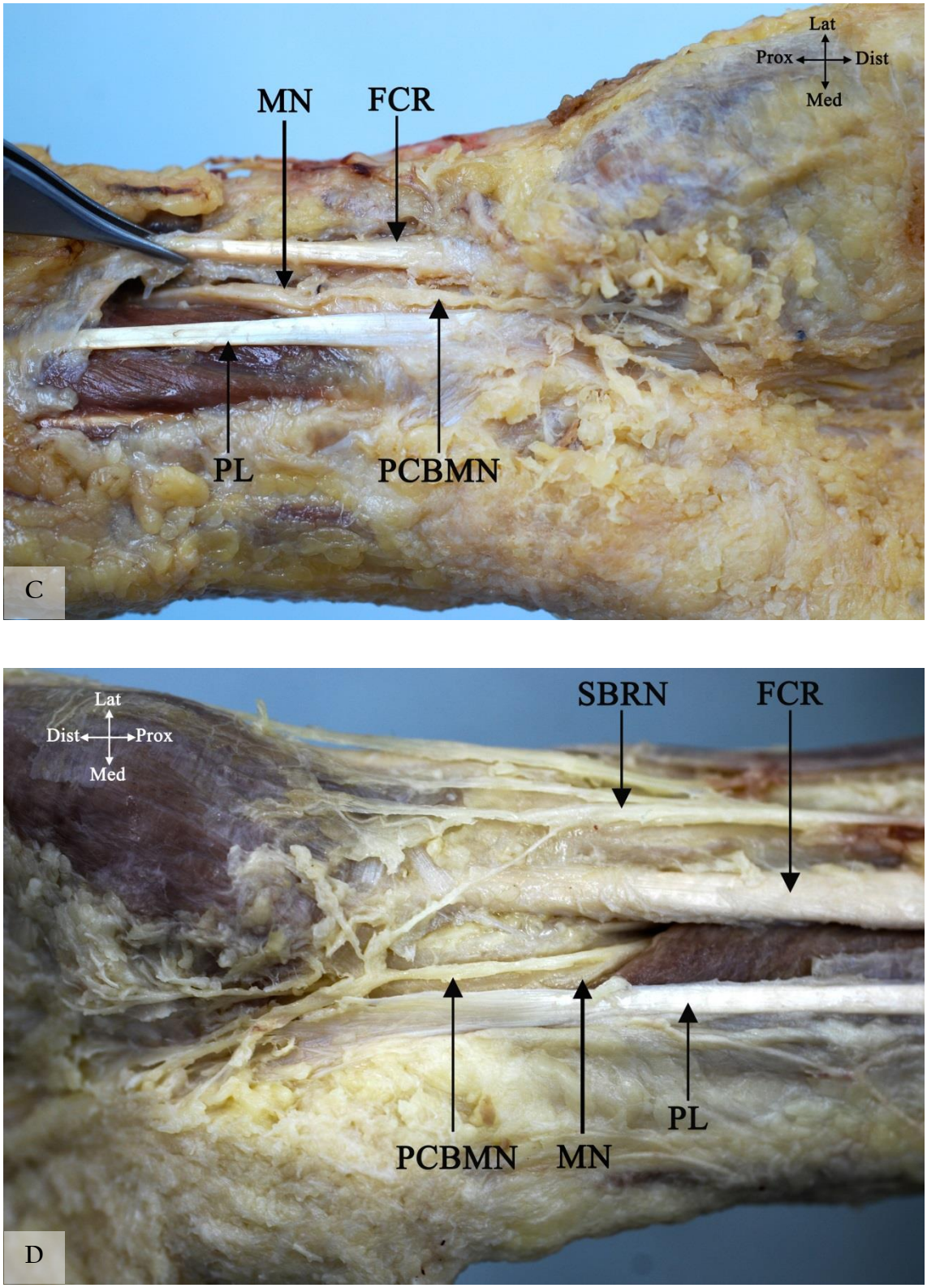

Figure 3.1: Different origin direction of the palmar cutaneous branch of the median nerve (PCBMN) from the main trunk of the median nerve (MN). (A) Lateral origin, (B) Posterolateral origin, (C) Medial origin, (D) Anterior origin. FCR, flexor carpi radialis; PL, palmaris longus; SBRN, superficial branch of the radial nerve; Lat, lateral; Med, medial; Prox, proximal; Dist, distal.

The PCBMN originated at a mean distance of 54.1±15.7 mm proximal to the WC, continued within the epineurium of the main trunk of the MN for a short distance and separated at a mean distance of 41.2±14.0 mm proximal to the WC (Table 3.3). The nerve then coursed distally medial to flexor carpi radialis and lateral to the palmaris longus tendon (if present). The nerve was noted to pass through the fascia of flexor carpi radialis tendon in 10 cases (8.3%) and posterior to the tendon in 5 cases (4.2%). At the distal forearm, the nerve penetrated the PCL creating a tunnel between the deep and superficial fibres and continued distally through the fibres of the TCL. The PCBMN tunnel was found to be 11.3±3.4 mm long (Figure 3.2, Table 3.3). It was also noted that the nerve passed superficial to the PCL in 18 cases (16.1%) while it passed deep to it in 14 cases (12.5%). Interestingly, the PCBMN was found to course deep to the TCL and pierced the ligament and palmar aponeurosis at several locations to supply the skin of the palm in one hand. The nerve entered the palm often penetrating the distal fibres of palmaris longus where it divided to supply the proximal two fifths of the palm.

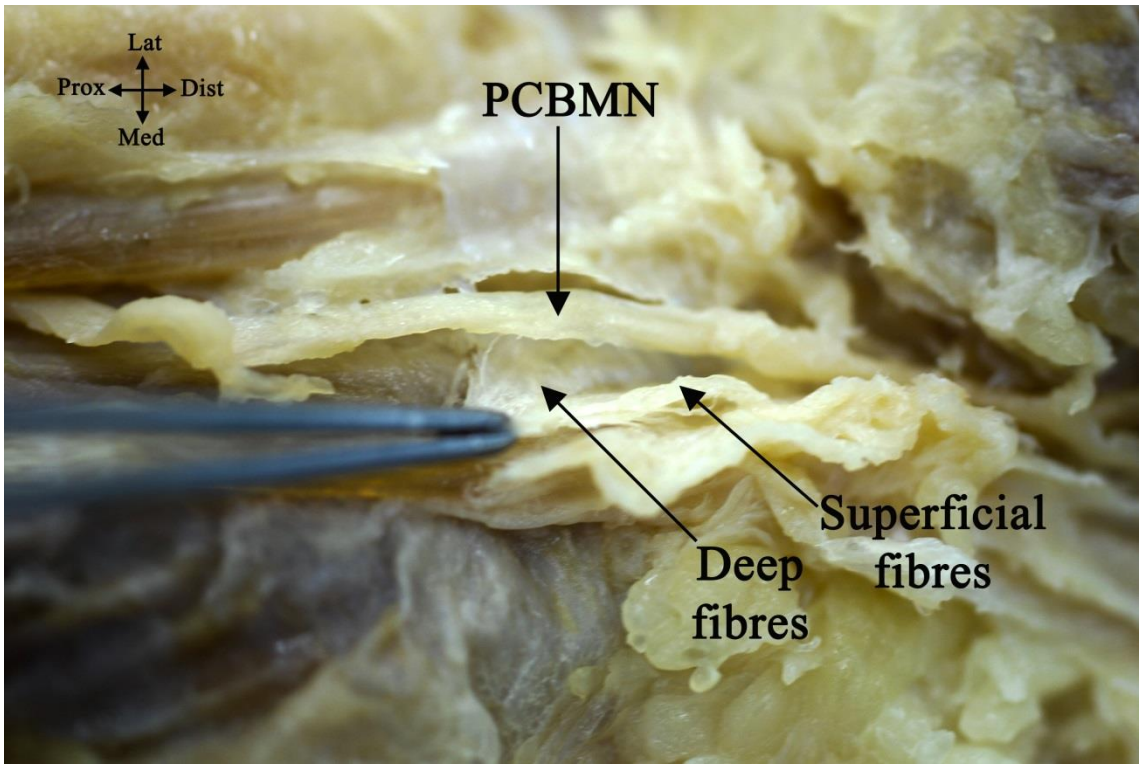

Figure 3.2: Palmar cutaneous branch of the median nerve (PCBMN) crossing between the superficial and deep fibres of the palmar carpal ligament to create a tunnel before entering the palm. Lat, lateral; Med, medial; Dist, distal; Prox, proximal.

Based on the division pattern of the nerve in the palm distal to the WC observed in 110 samples three patterns of division were identified:

Type I: The main trunk divides into Y-shaped ulnar and radial branches that continued to give tertiary branches as they course distally in the palm.

Variations to Type I: The main trunk gives several smaller branches before it divides into Y- shaped ulnar and radial major branches.

Type II: The PCBMN continues as one major branch that gives several minor branches as it courses distally in the palm.

Type III: The main trunk divides into three branches (radial, ulnar and middle) that all continue to give tertiary branches as they course distally in the palm.

Types I, II, and III were found in 40.0% (44/110), 36.4% (40/110), 14.5% (16/110) of the hands respectively. Furthermore, variations to Type I were found in 9.1% (10/110) of the hands investigated (Figure 3.3).

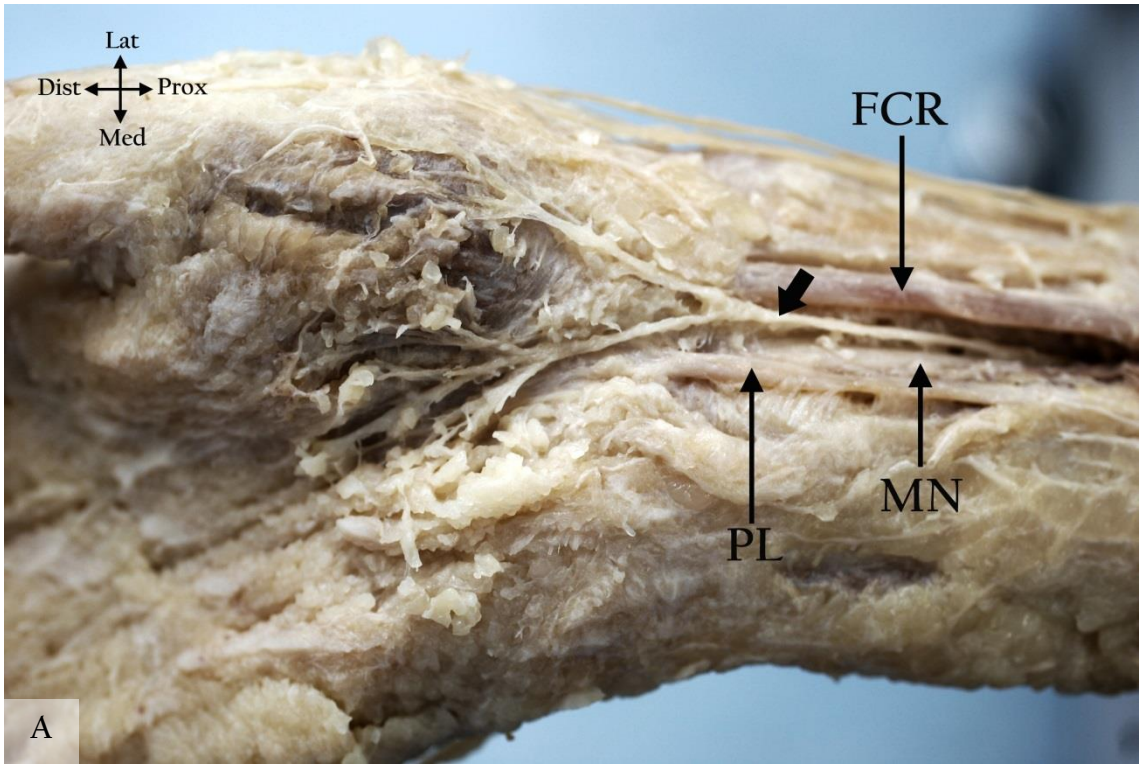
Lat
Dist
Prox
Med
FCR
MN
PL
A

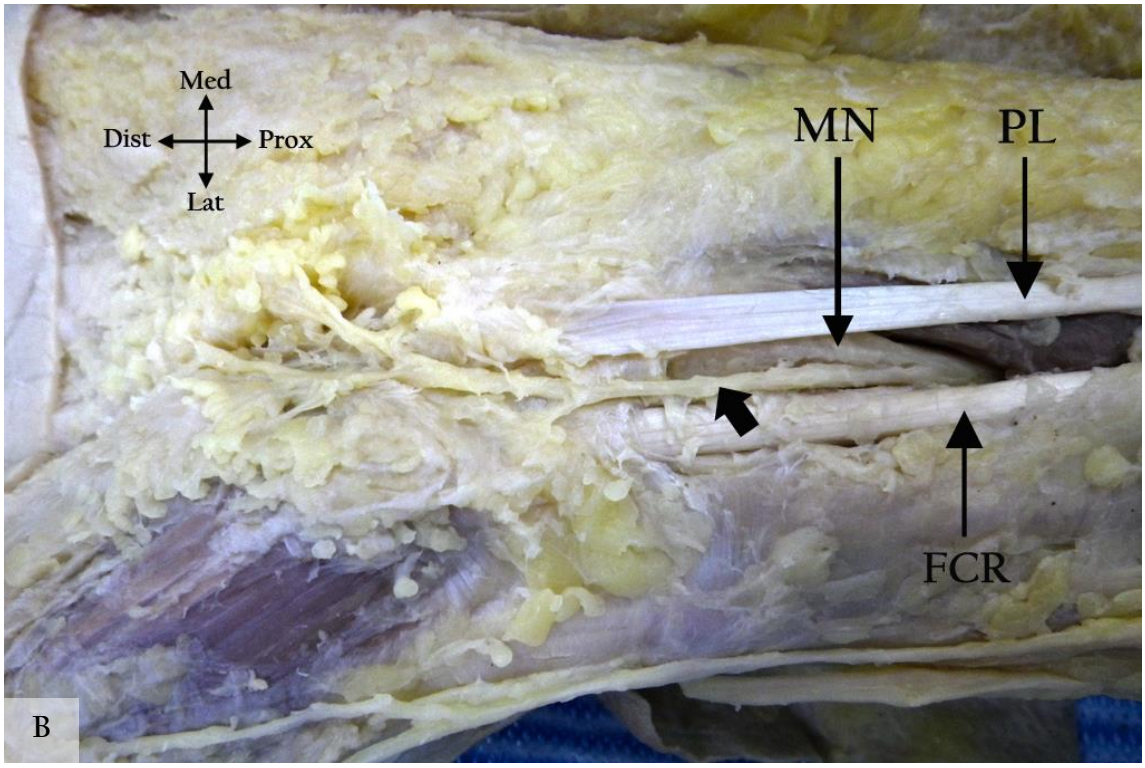
Med
Dist
Prox
Lat
MN
PL
FCR
B

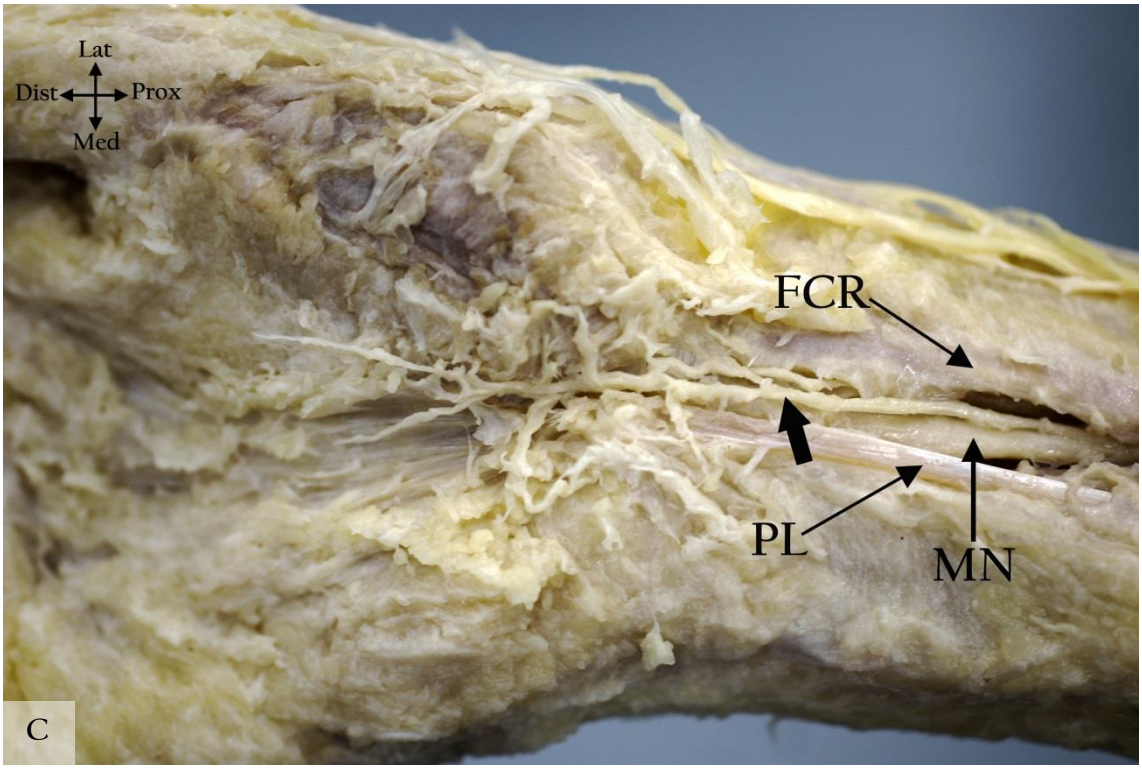

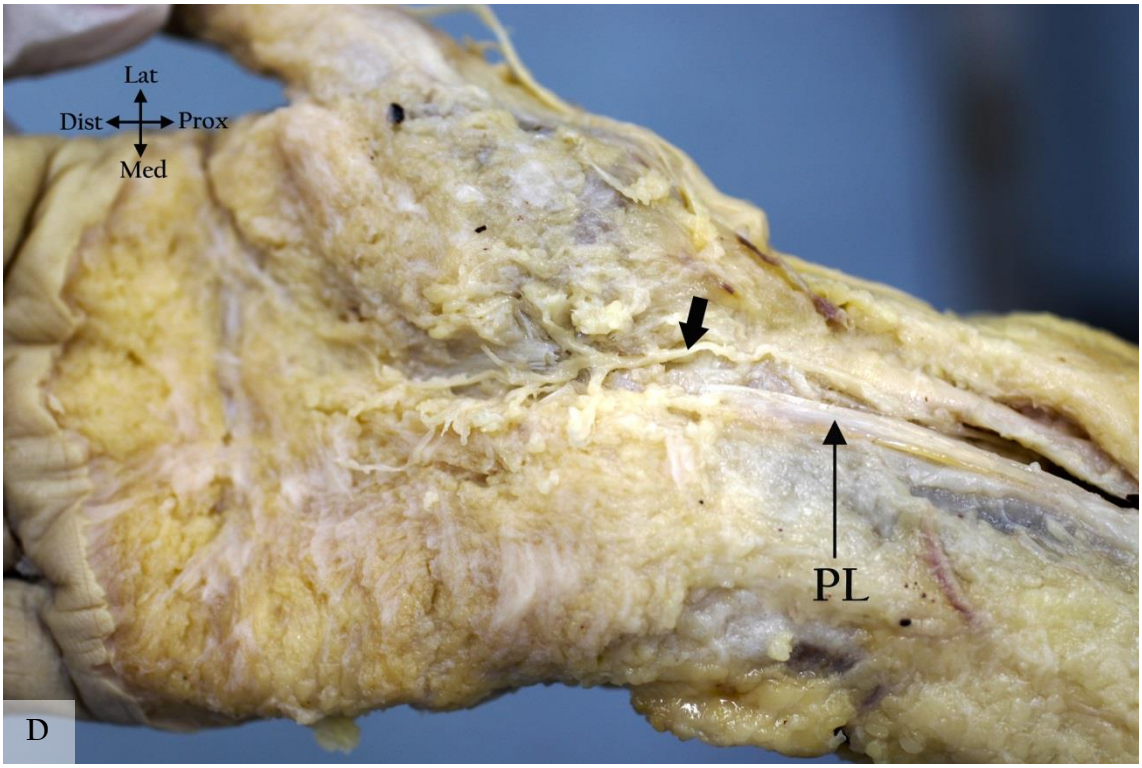

Figure 3.3: Branching patterns of the palmar cutaneous branch of the median nerve (PCBMN). (A) Type I, (B) Variation to Type I, (C) Type II and (D) Type III. PL, palmaris longus; FCR, flexor carpi radialis; bold arrow indicates the PCBMN; MN, median nerve, Med, medial; Lat, lateral; Dist, distal; Prox, proximal.

The angle between the major radial and ulnar branches in Type I was found to be 43.9±14.7°. PCBMN gave its first branch 1.2±8.1 mm distal to the WC. In 33 cases, the first branch of PCBMN originated proximal to the WC. Table 3.3 shows the major anatomical measurements recorded for the PCBMN.

Table 3.3: Anatomical measurements recorded for the palmar cutaneous branch of the median nerve (PCBMN) (mm)

	Mean	**SD**	**Max**	**Min**
Origin from main trunk	54.1	15.7	138.4	22.1
Detaches from main trunk	41.2	14.0	114.9	16.2
Length of PCBMN tunnel	11.3	3.4	24.5	5.7
Angle (degrees)	43.9	14.7	85.0	15.0
Distance of 1st branch to wrist crease	1.2	8.1	21.5	-18.2[1]

[1] Minus signs indicate that the point were located proximal to the level of the respective landmark

Two PCBMNs were noted in 11 cases (8.9%), 3 of which had different origin and detachment points. The proximal nerve originated at a mean distance of 70.9±20.6 mm (range: 100-42.1) and detached from the main trunk at a mean distance of 55.9±18.9 mm (range: 85.7-29.9) proximal to the WC. The distal nerve originated at a mean distance 64.8±17.8 mm (range: 92.3-42.1) and detached from the main trunk at a mean distance 46.5±16.7 mm (range: 77.0-27.9) proximal to the wrist crease (Table 3.4). In most cases, the two nerves joined proximal to, or at the level of, the WC forming a single nerve trunk before then dividing to innervate the palm. In most cases with two PCBMNs, the two branches took different courses, one medial to the FCR and the other within the tendon fascia. In relation to the PCL, one branch was found to course either superficially or through it, while the other was deep to the PCL fibres (Figure 3.4).

Table 3.4: Anatomical measurements recorded in cases where two palmar cutaneous branches of the median nerve were found (mm)

	Mean	**SD**	**Max**	**Min**
Origin of the proximal branch from main trunk of the median nerve	70.9	20.6	100	42.1
Detachment of the proximal branch from main trunk of the median nerve	55.9	18.9	85.7	29.9
Origin of the distal branch from main trunk of the median nerve	64.8	17.8	92.3	42.1
Detachment of the distal branch from main trunk of the median nerve	46.5	16.7	77.0	27.9

The PCBMN also communicated with other nerves supplying the region. It was found to communicate with the LABCN in 5 cases. The LABCN gives a branch to communicate with the PCBMN and therefore contributes to the innervation of the palm and the thenar eminence. In two of these cases the LABCN communicated with the SBRN earlier to its communication with the PCBMN (Figure 3.5). The nerve was also found to communicate solely with the SBRN (one case), with the recurrent motor branch of the median nerve (two cases) (Figure 3.6), with the palmar cutaneous branch of the ulnar nerve (one case) (Figure 3.7), and with the first CDN supplying the thumb (one case) (Figure 3.8).

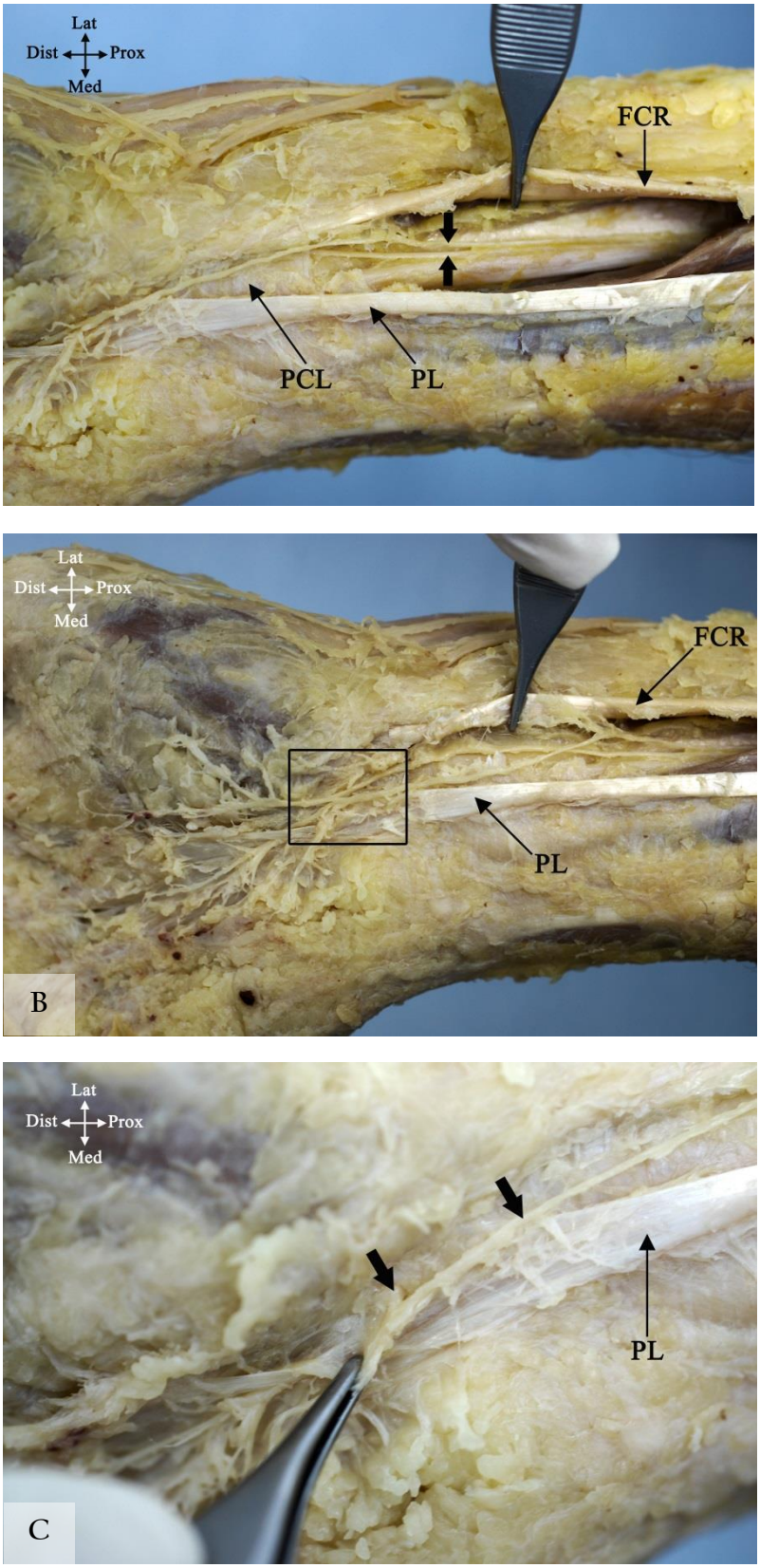

Figure 3.4: Two palmar cutaneous branches of the median nerve (PCBMN). (A) Shows the different course that each branch takes. (B) After full dissection of the palmar carpal ligament (PCL) to view the deeper branch, the rectangular area outlined is enlarged in (C). PL, palmaris longus; FCR, flexor carpi radialis; bold arrows indicate the PCBMN branches; Lat, lateral; Med, medial; Prox, proximal; Dist, distal.

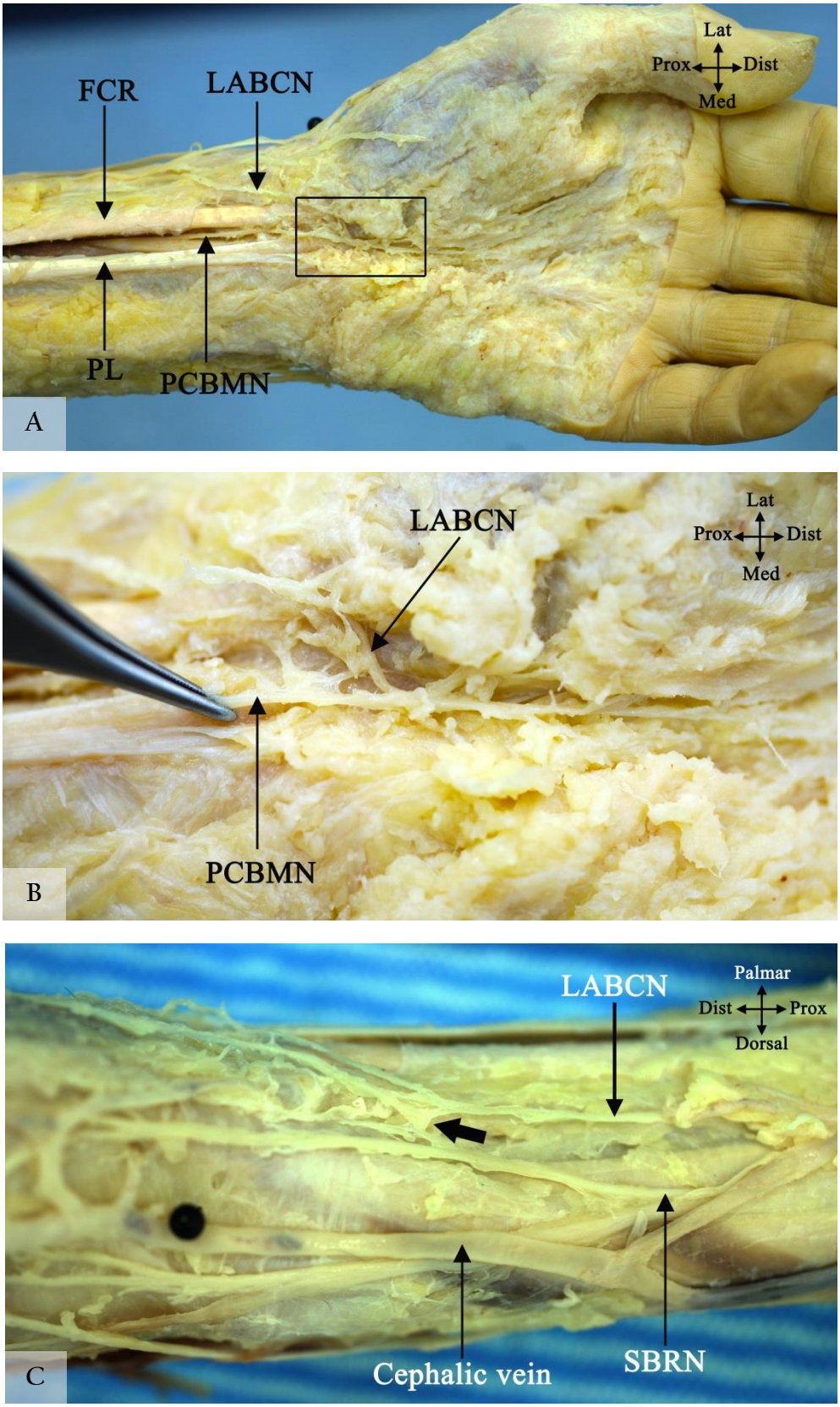

Figure 3.5: The palmar cutaneous branch of the median nerve (PCBMN) communicating with the lateral antebrachial cutaneous nerve (LABCN). (A) Full hand view showing the location of the two nerves, rectangular area outlined is enlarged in (B). (C) Shows the superficial branch of the radial nerve communicating with the LABCN prior to its communication with the PCBMN. PL, palmaris longus; FCR, flexor carpi radialis; Lat, lateral; Med, medial; Prox, proximal; Dist, distal; Palmar, palmar surface; Dorsal, dorsal surface.

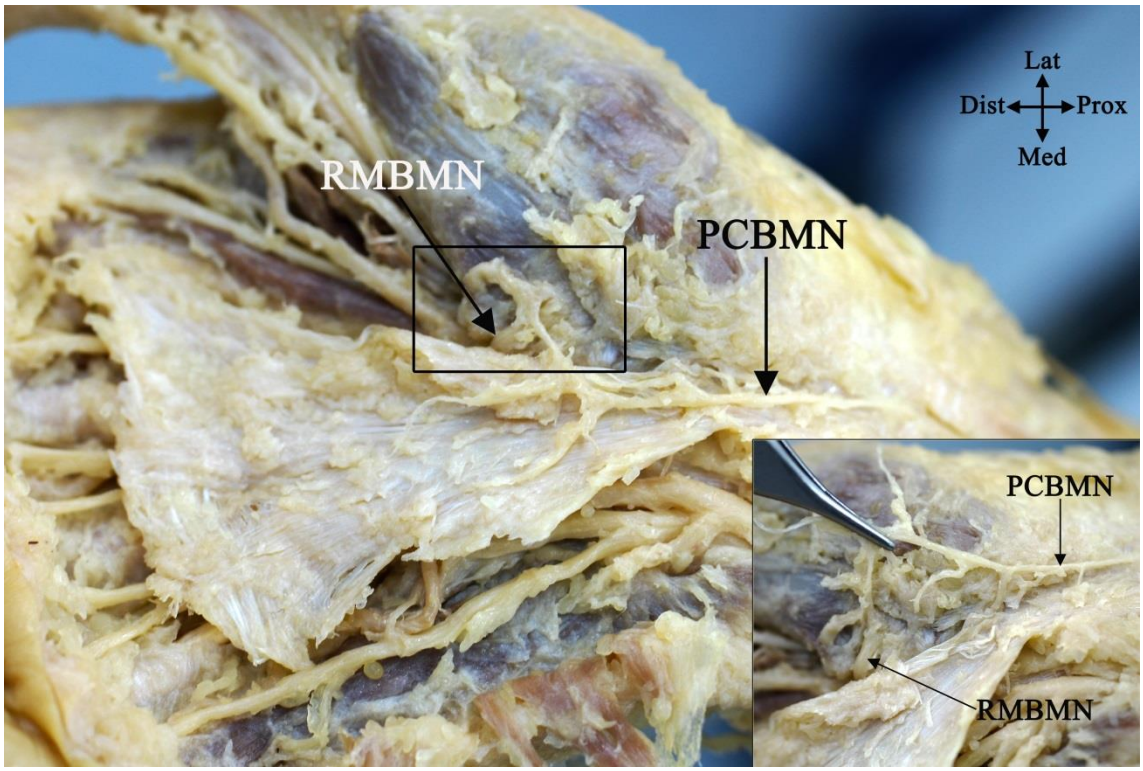

Figure 3.6: The palmar cutaneous branch of the median nerve (PCBMN) communicating with the recurrent motor branch of the median nerve (RMBMN). The rectangular area outlined is magnified at the corner. Lat, lateral; Med, medial; Prox, proximal; Dist, distal.

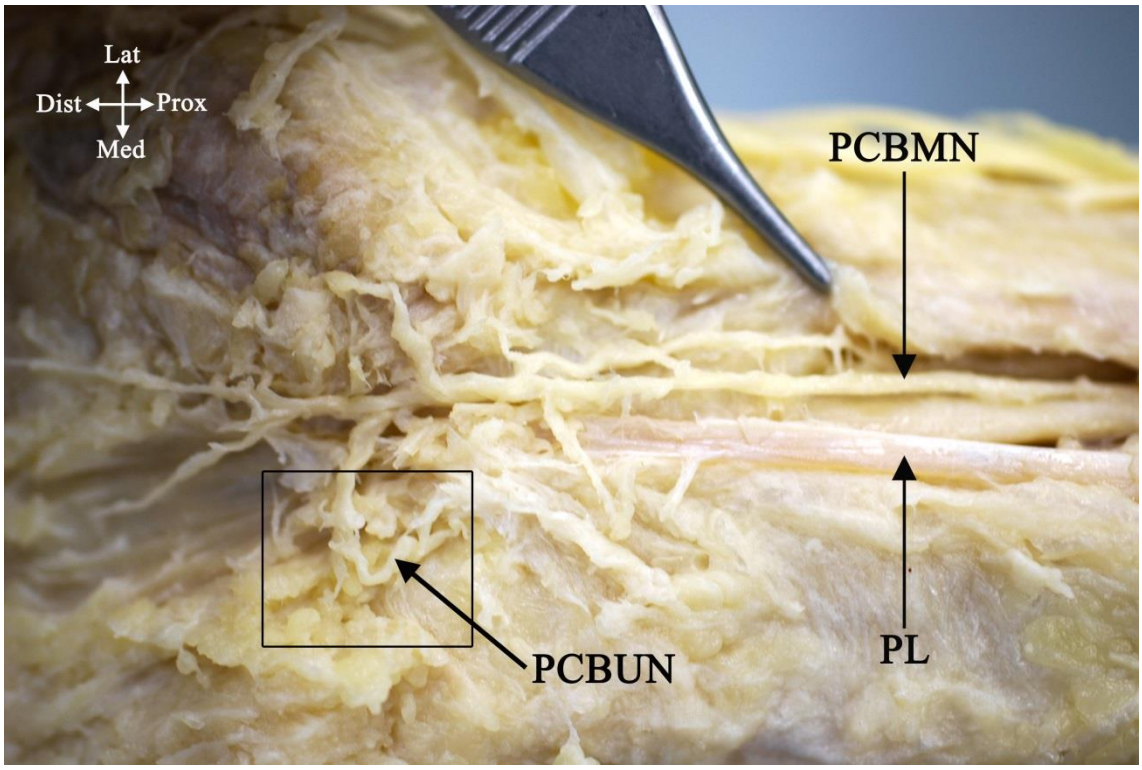

Figure 3.7: Palmar cutaneous branch of the median nerve (PCBMN) communicating with the palmar cutaneous branch of the ulnar nerve (PCBUN) at the rectangular area outlined. PL, palmaris longus; Lat, lateral; Med, medial; Prox, proximal; Dist, distal.

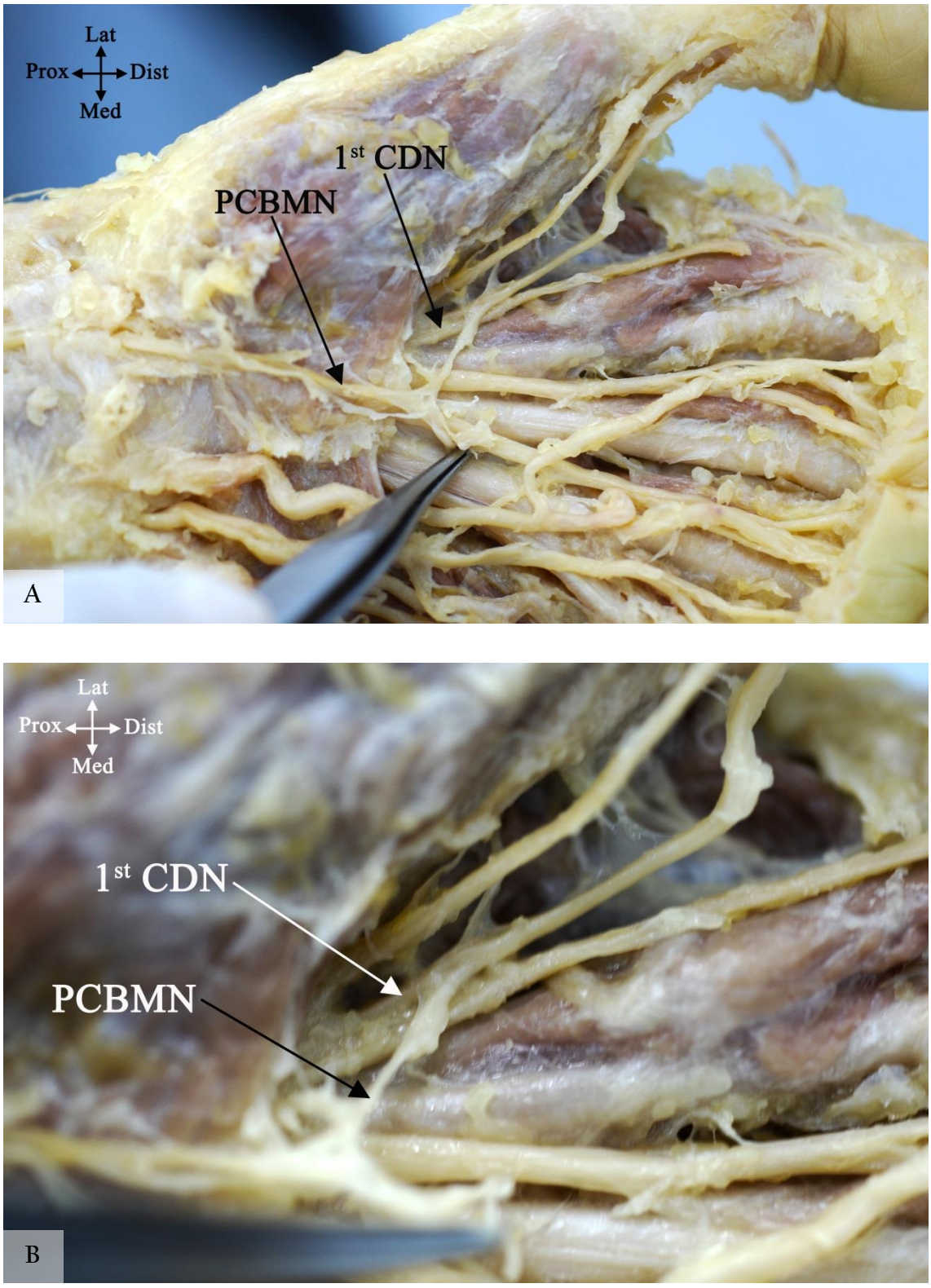

Figure 3.8: The palmar cutaneous branch of the median nerve (PCBMN) communicating with the first common digital nerve to the medial side of the thumb. (A) A full hand view. (B) Enlarged image of the communicating branch. Lat, lateral; Med, medial; Prox, proximal; Dist, distal.

An artery was observed to course along the lateral side of the main trunk of the MN in the distal forearm in one case. Distal to the detachment of the PCBMN, the artery coursed on top of the nerve separating the PCBMN from the MN, continuing on the medial side of the MN to enter the carpal tunnel along with the MN (Figure 3.9).

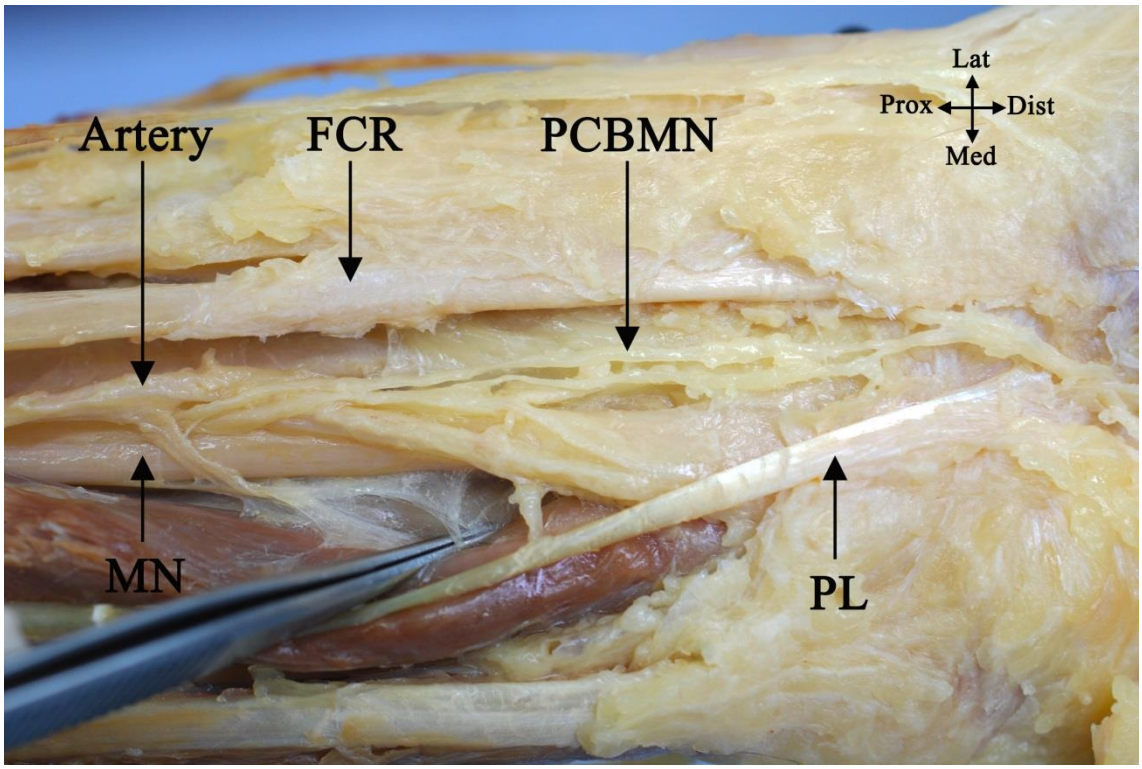

Figure 3.9: An artery crossing the median nerve (MN) and separating the two branches of the palmar cutaneous branch of the median nerve (PCBMN) from the MN trunk. PL, palmaris longus; FCR, flexor carpi radialis; Lat, lateral; Med, medial; Prox, proximal; Dist, distal.

The effect of sex and body side on the branching pattern was investigated. The branching pattern of the PCBMN was not influenced by sex (P value=0.506) or body side (P value =0.240). Appendix 1 shows the chi-square test results for both the effect of sex and body side.

3.3. Common digital nerves

The CDNs were investigated in 155 cadaveric palms from 80 cadavers: 68 (43.9%) hands were male and 87 (56.1%) female. Mean age was 82.4±9.6 (range: 101-53) years. The median nerve was found to pass through the carpal tunnel and divide into the first, second and third CDN within the tunnel or at the distal margin of the TCL in all cases. The fourth CDN and the PDN to the medial side of the little finger originated from the superficial division of the UN after it passed through Guyon's canal on the medial side of the palm.

The CDNs passed deep to the superficial palmar arch and divided into PDNs at various levels to supply the lateral and medial sides of the digits (Figure 3.10 A). In one case, the third CDN gave a branch that crossed superficial to the superficial palmar arch creating a neural loop around the arch: the branch then joined the third CDN again distally (Figure 3.10 B). Table 3.5 illustrates the branching points of the CDNs into PDNs with respect to different anatomic landmarks.

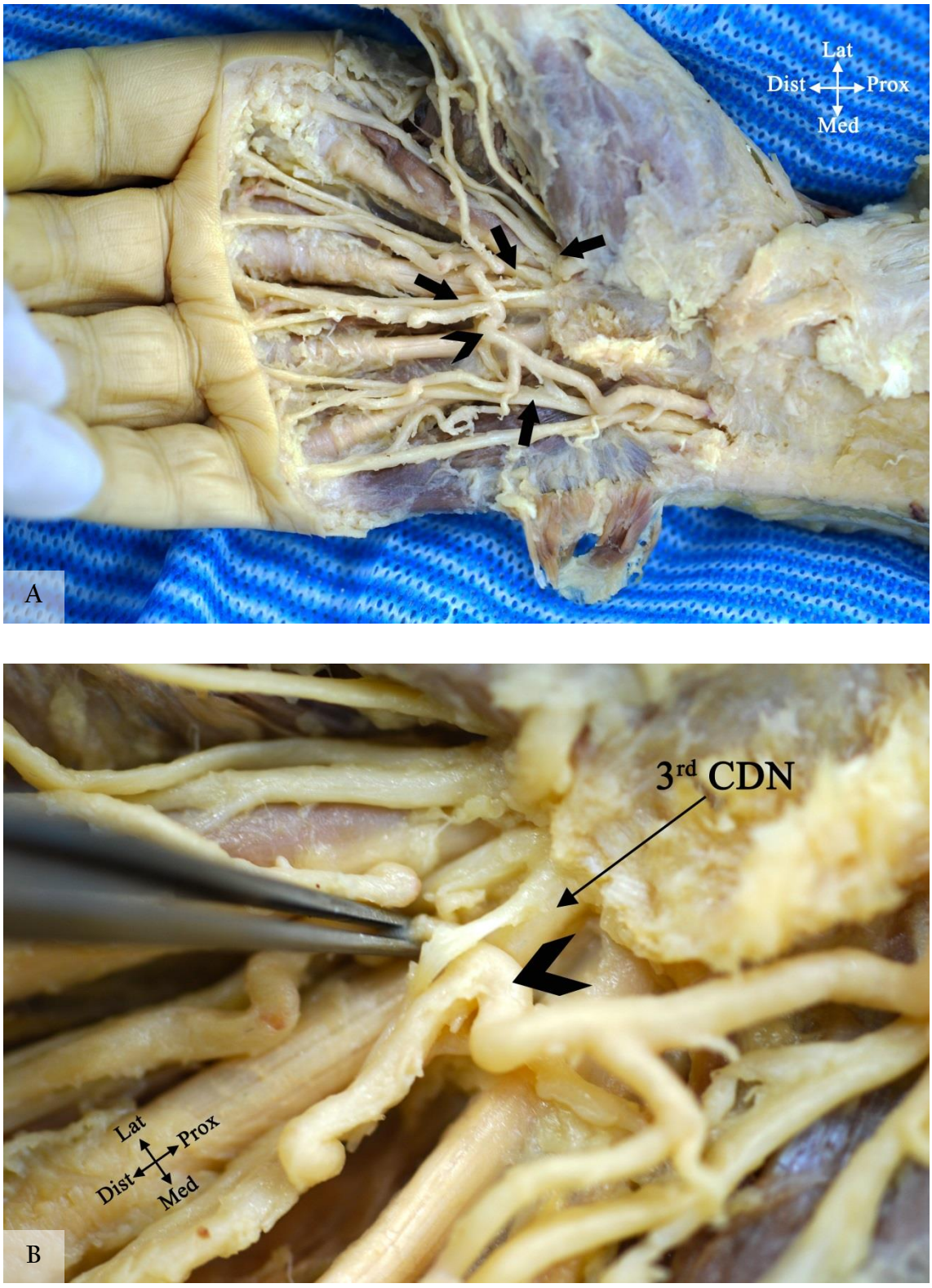

Figure 3.10: Common digital nerves (CDNs) and the superficial palmar arch. (A) Full hand view. (B) A neural loop is created by a branch from the 3rd CDN passing superficially to the superficial palmar arch. Arrow head indicates the superficial palmar arch; black arrows indicate the CDNs; Lat, lateral; Med, medial; Prox, proximal; Dist, distal.

Table 3.5: Absolute measurements for the branching points of the common digital nerves (CDNs) into proper digital nerves in the palm (mm)

		Mean	SD	Max	Min
First common digital nerve (CDN) first division	ST[1]	29.9	5.4	54.3	16.7
	BSL[2]	45.3	6.1	63.5	32.4
First CDN second division	ST	35.5	7.1	63.3	16.9
	BSL	51.7	7.4	71.9	35.4
Second CDN division	ST	59.8	7.9	81.1	42.9
	BSL	74.1	9.1	94.7	42.3
Third CDN division	ST	66.1	7.38	86.2	49.1
	BSL	78.9	7.7	99.5	60.1
Fourth CDN division	Pisiform	65.2	7.4	83.9	49.3
	BSL	72.6	7.7	92.2	55.0

[1] Scaphoid tubercle
[2]Bistyloid line

The second CDN was found to divide at a point located distal to the 70% of the distance between the third MCP joint and the BSL in 94.3% of cases. The third and fourth CDNs were found to divide distal to the 70% of the same distance mentioned earlier in 99.2% and 73.6% of the cases respectively. Relative measurements of the division points of the CDNs into the PDNs to the distance between the third MCP joint and the BSL are presented in Table 3.6. Values less that 100% indicate that the CDN divided proximal to the level of the third MCP joint whereas measurement values more than 100% indicate that the CDN divided distal to the level of the third MCP joint. The division points of the first and fourth CDNs were always proximal to the third MCP joint. However, the second CDN divided distal to the third MCP joint in 3 cases and the third CDN divided distal to the third MCP joint in 6 cases. Moreover, the third CDN branching point was at 86.5±8.3% (range: 107.1-51.3%) of the distance of the third MCP joint to the WC (Appendix II).

Table 3.6: Branching points of the common digital nerves (CDNs) into the proper digital nerves to the distance between the third metacarpophalangeal joint and the bistyloid line (%)

	Mean	SD	Max	Min
First common digital nerve (CDN) first division	51.2	5.3	63.3	40.2
First CDN second division	58.7	7.2	76.9	41.6
Second CDN division	83.8	8.6	101.5	39.4
Third CDN division	89.3	6.3	108.1	65.3
Fourth CDN division	74.2	7.6	93.7	55.4

Based on observations from 142 cadavers, the pattern of division of the first CDN supplying the thumb and the lateral side of the index finger was categorized into three types as suggested by Jolley et al. (1997):

Type I: A PDN to the lateral side of the thumb and a CDN further dividing distally to supply the medial side of the thumb and the lateral side of the index finger.

Type II: Trifurcation of PDNs to the thumb and the lateral side of the index finger.

Type III: A CDN further dividing to supply the lateral and medial side of the thumb and a PDN to the lateral side of the index finger.

Type I was found in 70.8%, Type II in 27.1% and Type III in 2.1% of the hands investigated (Figure 3.11).

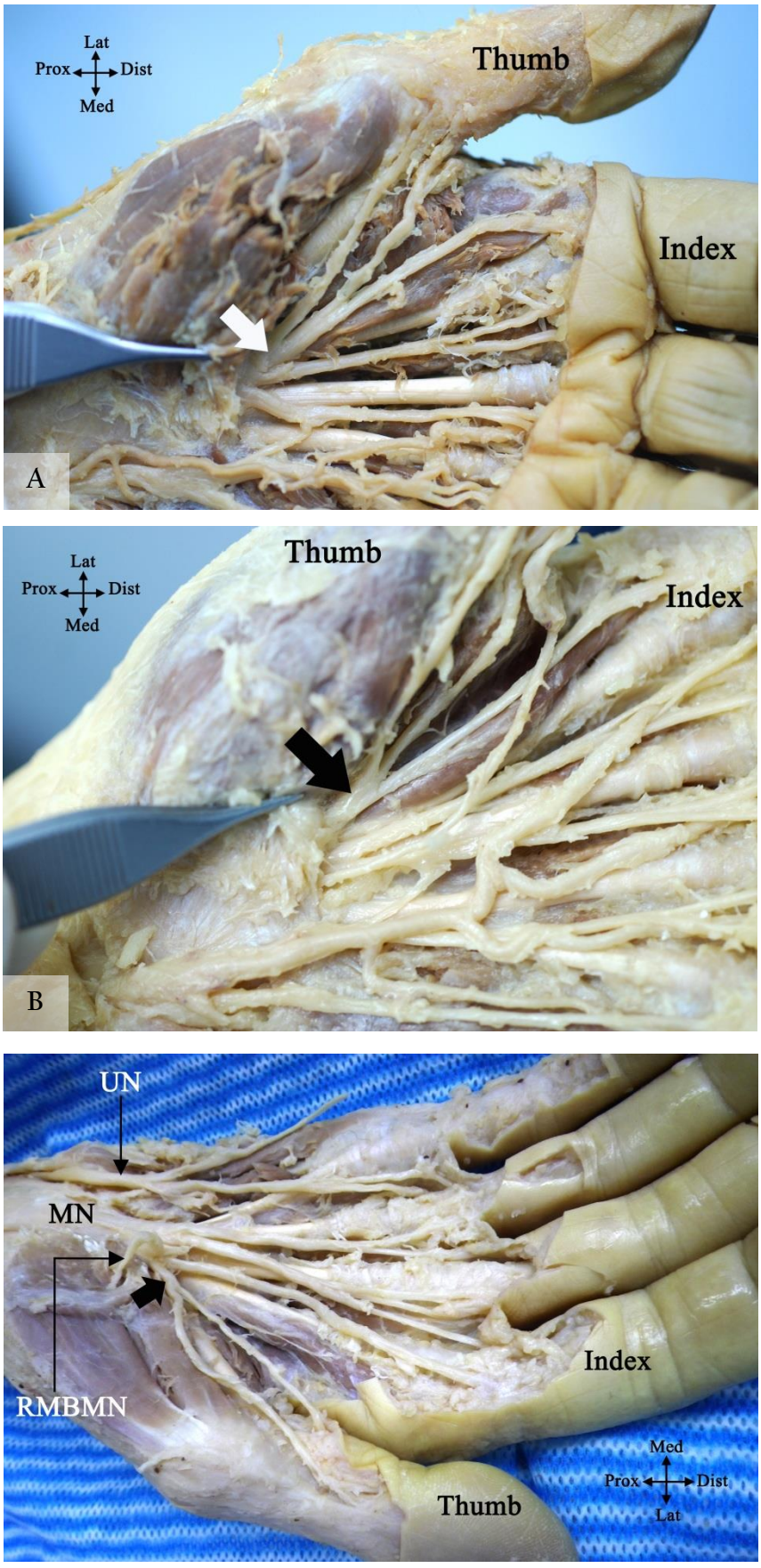

Figure 3.11: First common digital nerve (CDN) branching pattern. (A) Type I, (B) Type II, (C) Type III. The bold arrow indicates the first CDN; RMBMN, recurrent motor branch of the median nerve; MN, median nerve; UN, ulnar nerve; Lat, lateral; Med, medial; Prox, proximal; Dist, distal.

The effect of sex and body side on the branching pattern was investigated. The branching pattern of the first CDN was not influenced by sex (P value=0.186) but it was found to be influenced by body side (P value =0.041). Appendix 1 shows the chi-square test results for both the effect of sex and body side.

3.4.Ulnar nerve

The UN was examined in 144 cadaveric palms from 78 cadavers: 63 (43.8%) were male and 81 (56.3%) female. Mean age was 82.4±9.7 (range: 101-53) years. The ulnar nerve passed through Guyon's canal in all cases and divided into a deep motor branch that coursed deep to the hypothenar muscles and a superficial branch that supplied the little and medial side of the ring finger. The UN division in Guyon's canal was classified into two patterns based on the number of branches at the division point as suggested by Bonnel and Vila (1985):

Type I: UN bifurcates into one deep motor branch and a superficial sensory branch that further divides distally into a CDN supplying the fourth webspace and a PDN supplying the medial side of the little finger.

Type II: UN trifurcates into one deep motor branch, a CDN for the fourth webspace and a PDN supplying the medial side of the little finger.

Type I was found in 80.4% while Type II was found in 19.6% (Figure 3.12).

The effect of sex and body side on the branching pattern was investigated. The branching pattern of the UN was not influenced by sex (P value=0.258) or body side (P value =0.392). Appendix 1 shows the chi-square test results for both the effect of sex and body side.

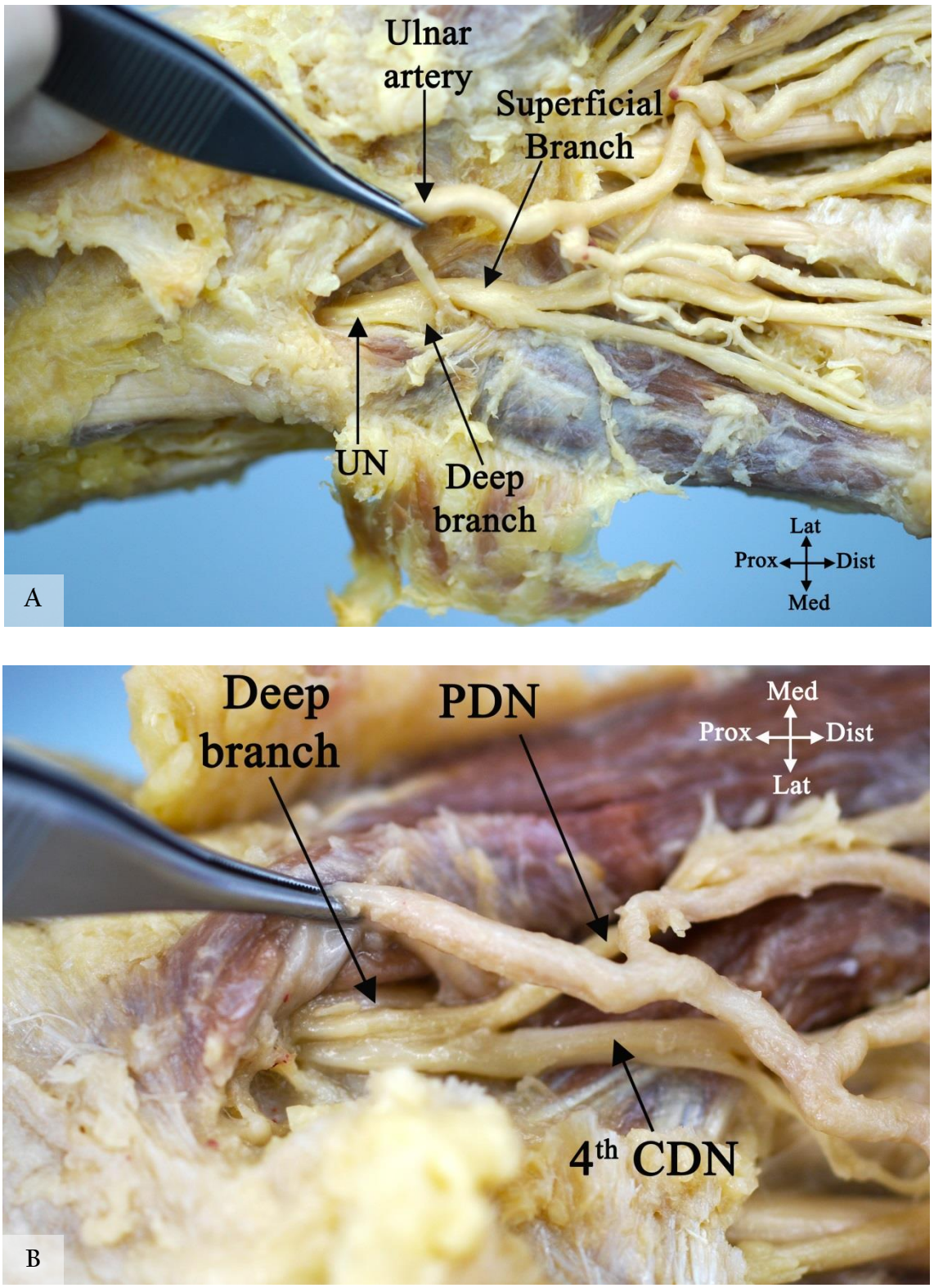

Figure 3.12: Patterns of division of the ulnar nerve (UN) in Guyon's canal. (A) Type I, (B) Type II. PDN, proper digital nerve; CDN, common digital nerve; Lat, lateral; Med, medial; Prox, proximal; Dist, distal.

In one case, the UN divided into 4 branches in Guyon's canal: one deep motor and three superficial sensory branches. The superficial branches were a PDN to the medial side of the little finger, a CDN to the fourth webspace and a CB communicating to the third CDN of the median nerve. The CB also communicated with the fourth CDN (Figure 3.13).

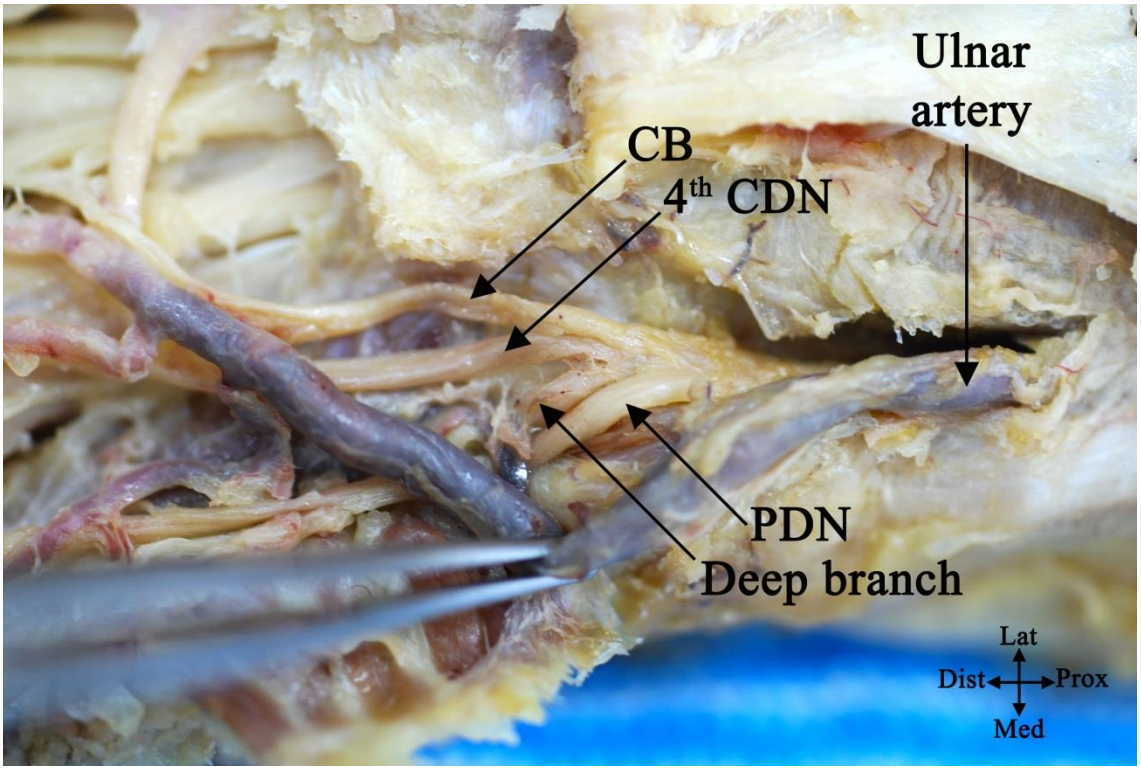

Figure 3.13: A special case where the ulnar nerve (UN) divided into four branches in Guyon's canal. PDN, proper digital nerve; CDN, common digital nerve; CB, communicating branch; Lat, lateral; Med, medial; Prox, proximal; Dist, distal.

The first and second branching points of Type I were measured to the proximal edge of the pisiform. Type II was found to divide 14.9±4.1 mm (range: 22.42-7.7) from its edge (Table 3.7).

Table 3.7: The first and second division points of Type I and the point of trifurcation of Type II to the proximal edge of the pisiform (mm)

	Mean	SD	Max	Min
Ulnar nerve division into deep & superficial (Type I first division point)	13.6	4.0	22.1	1.8
Superficial branch division into the 4th CDN[1] & PDN[2] (Type I second division point)	25.2	4.6	37.2	13.1
Ulnar nerve trifurcation into deep, 4th CDN & PDN (Type II trifurcation point)	14.9	4.1	22.42	7.7

[1] Common digital nerve
[2] Proper digital nerve to the medial side of the little finger

The sensory innervation of the little finger and medial side of the ring finger was supplied by the superficial division of the ulnar nerve in all except 6 cases where the ulnar nerve communicated with the DBUN (Kaplan anastomosis) and in another 4 cases where it received contributions from the median nerve.

The sensory distribution of the ulnar nerve in the palm was classified into two types based on the branches contributing to the innervation of the little and the medial side of the ring finger:

Type I: The little finger and the medial side of the ring finger were innervated by the superficial branch of the UN which could be:

A. Originating as a common trunk that divides distally to a PDN to the medial side of the little finger and a CDN to the fourth webspace. (Figure 3.12 A)
B. Originating as a PDN to the medial side of the little finger and a CDN to the fourth webspace. (Figure 3.12 B)

Type II: The little finger and the medial side of the ring finger were innervated by the superficial branch of the UN after it received a contribution from:

A. DBUN

i. The DBUN communicates with the superficial division of the UN before its division into CDN and PDN (Figure 3.14A).

ii. The DBUN communicates with the PDN to the little finger (Figure 3.14B).

B. Median nerve (Figure 3.15)

Type I A, I B, II A, and II B were found in 75.5%, 18.2%, 3.5% and 2.1% respectively. Contributions from both the median nerve and the DBUN were found in one case.

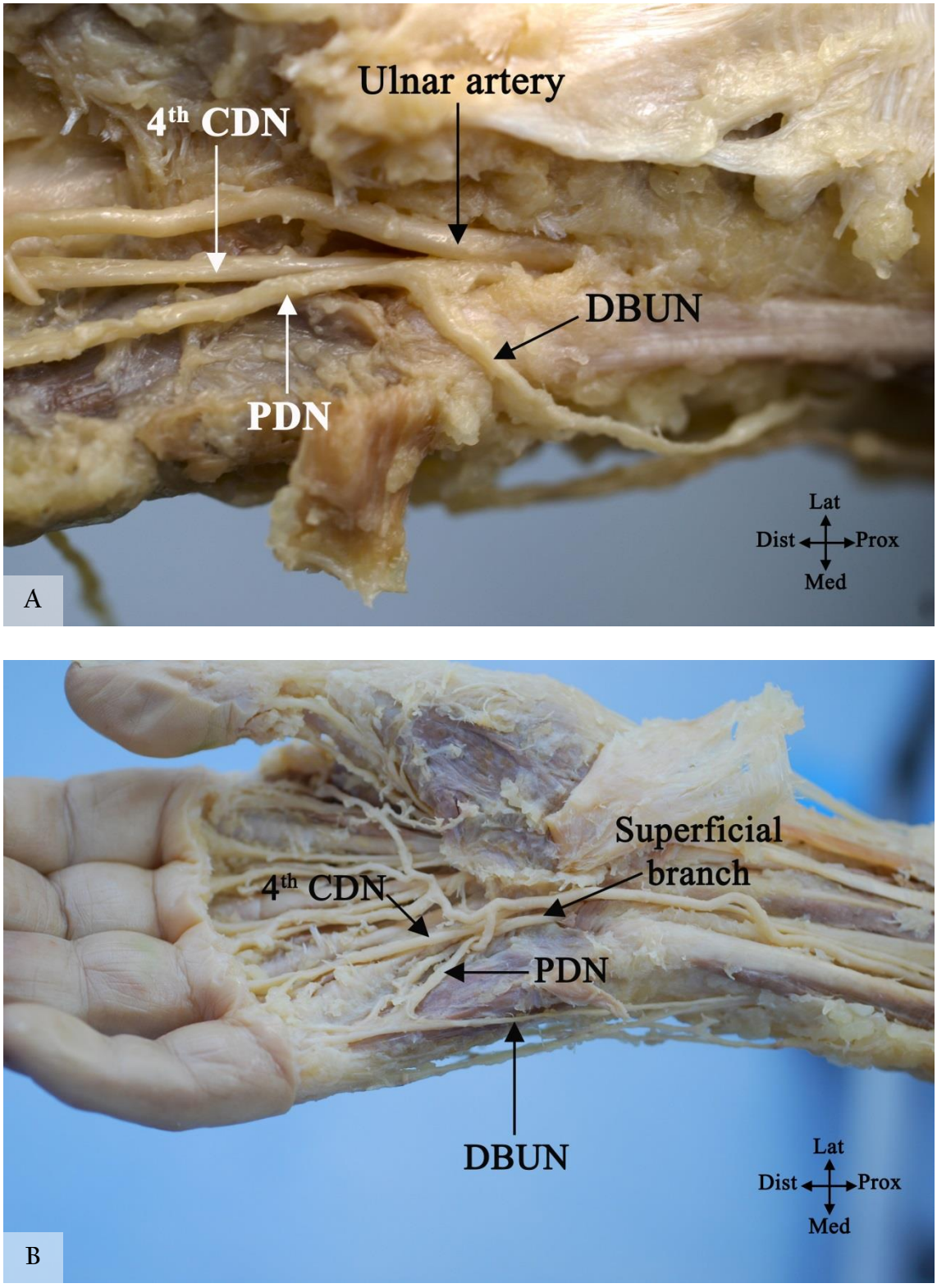

Figure 3.14: Kaplan anastomosis. (A) Dorsal branch of the ulnar nerve (DBUN) communicates with the superficial branch of the ulnar nerve. (B) DBUN communicates with the proper digital nerve to the little finger (PDN). CDN, common digital nerve; Lat, lateral; Med, medial; Prox, proximal; Dist, distal.

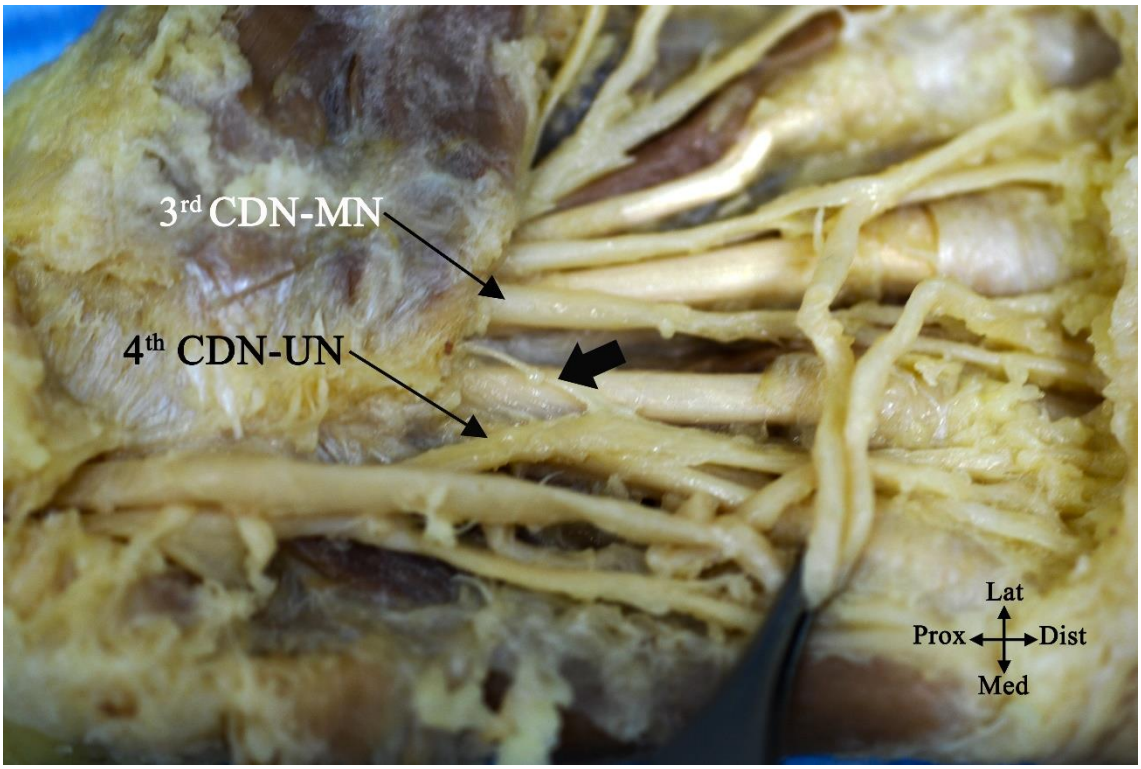

Figure 3.15: Fourth common digital nerve (CDN) receiving a branch from the third CDN which originate from the median nerve (MN). Bold arrow indicates the communicating branch. Lat, lateral; Med, medial; Prox, proximal; Dist, distal.

The fourth CDN can communicate with the PDN crossing the hypothenar eminence. This communication was found in 11 cases (7.7%) (Figure 3.16). Moreover, the deep motor branch sent a communicating branch through the hypothenar muscles to connect with the PDN to the medial side of the little finger in 7 cases (4.9%) (Figure 3.17).

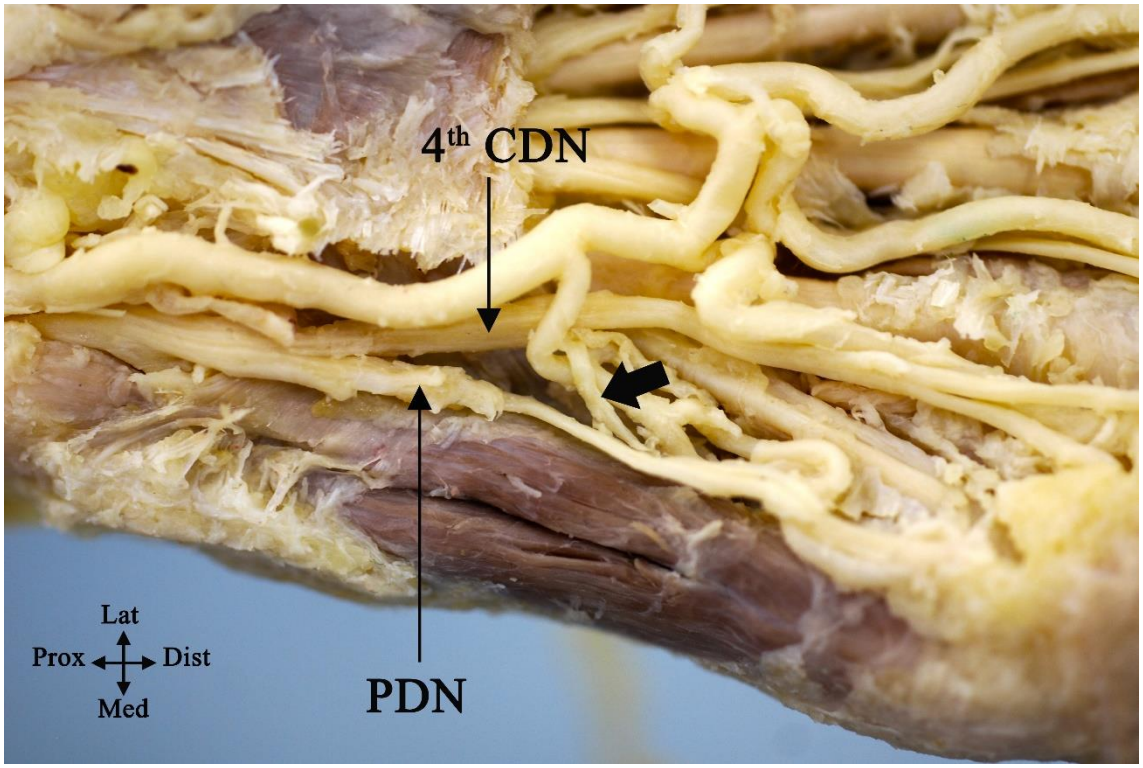

Figure 3.16: Fourth common digital nerve (CDN) communicating with the proper digital nerve (PDN) to the little finger. Bold arrow indicates the communicating branch. Lat, lateral; Med, medial; Prox, proximal; Dist, distal.

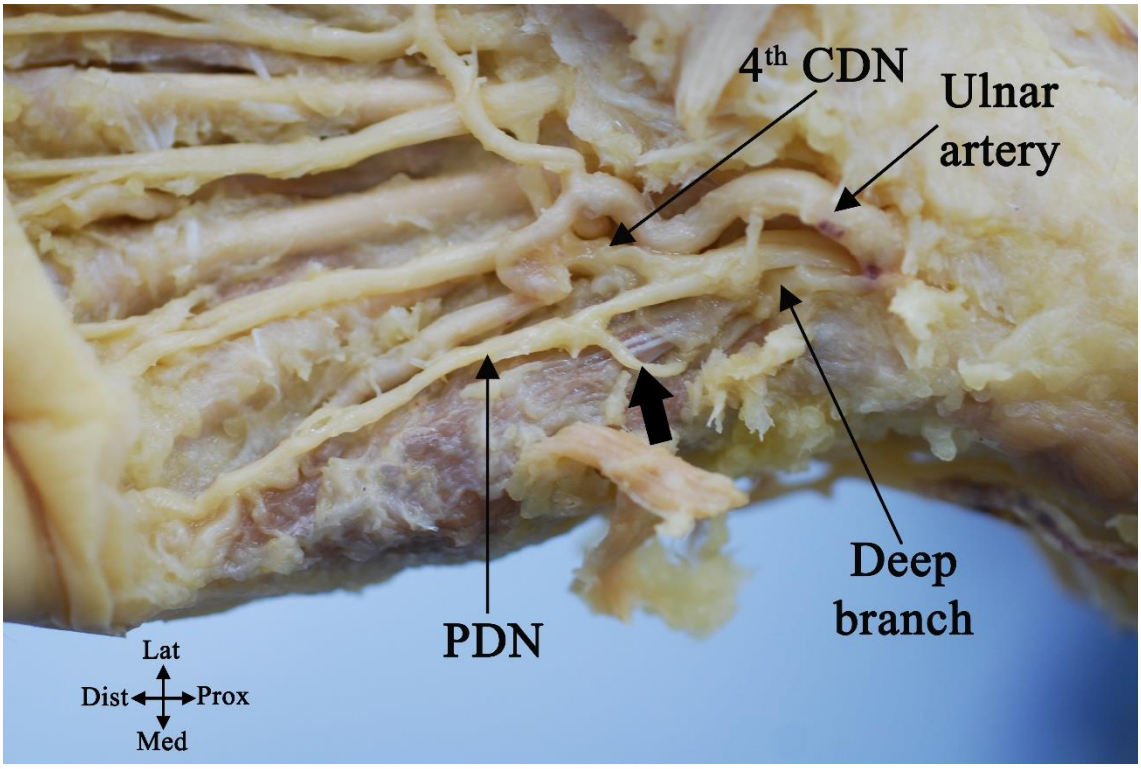

Figure 3.17: Deep motor branch of the ulnar nerve communicating with the proper digital nerve (PDN) to the little finger. CDN, common digital nerve; bold arrow indicates the communicating branch. Lat, lateral; Med, medial; Prox, proximal; Dist, distal.

In one case, the PDN to the little finger divided proximal to the fifth MCP joint and gave a branch to the dorsum of the hand. In another case, the UN divided high in the forearm. The UN divided 99.5 mm proximal to the pisiform into one superficial branch that passed superficial to Guyon's canal and another deep, passing through the canal. The superficial branch continued as the PDN to the medial side of the little finger and was joined by a branch from the DBUN. The deeper branch divided in the canal into the CDN to the fourth webspace and the deep motor branch crossing deep through the hypothenar muscles. The fourth CDN also received a contribution from the superficial branch. The ulnar artery did not pass through the canal; instead, it passed with the superficial division over the roof of the canal (Figure 3.18).

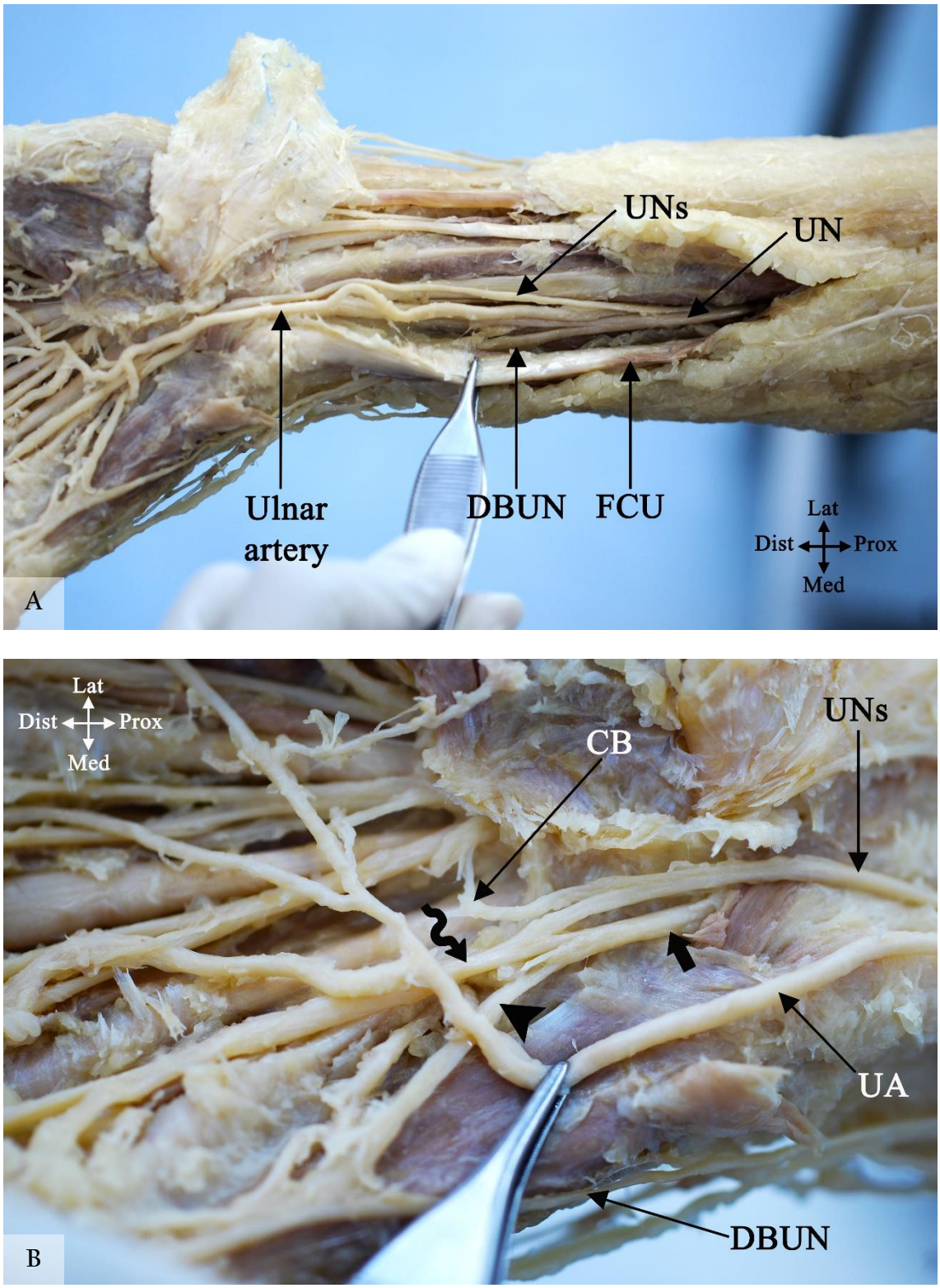

Figure 3.18: A special case of the ulnar nerve (UN) in Guyon's canal. (A) Distal forearm view. (B) Nerves after passing through Guyon's canal. FCU, flexor carpi ulnaris; UA, ulnar artery; UNs, superficial branch of the ulnar nerve; DBUN, dorsal branch of the ulnar nerve; CB, palmar communicating branch; arrow head indicates the proper digital nerve to the little finger; bold arrow indicates the deep branch of the ulnar nerve; tortuous arrow indicates the fourth common digital branch. Lat, lateral; Med, medial; Prox, proximal; Dist, distal.

3.5. Palmar communicating branch between the median and ulnar nerve

The palmar CB was investigated in 98 cadaveric palms from 62 cadavers: 45 (45.9%) male and 53 (54.1%) female. Mean age was 81.3±9.9 (range: 101-53) years.

To determine the incidence of the CB, 61 cadaveric palms were investigated (40 right hands and 21 left hands): the CB was found in all except 8 hands (13.1%).

Five patterns were noted according to the proximal and distal attachment of the CB:

Type I: The CB originated from the fourth CDN (ulnar nerve) and coursed distally to join the third CDN (MN) (Figure 3.19)

A. A single distal attachment
B. Multiple distal attachments

Type II: The CB originated from the third CDN (MN) and coursed distally to join the fourth CDN (UN) (Figure 3.20)

A. A single distal attachment
B. Multiple distal attachments

Type III: The CB coursed perpendicularly between the third and fourth CDNs (Figure 3.21).

A. A single attachments on both sides
B. Multiple attachments on one side

Type IV: The CB had multiple attachment points to both nerves in a diffuse manner (Figure 3.22 A).

Type V: The UN and MN gave branches that merged and continued distally to the lateral side of the ring finger (Figure 3.22 B).

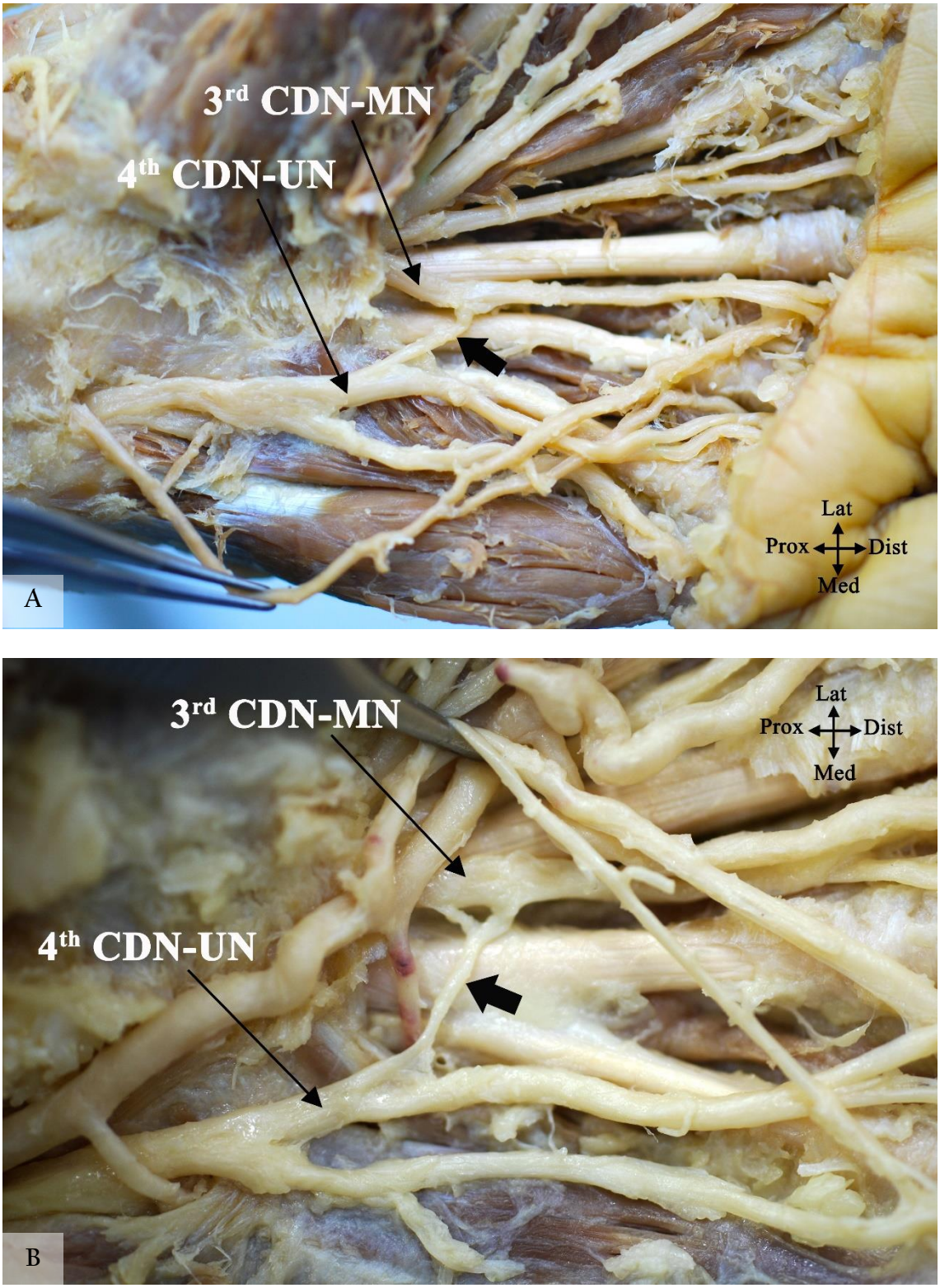

Figure 3.19: Branching pattern of the palmar communicating branch (CB) Type I. (A) Type I A, (B) Type I B. CDN, common digital nerve; MN, median nerve; UN, ulnar nerve, bold arrow indicates the palmar CB. Lat, lateral; Med, medial; Prox, proximal; Dist, distal.

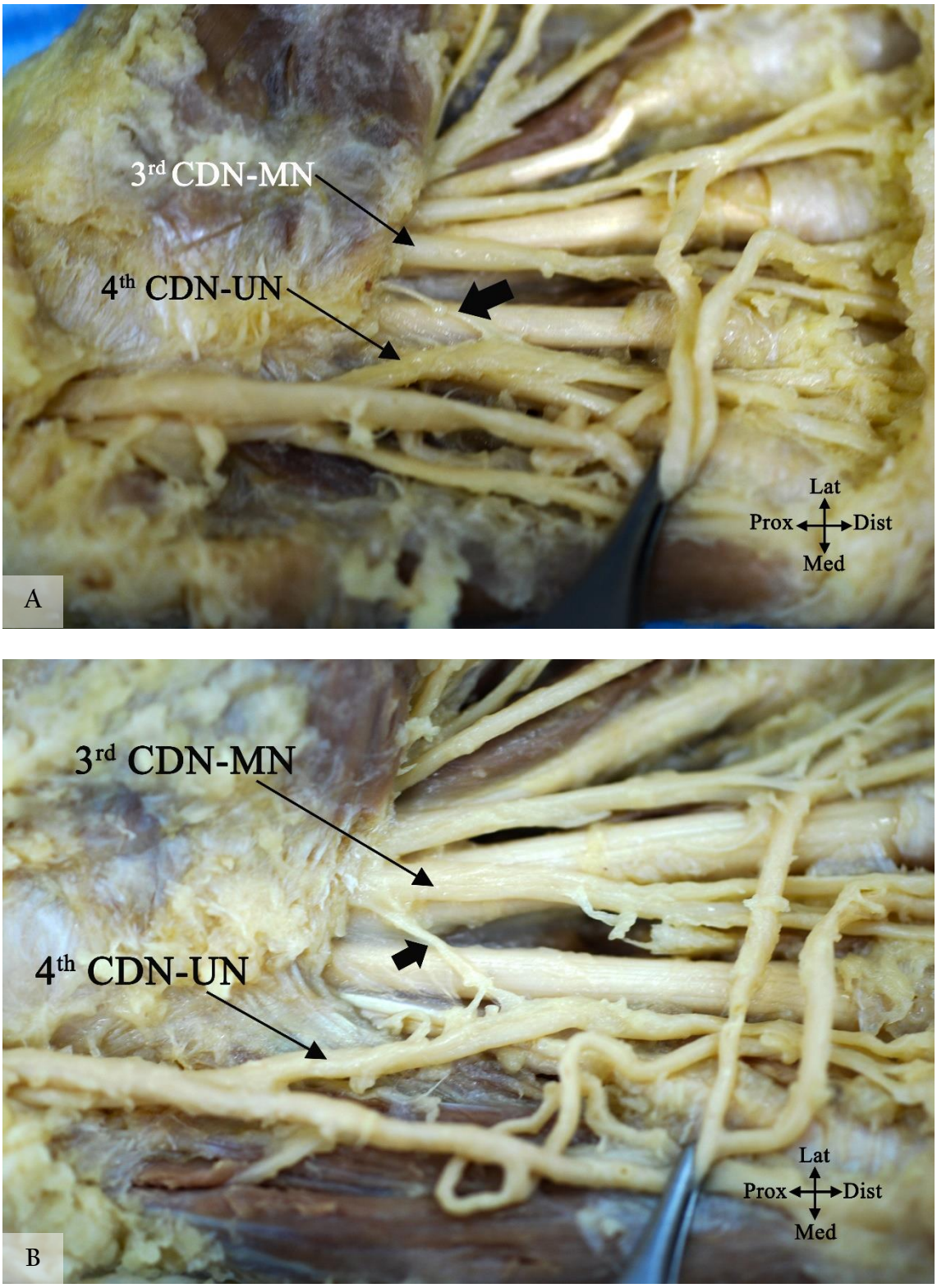

Figure 3.20: Branching pattern of the palmar communicating branch (CB) Type II. (A) Type II A, (B) Type II B. CDN, common digital nerve; MN, median nerve; UN, ulnar nerve; bold arrow indicates the palmar CB. Lat, lateral; Med, medial; Prox, proximal; Dist, distal.

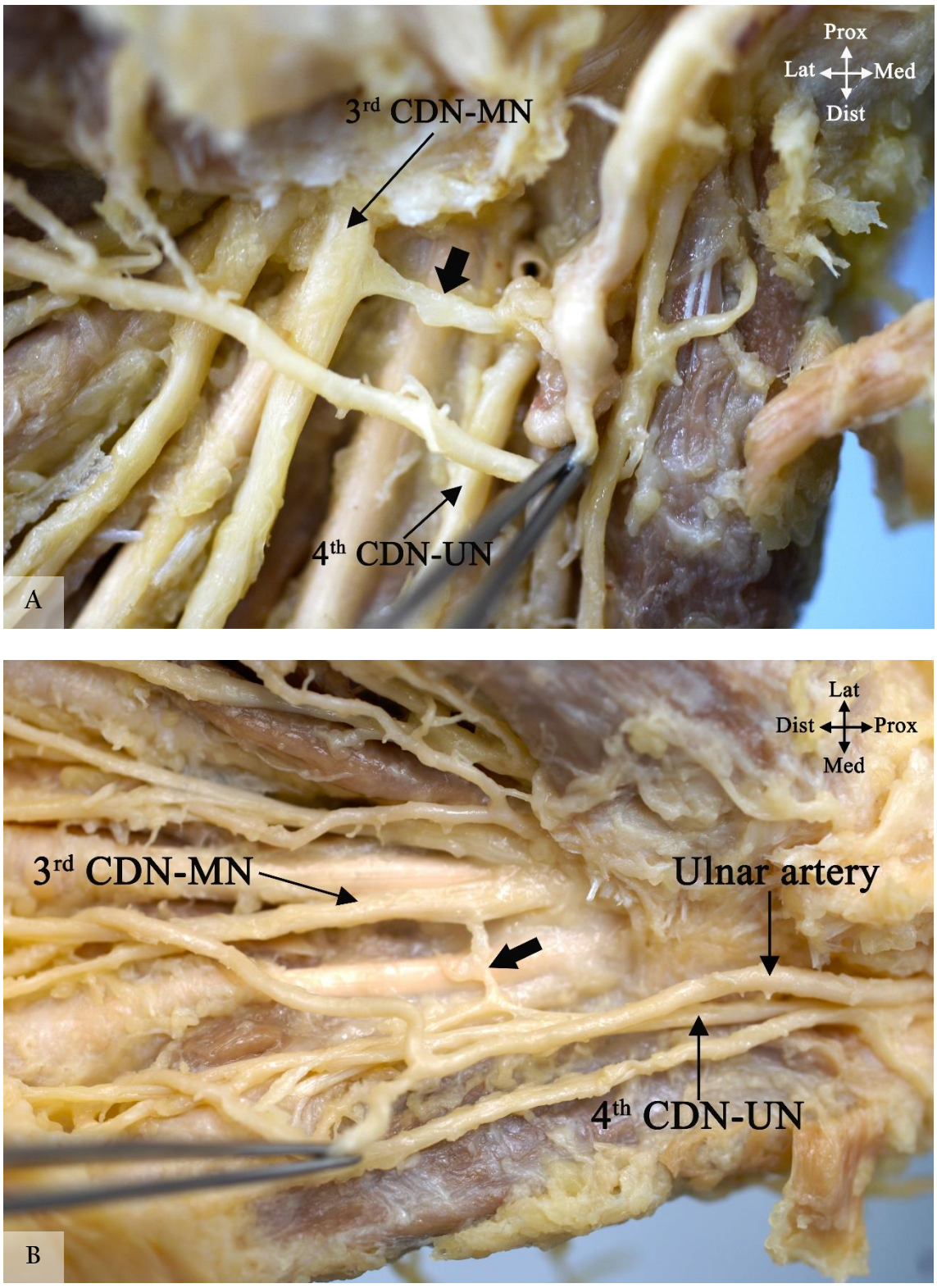

Figure 3.21: Branching pattern of the palmar communicating branch (CB) Type III. (A) Type III A, (B) Type III B. CDN, common digital nerve; MN, median nerve; UN, ulnar nerve; bold arrow indicates the palmar CB. Lat, lateral; Med, medial; Prox, proximal; Dist, distal.

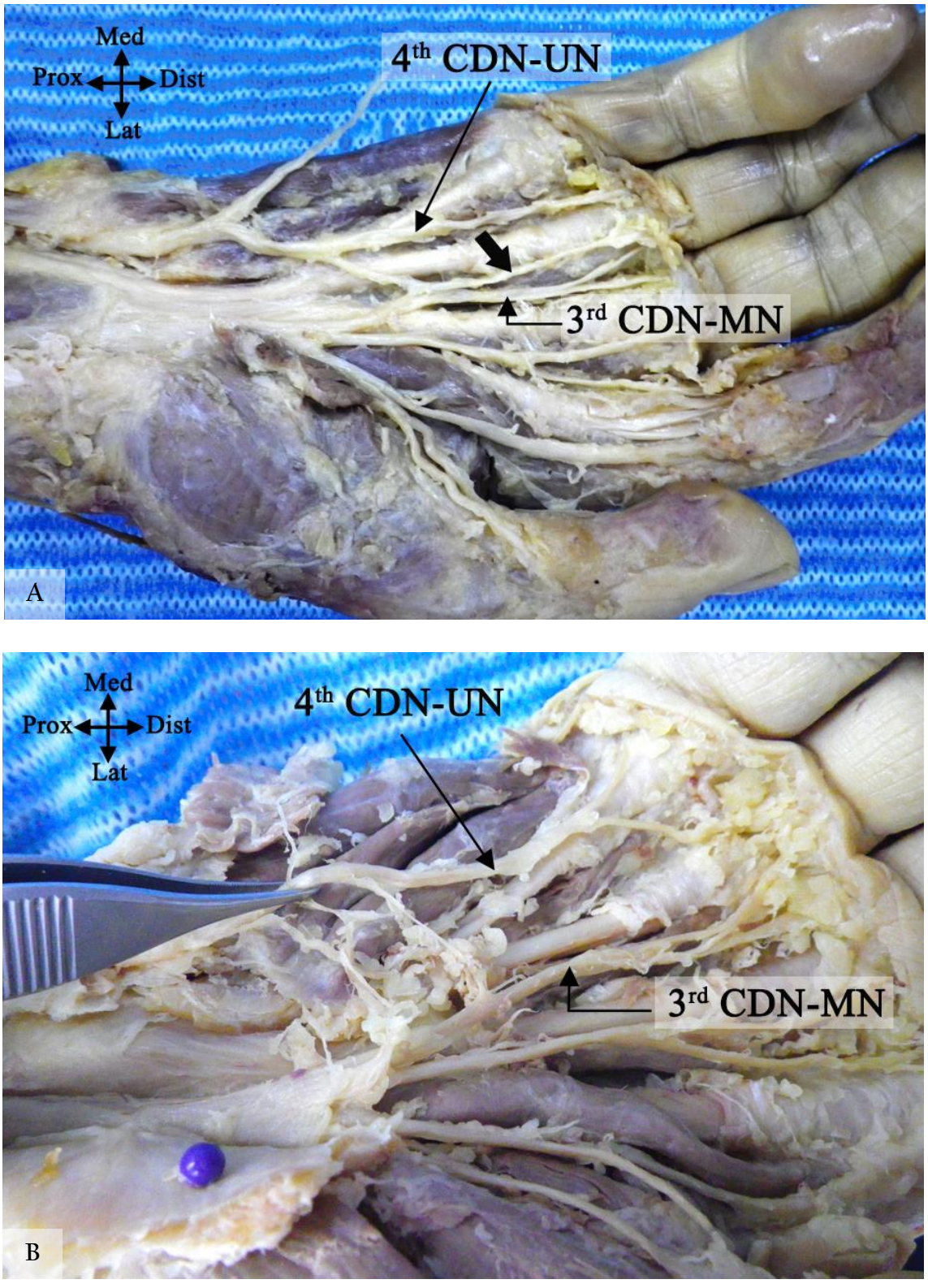

Figure 3.22: Branching pattern of the palmar communicating branch (CB) Type IV (A) and Type V (B). CDN, common digital nerve; MN, median nerve; UN, ulnar nerve; bold arrow indicates the palmar CB. Lat, lateral; Med, medial; Prox, proximal; Dist, distal.

Type I was found in 82.7% (81/98) of cases: it was noted that the CB had one distal attachment (60 cases, Type I A) or multiple distal attachments (21 cases, Type I B). Type II was found in 5.1% (5/98) of the cases investigated: similar to Type I, the distal attachment can be single (4 cases, Type II A) or multiple (1 case, Type II B). Type III was found in 5.1% (5/98), three of the five cases had multiple attachments to the fourth CDN (UN) (Type III B) and two had a single attachment to the fourth CDN and the third CDN (Type III A). Type IV and V were found in 4.1% (4/98) and 3.1% (3/98) cases respectively (Figures 3.16, 3.17, 3.18, 3.19, 3.20).

The proximal attachment of the CB was found 5.3±5.2 mm, 32.3±5.8 mm and 43.6±7.1 mm distal to the TCL, WC and to BSL respectively. The distal attachment was found 16.4±6.4 mm, 43.9±6.6 mm and 52.6±7.4 mm distal to the TCL, WC and BSL respectively. All measurements are shown in Table 3.8. Moreover, the CB was found to be 15.6±4.8 mm (range: 36.95-8.32) long and the proximal attachment originated at an angle averaging 142.7±17.7° (range: 180-90°). The angle at which the proximal attachment was found to branch off the UN or MN was found to be between 90-120°, 121-150° and 151-180° in 12.5%, 64.8% and 22.7% of the cases respectively.

Moreover, the proximal attachment of the CB was found between 25.9% and 60.3% of the distance between the third MCP joint and the WC; between 34.5% and 60.5% of the distance between the third MCP joint and the BSL. The distal attachment of the CB was found between 36.6% and 79.3% of the distance between the third MCP joint and the WC; between 41.8% and 75.4% of the distance between the third MCP joint and the BSL. The CB originated proximal to or at the level of the TCL in 13% of cases and less than 4 mm distal to the TCL in 38%.

Table 3.8: Distances measured for the proximal and distal attachments of the palmar communicating branch (CB) to different anatomical landmarks (mm)

Distance between:	Mean	SD	Max	Min
Proximal attachment of CB to TCL[1]	5.3	5.2	19.4	-10.6[2]
Distal attachment of CB to TCL	16.4	6.4	39.5	1.3
Proximal attachment of CB to WC[3]	32.3	5.8	46.6	20.5
Distal attachment of CB to WC	43.9	6.6	60.6	27.8
Proximal attachment of CB to BSL[4]	43.6	7.1	64.5	30.8
Distal attachment of CB to BSL	52.6	7.4	69.2	38.1

[1] Transverse carpal ligament
[2] Minus signs indicate that the point were located proximal to the level of the respective landmark
[3] Wrist crease
[4] Bistyloid line

The effect of sex and body side on the branching pattern was investigated. The branching pattern of the palmar CB was not influenced by sex (P value=0.335) or body side (P value =0.949). Appendix 1 shows the chi-square test results for both the effect of sex and body side.

3.6. Superficial branch of the radial nerve

The SBRN was investigated in 150 cadaveric hands from 76 cadavers: 60 (40%) male and 90 (60%) female. Mean age was 82.9±9.4 (range: 101-53) years.

The SBRN originated at the level of the elbow (the radial nerve divided into a superficial and a deep branch). In 17 cases (17/124, 13.7%), the SBRN originated proximal to the lateral epicondyle. It was found to originate 231.4±19.9 mm (range: 295-191.6) from the RSP and 13.3±13.9 (range: -35.0-57.0) mm from the lateral epicondyle. The SBRN coursed deep to brachioradialis and became subcutaneous 72.1±16.6 mm (range: 141.5-35.2) proximal to the RSP. Comparing the point where the SBRN pierces the antebrachial fascia to the total length of the radius, it is estimated that the SBRN

becomes subcutaneous in the distal 30.5±5.8% of the total length of the radius. The SBRN pierces the antebrachial fascia between the tendons of brachioradialis and extensor carpi radialis longus. In 3 cases (2%), the nerve pierced the tendon of brachioradialis to become subcutaneous.

The nerve continued distally and divided into two branches, one palmar and one dorsal, 51.4±14.9 mm proximal to the RSP. In 4 cases (2.7%), the SBRN divided into three branches rather than two (Figure 3.23). The nerve usually divided into its palmar and dorsal branches after it pierced the fascia; however, in one case the nerve divided deep to brachioradialis prior to becoming subcutaneous. In another case, the SBRN's first division originated at the level of the elbow. The SBRN originated as two nerves from the radial nerve: the superficial branch pierced brachioradialis, travelled in the substance of the muscle and became subcutaneous 119.7 mm proximal to the RSP as the palmar division of the SBRN. The deeper division continued deep to brachioradialis and became subcutaneous 97.7 mm proximal to the RSP as the dorsal branch of the SBRN. The palmar division connected with both the dorsal branch and the LABCN before it innervated the lateral side of the thumb and the thenar eminence. The dorsal branch continued to innervate the dorsum of the hand (Figure 3.24A-D).

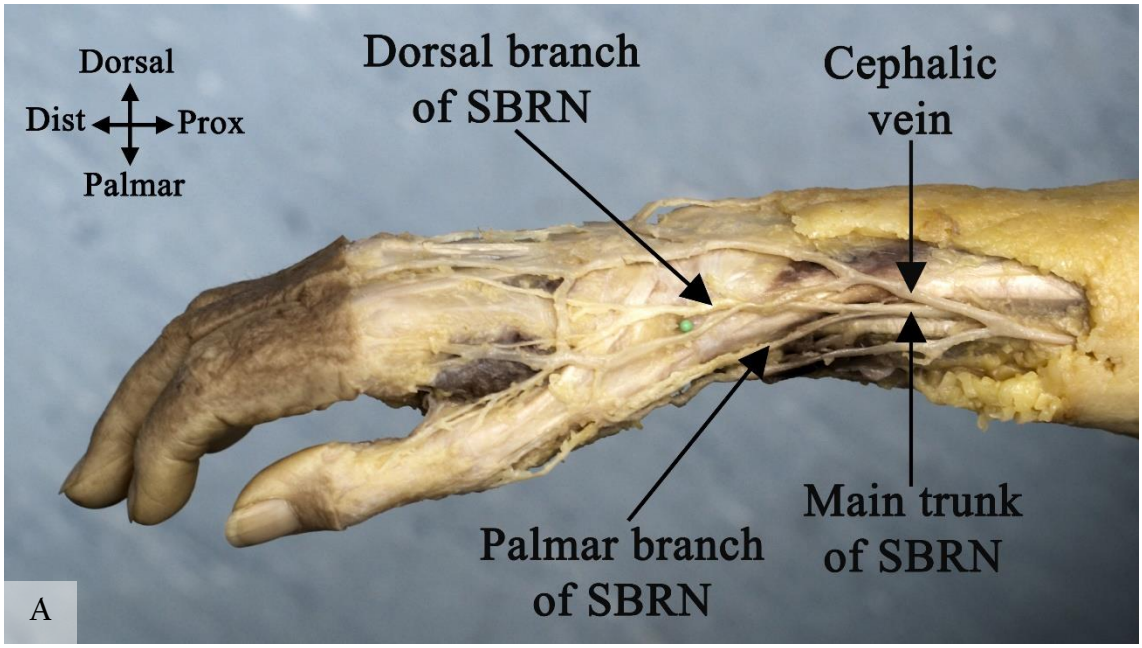

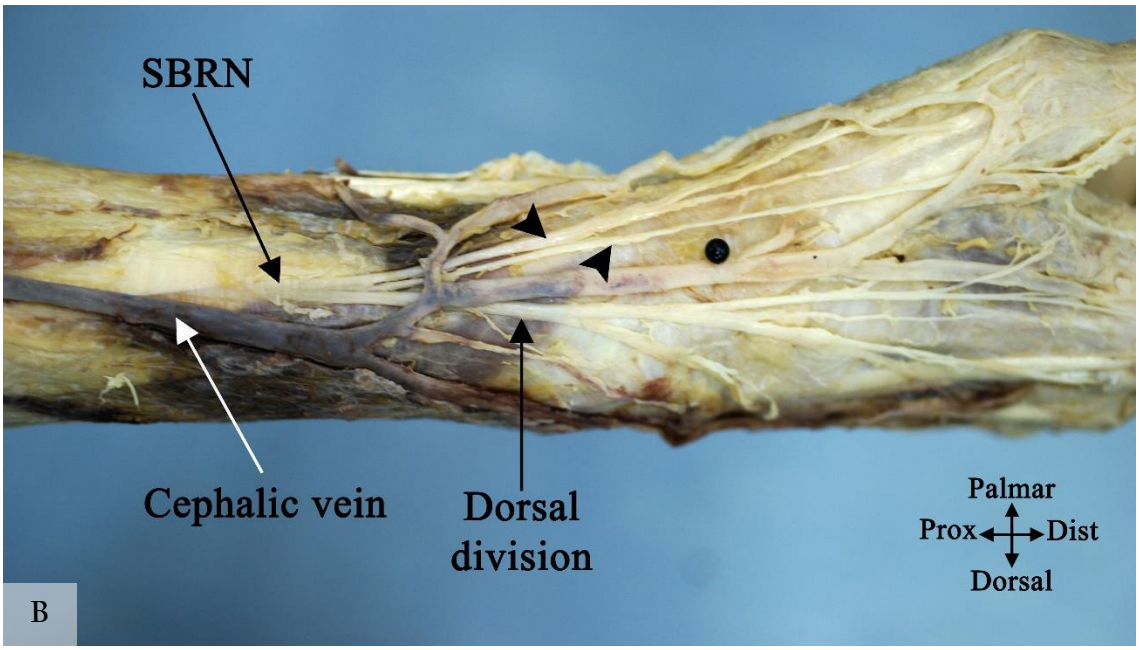

Figure 3.23: First division of the superficial branch of the radial nerve (SBRN) after it becomes cutaneous. (A) Palmar and dorsal divisions. (B) Three divisions, one dorsal and two palmar (indicated by the arrow heads); pins indicate the location of the radial styloid process. Prox, proximal; Dist, distal; palmar, palmar surface; Dorsal, dorsal surface.

Figure 3.24A: Special case of high division of the superficial branch of the radial nerve into palmar and dorsal divisions in the elbow region. Full hand view, arrow head indicates the dorsal branch; bold arrow indicates the palmar branch; black pin indicates the location of the radial styloid process. Prox, proximal; Dist, distal; Palmar, palmar surface; Dorsal, dorsal surface.

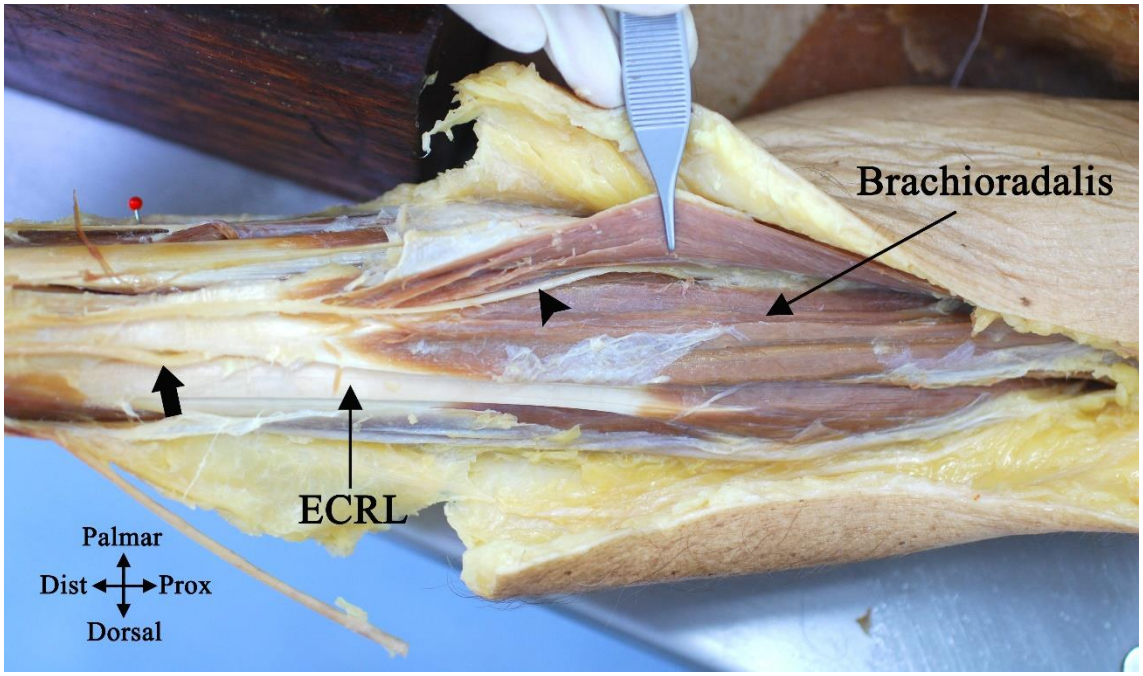

Figure 3.24B: Special case of high division of the superficial branch of the radial nerve into palmar and dorsal divisions in the elbow region. The palmar branch crossing through brachioradialis indicated by the arrow head; bold arrow indicates the dorsal branch coursing between brachioradialis and extensor carpi radialis longus (ECRL) tendons. Prox, proximal; Dist, distal; Palmar, palmar surface; Dorsal, dorsal surface.

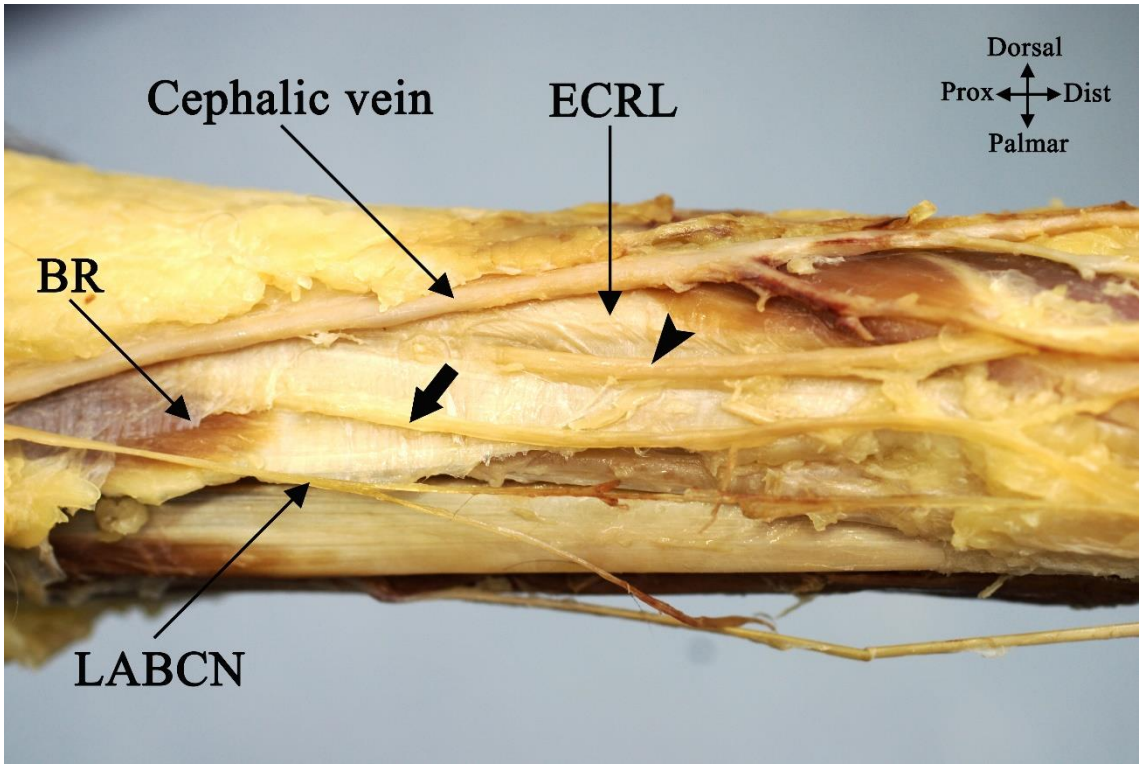

Figure 3.24C: Special case of high division of the superficial branch of the radial nerve into palmar and dorsal divisions in the elbow region. The two different points where the palmar (bold arrow) and dorsal (arrow head) branches pierce the antebrachial fascia. BR, brachioradialis; ECRL, extensor carpi radialis longus; LABCN, lateral antebrachial cutaneous nerve. Prox, proximal; Dist, distal; Palmar, palmar surface; Dorsal, dorsal surface.

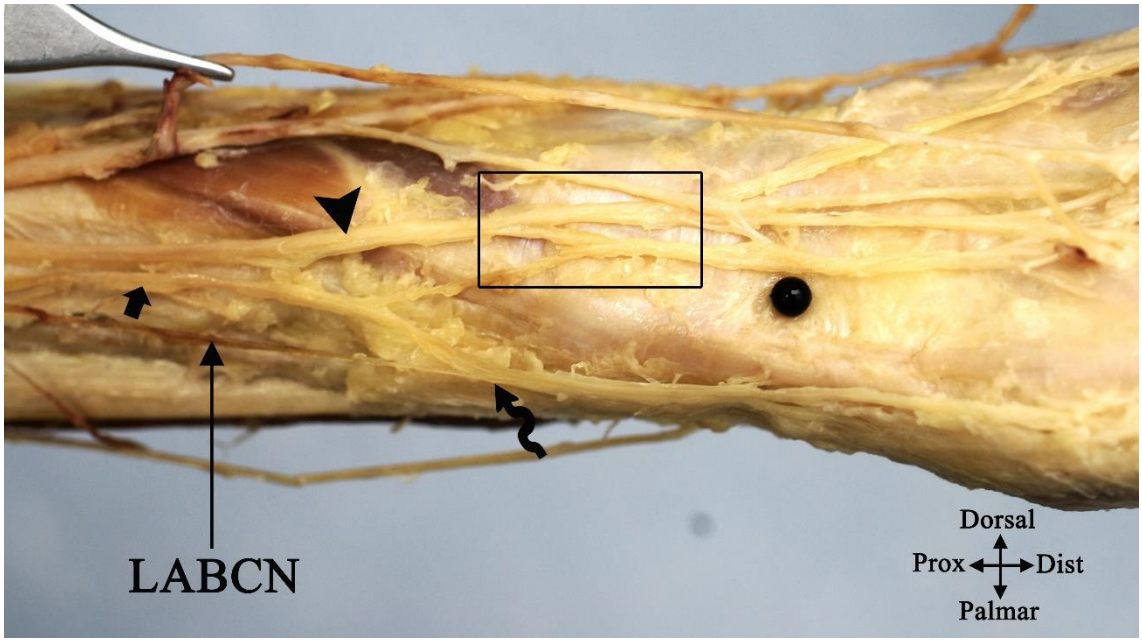

Figure 3.24D: Special case of high division of the superficial branch of the radial nerve into palmar and dorsal divisions in the elbow region. The palmar branch indicated by the bold arrow communicates with the lateral antebrachial cutaneous nerve (LABCN), communication point indicated by the tortuous arrow. Arrow head indicates the dorsal branch; rectangular area shows the palmar and dorsal branch communicating; black pin indicates the location of the radial styloid process. Prox, proximal; Dist, distal; Palmar, palmar surface; Dorsal, dorsal surface.

Prior to the first division, the SBRN diameter averaged 3.2±0.8 mm. All SBRN branches passed radial to LT with a mean distance of 14.1±3.8 mm (Table 3.9). The SBRN connected with the LABCN in 46 cases (30.7%) and crossed the cephalic vein for the first time after it became subcutaneous 47.9±19.3 mm proximal to the RSP. The SBRN branches often passed superficial to the anatomic snuff box. At the level of the RSP, the closest palmar and dorsal branches of SBRN passed 8.5±4.2 mm and 4.9±3.0 mm respectively. The closest palmar and dorsal branches to a point 25 mm proximal to the RSP passed 5.6±3.4 mm and 4.2±2.6 mm respectively (Table 3.9).

Table 3.9: Measurements of the closest branches of the superficial branch of the radial nerve (SBRN) to various anatomical points (mm)

	Mean	SD	Max	Min
Closest palmar branch at the level of the RSP[1]	8.5	4.1	17.8	0.7
Closest dorsal branch at the level of the RSP	4.9	3.0	14.7	1.1
Closest palmar branch to a point 25 mm proximal to the RSP	5.6	3.4	15.1	0
Closest dorsal branch to a point 25 mm proximal to the RSP	4.1	2.6	10.9	0
Closest branch to Lister's tubercle	14.1	3.8	23.1	4.6
First intersection between the SBRN and the cephalic vein	47.9	19.3	93.6	6.7
SBRN diameter prior to its first division	3.2	0.8	5.8	1.94

[1] Radial styloid process

The palmar branch of the SBRN usually supplied the thumb and the lateral side of the thenar eminence. The dorsal branch continued distally and divided in many configurations to supply the dorsum of the hand. The major division points of the palmar and the dorsal branches to the RSP are presented in Table 3.10.

Table 3.10: The major division points of the superficial branch of the radial nerve to the radial styloid process (mm)

	Mean	SD	Max	Min
First division point into palmar and dorsal branches	-51.4[1]	14.9	-14.5	-85.0
Palmar branch: Second major division point	-4.9	21.7	48.5	-54.0
Dorsal branch: Second major division point	-4.6	14.4	26.8	-48.2
Palmar branch: Third major division point	22.2	24.0	73.2	-30.7
Dorsal branch: Third major division point	22.3	13.1	62.2	-31.6[2]

[1] Minus signs indicate that the point were located proximal to the level of the respective landmark

The pattern of distribution of the SBRN had many configurations but was classified into six main types according to the extent of the sensory innervation in the dorsum of the hand modifying the suggested system recommended by Gupta et al. (2012):

Type I: The SBRN innervated the lateral two and half digits (Figure 3.25)

A. The main trunk bifurcated into S3 and a common trunk. S3 innervated the entire thumb, whereas the common trunk further divided into S2 and S1 distally
B. The main trunk bifurcated into S3 and a common trunk. S3 innervated the lateral side of the thumb, whereas the common trunk further divided into S2 and S1 distally
C. The main trunk trifurcated into three branches with a common origin point. The branches innervated the lateral side of the thumb, the medial side of the thumb and the lateral index, the medial index and the lateral middle fingers.

Type II: SBRN innervated the lateral 3 digits. The main trunk divided into medial and SR3 branches. The medial branch supplied the middle and index

fingers and occasionally the medial side of the thumb. SR3 supplied the thumb (Figure 3.26).

A. The main trunk divided into S3 and a common trunk. S3 innervated the entire thumb. The common trunk divided into S2 and S1 distally.
B. The main trunk divided into S3 and a common trunk, which divided distally to S1 and S2. S2 innervated the medial thumb and S1 the index and the middle finger.
C. The main trunk bifurcated into S3 and a common trunk. S3 innervated the lateral side of the thumb, whereas the common trunk further divided into two branches distally. The medial side of the thumb and the lateral side of the index fingers are innervated by the same branch.
D. The main trunk bifurcated into S3 and a common trunk. S3 innervated the lateral side of the thumb, whereas the common trunk further divided into three or four branches distally.
E. The main trunk trifurcated into three branches with a common origin point. The branches innervated the lateral side of the thumb, the medial side of the thumb, index and middle fingers.

Type III: SBRN innervated the lateral 3 and half digits. The main trunk divided into a medial and SR3 (Figure 3.27).

A. The main trunk bifurcated into S3 and a common trunk. S3 innervated the entire thumb, whereas the common trunk further divided into S2 and S1 distally.
B. The main trunk bifurcated into S3 and a common trunk. S3 innervated the lateral side of the thumb, whereas the common

trunk further divided into S1 and S2 distally. The medial side of the thumb and the lateral side of the index finger are innervated by the same branch.

C. The main trunk bifurcated into S3 and a common trunk. S3 innervated the lateral side of the thumb, whereas the common trunk further divided into S2 and S3 distally. S2 to the medial side of the thumb and S3 to the rest of the territory.

D. The main trunk bifurcated into S3 and a common trunk. S3 innervated the lateral side of the thumb, whereas the common trunk further divided into three or four branches distally.

Type IV: SBRN innervated the lateral four digits (Figure 3.28).

Type V: SBRN innervated the lateral four and half digits (Figure 3.29).

Type VI: SBRN innervated the full dorsum of the hand with the absence of the DBUN.

A. Trifurcation of the main trunk (Figure 3.30).

B. The main trunk bifurcated into S3 and a common trunk. S3 supplies the lateral side of the thumb. The common trunk further trifurcates (Figure 3.31).

C. The main trunk bifurcated into S3 and a common trunk. S3 supplies the lateral side of the thumb. The common trunk divided into S2 and S1. S2 supplies the medial side of the thumb and the lateral index finger. S1 supplies the rest of the territory (Figure 3.32).

D. The main trunk bifurcated into S3 and a common trunk. S3 supplies the lateral side of the thumb. The common trunk divided into S2 and S1. S2 supplies the medial side of the thumb index

and the lateral side of the middle fingers. S1 supplies the rest of the territory (Figure 3.33).

The most common type was Type I found in the 37.33% of the cases. Type II, III, IV, V and IV were found in 23.33%, 29.33%, 1.33%, 2% and 6.67% respectively. Tables 3.11-3.14 show the incidence rate for each type. Figures 3.25-3.33 show the different patterns of the SBRN.

Table 3.11: Incidence rate for superficial branch of the radial nerve (SBRN) Type I branching pattern

Type	No.	%
Type I	**56**	**37.3**
1A	8	5.3
1B	46	30.7
1C	2	1.3

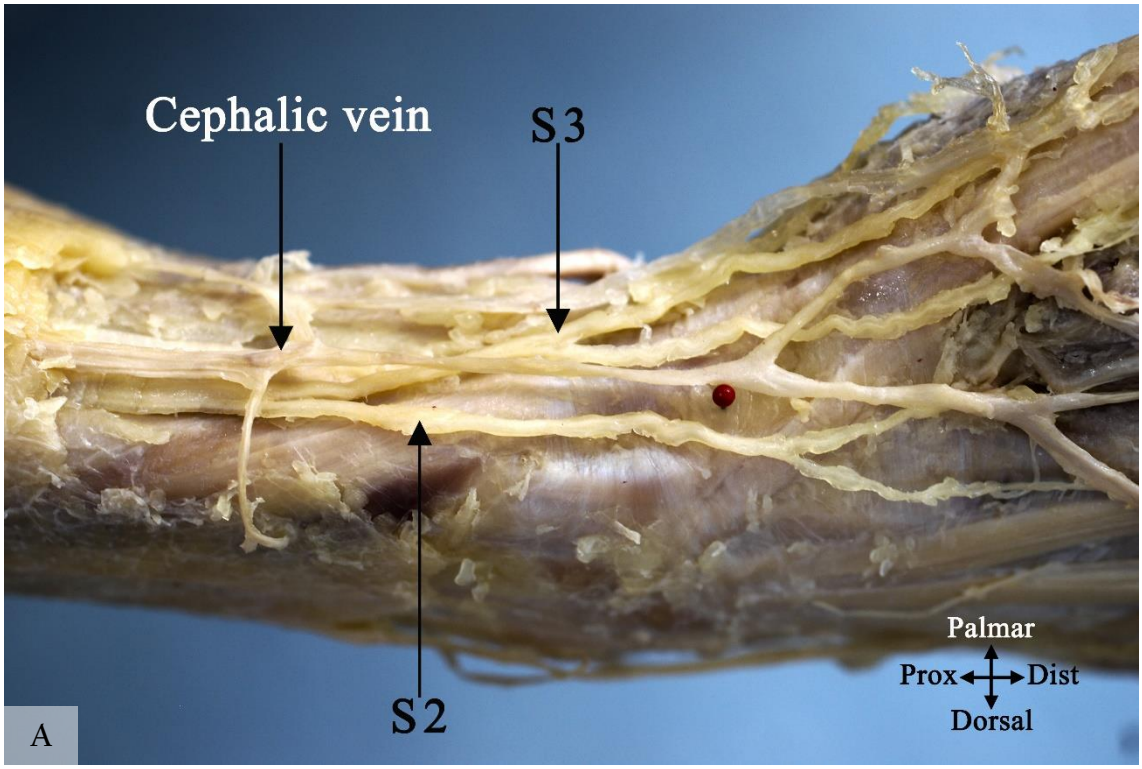

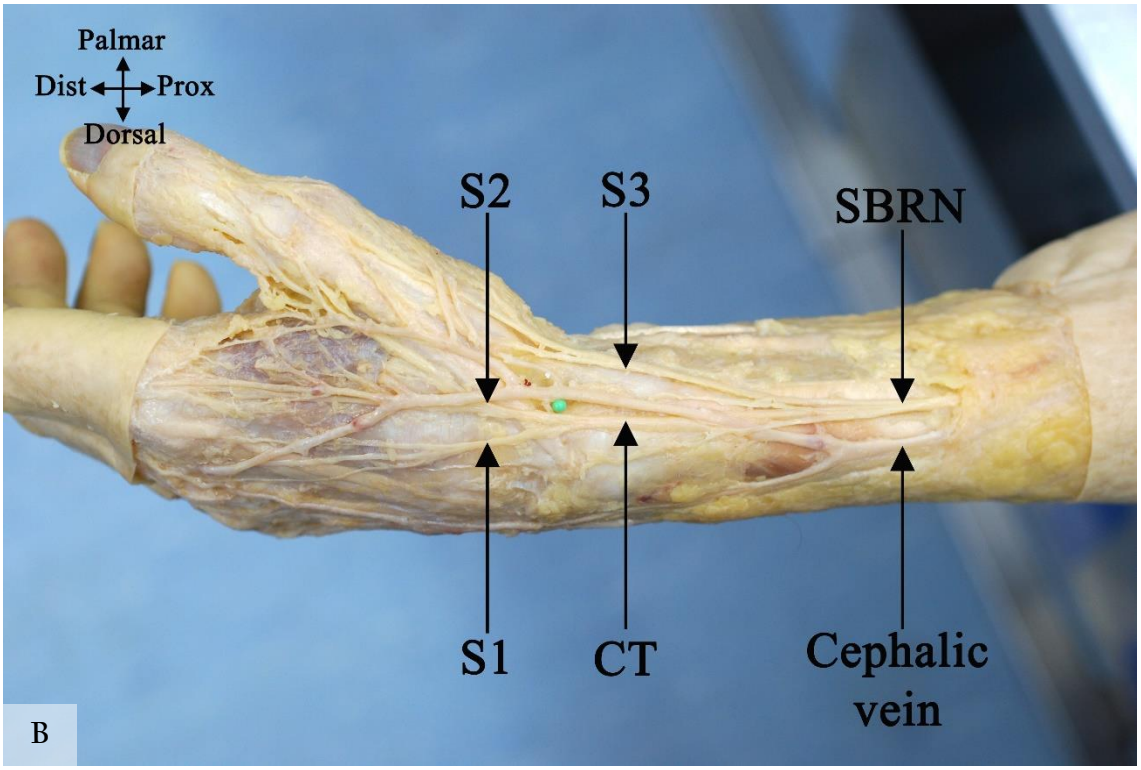

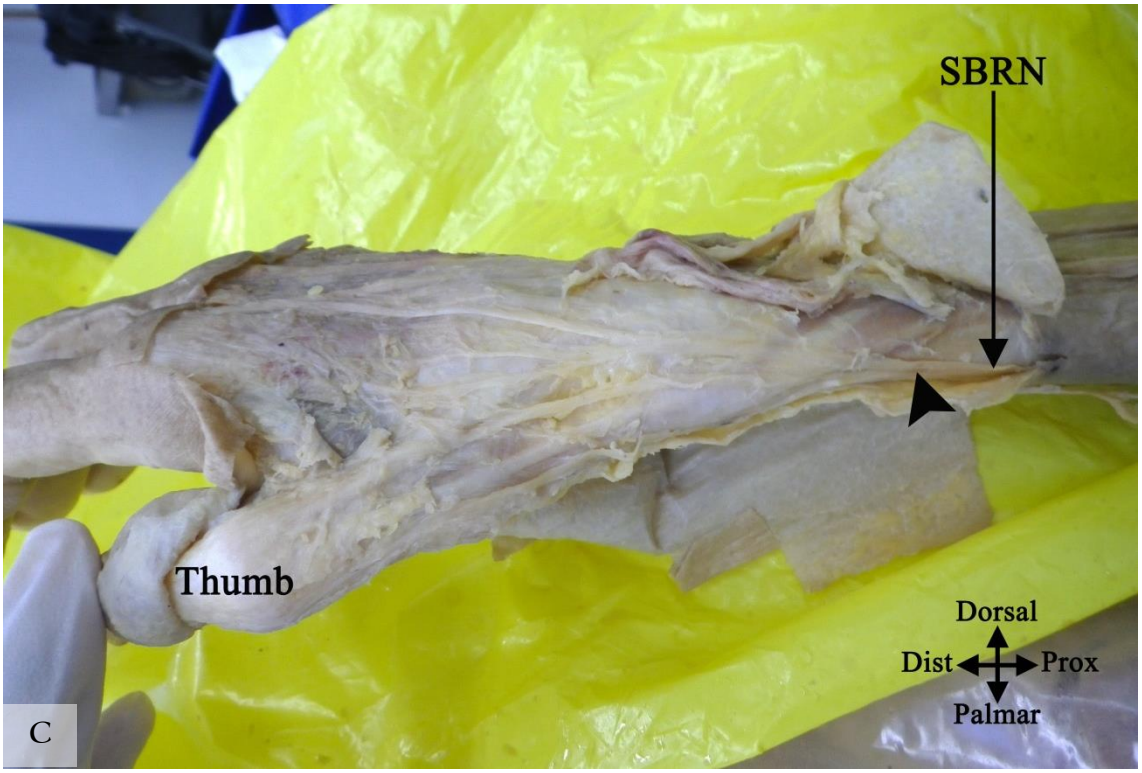

Figure 3.25: Branching pattern of the superficial branch of the radial nerve (SBRN) Type I. (A) Type I A. (B) Type I B. (C) Type I C. Arrow head indicates the trifurcation of the SBRN, pins indicate the location of the radial styloid process. Prox, proximal; Dist, distal; Palmar, palmar surface; Dorsal, dorsal surface.

Table 3.12: Incidence rate for superficial branch of the radial nerve (SBRN) Type II branching pattern

Type	No.	%
Type II	**35**	**23.3**
IIA	3	2
IIB	3	2
IIC	25	16.7
IID	3	2
II E	1	0.7

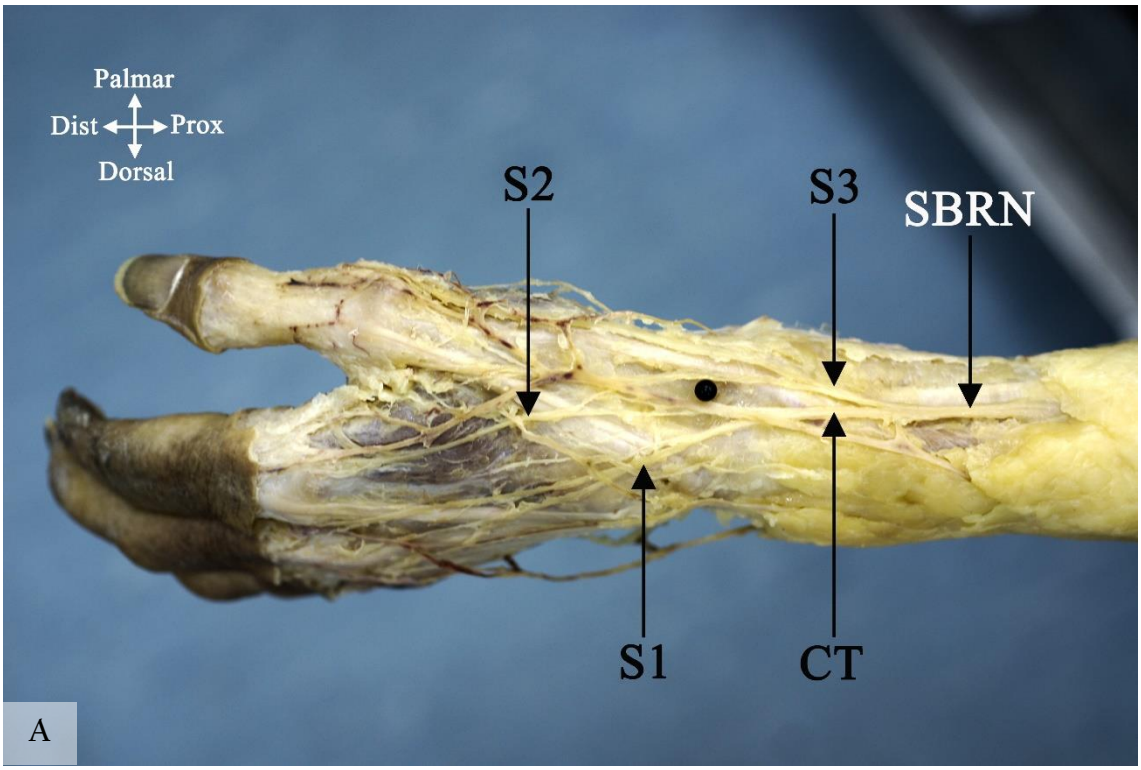

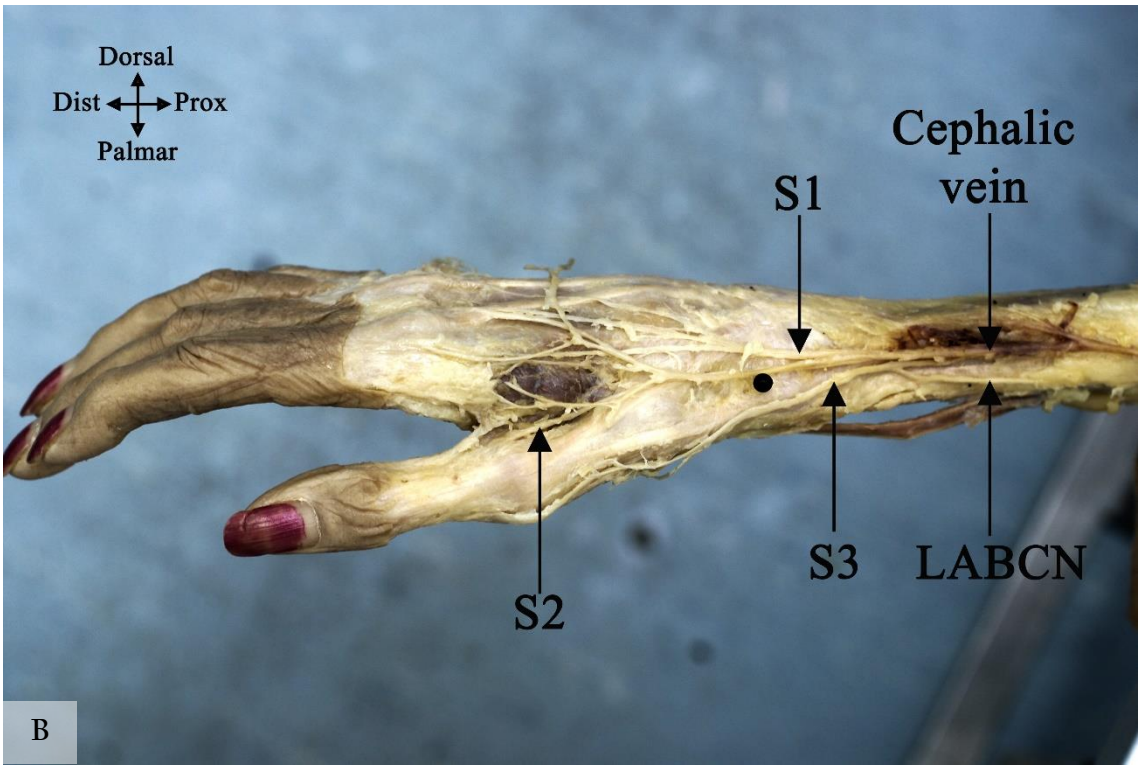
Dorsal
Dist
Prox
Palmar
Cephalic vein
S1
S3
LABCN
S2
B

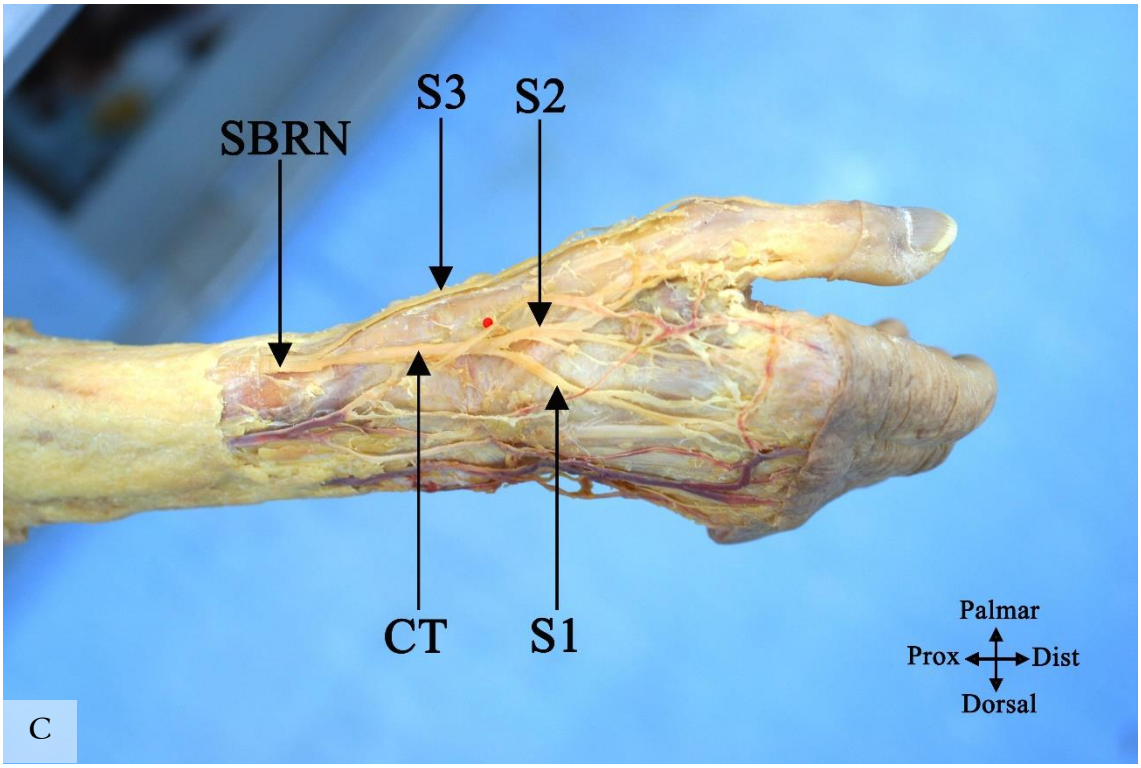
S3
S2
SBRN
CT
S1
Palmar
Prox
Dist
Dorsal
C

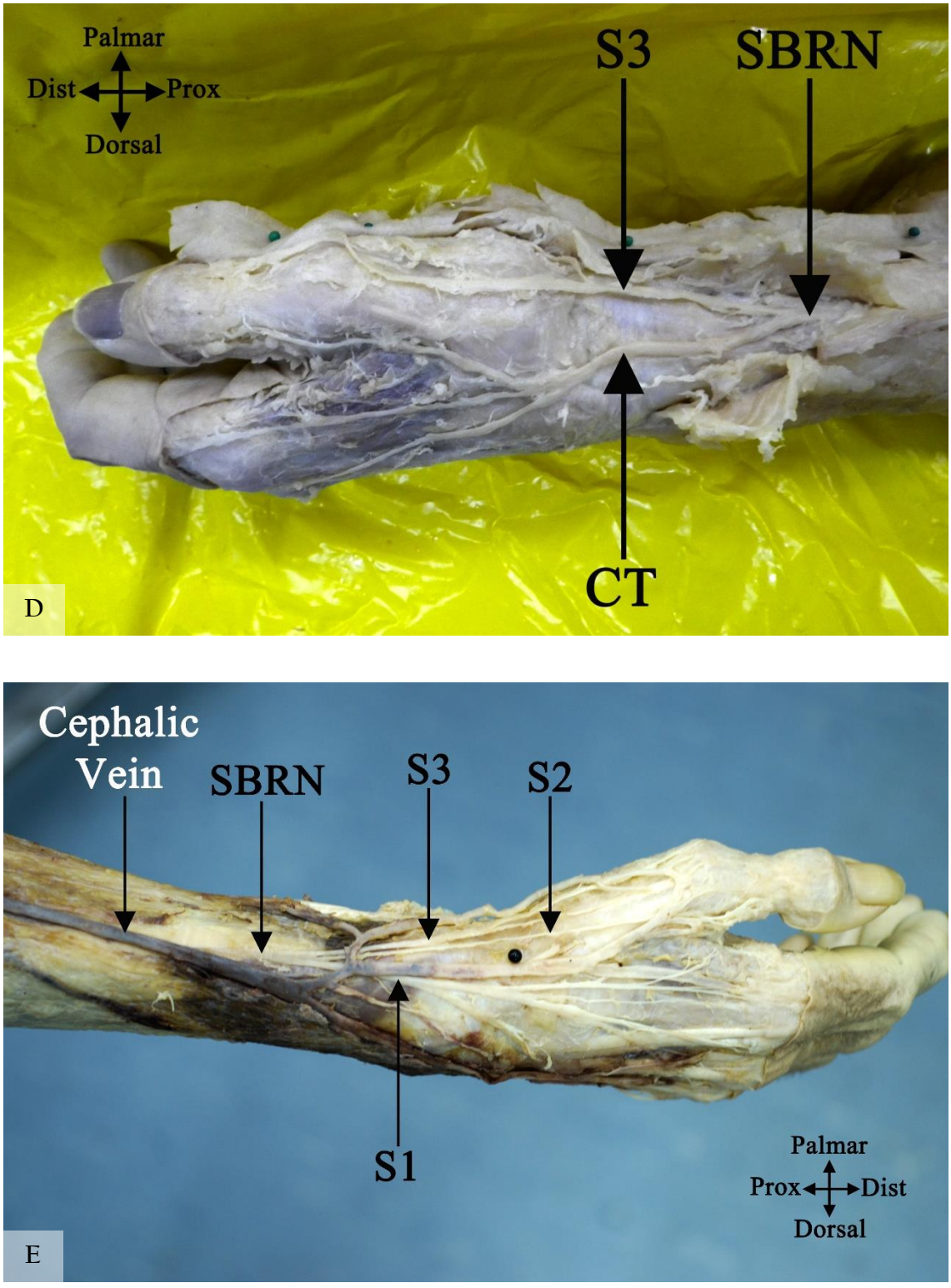

Figure 3.26: Branching pattern of the superficial branch of the radial nerve (SBRN) Type II. (A) Type II A. (B) Type II B (C) Type II C. (D) Type II D. (E) Type II E. CT, common trunk; LABCN, lateral antebrachial cutaneous nerve; pins indicate the location of the radial styloid process. Prox, proximal; Dist, distal; Palmar, palmar surface; Dorsal, dorsal surface.

Table 3.13: Incidence rate for superficial branch of the radial nerve (SBRN) Type III branching pattern

Type	No.	%
Type III	**44**	**29.3**
IIIA	6	4
IIIB	28	18.7
IIIC	5	3.3
IIID	5	3.3

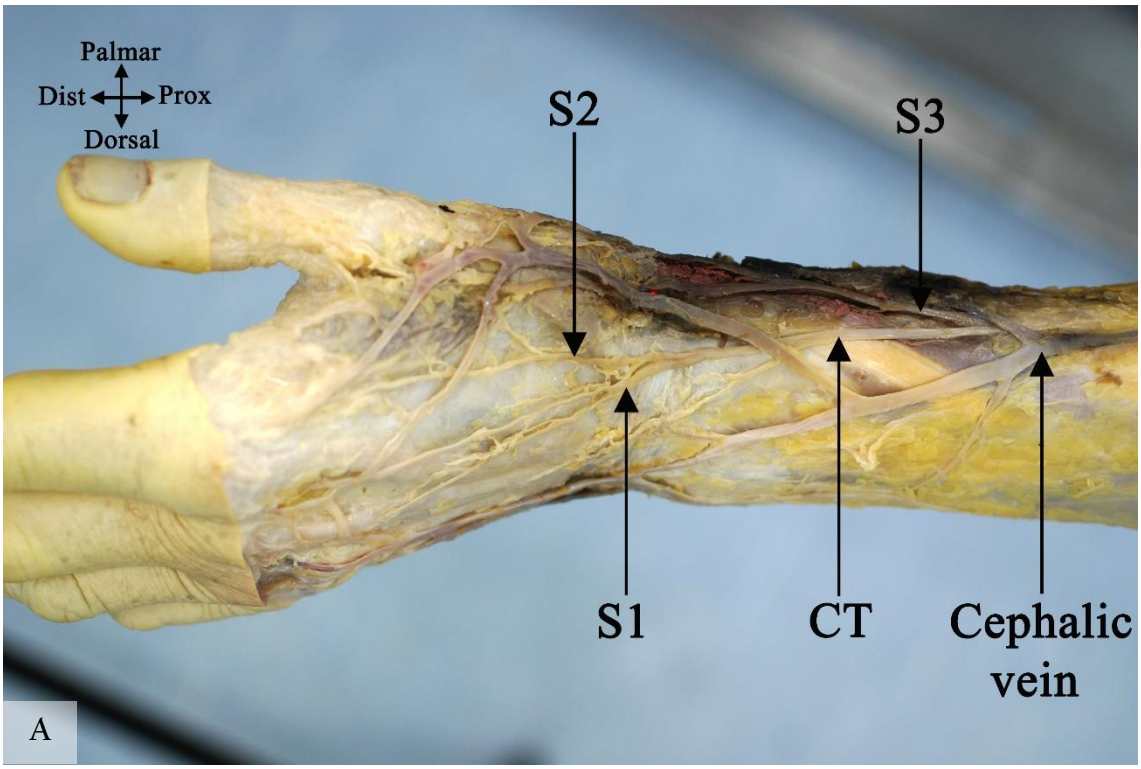

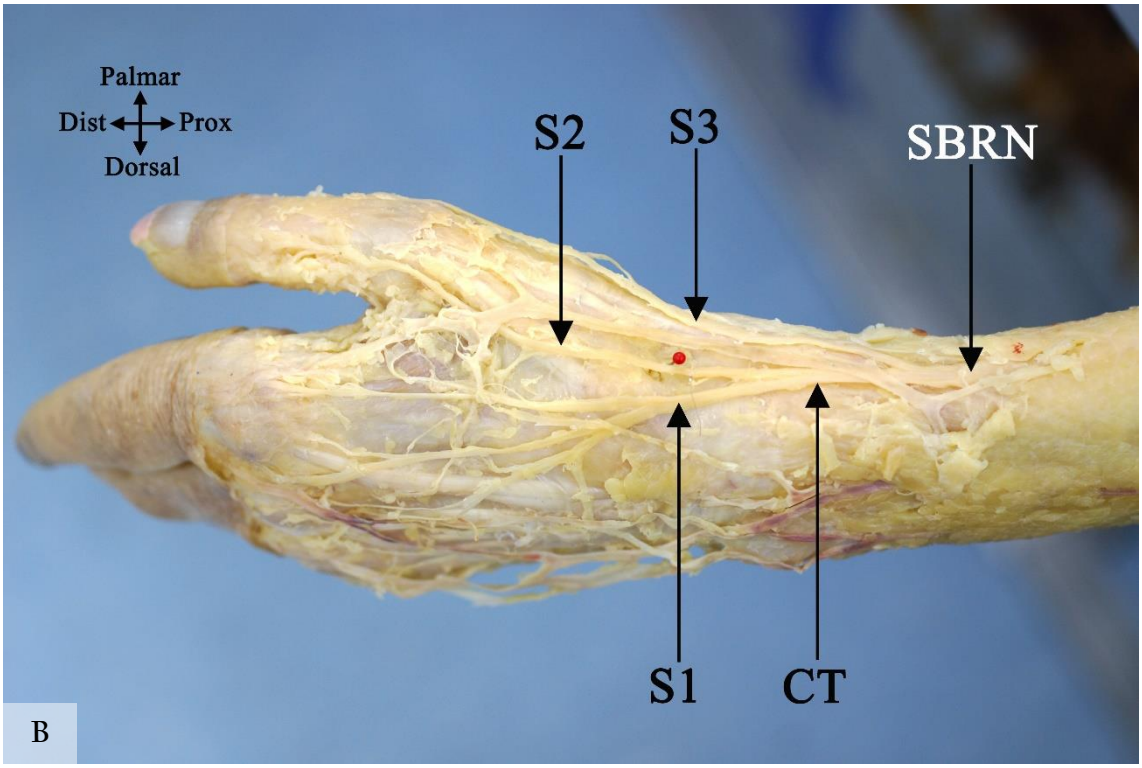
Palmar
Dist
Prox
Dorsal
S2
S3
SBRN
S1
CT
B

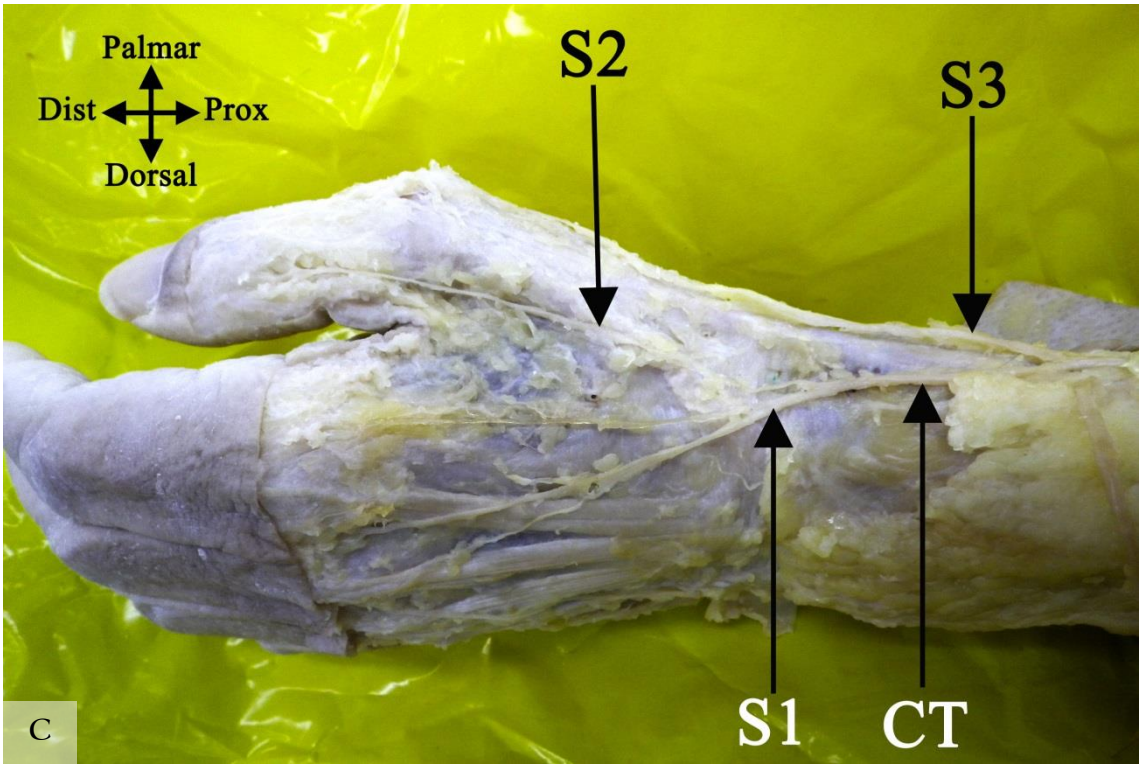
Palmar
Dist
Prox
Dorsal
S2
S3
S1
CT
C

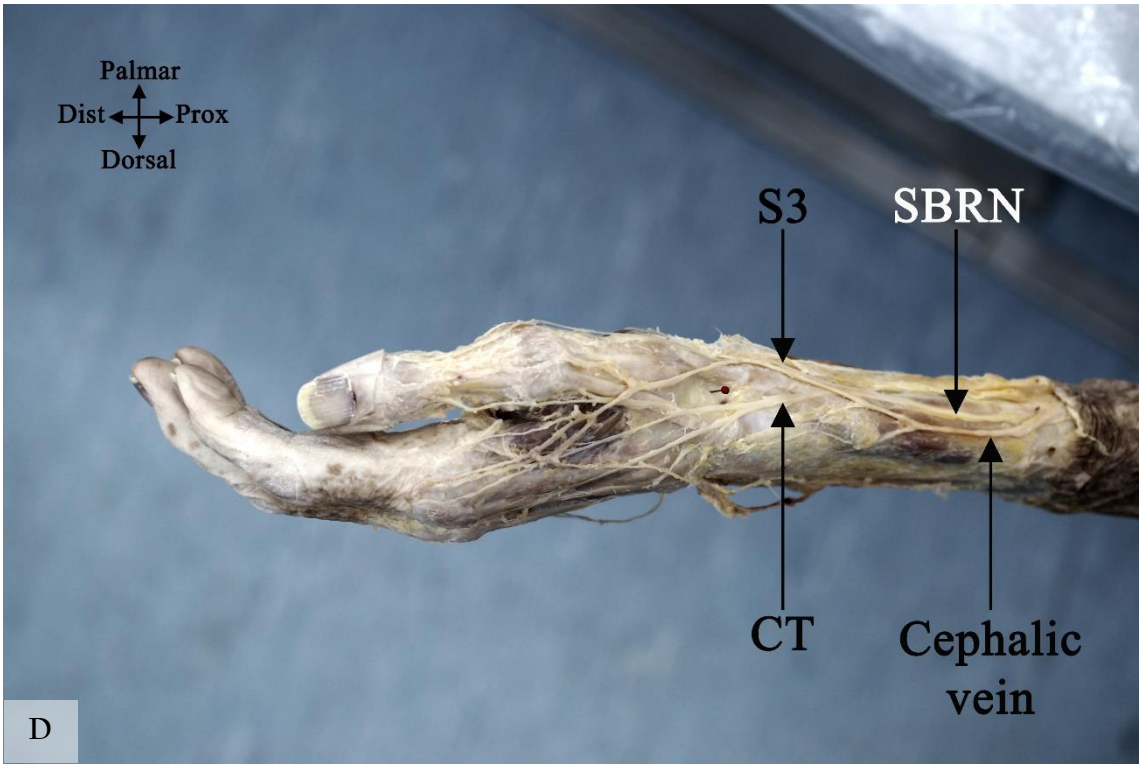

Figure 3.27: Branching pattern of the superficial branch of the radial nerve (SBRN) Type III. (A) Type III A. (B) Type III B (C) Type III C. (D) Type III D. CT, common trunk; pins indicate the location of the radial styloid process. Prox, proximal; Dist, distal; Palmar, palmar surface; Dorsal, dorsal surface.

Table 3.14: Incidence rates for superficial branch of the radial nerve (SBRN) Type IV, Type V and Type VI branching patterns

Type	No.	%
Type IV	2	1.3
Type V	3	2
Type VI	10	6.7
VIA	1	0.7
VIB	2	1.3
VIC	5	3.3
VID	2	1.3

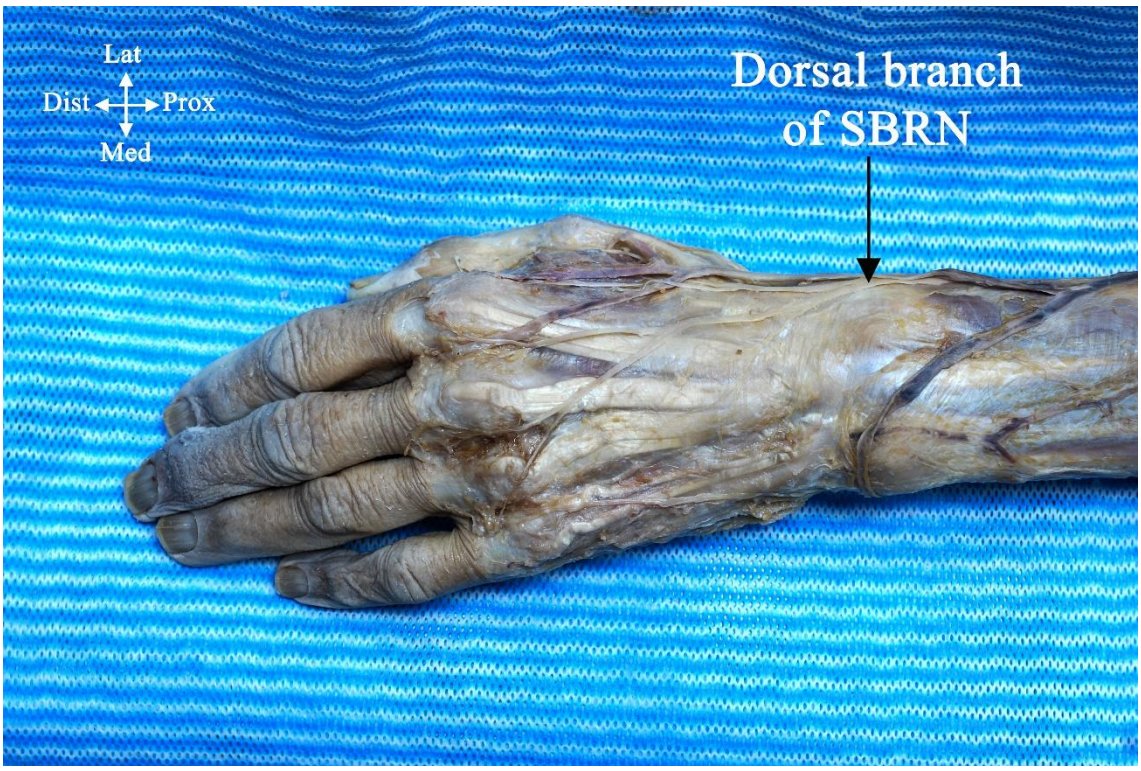

Figure 3.28: Branching pattern of the superficial branch of the radial nerve (SBRN) Type IV. Prox, proximal; Dist, distal; Lat, lateral; Med, medial.

Figure 3.29: Branching pattern of the superficial branch of the radial nerve (SBRN) Type V. Prox, proximal; Dist, distal; Lat, lateral; Med, medial.

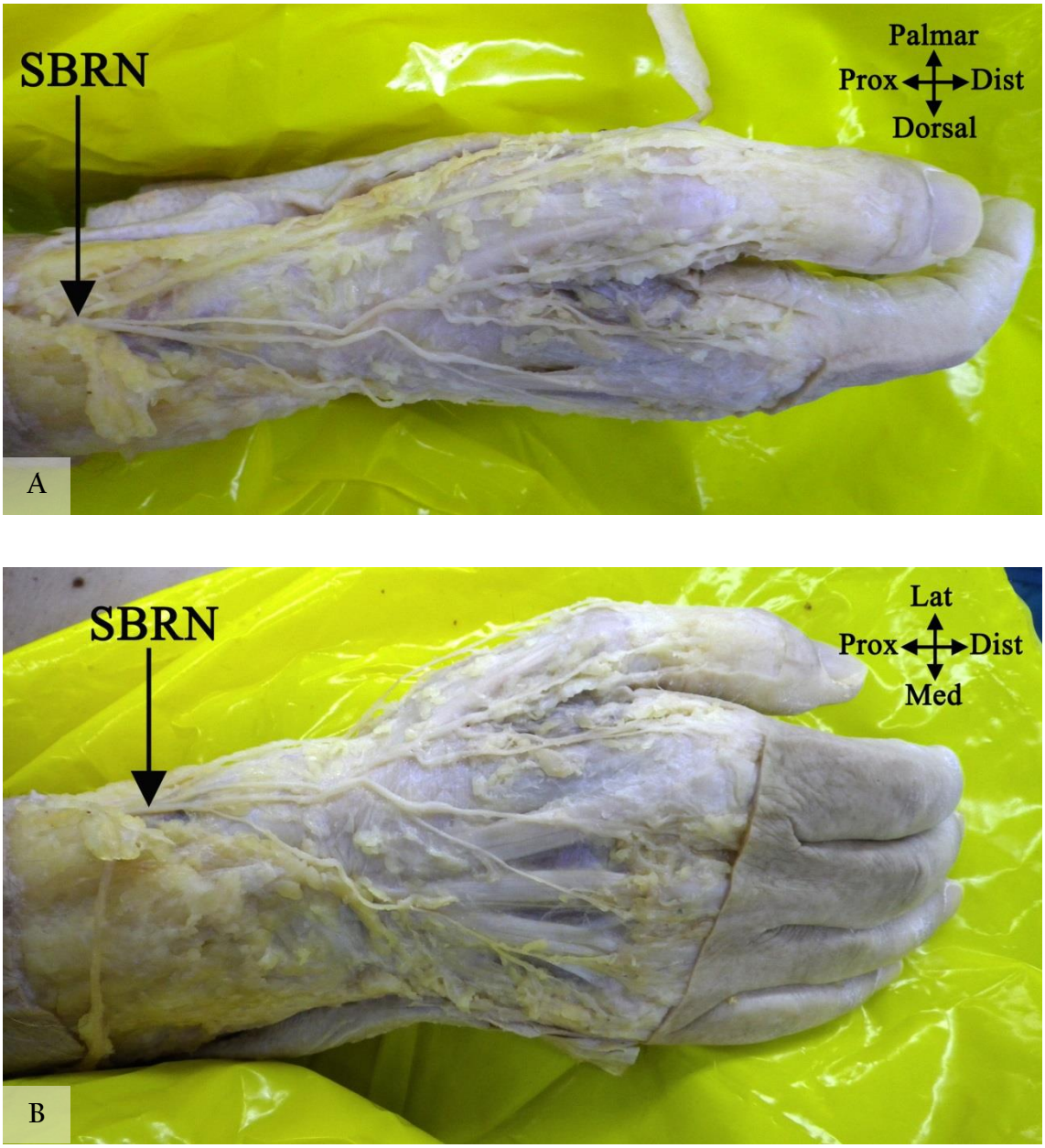

Figure 3.30: Branching pattern of the superficial branch of the radial nerve (SBRN) Type VI A. (A) Lateral view of Type VI A. (B) Dorsal view of Type VI A. Prox, proximal; Dist, distal; Med, medial; Lat, lateral; Palmar, palmar surface; Dorsal, dorsal surface.

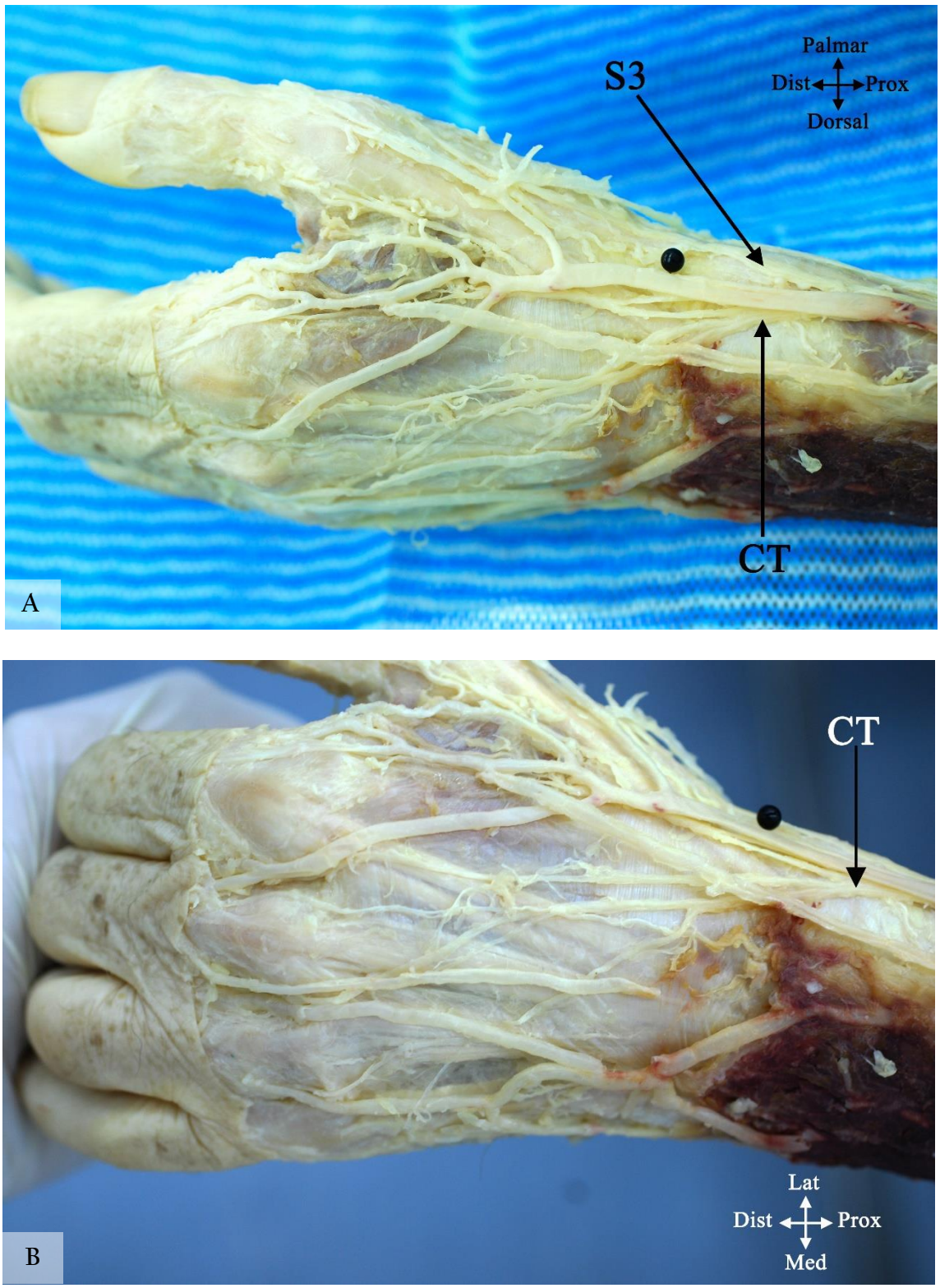

Figure 3.31: Branching pattern of the superficial branch of the radial nerve (SBRN) Type VIB. (A) Lateral view of Type VIB. (B) Dorsal view of type VIB. CT, common trunk; pins indicate the radial styloid process. Prox, proximal; Dist, distal; Lat, lateral; Med, medial; Palmar, palmar surface; Dorsal, dorsal surface.

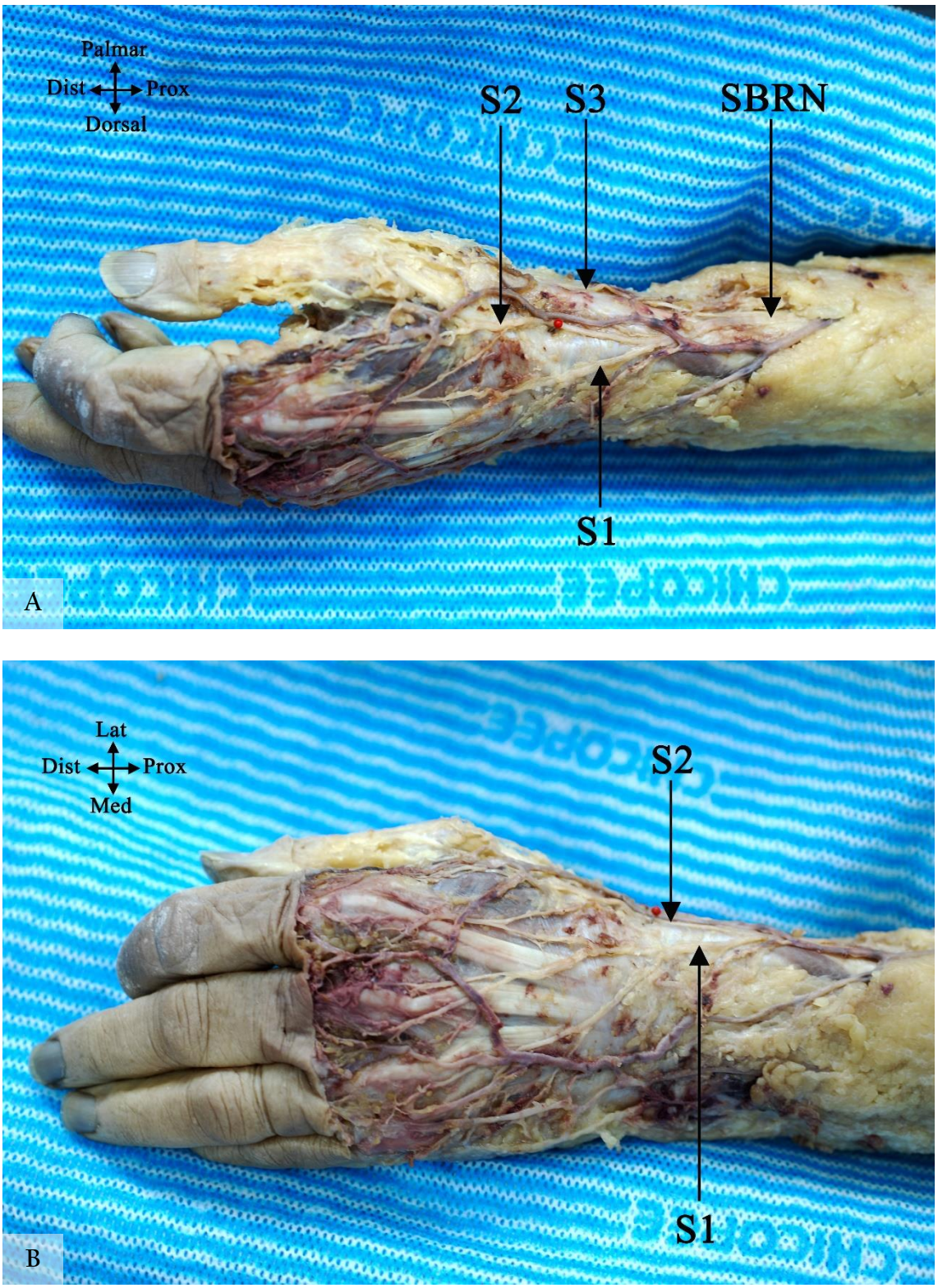

Figure 3.32: Branching pattern of the superficial branch of the radial nerve (SBRN) Type VI C. (A) Lateral view of Type VI C. (B) Dorsal view of Type VI C. Prox, proximal; Dist, distal; Lat, lateral; Med, medial; Palmar, palmar surface; Dorsal, dorsal surface.

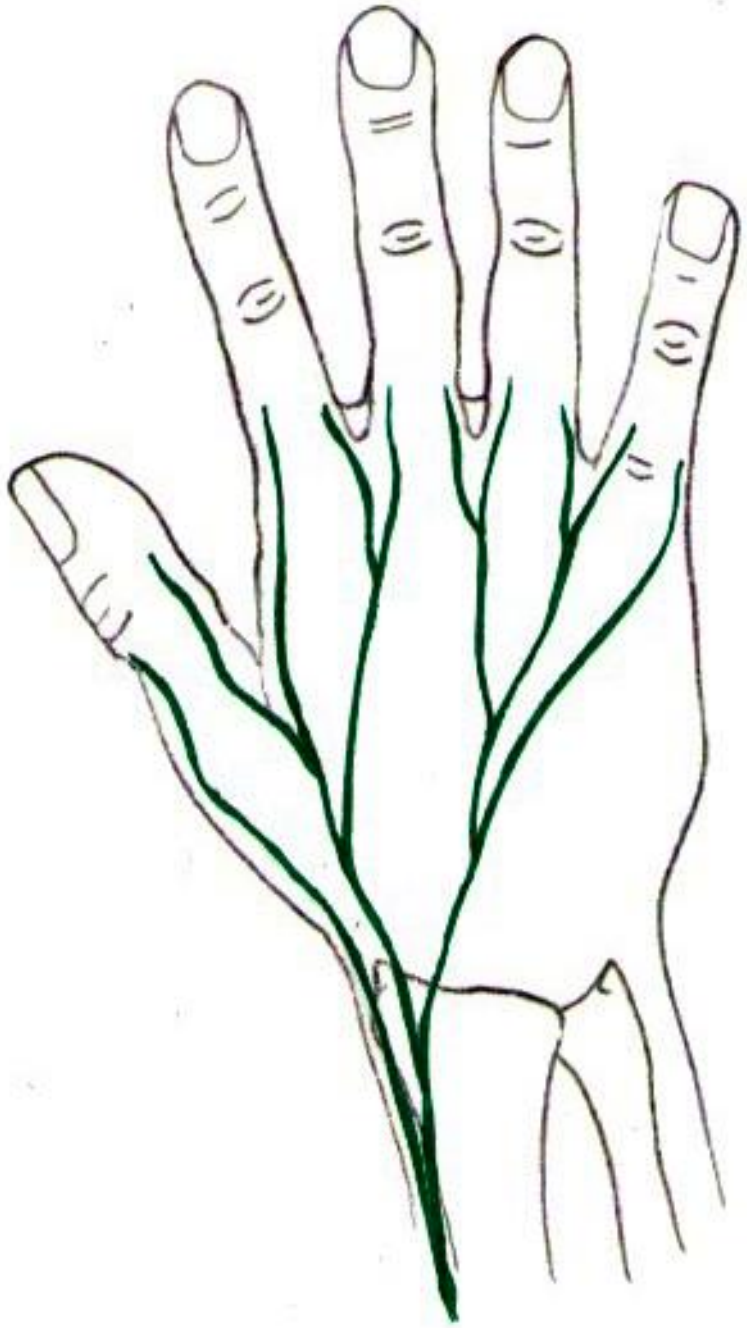

Figure 3.33: Branching pattern of the superficial branch of the radial nerve (SBRN) Type VI D. This type was found in cadaver number 896 right and left hands, pictures were lost and the sketch was prepared based on the sketches taken from the two hands where the type was found.

The effect of sex and body side on the branching pattern was investigated. The branching pattern of the SBRN was not influenced by sex (P value=0.966) or body side (P value =0.579). Appendix 1 shows the chi-square test results for both the effect of sex and body side.

3.7. Dorsal branch of the ulnar nerve

The DBUN was investigated in 139 cadaveric hands from 73 cadavers: 70 (50.3%) male and 69 (49.6%) female. Mean age was 82.6±9.5 (range: 101-53) years.

The nerve originated from the medial side of the main trunk of the ulnar nerve in the distal forearm. It originated 63.3±14.8 mm (range: 110.7-26.7) and 61.3±21.0 mm (range: 140-18.5) proximal to the proximal edge of the pisiform and proximal to the USP respectively. It was estimated that the nerve originated at the distal 23.6±7.7% of the total length of the ulna. The nerve pierced the fascia 18.1±7.1 mm (range: 33.1-1.74) proximal to the USP and continued to innervate the medial 1½-2½ digits in the dorsum of the hand. At the level of the USP, the closest branch of DBUN passed 6.8±3.1 mm (range: 14.0-0.4) to the USP (Table 3.15).

Table 3.15: Anatomical measurements recorded for the dorsal branch of the ulnar nerve (mm)

	Mean	SD	Max	Min
Origin from the ulnar nerve to the proximal edge of the pisiform	63.3	14.8	110	26.7
Origin from the ulnar nerve to the USP[1]	61.3	21.0	140	18.5
Pierced the fascia	18.1	7.1	33.1	1.74
Closest branch to USP	6.8	3.1	14.0	0.4

[1] Ulnar styloid process

Table 3.16 shows the major first and second division points of the DBUN. Prior to its division, the DBUN diameter was 2.2±0.7 mm (range: 3.68-0.62). The nerve consistently crossed a line between the USP and the fourth webspace. The DBUN crossed this line 18.1±9.1 mm (range: 40.4-3.4 mm) distal to the USP corresponding to 19.4±9.6% (range: 45.4-3.1) of the distance between the USP and the fourth webspace.

Table 3.16: Distances of the first and second major branching point of the dorsal branch of the ulnar nerve to the ulnar styloid process (mm).

	Mean	SD	Max	Min
First major branching point	-3.4[1]	17.4	53.4	-38.7
Second major branching point	39.2	13.2	73.6	-8.8

[1] Minus signs indicate that the point were located below the level of the respective landmark

3.8. Sensory distribution in the dorsum of the hand

The dorsum of the hand was supplied by branches of the SBRN and DBUN. The innervation territory showed many arrangements. Investigating 150 cadaveric hands, the dorsum of the hand innervation was outlined (Table 3.17).

Table 3.17: Sensory innervation in the dorsum of the hand with reference to digits

		SBRN[2]		DBUN[3]		UD[4]		Total
		n	%	n	%	N	%	
Index	lateral	150	100.0	0	0.0	0	0.0	150
	medial	147	98.0	0	0.0	3	2.0	150
Middle	lateral	146	97.3	0	0.0	4	2.7	150
	medial	57	38.0	57	38.0	36	24.0	150
Ring	lateral	28	18.7	89	59. 3	33	22.0	150
	medial	15	10.0	135	90.0	0	0.0	150
Little	lateral	14	9.3	136	90.7	0	0.0	150
	medial	10	6.7	140	93.3	0	0.0	150

[2] Superficial branch of the radial nerve
[3] Dorsal branch of the ulnar nerve
[4] Undetermined

The thumb and the lateral side of the index finger were always supplied by the SBRN; however, the SBRN communicated with the LABCN in 45 cases (30.0%), changing the innervation on the lateral side of the thumb in 37/45 (82.2%) by communicating with the palmar branch of the SBRN; and altering the innervation of the entire territory innervated by the SBRN by communicating with the main SBRN trunk or the dorsal branch of the SBRN in 8/45 (17.8%) (Figure 3.34). In one case, the lateral side of the thumb was entirely supplied by the LABCN and the medial side was supplied by a branch of the SBRN after it communicated with the LABCN (Figure 3.35). The SBRN innervated the lateral side of the middle finger in all cases except 4 (2.7%) in which the DBUN contributed to the innervation of the same area. Moreover, the SBRN innervated the medial side of the middle finger and the lateral side of the ring finger in only 38% and 18.7% respectively. When present, the DBUN always innervated the medial side of the little finger, the lateral side of the little finger and the medial side of the ring finger in the majority of cases, and the lateral side of the ring finger in more of half of the hands investigated.

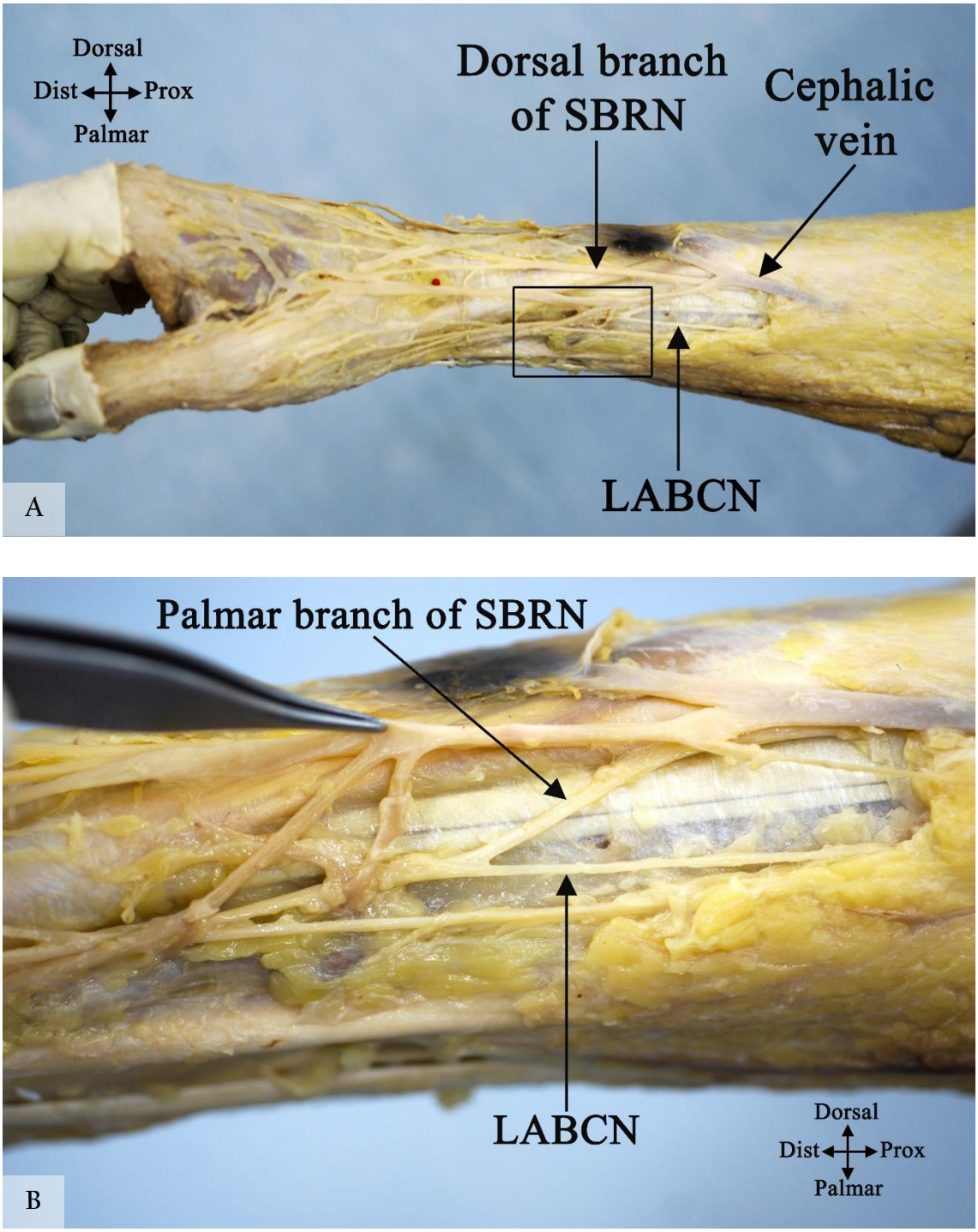

Figure 3.34: Superficial branch of the radial nerve (SBRN) communicating with the lateral antebrachial cutaneous nerve (LABCN) (A). The rectangular area outlined in (A) is enlarged and shown in (B). Prox, proximal; Dist, distal; Palmar, palmar surface; Dorsal, dorsal surface.

Figure 3.35: Lateral view of a special case of the lateral antebrachial cutaneous nerve (LABCN) entirely supplying the lateral side of the thumb. The medial side of the thumb is supplied by a branch of the superficial branch of the radial nerve (SBRN) after communicating with the LABCN (A). The rectangular area outlined in (A) is enlarged and shown in (B). Bold arrow indicates the communicating branch between the LABCN and the SBRN; Palmar, palmar surface; Dorsal, dorsal surface; Prox, proximal; Dist, distal.

The DBUN and the SBRN communicated in the dorsum surface of the hand in 37 cases (26.4%) altering the sensory innervation on the lateral side of the ring finger and medial side of the middle finger in 31/37 (83.8%) cases, the lateral side of the middle finger and medial side of the index finger in 3/37 (8.1%) cases, the medial side of the middle finger in 2/37 (5.4%) cases and the lateral side of the middle finger in one case. Dual innervation where both nerves overlap and contribute to the innervation of the same area with no communications were found in 4 cases. Dual innervation affected the medial side of the middle finger and lateral side of the ring finger in two cases, and the medial side of the middle finger only in a further two cases.

Comparing the branching pattern on the dorsum of the hand in 74 cadavers, symmetry was only found in 43.2% (32/74). Table 3.18 shows the different types of distribution on each body side. The symmetry in the palmar surface of the hand was not studied as it has less clinical implication.

Table 3.18: Distribution of the different branching patterns in the dorsum of the hand

		Right hand						**Total**
		Type 1	Type 2	Type 3	Type 4	Type 5	Type 6	
Left hand	Type 1	14*	9	4	0	1	1	29
	Type 2	5	5*	5	0	0	0	15
	Type 3	4	4	12*	0	0	1	21
	Type 4	1	0	0	0*	0	1	2
	Type 5	1	0	1	0	0*	0	2
	Type 6	1	2	1	0	0	1*	5
Total		26	20	23	0	1	4	74

* Showing the frequencies of symmetrical hands showing the same branching pattern in the left and right hand sides.

3.9. Dorsal communicating branch between the radial and ulnar nerve

The dorsal CB between the SBRN and the DBUN was found in 37/140 (26.4%) cadaveric hands of which 17 (46.0%) were from the right side and 20 (54.0%) were from the left side: 13 (35.1%) male and 24 (64.9%) female. Three types were identified based on the proximal attachment points:

Type I: The CB had a single attachment to the SBRN and the DBUN (Figure 3.36).

A. CB attached proximally to the SBRN
B. CB attached proximally to the DBUN
C. CB attached to the SBRN and DBUN at the same level

Type II: The CB had multiple attachment points to both the SBRN and DBUN (Figure 3.37 A).

Type III: The DBUN and SBRN both gave a branch that merged and sent branches to the dorsum of the hand (Figure 3.37 B),

Type I was found in 32.4% of the hands investigated. Moreover, subtype A, B, and C were noted in 4/37 (10.8%), 7/37 (18.9%) and 1/37 (2.7%) of the hands respectively. Type II and III were found in 10.8% (4/37) and 56.8% (21/37) of the hands respectively.

The effect of sex and body side on the branching pattern was investigated. The branching pattern of the dorsal CB was not influenced by sex (P value=0.830) or body side (P value =0.917). Appendix 1 show the chi-square test results for both the effect of sex and body side.

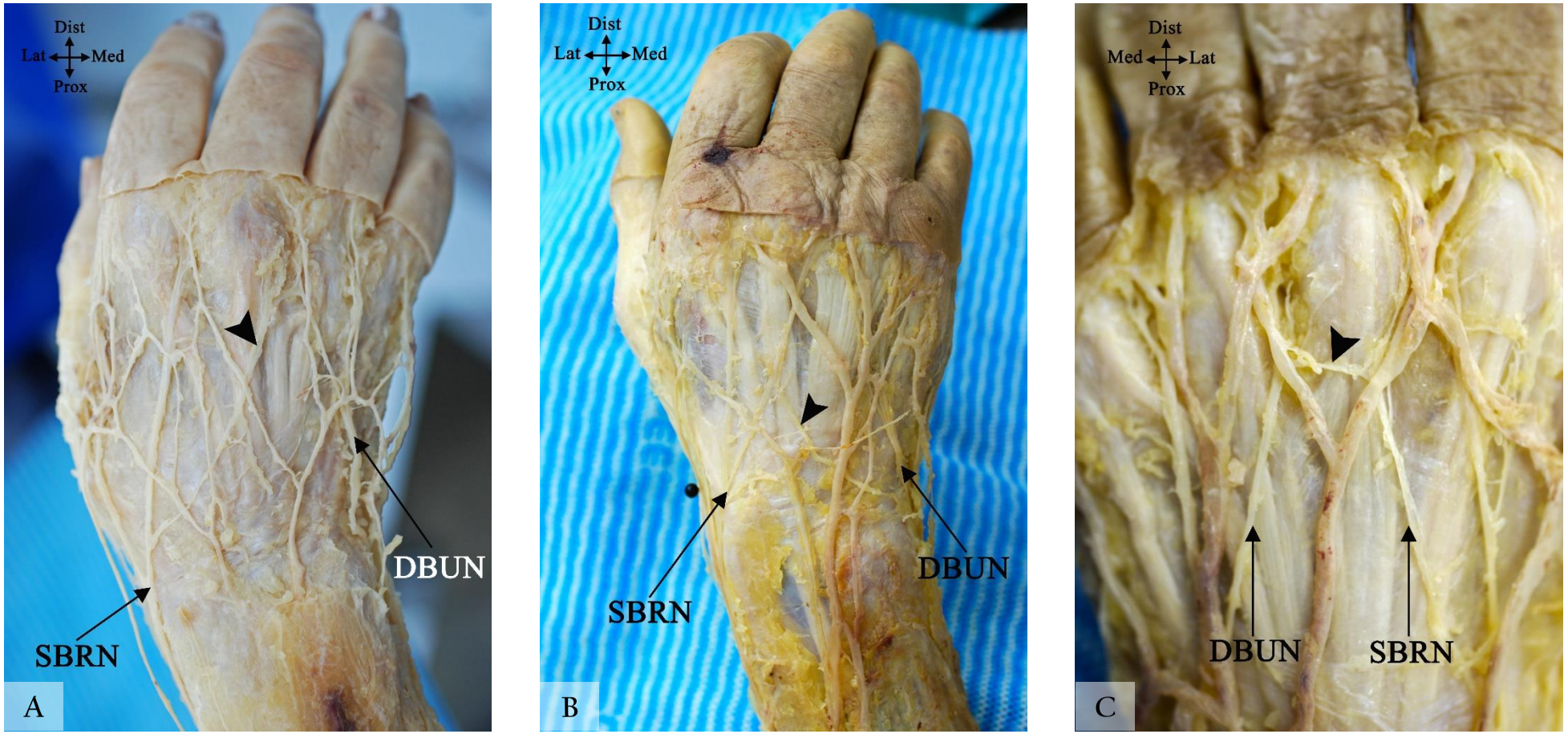

Figure 3.36: Dorsal communicating branch (CB) between the superficial branch of the radial nerve (SBRN) and the dorsal branch of the ulnar nerve (DBUN) Type I. (A) Type I A. (B) Type I B. (C) Type I C. The arrow head indicates the CB. Prox, proximal; Dist, distal; Lat, lateral; Med, medial.

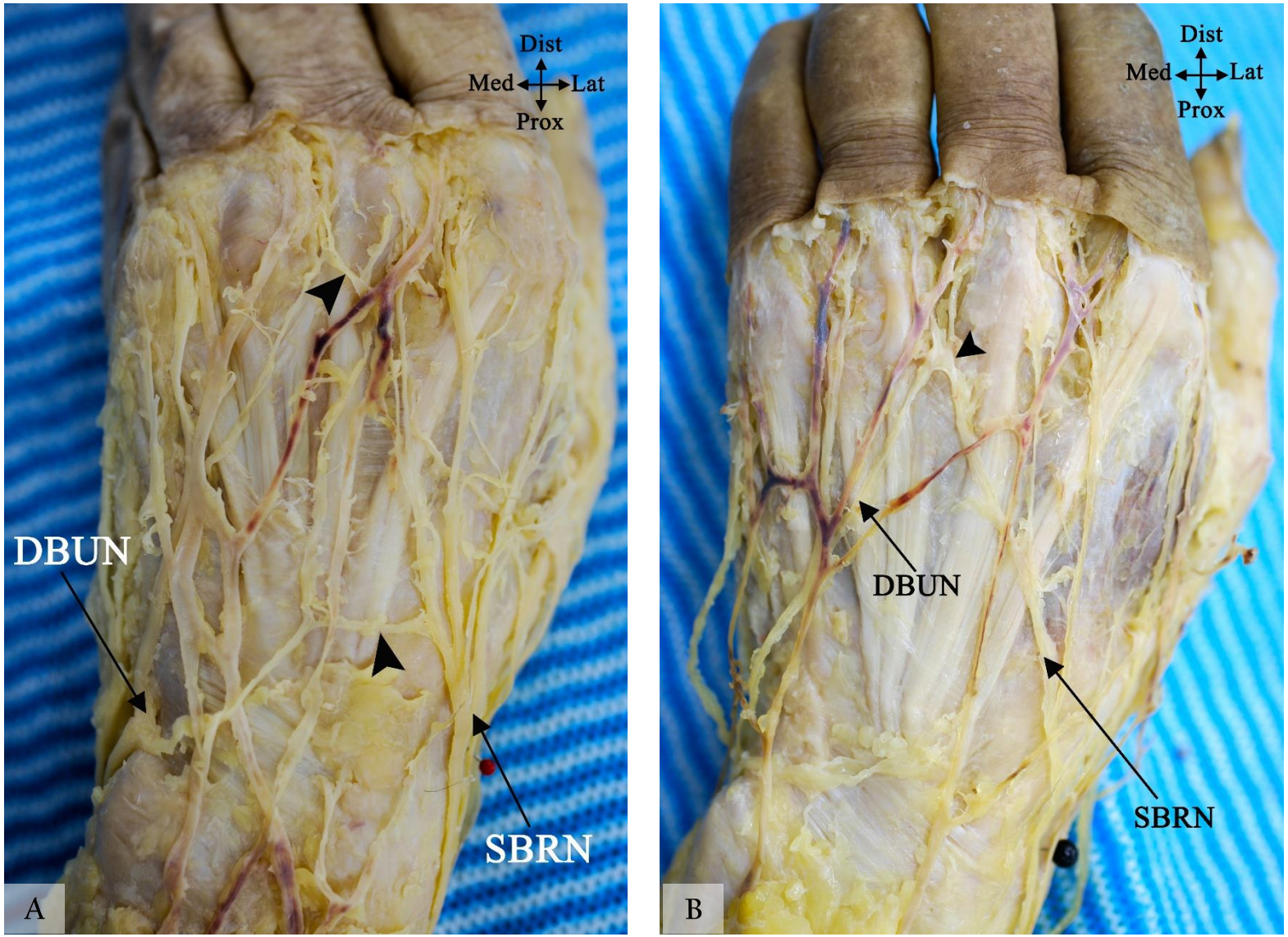

Figure 3.37: Dorsal communicating branch (CB) between the superficial branch of the radial nerve (SBRN) and the dorsal branch of the ulnar nerve (DBUN) (A) Type II. (B) Type III. The arrow head indicates the CB; Dist, distal; Prox, proximal; Lat, lateral; med, medial.

The location of the CB was variable. In Type I, The proximal attachment was found 18.5±22.0 mm to the BSL. The distal attachment was found to be 51.0±21.1 mm to the BSL. The CB average length was 54.6±19.5 mm and originated with a mean angle of 139±29.3° (Table 3.18).

The proximal attachment location measured to the BSL was located at the 25.4±30.6% (range: -7.6-85.6%) of the distance between the third MCP joint and the BSL. Moreover, the distal attachment position measured to the BSL was 65.4±24.5% (range: 32.9-98.4%) of the distance between the third MCP joint and the BSL (Appendix II).

In Type III, the merging of the two branches was found 71.3±9.8 mm to the BSL which is estimated to be located 87.0±6.9%% of the distance between the third MCP joint and the BSL (Table 3.19) (Appendix II).

Table 3.19: Anatomical measurements for the dorsal communicating branch between the superficial branch of the radial nerve and the dorsal branch of the ulnar nerve (mm)

	Mean	SD	Max	Min
Proximal attachment to the BSL[1] in Type I	18.5	22.0	62.9	-6.2[2]
Distal attachment to the BSL in Type I	51.0	21.1	93.4	25.3
Communicating branch length in Type I	54.6	19.5	86.3	30.6
Angle of origin in Type I	139	29.3	168	60
The merging point recorded in Type III	71.3	9.8	85.2	55.4

[1] Bistyloid line
[2] Minus signs indicate that the point were located proximal to the level of the respective landmark

4. Discussion

4.1. Palmar surface of the hand:

The palmar surface of the hand is innervated by branches from two nerves: the median and ulnar nerves. The median nerve gives the palmar cutaneous branch of the median nerve (PCBMN) in the distal forearm, and the first, second and third common digital nerves (CDNs) after it passes through the carpal tunnel. The MN is responsible for innervating the skin over the lateral and middle third of the palm, and the lateral 3½ digits as described by most anatomical textbooks. The UN is responsible for innervating the skin over the medial third of the palm and the medial 1½ digits by its superficial branch, which is given off in Guyon's canal. Although occasionally ignored by anatomical textbooks, the MN and UN can communicate across the palm deep to the superficial palmar arch allowing for exchange of fibres between the two nerves and thus changing the innervation boundary in the palm that is classically described as the middle of the ring finger.

4.1.1. Palmar cutaneous nerve of the median nerve

The PCBMN is the last nerve that arises from the median nerve in the forearm. It supplies the proximal middle and lateral two fifths of the palm. It was found in all 123 cases investigated in the current study. Originating 54.1±15.7 mm proximal to the WC, the nerve stayed in the same epineurium as the main trunk for a few millimetres (12.9±1.8) and detached 41.2±14.0 mm proximal to the WC. Taleisnik (1973) was the first to state that the PCBMN stays bound with the main body of the MN for a distance of 16-25 mm after its origin. The PCBMN can be compressed before its detachment from the MN as seen in pseudoanterior interosseous nerve syndrome when nerve fascicle compress before separation. Unknown masses or tendons compressing the

lateral aspect of the median nerve in the distal forearm or flexor carpi radialis fascia can also compress the nerve (Shimizu et al., 1988; Al-Qattan, 1997).

The origin point found in this study differed from that described in the literature. A higher origin point was reported by Hobbs et al. (1990) (84 mm proximal to the WC), Naff et al. (1993) (57 mm proximal to the RSP) and Martin et al. (1996) (59 mm proximal to the WC). A more distal origin point was reported by Bezerra et al. (1986) (45.6 mm proximal to the WC), Dowdy et al. (1994) (41 mm proximal to the WC), Watchmaker et al. (1996) (41 mm proximal to the WC), Matloub et al. (1998) (44 mm proximal to the WC), Chaynes et al. (2004) (44.3 mm proximal to the BSL), Cheung et al. (2004) (32 mm proximal to the WC) and Ozcanli et al. (2010) (39.2 mm proximal to the WC).

Interestingly, most anatomic studies do not usually differentiate between the origin point and the detachment point of the PCBMN from the main trunk of the MN[1]. The two words are usually used synonymously in the literature. In their study, Hobbs et al. (1990) had a high origin of the PCBMN reaching as high as 215 mm proximal to the WC, which is greater than any other report in the literature. This could be attributed to their dissection method continuing into the substance of the MN which they refer to as the PCBMN intraneural origin. Although not as high, Al-Qattan (1997) also reported an intraneural origin of the PCBMN in 10 cadaveric upper extremities at 70 mm (range: 40-150 mm) proximal to the WC. Most other studies report the origin point without specifying if it is the detachment, origin or intraneural origin point. However, the detachment point in this study is similar to the origin point reported by Ozcanli et al. (2010) (39.2 mm proximal to the WC), Dowdy et al. (1994) (41 mm proximal to the WC), Watchmaker et al. (1996) (41 mm proximal to the WC), and Matloub et al.

[1] How the origin and detachment points of the PCBMN were determined are explained in the methods section

(1998) (44 mm proximal to the WC) suggesting that those studies may have considered the detachment point of the PCBMN from the MN as the point of origin.

The PCBMN originated from the lateral side of the MN in most cases (93.5%); however, it also originated from the medial, posterolateral and the anterior side of the MN in 1.6%, 1.6%, and 3.3% respectively. Most literature mentions the PCBMN as originating from the lateral side, yet in their study of 60 Chinese cadavers, Cheung et al, (2004) reported 14 cases (11.7%) where the PCBMN originated from the medial side. Such a high number of variations in the origin direction may be explained by racial differences. Although Taleisnik (1973) described the PCBMN originating from the anterolateral side of the MN in all 12 cases investigated. No mention has been found in the literature of anterior or posterolateral origin; however this could be attributed to the limited number of samples involved in previous studies (see Table 1.1). Although small, it is important for surgeons to understand that such variations can exist to avoid complications in procedures involving the distal forearm.

The PCBMN coursed distally in the forearm between flexor carpi radialis and palmaris longus if present. In 10 cases (8.3%), the nerve passed through the fascia of flexor carpi radialis rather than medial to it and in a small number of cases posterior to the tendon (4.2%). Furthermore, it was not uncommon for the nerve to penetrate the fibres of palmaris longus as it blended with the palmar aponeurosis in the palm. This study's findings disagree with Matloub et al. (1998) who reported the PCBMN to pass through the fascia of flexor carpi radialis in the majority of cases (36/40), and was partially covered by palmaris longus tendon fibres at its insertion point into the palmar aponeurosis in a minority of cases (3/40). Such a position can put the nerve at risk of irritation or compression in cases of flexor carpi radialis tendinitis, trauma or inflammation leading to soft tissue swelling in the distal forearm, or ganglia arising

from the flexor carpi radialis sheath and atypical palmaris longus muscles (Al-Qattan, 1997).

The PCBMN has its own tunnel formed between the deep and superficial fibres of the TCL. Most literature describes the tunnel as starting at the level of the WC or at the level of the scaphoid tubercle (Matloub et al., 1998, Naff et al., 1993). In the current study, the tunnel started proximal to the WC between the superficial and deep fibres of the PCL and extended into the TCL. Al-Qattan (1997) mentioned that the PCBMN tunnel could be located within the antebrachial fascia, PCL, or the TCL. The average length of the tunnel was 11.3±3.4 mm which is longer than described by Matloub et al. (1998) who reported it at 8 mm long; however, it lies within the range described by Taleisnik (1973) (9-16 mm).

Al-Qattan (1997) described six zones where the PCBMN could be at risk of entrapment leading to compression syndrome. Distinguishing between entrapment of the PCBMN at those six zones and median nerve entrapment at the carpal tunnel can be challenging as the sensory innervation of the two nerves can greatly overlap. The two entrapments can be independent or associated. It is important to assess the possibility of the PCBMN entrapment in every patient with carpal tunnel syndrome (Wada et al. 2002).

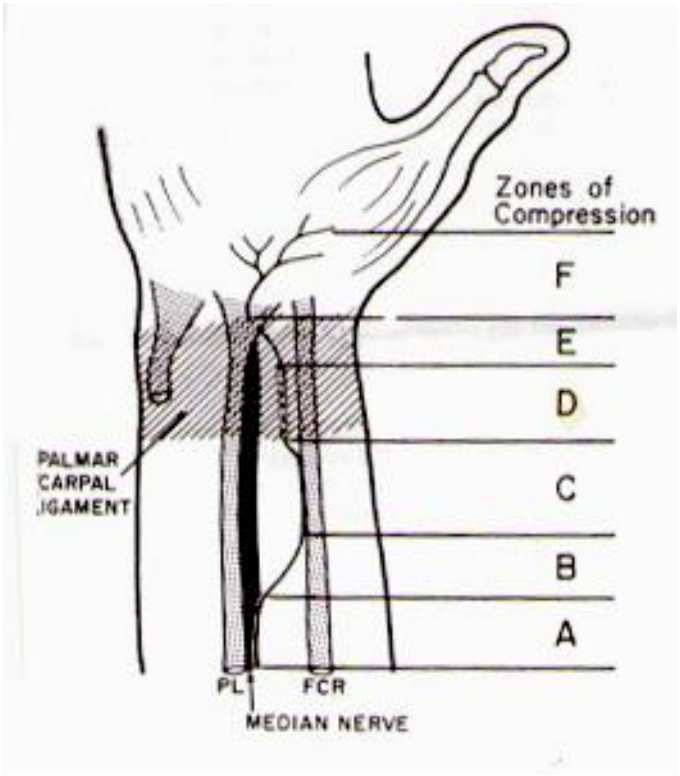

Figure 4.1: The six zones where the palmar cutaneous branch of the median nerve (PCBMN) is most likely to be entrapped as described by Al-Qattan (1997). (A) The PCBMN is bound to the main trunk of the median nerve; (B) The PCBMN detaches from the median nerve; (C) medial sheath of the flexor carpi radialis (FCR); (D) within the PCBMN tunnel; (E) in relation to the distal margin of palmaris longus (PL); (F) the PCBMN subcutaneous course prior to innervating the skin (Al-Qattan, 1997).

In a study of 12 cadaveric hands, Taleisnik (1973) described the branching pattern of the PCBMN as the nerve dividing into one larger lateral branch supplying the thenar area and several smaller medial branches. Although significant, the branching pattern described was not detailed enough as it did not include an outline of different patterns, variations, or mention incidence rates even though variations were found. Bezerra et al. (1986) investigated 50 cadaveric hands and classified the branching pattern into three types according to the palmar area innervated and the direction of the branches. In their classification, the PCBMN divided into two main branches in Type I and Type III; however the two types were distinguished by the innervation territories of the branches, and into three branches in Type II. In Type I, the PCBMN divided into a lateral branch innervating the thenar region and an intermediate branch innervating the intermediate third of the palm. Type III branches innervated the intermediate third of the palm by an intermediate branch and the thenar region by a medial branch. The medial branch might loop around to reach the laterally located thenar region. In Type

II, the PCBMN divided into lateral, intermediate and medial branches innervating the thenar, intermediate and hypothenar regions of the palm respectively (Bezerra et al., 1986). From the study by Bezarra et al. (1986), it could be concluded that the PCBMN divided into two or three main branches which correspond to Type I and Type III of the current study. Their study also reported that the medial branch was the shortest and present in only 42% of cases. This could be due to the medial third of the palm being innervated by the palmar cutaneous branch of the ulnar nerve, nerve of Henle and the transverse palmar nerves (Doyle and Botte, 2003; Tubbs et al., 2011).

DaSilva et al. (1996) described another type of branching pattern of the PCBMN. In their study of 12 cadaveric hands, the PCBMN divided into numerous non distinct small branches in 41.7% (5/12) (DaSilva et al., 1996). DaSilva's Type B described earlier resembles Type II of the current study which was found in 36.4% of cases (Table 4.1). Matloub et al. (1998) also described an additional pattern in their study after investigating 40 cadaveric hands. Type II, which was found in 35% (14/40) of cases, was described as the PCBMN giving several smaller branches before it divided into two main branches. However, in the current study, this type was only found in 7.21% of cases and is considered a variation of Type I. One reason that could explain the difference in incidence rates is that Matloub et al. (1998) and DaSilva et al. (1996) used fresh-frozen and fresh cadavers in their studies making it easier to locate and recognize smaller branches. Moreover, when three branches are present, the medial branch is described to be the smallest and shortest of the three.

In a more recent study conducted on 35 cadaveric hands, Chaynes et al. (2004) described two types of branching pattern based on the number of main branches. The PCBMN divided into two branches (Type I) or three branches (Type II). Their results

are similar to those reported by Bezerra et al. (1986) if the number of branches only is considered as the basis of classification in the two studies (Table 4.1).

Considering the branching patterns described in the literature, the need for a classification system of the branching patterns of the PCBMN in the palm becomes evident. Comparing different incidence rates reported in the literature is not easy as each study reports different patterns which are classified on a different basis. The present study suggests the following scheme which incorporates all patterns mentioned in the literature:

Type I: The main trunk divides into Y-shaped medial and lateral branches that continue to give tertiary branches as they course distally in the palm.

Variations to Type I: The main trunk gives several smaller branches before it divides into a Y-shaped medial and lateral major branches.

Type II: The PCBMN continues as one major branch that gives several minor branches as it courses distally in the palm.

Type III: The main trunk divides into three branches (lateral, medial and intermediate) that all continue to give tertiary branches as they course distally in the palm.

Table 4.1: Incidence rates of different patterns of distributions of the palmar cutaneous nerve of the median nerve in the literature compared with the types found in the current study

No	Reference	Type I		Type II	Type III
		Typical	Variation		
1.	Current study	40%	9.1%	36.4%	14.5%
2.	Bezerra et al. (1986)[1]	66%	-	-	34%
3.	DaSilva et al. (1996)	-	-	41.7%	58.3%
4.	Matloub et al. (1998)[2]	50%	35%	-	
5.	Chaynes et al. (2004)	60%	-	-	40%

[1] The study reported three types based on the region each branch innervated. Some percentages were combined to allow comparison with this study (Type I and Type III).
[2] The study reported a Type III (15%) where two PCBMN originate from the MN. This type was omitted from the table.

The literature distinguishes between duplicate PCBMN and two PCBMN branches; however, the two words are used synonymously in most publications. Moreover, it is important to distinguish between two PCBMNs and a nerve with high division. In the current study, two PCBMN branches where noted in 11 cases (8.9%), of which 2/11 had different origin and detachment points, 4/11 had the same origin point but different detachment points, 1/11 had different origin points but the same detachment point, and 4/11 had the same origin and detachment points. The incidence rate in the current study is lower than that described by Hobbs et al. (1990), DaSilva et al. (1996) and Matloub et al. (1998) who reported the presence of two PCBMN branches in 16%, 16.7%, and 15% of their cases respectively. However, it is similar to studies by Martin et al. (1996) and Watchmaker et al. (1996) who stated that two PCBMN were found in 8% of their cases. It is important to appreciate the possibility of having two PCBMN branches with different origin points, especially when planning local and regional anaesthesia of the wrist and distal forearm. The PCBMN branches can be vulnerable to injury due to compression, retraction or dissection during surgical procedures performed in the distal forearm if they are not recognized by the surgeon.

It is not uncommon for the PCBMN to communicate with the SBRN. However, such communications have been reported with different incidence rates in the literature: Bezerra et al. (1986) reported it in 4%, Hobbs et al. (1990) in 8%, and Chaynes et al. (2004) in 14.3%. Such communication was found in only one case in the current study (0.8%). Also, in the current study, the PCBMN was found to communicate with other nerves in the region. As previously described by Bezerra et al. (1986), the PCBMN was found to communicate with the first CDN in one case. Watchmaker et al. (1996) reported that the nerve overlapped with the LABCN in one case; however, in the current study, the nerve was found to communicate with the LABCN in 5 cases, in two of which the LABCN communicated with the SBRN prior to its communication with the PCBMN which might suggest that the PCBMN received fibres not only from the LABCN but also from the SBRN. The PCBMN was also found to communicate with the recurrent motor branch of the median nerve (two cases), which as far as can be ascertained, has not been reported in the literature. Such communications could explain sensory disturbances in the palm when injury to the SBRN or the LABCN occurs. It could also explain extended sensory disturbances in the palm after carpal tunnel release. Moreover, motor fibres can have a collateral pathway through the PCBMN and thus motor dysfunction of the thumb can occur if the PCBMN is injured or compressed.

4.1.2. Common Digital Nerves

The median nerve becomes superficial in the distal forearm, coursing between palmaris longus and flexor carpi radialis. It usually enters the carpal tunnel as one trunk, although high bifurcation of the MN has been reported in the literature (Berry et al., 2003; Sundaram et al., 2008; Bagatur et al., 2013). The CDNs course deep to the superficial palmar arch; however in the current study, in one case the third CDN gave a

branch that coursed superficially to the superficial arch creating a neural loop. Presence of such loops in the palm has been mentioned in the literature. They could result in digital nerve compression and sensory disturbances in cases of palmar aneurysm (O'Connor, 1972).

In the carpal tunnel or at its distal edge, the MN divides into three CDNs. Few reports are found in the literature that detail the location or the division point of the CDNs into PDNs. In their study of 12 cadaveric hands, Torrez and Olave (2008) reported that the first, second, third and fourth[1] CDNs were found 43.5±9.1, 68.1±10.5, 72.6±8.9 and 66.1±9.8 mm from the WC respectively. Although, the first CDN gives off three PDNs, two supplying the medial and lateral sides of the thumb and one supplying the lateral side of the index finger, they do not usually branch off at the same level, Torrez and Olave (2008) do not specify which division of the first CDN branching is reported. The BSL and the WC are closely related anatomical landmarks and are frequently used in anatomical studies. However, the two landmarks vary in their location to each other. Chaynes et al. (2004) reported that the BSL could be found as far as 11.2 mm proximal to the WC, and the BSL and WC were found at the same level in only 40% (14/35) of the hands investigated. This could explain the difference between the results reported by Torrez and Olave (2008) and the current study as there is a constant ~5 mm difference between the measurements reported for the second, third and fourth CDNs in Torrez and Olave (2008) and the measurements taken in this study.

In their study of the ulnar nerve in the palm, Bonnel and Villa (1985) reported that the fourth CDN divided into two proper digital nerves to the medial side of the ring finger and the lateral side of the little finger 68 mm from the BSL. Similarly, in the current study, the same division occurred 72.6±7.7 mm distal to the middle of the BSL and 65.2±7.4 mm distal to the pisiform.

[1] Although the fourth CDN originates from the ulnar nerve, it is discussed here for comparison purposes.

The current study also represented the distances in relative values with respect to the distance between the BSL and the third MCP joint. Such representation overcomes the effect of different hand sizes in the sample investigated. The CDNs were found to divide into PDNs proximal to the third MCP joint in the majority of cases and at different levels (see Table 3.4). Such indices of where the CDNs divide in the palm with respect to different anatomical landmarks are important for clinicians to better diagnose and assess hand pathologies, plan and implement effective therapeutic procedures.

The first CDN divides into three PDNs that supply the thumb and the lateral side of the index finger in three possible patterns first described by Jolley et al. (1997):

Type I: A PDN supplying the lateral side of the thumb and a CDN that further divides to supply the medial side of the thumb and lateral side of the index finger.

Type II: A trifurcation to produce three PDNs to supply the thumb and lateral side of the index finger.

Type III: A CDN that further divided to supply the medial and lateral sides of the thumb and a PDN that continued distally to supply the index finger.

The three types were found by Jolley et al. (1997) in 69%, 25%, and 6% of hands respectively. In the current study the three types were found in 70.8%, 27.1% and 2.1% respectively. The description of the different patterns of the first CDN is rarely mentioned in anatomical textbook, thus it could be overlooked by clinicians. It was interesting to notice that the branching pattern of the first CDN is influenced by body side (P-value = 0.041). This could be explained by the sample distribution being skewed into Type I affecting the Chi-Square results.

4.1.3. Ulnar nerve

The ulnar nerve enters the palm through Guyon's canal where it divides into a superficial sensory branch and a deep motor branch. Bonnel and Villa (1985) were the first to classify the division of the ulnar nerve in the palm into two branching patterns:

Type I: The ulnar nerve bifurcated into one sensory nerve and one motor nerve.

Type II: The ulnar nerve trifurcated into two sensory nerves and one motor nerve.

Type I was found in 78% (39/50) while Type II was found in 22% (11/50) (Bonnel and Villa, 1985). In their study of 31 cadaveric hands, Lindsey and Watumull (1996) reported that Type I and Type II were found in 80.6% (25/31) and 19.4% (6/31) respectively. The reported incidence rates agree with the findings of this current study where Type I and Type II were found in 80.4% and 19.6% respectively.

Bonnel and Villa (1985) also used morphometric measurements to locate the division point of the UN into a PDN to the medial side of the little finger and a fourth CDN; however their measurements were taken to the BSL (29 mm distal to the BSL) averaged for both types, whereas the measurements for the same division point was taken to the proximal edge of the pisiform in the current study. In the current study, the division point where the UN divided into deep and superficial branches in Type I and the division point where the UN trifurcated in Type II were found to be 13.6±4.0 mm and 14.9±4.1 mm distal to the pisiform respectively. The second division where the superficial branch of the ulnar nerve divides into a PDN to the medial side of the little finger and the fourth CDN in Type I was found 25.2±4.6 mm distal to the pisiform. The pisiform is located on or slightly distal to the wrist crease which in turn is located 11.7±4.3 mm distal to the ulnar styloid process (Bugbee and Botte, 1993). In Type I, the

division of the superficial branch of the UN into a PDN to the medial side of the little finger and the fourth CDN occurs 25.2±4.6 mm distal to the pisiform corresponding to 36.9±8.9 mm to the ulnar styloid process which is more distally than that reported by Bonnel and Villa (1985).

The UN innervates the skin of the medial third of the palm and the medial one and half digits. However, the UN can receive fibres from the MN or the DBUN. The palmar CB originating proximally from the MN and inserting distally into the UN was found in 5 cases in the current study[1]. With the assumption that nerve fibres always move proximally to distally, it is possible that the UN receives fibres from the MN in these 5 cases. The UN can also communicate with the DBUN: this communicating branch is called a Kaplan anastomosis and is considered rare in the literature. Kaplan anastomoses were found in 4.2% (6/144 cases) in the current study. Based on cases reported in the literature and findings from this study, Kaplan anastomosis branching patterns could be classified into four types:

Type A: The CB connects to the UN before division into superficial and deep branches.

Type B: The CB connects to the superficial division before it branches into sensory digital nerves.

Type C: The CB connects to the deep motor division of the UN.

Type D: The CB connects to the PDN to the medial side of the little finger.

Kaplan (1963) was the first to describe this communication between the superficial branch of the UN and the DBUN. Bonnel and Villa (1985) (1/50; 2%) and Murata et al. (2004) (1/35; 2.9%) reported similar cases which correspond to Type D of the

[1] The palmar communicating branch between the median and ulnar nerves is discussed in section 4.1.4.

previously mentioned classification. Five cases were found in the current study that resembled Type D.

Hoogbergen and Kauer (1992) reported another case of Kaplan anastomosis where the CB joined the deep branch of the ulnar nerve. This description corresponds to Type C of the previously mentioned classification and was not found in the current study. Furthermore, Paraskevas et al. (2008) reported a Kaplan anastomosis where the CB joined to the main trunk of the UN before its division into deep and superficial branches. This description corresponds to Type A in the previously mentioned classification and was not found in the current study. Type B of the classification where the CB joins the superficial branch of the UN was only found in one case in the current study. This type does not appear to have been described in the English literature.

Although considered rare, it is important to appreciate the significance and clinical impact of a Kaplan anastomosis. A Kaplan anastomosis receives fibres from the DBUN, which do not pass through Guyon's canal, therefore signs and symptoms of ulnar nerve injury or compression at the wrist area as a result of ulnar artery aneurysm, trauma, and flexor carpi ulnaris tendinitis might not show typical presentation. Furthermore, the CB is only covered by skin and fat which makes it vulnerable to compression and trauma. The CB could also be at risk of injury in cases such as pisiform fractures, Guyon's canal exploration, or clinical procedures performed on the medial side of the wrist.

Based on nerve branches innervating the little and the medial side of the ring finger, this study suggests the following classification:

Type I: The little finger and the medial side of the ring finger are solely innervated by the superficial branch of the UN which could be:

A. Originating as a common trunk that divides distally into a PDN to the medial side of the little finger and a CDN to the fourth webspace.
B. Originating as a PDN to the medial side of the little finger and a CDN to the fourth webspace.

Type II: The little finger and the medial side of the ring finger are innervated by the superficial branch of the UN after it receives contribution from:

A. DBUN
    i. The DBUN communicates with the superficial division of the UN before its division into CDN and PDN.
    ii. The DBUN communicates with the PDN to the little finger.
B. Median nerve

The fourth CDN communicated with the PDN to the medial side of the little finger in 7.6% (11/144) cases creating a neural loop across the hypothenar area. The deep motor branch was also found to give a branch to the PDN of the medial side of the little finger in 4.9% (7/144) of cases. Both communication branches can be at risk of injury during surgical procedures in the medial palm if the surgeon is not aware of their presence. Furthermore, these CBs could also be compressed due to ganglion cyst formation, artery aneurysms and lipomas resulting in atypical ulnar nerve neuropathy presentation.

4.1.4. Communicating branch between the median and ulnar nerves

The palmar surface of the hand is innervated by the median and ulnar nerves with the middle of the ring finger being the classical boundary. The median nerve innervates the lateral 3½ digits whereas the ulnar nerve innervates the medial 1½ digit. Sensory variations to this classical description have been reported in the literature and

attributed to the presence of the superficial palmar communicating branch (CB) between the MN and UN (May Jr and Rosen, 1981; Arner et al., 1994).

The CB between the UN and MN was first described by the famous painter Pietro (Berrettini) Da Cortona in the anatomical atlas (Tabulae Anatomicae) published in 1741. However, it was not until 1991, when Meals and Calkins introduced the name Berrettini branch into the literature (Stančić et al., 1999). The communicating branch is also referred to as "ramus communicans", the superficial palmar communication or the palmar communicating branch in some literature (Stančić et al., 1999; Loukas et al., 2007; Tagil et al., 2007).

Modern literature has investigated the palmar CB; however, different and sometimes contradicting reports have been made regarding its incidence, pattern and common location. With great variability, the incidence of the CB was reported to be 100% by Bonnel and Vila (1985), 96.4% by Olave et al. (2001), 95% by Ferrari and Gilbert (1991), 85% by Loukas et al. (2007), 81% by Stančić et al. (1999), 74% by Biafora and Gonzalez (2007), 67% by Bas and Kleinert (1999), 29.5% by Dogan et al. (2010) and 4% by Hoogbergen and Kauer (1992). In the current study, with the purpose of establishing an incidence rate for the presence of the palmar CB, 61 cadaveric palms were dissected and the palmar CB was found in 53/61 (86.9%) specimens. The results obtained from this study, along with most reports indicate a high incidence rate of the CB, supporting the idea that the presence of the palmar CB is a normal anatomical finding rather than an anomaly or variation.

The palmar CB is classified in the literature based on origin and termination of the CB and its relationship to the TCL into different morphological patterns. Many reports carried different descriptions of the CB; however the first classification was by Meals

and Shaner (1983) based on the direction of the nerve fibres into three types, of which Type I was further subdivided into 3 subtypes. Their classification is:

Type I: The CB passed from the 4th CDN (ulnar) to the 3rd CDN (median).

- Type IA: Fibres entered the lateral side of the ring finger.
- Type IB: Fibres entered the lateral side of the ring finger and the medial side of the middle finger.
- Type IC: Final destination of the fibres could not be determined

Type II: The CB passed from the 3rd CDN (median) to the 4th CDN (ulnar).

Type III: Both the 3rd and 4th CDNs gave a branch that merged and continued in the midpalm.

Other studies have modified the previous classification based on their observations and findings; however the basis of the classification remains the direction of the fibres. Bas and Kleinert (1999) were the first to incorporate diffuse interconnection patterns of the CB into the classification system, after it was described by Gehwolf (1921). This pattern corresponds to Type IV of the current study. In 2000, Don Griot et al. described a transverse CB that coursed perpendicular to the TCL corresponding to Type III of the current study. An interesting classification system suggested by Kawashima et al. (2004) and later modified by Dogan et al. (2010) included the absence of the CB as a type reflecting that the presence of the CB is common and should be considered typical rather than an anomaly.

Another classification system was suggested by Ferrari and Gilbert (1991) based on the relationship of the CB to the transverse carpal ligament and the angle of origin. The

classification included Groups I, II, III and IV found in 48.9%, 24.4%, 22.2% and 4.4% of cases respectively and were described as:

Group I: The CB coursed obliquely from the 4th CDN (ulnar) to 3rd CDN (median), the distance between the origin of the CB and the distal margin of the TCL was more than 4 mm and the origin angle less than 54°.

Group II: The CB courses from the 4th CDN (ulnar) to 3rd CDN (median) parallel to the distal margin of the TCL, the distance between the origin of the CB and the distal margin of the TCL was less than 4 mm with a right angle to the ulnar nerve.

Group III: The CB coursed obliquely from the 4th CDN (ulnar) to 3rd CDN (median), originated below the distal margin of the TCL, the origin angle is very acute.

Group IV: The CB branched from the 3rd CDN (median) to 4th CDN (ulnar).

This classification system is considered arbitrary and ambiguous by many authors; however it was used by Stančić et al. (1999) who reported the different incidence rates of the four types as 14.81%, 19.75% 65.43% and 0% respectively.

In the current study, a total of 98 cadaveric palms with palmar CBs were investigated. Five patterns were noticed and were classified according to the proximal and distal attachment points into:

Type I: The CB originated from the fourth CDN (UN) and coursed distally to join the third CDN (MN)

A. A single distal attachment

B. Multiple distal attachments

Type II: The CB originated from the third CDN (MN) coursed distally to join the fourth CDN (UN)

A. A single distal attachment

B. Multiple distal attachments

Type III: The CB coursed perpendicularly between third and fourth CDNs.

A. A single attachment on both sides

B. Multiple attachments on one side

Type IV: The CB had multiple attachment points to both nerves in a diffuse manner.

Type V: The UN and MN gave branches that merged and continued distally to the lateral side of the ring finger.

Table 4.2 shows the incidence of the different patterns as reported in the literature in comparison to the findings of this study. The classification system suggested in this study focuses on the proximal and distal attachments; it is easy to follow, clear and incorporates other classification systems mentioned in the literature. Different frequencies reported in the literature can be attributed to the sample size used in each study, and using different classifications that might not include all types thus affecting the frequency distribution across the suggested patterns. A consistent note found in all studies is that the most common topography of the CB corresponds to Type I in this study. Type II has been mentioned at various frequencies yet are lower than that described for Type I. Type III, IV and V have not been found in all studies. However,

adding the absence of the CB as a type in the classification is recommended to fully describe the innervation of the palmar surface of the hand.

Table 4.2: Different incidence rates of the palmar communicating branch patterns as reported in the literature in comparison to the current study findings

No	Reference	Type I	Type II	Type III	Type IV	Type V
1.	Current study	82.7%	5.1%	5.1%	4.1%	3.1%
2.	Meals and Shaner, 1983	95%	2.5%	-	-	2.5%
3.	Bonnel and Villa, 1985	92%	-	-	-	8%
4.	Bas and Kleinert, 1999	55%	20%	-	25%	-
5.	Olave et al., 2001	83.3%	14.8%	-	1.9%	-
6.	Don Griot et al., 2000	88%	4%	8%	-	-
7.	Kawashima et al., 2004[1]	72.5%	22%	-	4.6%	-
8.	Biafora and Gonzalez, 2007	91.9%	8.1%	-	-	-
9.	Loukas et al., 2007	84.1%	7.1%	3.5%	5.3%	
10.	Tagil et al. , 2007	66.7%	5.5%	11.1%	16.7%	-
11.	Dogan et al. 2010[2]	71.2%	16.9%	-	5.1%	3.4%

[1]The classification describe a CB branching from the 4th CDN to the lateral side of the ring finger found in one case (0.92%) which could be also described as Ulnar-Median CB putting it under Type I.
[2] The classification describe a CB branching from the 4th CDN to the lateral side of the ring finger found in one case (3.4%) which could be also described as Ulnar-Median CB putting it under Type I.

Knowledge of the morphology of the CB is important in understanding sensory alterations that do not conform to the typical description of the 3½-1½ median-ulnar innervation described in the literature. Fibres passing between the two nerves result in mixed sensation in the area extending from the medial side of the middle finger to the ring finger resulting in reduced and not total absence of sensation in the area if the CB was damaged. Moreover, the presence and topography of the CB can explain why patients with carpal tunnel syndrome could have symptoms extending to the medial side of the ring finger even though involvement of Guyon's canal cannot be confirmed.

It can also explain why some patients will have persistent sensation in their ring and middle fingers with complete laceration of the MN.

The earliest understanding of the sensory innervation of the hand comes from a study conducted in 1918 by Stopford on 1000 gunshot victims following World War I. In this study, sensory distribution in cases of UN injury extended beyond the typical medial 1½ digits in 21% of cases. Similarly, Linell (1921) investigated 20 palms and reported that the UN sensory innervation extends beyond the typical arrangement in 20% of cases. Although significant, such studies indicate that the presence of the palmar CB, which explains the sensory deviations, is not a common finding. Mononeural innervation to the ring finger was not generally supported by electrophysiological studies (Laroy et al., 1999). In an electrophysiological study of the palmar surface of the hand, Laroy et al. (1998) stated that the ring finger received contributions from the ulnar and median nerves in all cases: no case was found where a mononeural innervation was present. In another study conducted in 1999, Laroy et al. mentioned that the absence of either UN or MN contribution to the ring finger was always accompanied with neural pathology and was not due to anatomical variation. Interestingly, Stappaerts et al. (1996) reported that MN stimulation resulted in recordings obtained from the little finger in 2/31 cases, whereas stimulation of the UN resulted in recordings obtained from the middle finger in 3/31 cases. Such studies clearly demonstrate the difference between the incidence rate of the palmar CB in dissection based and electrophysiological studies. Physicians should be aware of the possible presence of the CB in the palm even when electrophysiological results suggest otherwise, and not use velocity study results as an absolute reference in evaluating and assessing sensory innervation in patients.

Based on their observations, Ferrari and Gilbert (1991) described a triangular area where the CB is most likely to be found. The area extended from the middle half of the hypothenar eminence to the proximal transverse crease of the palm distally and bounded by the inter-thenar crease laterally. Don Griot et al. (2000) described the relationship of the CB to the bistyloid line and by using morphometric data outlined an area where the CB is most likely to be encountered. The risk zone described extends more distally and less bilaterally than that described by Ferrari and Gilbert (1991), located between 22%-81% of the distance between the third MCP joint and the BSL with 90% of the CB being found between 33%-67% of the same distance. In the current study, the palmar CB was found to be located between 34.5%-75.4% of the distance between the third MCP joint and the middle of the BSL. Using the middle of the CB as a reference point rather than the proximal and distal attachment points, Loukas et al. (2007) reported that the palmar CB was encountered between 12.5%-85% of the distance between the third MCP joint and the BSL, with 83% of the specimens located between 35%-62% of the same distance.

The palmar CB has also been described with reference to its location to the WC (Olave et al., 2001). The proximal attachment was found to be 33.9±5.5 mm and 30.2±8.2 mm to the WC in male right and left sides respectively and 28.5±6.2 mm and 27.1±3.3 mm to the WC in female right and left sides respectively. As for the distal attachment, the study mentions it was found 43.6±6.9 mm and 40.2±6.2 mm to the WC in male right and left sides respectively and 40.7±7.8 mm and 34.4±1.6 mm to the WC in female right and left sides respectively. In another study of 37 palmar CBs, the UN attachment point, which is the proximal attachment in 34/37 specimens, was found to be 31.7±7.5 mm distal to the WC, whereas, the MN attachment point was found 39.03±7.3 mm distal to the WC. The study also outlined the axis of the third webspace and the fifth ray as the lateral and medial boundaries of the risk area where the CB is most likely to

be encountered (Biafora and Gonzalez, 2007). Similarly in the current study, the proximal attachment of the palmar CB was found 32.3±5.8 mm and the distal attachment was found 43.9±6.6 mm to the WC respectively.

The palmar CB is at high risk during carpal tunnel release due to its close proximity to the TCL. In the current study, 13% of the CB proximal attachment originated at or below the level of the TCL, and 38% had a proximal attachment originating below the level or 4 mm distal to the TCL. Ferrari and Gilbert (1991) reported that the CB originated below the level of the TCL in 22.2% of cases. Stančić et al. (1999) reported that 65.4% of specimens had a proximal attachment below the level or 4 mm distal to the TCL. This close position also puts the CB at risk during exploration of Guyon's canal. Moreover, the palmar CB was reported to be 6.2±3.7 mm and 5.1±2.8 mm distal to the distal edge of the TCL at the level of the axis of the 4th metacarpal bone in male right and left sides and 5.3±3.7 mm and 4.0±1.9 mm distal to the distal edge of the TCL at the level of the axis of the 4th metacarpal bone in female right and left sides (Olave et al., 2001).

The angle at which the CB leaves its proximal attachment is important clinically as the angle approaches a right angle the greater chance it may be injured during surgical procedures in the area. In the current study, the palmar CB detached from the proximal attachment point at an angle 139.9±18.3°, and was found to be 15.6±4.8 mm long extending between the third and fourth CDN in all cases. The angle at which the proximal attachment branched off the UN or MN was found to be between 90-120°, 121-150° and 151-180° in 12.5%, 64.8% and 22.7% of cases respectively. Ferrari and Gilbert (1991) reported 24.4% (11/45) of their cases to originate at a right angle, whereas, Stančić et al. (1999) found it in 19.8% (16/81).

The palmar CB has been reported to communicate with the second CDN; the MN trunk prior to its division into CDNs; the PDN to the lateral side of the middle finger after it arises from the UN; communicate with the UN and the PDN to the medial side of the little finger after it arises from the MN (Ferrari and Gilbert, 1991; Loukas et al., 2007) but none of these patterns were found in the current study.

The importance of appreciation of the topography and location of the palmar CB is clearly shown in such cases as reported by Arner et al. (1994). Investigating 53 two-portal elective carpal tunnel release operations, the study reported 10 patients developing a new sensory disturbance in the ring and middle or little fingers. Six patients continued having symptoms 4 months postoperatively. While the patients described their symptoms as tingling sensation or hyperesthesia rather than numbness, which can mislead physicians to erroneously interpreting it as residual median nerve compression; compression or division injury to the palmar CB was concluded to be the cause of the symptoms (Arner et al., 1994). In another case reported by May Jr and Rosen (1981), numbness on the lateral side of the ring finger developing into a severe tingling sensation over three months was described by a patient following an elective carpal tunnel release. After exploration a large neuroma was found on the palmar CB; following treatment the symptoms were relieved. In a case report, by Rollins and Meals (1985), of a complete laceration of the palmar CB following an accident, the palmar CB was almost equal in diameter to the third CDN prior to their merger indicating the large contribution of the CB in the formation of the PDNs. Moreover, Ferrari and Gilbert (1991) described the palmar CB contributing 30% of the fibres supplying the lateral side of the ring finger in 5 cases and 10% in two cases. Such reports emphasize the importance of the palmar CB in the exchange of fibres in the palm.

According to the morphometric data obtained in this study, a risk area can be outlined where the CB is most likely to be encountered. Figures 4.2 and 4.3 show the risk area with reference to the WC and the BSL respectively. The palmar CB is at risk of injury during carpal tunnel release, flexor tendon surgery of the ring finger, Dupuytren's release, and mobilization of neurovascular island flaps. Palmar pain and digital sensory disturbances resulting from its injury can be erroneously attributed to retraction or scarring if clinicians fail to recognize its involvement. Having morphometric indices provide a precise description of the likely location of the palmar CB overcoming the differences in hand size between individuals and genders. It furthermore compensates for any changes incurred due to the fixation methods. Yet, it is important to appreciate that these indices should not be treated as an absolute reference and that human variations can still surprise.

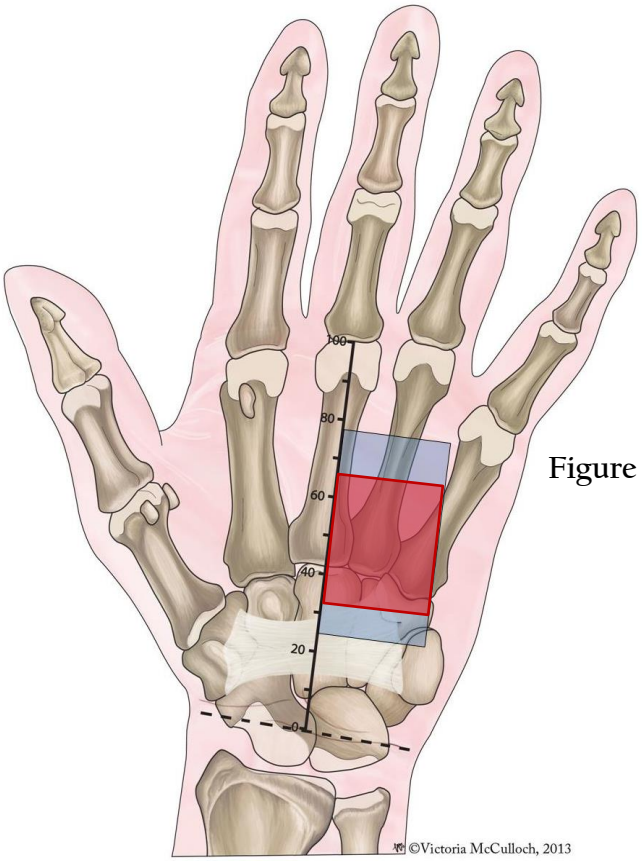

Figure 4.2: Risk area of where the palmar communicating branch is most likely to be found with reference to the wrist crease. Full range is shown by light blue area, 80% of the samples are located in the area indicated by the red box.

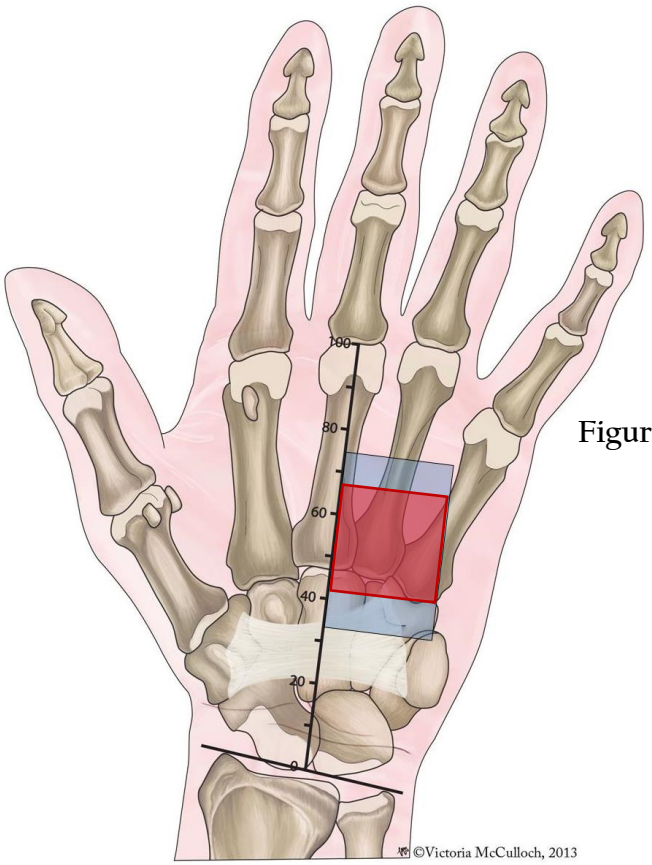

Figure 4.3: Risk area of where the palmar communicating branch is most likely to be found with reference to the bistyloid line. Full range is shown by light blue area, 80% of the samples are located in the area indicated by the red box.

4.2. Dorsal surface of the hand:

The dorsum of the hand is supplied mainly by three nerves: the superficial branch of the radial nerve (SBRN), the dorsal branch of the ulnar nerve (DBUN) and occasionally by the lateral antebrachial cutaneous nerve (LABCN). With various configurations the SBRN innervates the skin covering the lateral 3½-2½ digits, whereas the DBUN innervates the skin covering the medial 1½-2½ digits. The LABCN can extend more distally and innervate the lateral side of the thumb. These nerves are variable in their branching pattern putting them in danger of injury during various clinical procedures performed in the distal forearm, wrist and dorsum of the hand. Understanding the course and appreciating the relationship between these nerves and other anatomical structures is vital to properly diagnose, plan and perform a clinical procedure successfully.

4.2.1. Superficial branch of the radial nerve

The superficial branch of the radial nerve (SBRN) innervates the dorsolateral side of the hand and the dorsal skin covering the lateral 3½-2½ digits up to the proximal interphalangeal joint. The nerve's course and branching patterns have proven to be variable in the literature. Such variability puts the nerve in jeopardy of injury during different clinical procedures performed in the distal forearm or wrist area. Knowledge of the anatomical course of the SBRN, appreciation of the anatomic relationship with other structures in the area, and understanding the possible anatomical variations and their clinical significance can ensure minimal iatrogenic injuries, better application of current procedures, and provide the basis for new opportunities to create novel applications or approaches.

The SBRN originates at elbow level as one of the terminal branches of the radial nerve. In the current study, it was found to originate proximal to the lateral epicondyle in 13.7% of cases. Abrams et al. (1992) reported that the SBRN was found to originate at the level of the lateral epicondyle in 8/20 (40%) cases and within 21 mm distal to the epicondyle in the remaining 12/20 (60%) cases. In the current study, the nerve coursed deep to brachioradialis and became subcutaneous by piercing the antebrachial fascia 72.1±16.6 mm proximal to the RSP, between the tendons of brachioradialis and extensor carpi radialis longus. This finding is similar to that reported in the literature where the SBRN was found to become subcutaneous 73±1.5 mm, 81.6 mm, 83.1±11.4 mm and 85.4±1.32 mm by Huanmanop et al. (2007), Vialle et al. (2001), Robson et al. (2008) and Samarakoon et al. (2011) respectively. The distances in the current study are less than those reported by Abrams et al. (1992) and Ikiz and Üçerler (2004) who reported the SBRN to become subcutaneous at 90±14 mm and 92±14mm respectively. In the current study, the nerve was found to pierce the tendon of brachioradialis to become subcutaneous in 2% (3 cases), which is less than that reported by Abrams et al. (1992) (10%); yet similar to the findings of Huanmanop et al. (2007) (3.8%). Such a course can put the SBRN in danger of entrapment.

In the current study, the point where the SBRN becomes subcutaneous is estimated to be located at the distal 30.5±5.8% of the total length of the radius. Also Robson et al. (2008) found the SBRN to become subcutaneous in the distal 32.8±4.1% of the total length of the forearm; however, the SBRN is reported to become subcutaneous, on average, in the distal 36% of the distance between the lateral epicondyle to the RSP (Abrams et al., 1992). In this region the nerve is only covered by skin and subcutaneous fat making it vulnerable to injury due to trauma or compression in cases of tight handcuffs, tight watches or bracelets. Compressive or badly made casts or fracture bracelets can lead to nerve irritation complicating the treatment process. Moreover,

clinical procedures performed in the distal third of the forearm should be conducted with caution.

The SBRN divided into two branches: one palmar and one dorsal (97.3%) or three branches (2.7%) 51.4±14.9 mm proximal to the RSP. Although different, both Abrams et al. (1992) and Ikiz and Üçerler (2004) reported a higher incidence rate at 15% and 8.33% of which the SBRN divides into three branches after it became subcutaneous. Moreover, this division pattern was not found by Klitscher et al. (2007) or Samarakoon et al. (2011). Table 4.3 shows different anatomical measurements taken for the SBRN as reported in the literature in comparison to the current study.

Table 4.3 Anatomical measurements for the superficial branch of the radial nerve (SBRN) as reported in the literature in comparison to the current study (mm).

No	Reference	Becoming subcutaneous to the RSP[1]	1st major branch to the RSP	2nd major branch to the RSP	Closest branch to LT[2]
1.	Current study	70.8±15.9	50.9±14.7	Palmar: 4.3±21.7 Dorsal: 4.3±14.4	14.1±3.8
2.	Abrams et al. (1992)	90±18	51±18		16±0.5
3.	Tellioglu et al. (2000)		46±5.7	Palmar: 4.8±2.1 Dorsal: 16±2.3	
4.	Ikiz & Üçerler (2004)	92±14	49±12		15.8±12
5.	Huanmanop et al. (2007)	73±1.5	46±1.5		10±3.8
6.	Klitscher et al. (2007)		54.7±12.2	0.0±5.7	16.4±3.7
7.	Robson et al. (2008)	83.1±11.4	49.2±14.4		14.9±5.3
8.	Korcek & Wongworawat (2011)		31.46±10.73 to a line between the RSP & LT	4.18±10.23	
9.	Samarakoon et al. (2011)	85.4±13.2	55.7±14.3		

[1] Radial styloid process
[2] Lister's tubercle

Due to the variable course of the SBRN in the distal forearm and the wrist area, the nerve is at risk of injury during various clinical procedures including reduction and stabilization of distal radial fractures, wrist arthroscopy, radial artery harvest, wrist denervation, nerve blockade, De Quervain's release, and bone graft harvest.

SBRN can be injured directly as a result of distal radial fractures, or indirectly as a result of reduction and fixation of those fractures. Anderson et al. (2004) reported neuropathies related to the SBRN following the insertion of external fixator pins in 8.3% of cases investigated. An open technique for placing the pins is advocated to reduce nerve irritation (Anderson et al., 2004).

Kirschner wires (K-wires) are also used to treat and stabilize distal radial fractures. The RSP is commonly used as an insertion point for these wires. In the current study, branches of the SBRN were found to pass as close as 0.7 mm to the RSP putting the nerve branches at high risk of injury. Steinberg et al. (1995) reported that 20% of the deep structures including the SBRN were injured as a result of inserting K-wires through the anatomic snuffbox. The study also described a safe-zone area of 68 mm^2 where the wires can be inserted safely (Steinberg et al., 1995). However, this safe-zone was evaluated by Korcek and Wongworrawat (2011) who concluded that the variability of the SBRN in this area makes it difficult to assign any true safe zone. In another study, Singh et al. (2005) reported neuropathies related to the SBRN in 20% following the insertion of K-wires. Patients presented symptoms of sensory disturbances, complete sensory loss and painful neuroma formation (Singh et al., 2005). Hochwald et al. (1997) stated that the anatomic snuffbox contained on average 3 nerve branches coursing as close as 3 mm from the RSP; and recommended limited open technique where the SBRN branches can be identified and preserved prior to the insertion of the wires. Nerve irritation can also occur during the removal of the wires,

the reduction process or due to the continuous friction between the nerve and the buried part of the wire if it is placed too close to the nerve. An open technique or a limited-open technique allows the surgeon to place the wires at a safer distance from any nearby nerves (Hochwald et al. 1997; Singh et al., 2005; Sharma et al., 2006). As an alternative and if the case permits, LT can be used as a safe insertion point for the K-wires. In the current study, branches of the SBRN passed 14.1±3.8 mm from the LT.

Elastic stable intramedullary nailing is frequently used to treat paediatric open, unstable or irreducible fractures due to its cosmetic and functional advantages (Cumming et al., 2008). The nails are usually inserted dorsally between the first and second dorsal compartment using a 20-30 mm proximal incision starting at the level of the physis. Kang et al. (2011) reported sensory disturbances in two patients (2.2%) following treatment by elastic intramedullary nailing, whereas Cumming et al. (2008) found it in 1/19 (5.2%). In a larger retrospective study of 553 cases, 15 (2.7%) cases were reported to have developed a lesion of the SBRN as a result of the primary operation or nail removal (Fernandez et al., 2010). With careful dissection to identify the SBRN branches present in the area, complications can be reduced.

Arthroscopy can be used as a diagnostic or therapeutic tool. It can be used in many cases including triangular fibrocartilaginous tears, carpal interosseous ligament injuries, intra-articular distal radial fractures, wrist pain and dorsal ganglia. Wrist arthroscopy has a complication rate of 2% (Culp, 1999); however, with the increase in medical procedures involving arthroscopy, the actual complication rate is thought to be higher. Tryfonidis et al. (2009) reported that superficial nerves pass at a mean distance of 1.8 mm, 4.9 mm, 2.5 mm and 6.7 mm from portals 1-2, 3-4, 6U, and MCP respectively putting them at high risk during the establishment of portals. Arthroscopic portals are designed in relation to their relationship to the extensor compartment. As the

procedures can be performed on the radial side of the hand depending on the portals established, the SBRN can be at risk of injury or irritation as it passes near to or directly below these portals. Understanding the course and anatomic relation of the superficial nerves in the area can help clinicians to better preserve and avoid iatrogenic injuries to those nerves. Furthermore, the SBRN can also be injured during arthroplasty, arthrotomy, bone graft harvest or wrist denervation procedures as the nerve branches course under the portals or incision lines. Bone grafts can be obtained from the distal radius between the first and second dorsal compartment. Arthroplasty of the distal scaphoid joint (triscaphe joint) is performed via a longitudinal incision between the tendons of the first extensor compartment with a SBRN neuropathy complication rate of 4.1% (Wessels, 2004). SBRN branches can course through this area in various configurations and be at risk if the surgeon is unaware of their presence. Wrist denervation is used to treat patients with chronic pain originating as a result of many pathological conditions of the wrist by surgically dividing articular branches from the median, ulnar, radial and LABCN. Good understanding of the relative anatomy of the nerves in the area is important to be able to conduct the procedure safely and successfully.

During De Quervain's release of the first dorsal compartment, the SBRN branches can be injured as they cross closely, or through the area. Abrams et al. (1992) mentioned that branches of the SBRN were found over the first dorsal compartment in 35% of cases, Ikiz and Üçerler (2004) reported it in 16.67%, while Huanmanop et al. (2007) found it in 38%. Depending on the severity of the condition, a surgical release of the first dorsal compartment may be required. Surgical release can be performed by a longitudinal, transverse, or a Z-incision line. Mellor and Ferris (2000) reported SBRN injury in 6/17 (35.3%) of cases following a longitudinal incision. At the level of the RSP, branches of the SBRN pass as close as 2 mm to the first dorsal compartment (Klitscher

et al., 2007). Robson et al. (2008) mentioned that a transverse or a Z-incision will cross the SBRN branches in all cases investigated. The study suggested a 25 mm incision at the RSP and extending proximally which spared any SBRN branches in 68% of the cases investigated. In the current study, the SBRN crossed the most proximal edge of the incision described by Robson et al. (2008) in 10.7% and the SBRN branches were found to course closer to the RSP axis in 41.7% of the cases investigated. Agreeing with the literature, the SBRN has a variable course, a safe incision zone cannot be identified, and careful dissection intra-operatively is strongly recommended to identify and preserve nerve branches in the area.

As the radial artery is frequently used for obtaining samples during arterial blood gas testing, the SBRN can be at risk of injury due to its close proximity to the radial artery at the wrist. Several attempts may be required before a successful sample is obtained; moreover, several samples can be required to test a patient's respiratory status in some conditions. Robson et al. (2008) described a close association between the SBRN branches and the radial artery in 48% of cases. An ulnar approach to the radial artery is suggested to minimize SBRN injury (Robson et al., 2008).

Neurological complications related to the SBRN have been reported following radial artery harvest for coronary surgeries. In their study of 54 patients that underwent radial artery harvest for coronary surgery, Siminelakis et al. (2004) reported sensory disturbances related to the dorsum of the hand in 31.28% of cases. Neuropathies can be as a result of direct trauma during the harvest, compression secondary to edema, history of clinical conditions affecting the vasculature such as diabetes or smoking, or ischemia secondary to reduced blood supply when the nerves are supplied by branches from the radial artery (Denton et al., 2001). Galajda et al. (2002) discussed the importance of the harvest technique, mainly the mechanical or thermal damage that

occurs during the harvest as the main reason for SBRN damage. Neuropathies in the SBRN territory were reported as high as 16.2% when the radial artery was harvested using the traditional method and 2% when the radial artery was harvested by a novel approach they developed but have not explained in their publications (Galajda et al., 2002). In another study by Bleiziffer et al. (2008), an open technique for radial artery harvest patients reported less sensory disturbances related to SBRN (22.6%) than endoscopic technique for the radial harvest group (45.3%); however, the authors still advocate the endoscopic technique for its cosmetic advantages and lower post-operative wound complications.

The SBRN has a close association with the cephalic vein. Robson et al. (2008) reported a close association between the SBRN and the cephalic vein in 80% cases investigated. In the current study they both crossed for the first time after the nerve became subcutaneous at 47.9±19.3 mm (range: 93.6-6.7 mm) proximal to the RSP. Similarly, Klitscher et al. (2007) reported a mean distance between the RSP and the crossing point of the two structures at 54.3±7.6 mm. Gupta et al. (2012) investigating spontaneously aborted foetuses reported that the cephalic vein crossed the nerve twice in 80% of the cases studied. Cephalic vein cannulation is a common procedure that puts the SBRN at risk of injury if the vein wall is punctured. Sawaizumi et al. (2003) reported 11 cases of SBRN injury after venepuncture of the cephalic vein patients complained of pain, numbness and sensory disturbances in the dorsal region of the hand; of which 7/11 (63.6%) continued to show sensory symptoms at three month follow up. Vialle et al. (2001) stated that the SBRN and the cephalic vein crossing point ranged between 90 mm proximal to 45 mm distal to the RSP. Although the current study only focused on the crossing point proximal to the RSP, it is evident that the crossing point and the relation between the SBRN and the cephalic vein are highly variable and that no safe zone can be assigned. Venepuncture of the cephalic vein at the

wrist or the distal third of the forearm, where the SBRN becomes subcutaneous, should only be used when no other alternative is available.

Radial forearm fasciocutaneous free flaps are used for reconstructive surgery. Morbidity at the donor site has been of concern. Richardson et al. (1997) reported sensory disturbances in 32% of cases following the harvest, whereas Lutz et al. (1999) reported it in 54%. Grinsell and Theile (2005) described different incidence rates depending on the draining system harvested with the flap; double the rate of sensory disturbances are associated with neural injury if the cephalic vein is harvested (18%) in comparison to harvesting the venae commitantes (9%). This finding coincides with the close association that the cephalic vein has with the SBRN that could put the neural structures in danger if the cephalic vein was raised.

The SBRN and LABCN can overlap. Mackinnon and Dellon (1985) reported a complete or a partial overlap between the two nerves in 75% of cases. Steinberg et al. (1995) reported that the LABCN was found to course through the anatomic snuffbox in 45% of the cases investigated and was in danger of injury by a K-wire in 40%. Similarly, Korcek and Wongworrawat (2011) described a close association between the SBRN and LABCN. The LABCN was found to be present over the anatomic snuff box in 52.5% of cases, innervating the same area of the SBRN in 10% of cases. Furthermore, the LABCN was found to take over the innervation of the lateral side of the thumb with the absence of the S3 branch from the SBRN in 5% of cases (Korcek and Wongworrawat, 2011) and in 4.7% (Huanmanop et al., 2007). Other studies have differed in the communication rate between the SBRN and LABCN. It was reported to be 43% by Huanmanop et al. (2007), 35% by Abrams et al. (1992) and 20.8% by Ikiz and Üçerler (2004). In the current study, the LABCN communicated with the SBRN in 30.7% of cases. Due to its variability in communicating with the SBRN, extensions and

distribution patterns; it is difficult to assign sensory deficiencies or neuromas to one of the nerves and not the other. Furthermore, because of its presence over the anatomic snuffbox and the first dorsal compartment, it is at as much risk of injury as the SBRN during procedures performed in this area. This association between the two nerves should be considered when evaluating sensory deficiencies and planning nerve blockade in the wrist area.

Injury to the SBRN can be very painful and require a long recovery time and may require further surgery. Patients may complain of paraesthesia or hypesthesia in branches of the SBRN and pain secondary to nerve lesions or neuroma formation affecting their daily activities leading to various forms of disability. Careful technique, through understanding the course and division points of the nerves in the area in relation to anatomical landmarks can minimize postoperative complications and help clinicians during the procedures mentioned above.

The branches arising from the main trunk of the SBRN are usually labelled from medial to lateral as superficial radial 1 (SR1), SR2 and SR3 (Steinberg et al., 1995). The variability of the SBRN branching and innervation territory made it difficult to classify the nerve into a system. Ikiz and Üçerler (2004) classified the SBRN into three types based on the number of branches. Huanmanop et al. (2007) modified the system by adding a new type that accounts for cases where SR3 is absent and the area of innervation is taken over by the LABCN. Although significant, this classification system does not account for all the variations in the branching patterns described for the SBRN or for the different innervation territories encountered. Another classification system described by Korcek and Wongworawat (2011) is based on the arrangement by which SR1, SR2 and SR3 comes off the main trunk of the SBRN. Yet, this system does not account for all the variations for the SBRN. Gupta et al. (2012)

described another system based on firstly the innervation territory of the SBRN, and secondly by the number and arrangement of the branches coming off the main trunk of the SBRN. The system describes only three types, where the SBRN extends to innervate the lateral three and half digits. However, in the current study cases were identified where the SBRN innervation territory extended beyond the lateral three and half digits. Those cases are not accounted for in the classification suggested by Gupta et al. (2012).

The current study proposes modifying the classification suggested by Gupta et al. (2012) to include different innervation territories.

Type I: The SBRN innervated the lateral two and half digits

A. The main trunk bifurcated into S3 and a common trunk. S3 innervated the entire thumb, whereas the common trunk further divided into S2 and S1 distally
B. The main trunk bifurcated into S3 and a common trunk. S3 innervated the lateral side of the thumb, whereas the common trunk further divided into S2 and S1 distally
C. The main trunk trifurcated into three branches with a common origin point. The branches innervated the lateral side of the thumb, the medial side of the thumb and the lateral index, the medial index and the lateral middle fingers.

Type II: The SBRN innervated the lateral 3 digits. The main trunk divided into medial and SR3 branches. The medial branch supplied the middle, index finger and occasionally the medial side of the thumb. SR3 supplied the thumb.

A. The main trunk divided into S3 and a common trunk. The S3 innervates the entire thumb. The common trunk divides into S2 and S1 distally.
B. The main trunk divided into S3 and a common trunk, which divided distally to S1 and S2. S2 innervates the medial thumb and S1 to the index and the middle fingers.
C. The main trunk bifurcated into S3 and a common trunk. S3 innervated the lateral side of the thumb, whereas the common trunk further divided into two branches distally. The medial side of the thumb and the lateral side of the index fingers are innervated by the same branch.
D. The main trunk bifurcated into S3 and a common trunk. S3 innervated the lateral side of the thumb, whereas the common trunk further divided into three or four branches distally.
E. The main trunk trifurcated into three branches with a common origin point. The branches innervated the lateral side of the thumb, the medial side of the thumb, index and middle fingers.

Type III: The SBRN innervated the lateral 3 and half digits. The main trunk divided into medial and SR3 branches.

A. The main trunk bifurcated into S3 and a common trunk. S3 innervated the entire thumb, whereas the common trunk further divided into S2 and S1 distally.
B. The main trunk bifurcated into S3 and a common trunk. S3 innervated the lateral side of the thumb, whereas the common trunk further divided into S1 and S2 distally. The medial side of

the thumb and the lateral side of the index finger are innervated by the same branch.

C. The main trunk bifurcated into S3 and a common trunk. S3 innervated the lateral side of the thumb, whereas the common trunk further divided into S2 and S3 distally. S2 to medial thumb and S3 to the rest of the territory.

D. The main trunk bifurcated into S3 and a common trunk. S3 innervated the lateral side of the thumb, whereas the common trunk further divided into three or four branches distally.

Type IV: SBRN innervated the lateral four digits.

Type V: SBRN innervates the lateral four and half digits

Type VI: SBRN innervates the full dorsum of the hand with the absence of the DBUN.

A. Trifurcation of the main trunk.

B. The main trunk bifurcated into S3 and a common trunk. S3 supplies the lateral side of the thumb. The common trunk further trifurcates.

C. The main trunk bifurcated into S3 and a common trunk. S3 supplies the lateral side of the thumb. The common trunk divided into S2 and S1. S2 supplies the medial side of the thumb and the lateral index finger. S1 supplies the rest of the territory.

D. The main trunk bifurcated into S3 and a common trunk. S3 supplies the lateral side of the thumb. The common trunk divided into S2 and S1. S2 supplies the medial side of the thumb

index and the lateral side of the middle fingers. S1 supplies the rest of the territory.

The aim of this classification is not to produce a system to be memorized, but rather to ease the understanding of the different branching patterns of the SBRN in the dorsum of the hand. The most common type was Type I, where the SBRN extends to innervate the 2½ lateral digits. Table 4.4 shows the incidence rate of the 6 types found in this study.

Table 4.4: Incidence rates of the branching patterns of the superficial branch of the radial nerve found in the current study

Type	No.	%
Type I	56	37.3
Type II	35	23.3
Type III	44	29.3
Type IV	2	1.3
Type V	3	2
Type VI	10	6.7

4.2.2. Dorsal branch of the ulnar nerve:

The dorsal branch of the ulnar nerve (DBUN) is one of the terminal branches of the UN. It supplies the dorsomedial aspect of the dorsum of the hand and skin covering the dorsal medial 1½ digits. In the current study it was found to originate from the medial side of the main trunk of the UN 63.3±14.8 mm from the USP and 61.3±21.0 mm from the proximal edge of the pisiform. The origin point found in this study differs to those mentioned in the literature. The DBUN was found to originate more proximally by Botte et al. (1990), Casoli et al. (2004), and Cavusoglu et al. (2011) reporting it to be 83.±24 mm, 80 mm and 83.6±2.4 mm proximal to the pisiform respectively. It has also been reported to originate more distally than in the current study by Goto et al. (2010)

and Puna and Poon (2010) who reported the origin point to be 34±13 mm and 51±14 mm proximal to the USP respectively. The origin point corresponds to a point located in the distal 26% of the total length of the ulna (Botte et al., 1990); similarly, it was found to be located 23.6±7.7% of the total length of the ulna in the current study.

In the current study, the nerve courses medially and distally deep to flexor carpi ulnaris before it emerges at the dorsomedial border to become subcutaneous 18.1±7.1 mm proximal to the USP. Botte et al. (1990) and Cavusoglu et al. (2011) reported the DBUN pierced the antebrachial fascia 50±18 mm and 54.7±1.5 mm proximal to the pisiform respectively. Although mentioned with reference to a different bony landmark (the pisiform), which is located 11.7±4.3 mm distal to the USP, the point where the nerve becomes subcutaneous is located more distally in the current study. In their study, Mok et al. (2006) reported the DBUN becoming subcutaneous 26±8.3 mm proximal to the USP.

The DBUN innervates the medial side of the dorsal hand and the skin covering the medial 1½-2½ digits by dividing into two major branches. In the current study, the first division was found to originate anywhere between 38.7 mm proximal to the USP and 53.4 mm distal to the USP (mean: -3.4±17.4 mm). The second division was also found to be variable, dividing anywhere between 8.8 mm proximal to the USP and 73.6 mm distal to the USP (mean 39.2±13.2 mm). Mok et al. (2006) reported different measurements for the location of the first and second branches of the DBUN. In their study, the first branch occurred 20±14.7 mm proximal the USP while the second branch occurred 26±11.4 mm distal to the USP. The differences between the two studies could be attributed to the different definition of the major branches Mok et al. (2006) used in their study. They described the major branches as being the nerves terminating in the

dorsal digits with no further divisions, whereas this study considered the division points as they occur along the course of the DBUN.

These anatomical measurements are important to appreciate when performing a direct approach to the subcutaneous border of the ulna where the DBUN is at high risk of injury such as in cases of open reduction and internal fixation of ulna fractures, treatment of delayed union or non-union of ulnar fractures and chronic osteomyelitis, osteotomy of the ulna and lengthening or shortening of the ulna (Le Corroller et al., 2013). Injury to the DBUN could be presented as dysesthesia and numbness to the dorsomedial area of the hand. It can also result in neuroma formation which is usually more painful and disabling to the patient than sensory disturbances.

Moreover, understanding the anatomy and course of the DBUN is important in planning and preparing nerve grafts of up to 100 mm. Neurovascular flaps from the DBUN are preferable because of their limited donor site morbidity, cosmetic advantages, restricted vascular sacrifice, and the simple and rapid dissection required in their preparation. It is also important to appreciate the anatomical relations of the DBUN in planning nerve blockade, assessing iatrogenic injuries and restoration of sensory innervation after UN lesions.

The DBUN is at risk during wrist arthroscopy as it passes close to the 6 Radial (6R) portal. Grechenig et al. (1999) reported that the most common complication found after performing wrist arthroscopy on 96 patients was irritation of the DBUN, reported in 3.1% of cases. The nerve consistently crossed a line between the USP and the fourth webspace. The DBUN crossed this line 18.1±9.1 mm distal to the USP corresponding to 19.4±9.6% of the distance between the USP and the fourth webspace. Tindall et al. (2006) found the DBUN to be more constant crossing the same line 24 mm (range: 18-28 mm) distal to the USP, corresponding to a point 23±2.5% of the distance between

the USP and the fourth webspace. In their study, Tindall et al. (2006) recommend that the 6R portal is placed in the proximal 19% of the distance to avoid injury to the DBUN. However, according to the results obtained from the current study, the DBUN crossed the distance between the USP and the fourth webspace within the proximal 19% in almost 50% of the specimens. Agreeing with Tindall et al. (2006) that this area should be approached with caution and that those measurements should not be taken as absolute reference.

4.2.3. Sensory distribution in the dorsum of the hand

Anatomical textbooks usually describe the sensory distribution in the dorsum of the hand as being supplied by the SBRN and the DBUN. Gray's Anatomy for Students 2nd edition describe the innervation territory of the SBRN as supplying "*the dorsolateral aspect of the palm and the dorsal aspects of the lateral three and one-half digits distally to approximately the terminal interphalangeal joints*"; however, illustrations show that the innervation territory extends only to the dorsal skin covering the lateral three digits (Drake et al., 2010). A similar discrepancy between text and illustrations is present describing the DBUN innervation territory. While the text describes the DBUN as innervating the dorsal skin covering the medial one and half digits, the illustration shows the innervation territory to extend to cover the dorsal skin covering the medial two digits (Drake et al., 2010). Similarly, illustrations are shown in Gray's Atlas of Anatomy where the SBRN innervates the dorsal skin covering the lateral three digits whereas the DBUN innervates that covering the medial two digits (Drake et al., 2008).

In other textbooks (Moore et al., 2011; Moore et al., 2013), the dorsum of the hand innervation is illustrated to show the classical description of the SBRN innervating the dorsal two thirds of the dorsal hand and the dorsal skin covering the lateral three and half digits, with the DBUN innervating the rest of the hand.

Grant's Atlas of Anatomy 12th edition shows the dorsum of the hand to be split between the two nerves at the middle of the ring finger: the SBRN innervating half of the dorsum hand and the dorsal skin covering the lateral three and half digits whereas the DBUN innervates the medial half of the dorsal hand and the dorsal skin covering the medial two and half digits. The atlas also shows several variations in the innervation of the dorsum of the hand (Agur et al., 2009).

An understanding of the sensory distribution in the dorsum of the hand comes mainly from historical large studies such as that conducted by Stopford (1918) examining gunshot victims from World War I. By testing for sensory loss, it was possible to describe the outline known today. In UN injuries, the study described anaesthesia in the medial one and half digits in 79%, and in the entire little and ring fingers in only 15% setting the typical distribution of the DBUN to be limited to the medial dorsum of the hand and the skin covering the medial one and half digits. Although significant, the study set loss of sensation as the variable tested which could be misleading when it comes to outlining the extent of the sensory distribution of the dorsal nerves. Such a definition does not account for communicating branches between the dorsal nerves and/or other nerves in the area that allows for exchange of fibres and thus sensory retention in an area that is supposed to be anaesthetised if the injured nerve was solely responsible for innervating that area. In another study, Linell (1921) reported that the typical distribution of the medial one and half digits was only found in 12.5% of cases, whereas the DBUN extended to innervate the skin covering the medial two and half digits in 68.8%. Auerbach et al. (1994) also reported that the SBRN innervated the dorsal skin covering the lateral three digits in 55%, and followed the typical description of innervating the lateral three and half digits in only 5%. In a more recent study by Mok et al. (2006), the DBUN was found to follow the classical description of innervating the medial one and half digits in only 13.3%. In the current study, the SBRN

was found to follow the classical description and solely innervate the lateral three and half digits in only 18.7%. It was noted that the SBRN extended less medially than the classical description agreeing with the results of Mok et al. (2006). The most common distribution found in the current study was the SBRN innervating the lateral dorsal skin and the skin covering the lateral two and half digits. Furthermore, the DBUN was found to innervate the medial dorsal skin and the skin covering the medial two and half digits in 38.0% setting it as the most common pattern. Similarly, Vergara-Amador and Nieto (2010) reported that the most common branching pattern of the SBRN seen in 56% extended to innervate the lateral two and half digits.

Electrophysiological studies have also highlighted the variability of the distribution patterns in the dorsum of the hand. Stappaerts et al. (1996) mentioned that action potential results were obtained from the little and ring fingers in 52% after stimulation of the DBUN, and from the middle finger in 26% after stimulating the same nerve. Laroy et al. (1998) mentioned that the action potential is reduced laterally to medially when the SBRN was stimulated and medially to laterally when the DBUN was stimulated and become increasingly unobtainable at the level of the ring finger.

It is not uncommon for the SBRN and DBUN to communicate in the dorsum of the hand[1] changing the sensory distribution in the dorsum of the hand. In the current study, the two nerves communicated in 37 (26.4%) cases altering the sensory innervation on the medial side of the ring finger and lateral side of the middle finger in the majority of cases (31/37; 83.8%); however, it is still possible for the communication to affect other areas as the lateral side of the middle finger and the medial side of the index finger, and the medial side of the middle finger as seen in the current study in 8.1% (3/37) and 5.4% (2/37) of cases respectively. Furthermore, dual innervation where the two nerves overlap and contribute to the innervation of the same territory with no

[1] The dorsal communicating branch between the SBRN and the DBUN is discussed in the next section

clear communication has been reported in the literature. Mok et al. (2006) reported dual innervation in 10/30 (33.3%) where both nerves supply the medial side of the middle finger and the lateral side of the ring finger (6/10), the medial side of the middle finger (3/10), and the medial side of the ring finger (1/10). In the current study, dual innervation was noted in only 4 cases (2.9%) affecting the medial side of the middle finger and the lateral side of the ring finger in two cases, and the medial side of the middle finger only in the other two. Communicating branches and dual innervation in the dorsum of the hand can complicate the interpretation of the velocity test results by producing a low or absent response; create complications during surgery, and leads to misevaluation of nerve pathology if the clinician is not aware of their presence.

LABCN can contribute to the innervation of the dorsum of the hand. It was also reported that the LABCN completely takes over the innervation of the lateral side of the thumb when SR3 is absent (Madhavi and Holla, 2003; Huanmanop et al., 2007; Korcek and Wongworawat, 2011). Such variation was noticed in one case in the current study. The incidence rate for the communication between the two nerves varies between 20.8-43% in the literature. Interestingly, in the current study, the SBRN communicated with the LABCN in 30.0% of cases of which the LABCN communicated with SR3 allowing both nerves to contribute in the innervation of the lateral side of the thumb (37/45; 82.6%) and communicated to the main trunk of the SBRN allowing both nerves to contribute in the innervation of the entire territory of the SBRN (8/45; 17.4%). Martín Inzunza et al. (2011) reported a similar case where the LABCN communicated with the SBRN and continued to supply the entire SBRN territory. Clinicians evaluating neuromas, nerve pathology and sensory disturbances in the dorsum of the hand should be aware of the possible involvement of the two nerves.

Full supply of the dorsum of the hand by the SBRN with the absence of the DBUN has been described in the literature. Dissection based studies and velocity conduction studies report different incidence rates. In dissection based studies it was found in 4.16% as reported by Botte et al. (1990), 3.3% by Mok et al. (2006), 5.5% by Tiznado et al. (2012) and 8% by Robson et al. (2008). In velocity conduction studies it was reported in 19% by Pollak et al. (2013) and 12.9% by Stappaerts et al. (1996). In the current study it was found in 6.7% of cases. Failure to recognize the presence of this pattern can lead to misinterpretation of the velocity conduction test results and nerve injury promoting inappropriate treatment and unnecessary surgical intervention. If a response from the DBUN cannot be obtained, a full investigation of the hand is recommended.

Patterns of innervation in the dorsum of the hand are variable across individuals; however, it is also variable between the two hands of the same individual. Investigating 30 fetuses, asymmetry between left and right hand sides was found in 17% as reported by Gupta et al. (2012). In another study performed on 40 Thai cadavers, asymmetry was observed in 42.5% of the cases (Huanmanop et al., 2007). In velocity conduction studies, Stappaerts et al. (1996) reported symmetry for the dorsum of the hand after stimulating both SBRN and DBUN in 29% of the cases only, whereas Dutra de Oliveira et al. (2000) reported significant differences in the results obtained in 21%. It is important to appreciate the differences between the two sides of the same individual. In the current study, symmetry was found in 43.2% of cases. The electrophysiological test results obtained from the healthy hand should not be used as an absolute reference to evaluate pathology in the other hand.

Electrophysiological studies are an important tool in mapping sensory nerves in the hand; however, they should be used with caution. Low or absent responses when the

nerves are stimulated does not necessarily mean that the tested nerve is absent as nerve axons could be too few and/or their diameter too small to produce an action potential high enough to be recorded. This explains the differences in incidence rate of all-radial-supply between dissection based and velocity conduction studies. Not appreciating the presence of the communicating branches can lead to misdiagnosis of neural entrapment and pathologies in the wrist and forearm. Moreover, asymmetry is not uncommon in the dorsum of the hand and the healthy hand should not be considered an absolute reference when evaluating pathologies in the other hand. Full hand investigation is recommended to have a better understanding of the pattern of the dorsal nerves and thus avoid preoperative and postoperative complications.

4.2.4. Dorsal communicating branch between the superficial branch of the radial nerve and the dorsal branch of the ulnar nerve

The sensory innervation of the dorsum of the hand can be quite variable. The presence of a dorsal communicating branch (CB) between the SBRN and the DBUN can explain sensory deviations in the dorsum of the hand. It can provide collateral pathways for nerves to supply a region otherwise anaesthetised due to injury or pathology. In electrophysiological studies, the presence of dorsal CB can alter the results leading to misdiagnosis and unnecessary therapeutic measures. Furthermore, it can be a complicating factor if injured during surgical procedures to the dorsum of the hand. The dorsal CB is at risk of injury during surgical procedures performed in the dorsum of the hand such as fracture repairs of the fourth and fifth metacarpal bones, and dorsal approaches to the carpal tunnel resulting in sensory disturbances and painful neuroma formation. Consequently, understanding the topography and the common location of the dorsal CB is important to properly diagnose and treat various hand related pathologies.

The dorsal CB was reported in the literature with various incidence rates. Botte et al. (1990) found it in one specimen of 24 (4.16%), Auerbach et al. (1994) reported it in 15% of the 20 hands explored, while Loukas et al. (2008) investigated 200 formalin fixed adult cadaveric hands and reported the incidence of the communicating branch between the DBUN and the SBRN to be 60% (120/200). Interestingly, in their study of 30 cadaveric hands outlining in detail the different nerves contributing to the dorsal innervation of the hand, Mok et al. (2006) made no mention of the dorsal CB.

The DBUN is usually used for preparing nerve grafts for its minimum donor morbidity. Cavusoglu et al. (2011) reported that due to the many communications between the DBUN and the SBRN in the dorsum of the hand, excision of the DBUN may not result in numbness. However, in the current study the dorsal CB was only found in 26.4% of cases. Collateral, dual and dorsal CB can explain the minimal sensory loss in the donor site, but according to the results obtained from this study, clinicians need to be careful not to develop therapeutic choices on inaccurate assumptions.

Loukas et al. (2008) suggested classifying the dorsal CB into four types based on the direction of the CB. The current study suggests classifying the dorsal CB into three types based on the number of attachment points between the SBRN and the DBUN:

Type I: The CB had a single attachment to the SBRN and the DBUN.

A. CB attached proximally to the SBRN
B. CB attached proximally to the DBUN
C. CB attached to the SBRN and the DBUN at the same level

Type II: The CB had multiple attachment points to both the SBRN and DBUN.

Type III: The DBUN and SBRN both gave a branch that merged and sent branches to the dorsum of the hand.

Type I A, I B and I C correspond to the Types I, II and III suggested by Loukas et al. (2008) respectively. Types I A, I B and I C were found in 10.8%, 18.9% and 2.7% in the current study; however were found in 59.1%, 19.1% and 3.3% by Loukas et al. (2008). The most common type found in this current study was Type III (56.8%).

Loukas et al. (2008) described a risk zone where the dorsal CB is most likely to be found. The dorsal CB was found 41% of the distance between the USP and the fourth metacarpophalangeal joint with a range of 12-78%. With such a big range, the authors used a prevalence of 85% of the samples to make the risk area smaller and more useful and reported the dorsal CB to be present between 28-60% of the distance between the USP and the fourth metacarpophalangeal joint (Loukas et al., 2008). In the current study, the dorsal CB was defined by its proximal and distal attachment points. The proximal attachment of Type I of the dorsal CB was found between -7.6-85.6% of the distance between the third MCP joint and the BSL, whereas the distal attachment was found between 32.9-98.4% of the same distance. With the large variability in the dorsum of the hand and limited number of samples, it is difficult to identify a risk-zone. The majority of cases in this study belong to Type III (56.8%) where the merging point of the two nerves was at 83.9±17.0% of the distance between the third MCP joint and the BSL. This type has not been described before in the literature. In their study detailing the nerves in the dorsum of the hand, Mok et al. (2006) suggested a safe area where no nerves pass through in the dorsum of the hand. The suggested area overlaps with the risk area suggested by Loukas et al. (2008) and with the findings of this current study. In their study of the nerves of the dorsum of the hand, Cirpar et al. (2012) reported that the great variability of the branching patterns of the dorsal nerves

and the presence of communicating branches between nerves prevents any suggestion of a safe zone in the dorsum of the hand.

5. Conclusion

Understanding the cutaneous innervation of the hand is the first step in understanding hand anatomy. With the on-going effort to decrease postoperative complications and provide high quality medical services, an understanding of the anatomy of the cutaneous nerves of the hand, their distribution, CBs, and variations is essential for assessing and managing various clinical conditions. The description of the typical anatomy and innervation areas in the hand needs to be reassessed. Textbooks usually describe the typical anatomy ignoring important anatomical anomalies and their clinical significance. The literature, on the other hand, gives vague and sometimes contradicting reports on the incidence, course and characteristics of the sensory nerves of the hand. Although important, some reports give confusing descriptions and unclear measurements limiting the use of the data in clinical settings. The main aim of this project was to clarify the complex relations of the cutaneous nerves of the hand and evaluate their significance in clinical settings.

The PCBMN has been described in many reports in the literature. However; studies have usually been conducted on a limited number of samples, on cadavers who underwent different fixation methods, and by using different bases of measurement and classification influencing the consistency of the descriptions of the anatomical characteristics of the nerve and leading to variable and sometimes confusing reports. The origin point of the PCBMN has been used to describe the intraneural origin, detachment point, and the point where the PCBMN can be distinguished from the MN but still enclosed in the same neural sheath. Moreover, reports have failed to agree on the description of the branching patterns and the basis of classifying those patterns. The PCBMN was classified by the number of branches emerging from the MN, the sub-branches coming off the PCBMN or/and the territory innervated by each sub-branch.

The current study suggests a classification system based on the number and direction of the sub-branches coming off the PCBMN and incorporating other patterns described in the literature. The current study also highlights variations to the most common branching patterns described, the origin of the nerve from the main trunk of the MN, the relationship of the nerve to other structures in the distal forearm and communications with other nerves in the region. Knowledge of the anatomical characteristics of the PCBMN and the appreciation of possible variations in the distal forearm and proximal palm is important to properly diagnose and evaluate pathologic or postoperative signs and avoid injuries to the nerve during surgical interventions to the distal forearm and proximal palm.

The CDNs have been neglected in the literature. With few studies describing their branching points to PDNs and their relationship to other structures in the palm. The current study describes the CDNs division points to PDNs to various bony landmarks with absolute and relative values providing clinicians with indices that can be used as a tool in clinical procedures (Figure 5.1 A).

The UN innervates the palmar and dorsal medial hand and the skin covering the medial 1½ digits by the superficial branch of the UN that originates from the UN as it passes through Guyon's canal, and the DBUN which originates from the UN in the distal forearm and courses dorsally to supply the medial dorsal hand. The current study investigated the branching pattern of the UN in Guyon's canal, discussed variations and communicating branches present in the area, and suggested a scheme to classify the neural contribution supplying the palmar skin of the little and medial side of the ring finger. Neural contributions, other than from the UN, are overlooked and sometimes underestimated in the literature. The suggested classification emphasises the possible palmar-dorsal communications (Kaplan anastomosis) and median-ulnar

communications which could be a source of postoperative complications if injured during surgical interventions in the area. Moreover, the DBUN is at risk during clinical procedures performed to the distal ulna or the wrist area. Understanding the course of the DBUN will help clinicians to preserve the nerve during these procedures and help to better evaluate and assess the nerve involvement in hand neuropathology. Furthermore, knowledge of the anatomical relation of the DBUN will aid in the preparation and planning of nerve grafts.

The palmar CB has been investigated in the literature; however, with different and often contradicting reports regarding incidence rate, branching patterns and most common location. The current study investigates discrepancies in previous reports and suggests a classification scheme incorporating other systems mentioned in the literature. This study also outlines a risk-zone where the palmar CB is most likely to be found (Figure 5.1 B). Recognizing the topography of the palmar CB is important to understand palmar sensory alteration to the typical description and to properly evaluate possible nerve involvement following surgical procedures in the palmar area. The study also provides guidelines of where the palmar CB is most likely to be found in relation to various anatomic landmarks which can be helpful to surgeons in avoiding injury to the CB during any surgical intervention in the area.

Risk areas where the palmar CB, division points of the CDNs into PDNs, CBs in the medial side of the palm are most likely to be found are illustrated in Figure 5.1.

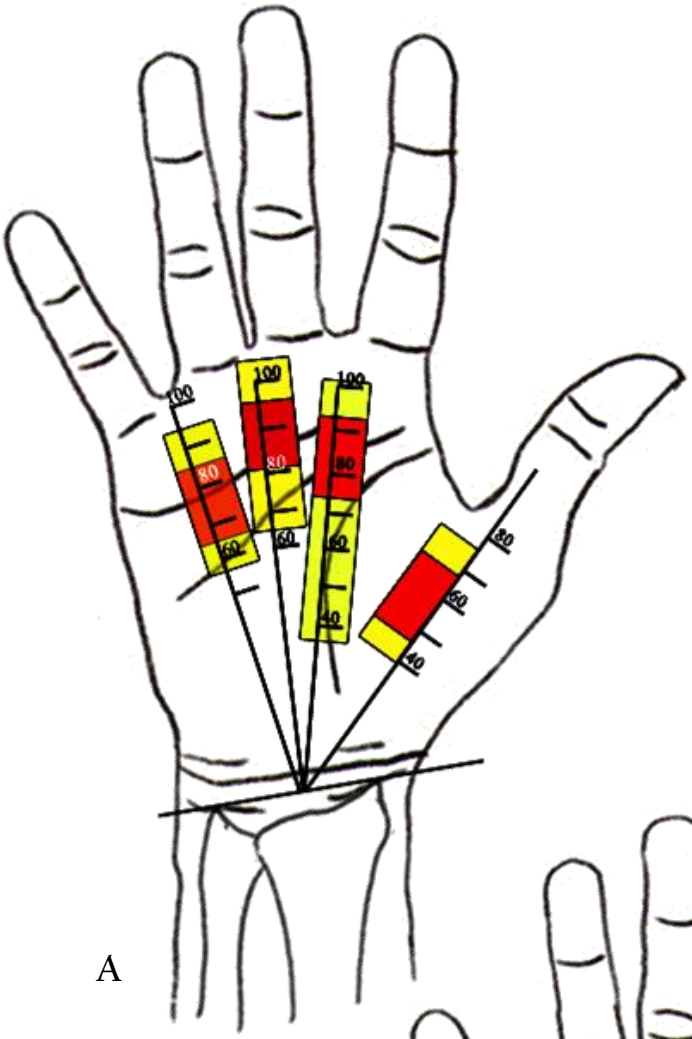
100
80
60
100
80
60
100
80
60
40
80
60
40

A

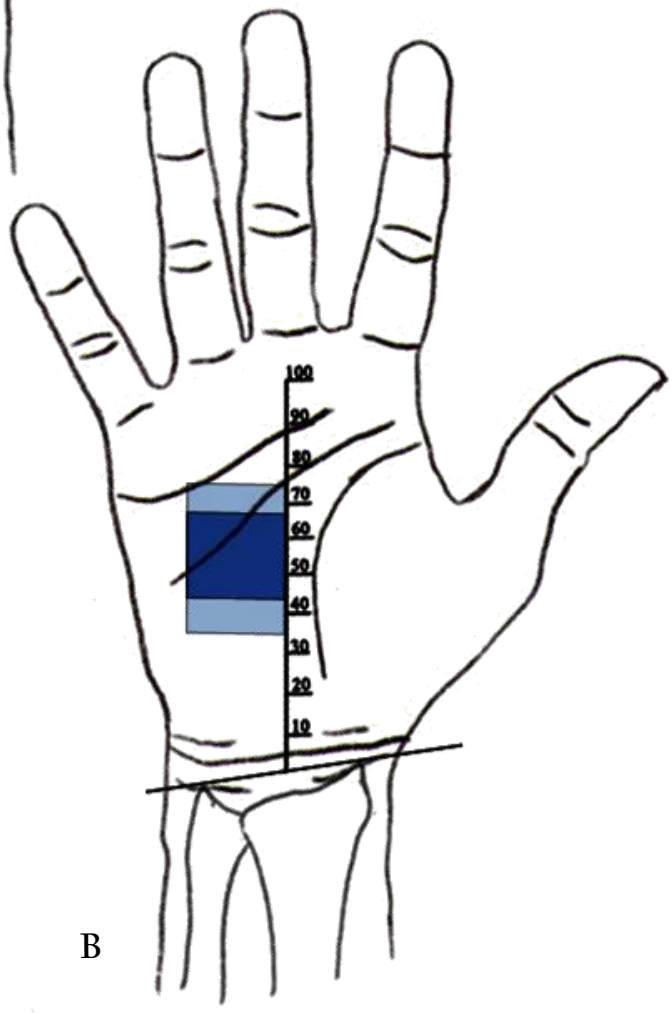
100
90
80
70
60
50
40
30
20
10

B

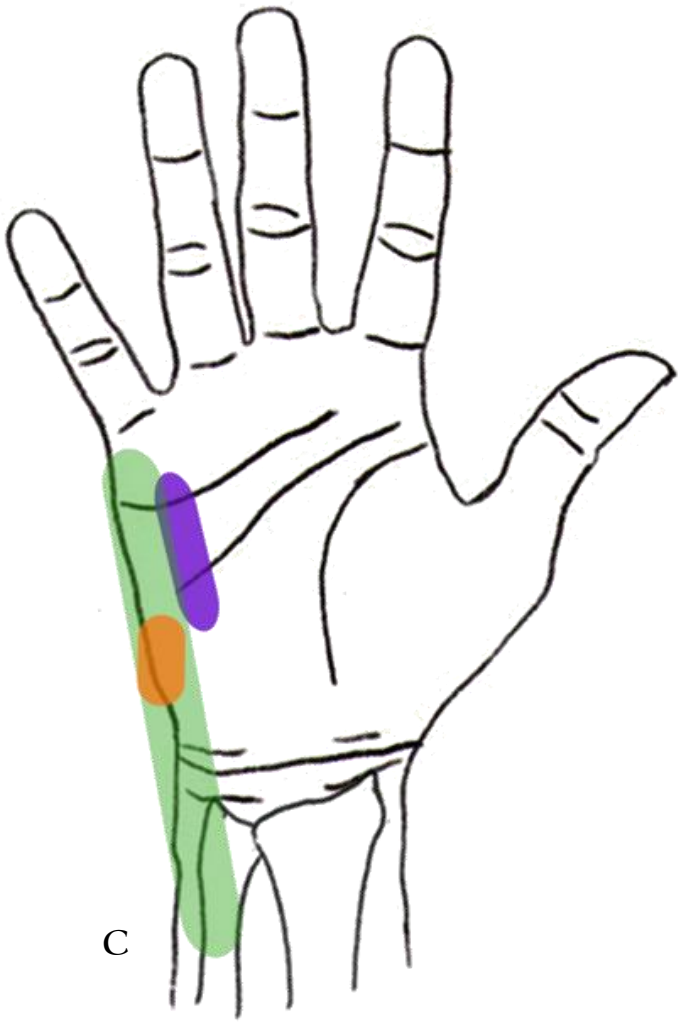

Figure 5.1: Risk areas in the palm. (A) Risk area representing the location of the division points of the common digital nerves into proper digital nerves, Yellow boxes represent the full range, Red boxes show the high risk area of 80% of the samples; (B) Risk area where the palmar communicating branch between the median and ulnar nerves is most likely found (incidence rate 86.9% in the current study), Light blue box represent the full range, dark blue box show the high risk area of 80% of the samples; (C) Green area shows the most common location of Kaplan anastomosis (incidence rate 4.2% in the current study); Orange area represents the risk area where the motor division of the ulnar nerve sends a communicating branch into the PDN of the medial side of the little finger (incidence rate 4.9%); Purple area represents the risk area where the fourth CDN sends a communicating branch to the PDN of the medial side of the little finger (incidence rate 7.7% in the current study); the location of the green, orange and purple area are based on observations.

The SBRN can be at risk directly due to trauma or injury in cases of fracture, compressive bracelets or watches; or indirectly as a result to treatment of fractures or during clinical procedures such as wrist arthroscopy, radial artery harvest, blood gas testing, cephalic vein cannulation and De Quervain's release. Understanding the anatomical course of the SBRN and its relationship to other structures in the distal forearm and wrist is vital for safe clinical practice. Moreover, appreciation of possible variations and communicating branches with other nerves in the area will aid clinicians to better assess and evaluate neuropathologies.

The literature has differed in the description of the sensory distribution territories in the dorsum of the hand with many studies giving different and inconstant reports and findings. Electrophysiological studies have also been conducted to better understand the sensory distribution in the dorsum of the hand; however, they provided different incidence rates to patterns and variations than those mentioned by dissection based studies. The most common branching pattern in the dorsum of the hand found in the current study is illustrated in Figure 5.2. Dorsal communicating branches can explain the deviation in the sensory distribution from the typical descriptions; however, the literature has differed in the incidence rate of these CBs, and often ignored their presence in the dorsum of the hand. The current study discusses the sensory distribution in the dorsum of the hand, gives incidence rates for the common patterns and variations to those patterns. It also discusses the different CBs in the dorsum of the hand and their significance in clinical settings. Understanding the sensory distribution in the dorsum and possible CBs is important to better diagnose signs and symptoms presented and assess the involvement of different nerves. Knowledge of the variations in the sensory distribution helps to correctly interpret velocity conduction studies results thus better design and implement an appropriate therapeutic plan. Risk areas where the dorsal CB between the SBRN and DBUN (Type III) is most likely to be found

and where the DBUN courses through a line between the USP and the fourth webspace are illustrated in Figure 5.2.

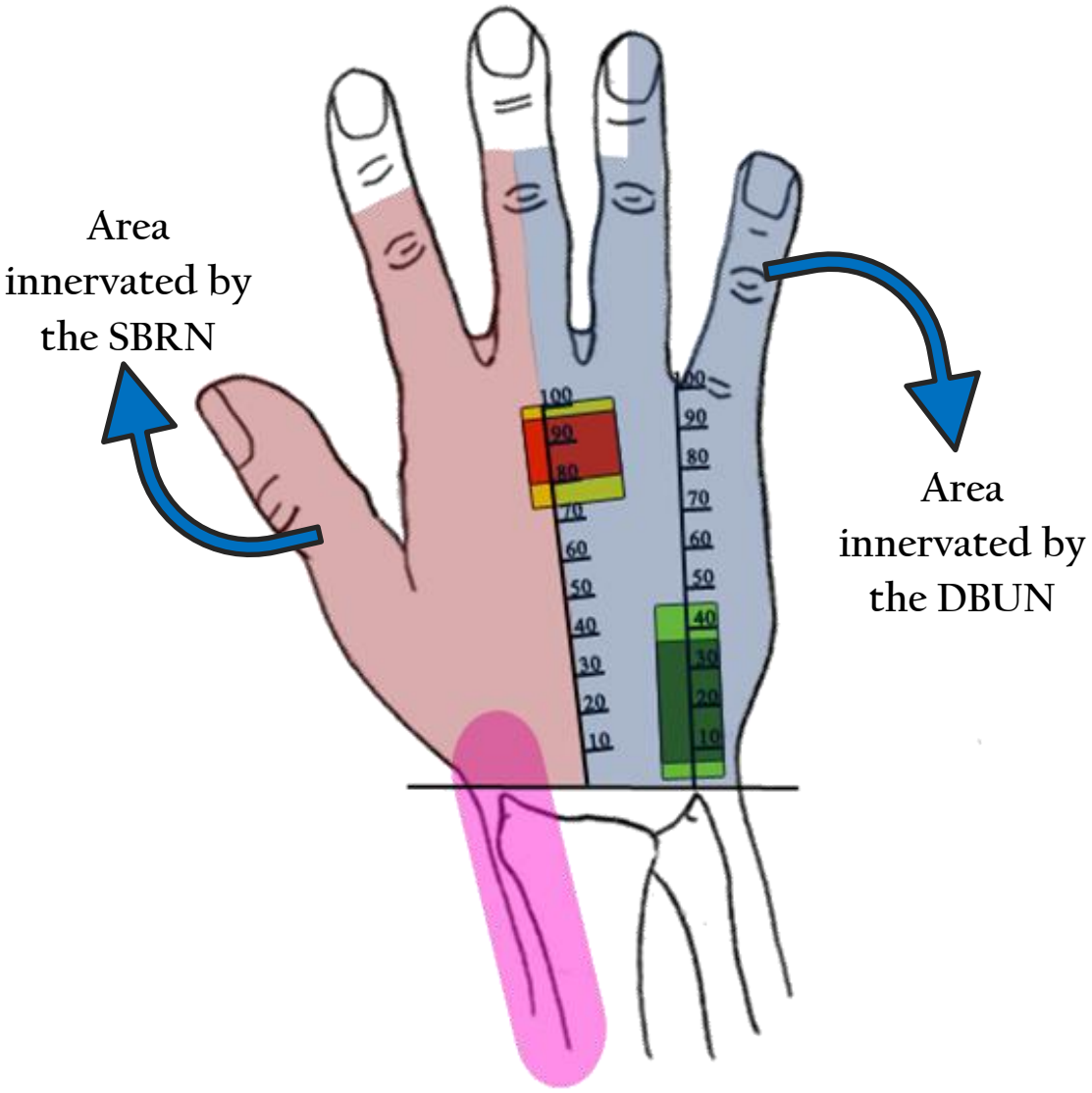

Figure 5.2: The most common sensory innervation pattern and risk areas in the dorsum of the hand as found in the current study. Yellow box represent full range of the most common location of the dorsal communicating branch between the superficial branch of the radial nerve (SBRN) and the dorsal branch of the ulnar nerve (DBUN) (Type III) relative to the distance between the third metacarpophalangeal joint and the middle of the bistyloid line, 80% of the samples are found in the area indicated by the red box; Light green area represent the full range of the area where the DBUN crosses a line extending between the ulnar styloid process and the fourth webspace, 80% of the samples are found in the area indicated by the dark green box; Pink area represent a risk area where the lateral antebrachial cutaneous nerve communicate with the SBRN (incidence rate 30.0%, this area is based on observations).

With the continuous development of clinical procedures and techniques, a detailed knowledge and understanding of the typical anatomy, course, patterns of distribution and the appreciation of possible variations of the nerves of the hand is essential for safe and optimal clinical practice. This study described the course of the cutaneous nerves in the hand and their relations to other structures in the distal forearm and wrist. It outlined the most common topographical patterns of these nerves, variations to these patterns and their clinical significance. Using morphometric data, the most common location of palmar CBs were outlined with reference to identifiable landmarks. The findings obtained from this study will help clinicians to plan and prepare various procedures in the distal forearm and wrist. It will help in evaluating the involvement of different nerves by better assessing signs and symptoms presented in different hand neuropathologies. Moreover, it will have a positive impact in reducing postoperative complications and increasing patient satisfaction. Furthermore, knowledge of the anatomical course and appreciation of possible variations and communicating branches of the cutaneous nerves of the hand will provide opportunities to create novel procedures in the wrist and hand.

6. References

- AARON, S. D., VANDEMHEEN, K. L., NAFTEL, S. A., LEWIS, M. J. & RODGER, M. A. 2003. Topical tetracaine prior to arterial puncture: A randomized, placebo-controlled clinical trial. *Respiratory Medicine*, 97, 1195-1199.

- ABRAMS, R. A., BROWN, R. A. & BOTTE, M. J. 1992. The superficial branch of the radial nerve: An anatomic study with surgical implications. *Journal of Hand Surgery*, 17, 1037-1041.

- AGUR, A. M. R., DALLEY, A. F. & GRANT, J. C. B. 2009. *Grant's atlas of anatomy*, Philadelphia, Pa, Lippincott Williams & Wilkins, pages: 554-587.

- AHČAN, U., ARNEŽ, Z. M., BAJROVIĆ, F. F. & ZORMAN, P. 2002. Surgical technique to reduce scar discomfort after carpal tunnel surgery. *Journal of Hand Surgery*, 27, 821-827.

- AHČAN, U., ARNEŽ, Z. M., BAJROVIĆ, F. F., HVALA, A. & ZORMAN, P. 2003. Nerve fibre composition of the palmar cutaneous branch of the median nerve and clinical implications. *British Journal of Plastic Surgery*, 56, 791-796.

- AHN, D. S., YOON, E. S., KOO, S. H. & PARK, S. H. 2000. A prospective study of the anatomic variations of the median nerve in the carpal tunnel in Asians. *Annals of Plastic Surgery*, 44, 282-287.

- AHSAN, Z. S. & YAO, J. 2012. Complications of wrist arthroscopy. *Arthroscopy: Journal of Arthroscopic and Related Surgery*, 28, 855-859.

- ALIZADEH, K., LAHIJI, F. & PHALSAPHY, M. 2006. Safety of carpal tunnel release with a short incision: A cadaver study. *Acta Orthopaedica Belgica*, 72, 415-419.

- AL-QATTAN, M. M. 1997. Anatomical classification of sites of compression of the palmar cutaneous branch of the median nerve. *Journal of Hand Surgery: European Volume*, 22, 48-49.

- ANDERSON, J. T., LUCAS, G. L. & BUHR, B. R. 2004. Complications of treating distal radius fractures with external fixation: a community experience. *The Iowa Orthopaedic Journal*, 24, 53-59.

- ARIYAN, S. & WATSON, H. K. 1977. The palmar approach for the visualization and release of the carpal tunnel. An analysis of 429 cases. *Plastic and Reconstructive Surgery*, 60, 539-547.

- ARNER, M., HAGBERG, L. & ROSEN, B. 1994. Sensory disturbances after two-portal endoscopic carpal tunnel release: A preliminary report. *Journal of Hand Surgery*, 19, 548-551.

- AUERBACH, D. M., COLLINS, E. D., KUNKLE, K. L. & MONSANTO, E. H. 1994. The radial sensory nerve: An anatomic study. *Clinical Orthopaedics and Related Research*, 308, 241-249.

- AVCI, S. & SAYLI, U. 2000. Carpal tunnel release using a short palmar incision and a new knife. *Journal of Hand Surgery*, 25 B, 357-360.

- BAGATUR, A. E., YALCINKAYA, M. & ATCA, A. O. 2013. Bifid median nerve causing carpal tunnel syndrome: MRI and surgical correlation. *Orthopedics*, 36, e451-e456.

- BAS, H. & KLEINERT, J. M. 1999. Anatomic variations in sensory innervation of the hand and digits. *Journal of Hand Surgery*, 24, 1171-1184.

- BEREDJIKLIAN, P. K., BOZENTKA, D. J., LEUNG, Y. L. & MONAGHAN, B. A. 2004. Complications of wrist arthroscopy. *Journal of Hand Surgery*, 29, 406-411.

- BERRETTINO, P. C. & PETRIOLI, C. R. 1741. Tabulae Anatomicae. *Rome: Typographia Antonii de Rubeis*, 1-4 as cited in STANČIĆ, M. F., MIĆOVIĆ, V. & POTOČNJAK, M. 1999. The anatomy of the Berrettini branch: Implications for carpal tunnel release. *Journal of Neurosurgery*, 91, 1027-1030.

- BERRY, M. G., VIJH, V. & PERCIVAL, N. J. 2003. Bifid median nerve: Anatomical variant at the carpal tunnel. *Scandinavian Journal of Plastic and Reconstructive Surgery and Hand Surgery*, 37, 58-60.

- BERTELLI, J. A. & PAGLIEI, A. 1998. The neurocutaneous flap based on the dorsal branches of the ulnar artery and nerve: A new flap for extensive reconstruction of the hand. *Plastic and Reconstructive Surgery*, 101, 1537-1543.

- BEZERRA, A. J., CARVALHO, V. C. & NUCCI, A. 1986. An anatomical study of the palmar cutaneous branch of the median nerve. *Surgical and Radiologic Anatomy*, 8, 183-188.

- BIAFORA, S. J. & GONZALEZ, M. H. 2007. Sensory communication of the median and ulnar nerves in the palm. *Journal of Surgical Orthopaedic Advances*, 16, 192-195.

- BLEIZIFFER, S., HETTICH, I., EISENHAUER, B., RUZICKA, D., VOSS, B., BAUERNSCHMITT, R. & LANGE, R. 2008. Neurologic sequelae of the donor arm after endoscopic versus conventional radial artery harvesting. *Journal of Thoracic and Cardiovascular Surgery*, 136, 681-687.

- BOESON, M. B., HRANCHOOK, A. & STOLLER, J. 2000. Peripheral nerve injury from intravenous cannulation: a case report. *Journal of the American Association of Nurse Anesthetists*, 68, 53-57.

- BONNEL, F. & VILA, R. M. 1985. Anatomical study of the ulnar nerve in the hand. *Journal of Hand Surgery*, 10, 165-168.

- BORN, T. & MAHONEY, J. 1995. Cutaneous distribution of the ulnar nerve in the palm: Does it cross the incision used in carpal tunnel release? *Annals of Plastic Surgery*, 35, 23-25.

- BOTTE, M. J., COHEN, M. S., LAVERNIA, C. J., VON SCHROEDER, H. P., GE LLMAN, H. & ZINBERG, E. M. 1990. The dorsal branch of the ulnar nerve: An anatomic study. *Journal of Hand Surgery*, 15, 603-607.

- BOZKURT, M. C., CEZAYIRLI, E. & TAGIL, S. M. 2002. An unusual termination of the ulnar nerve in the palm. *Annals of Anatomy*, 184, 271-273.

- BOZKURT, M. C., TAGIL, S. M. & ÖZÇAKAR, L. 2004. An aberrant sensory innervation of the little finger by the ulnar nerve: A cadaveric observation. *Plastic and Reconstructive Surgery*, 113, 1531-1532.

- BUCKMILLER, J. F. & RICKARD, T. A. 1987. Isolated compression neuropathy of the palmar cutaneous branch of the median nerve. *Journal of Hand Surgery*, 12, 97-99.

- BUGBEE, W. D. & BOTTE, M. J. 1993. Surface anatomy of the hand: The relationships between palmar skin creases and osseous anatomy. *Clinical Orthopaedics and Related Research*, 296, 122-126.

- BURNETT, M. G. & ZAGER, E. L. 2004. Pathophysiology of peripheral nerve injury: a brief review. *Neurosurgical focus*, 16, 1-7.

- CAMPBELL, W. W. 2008. Evaluation and management of peripheral nerve injury. *Clinical Neurophysiology*, 119, 1951-1965.

- CASOLI, V., VÉROLINO, P., PÉLISSIER, P., KOSTOPOULOS, E., CAIX, P., DELMAS, V., MARTIN, D. & BAUDET, J. 2004. The retrograde neurocutaneous island flap of the dorsal branch of the ulnar nerve: Anatomical basis and clinical application. *Surgical and Radiologic Anatomy*, 26, 8-13.

- CAVUSOGLU, T., OZDEN, H., COMERT, A., YAZICI, I., ACAR, H. I., TELLIOGLU, A. T. & TEKDEMIR, I. 2011. Topographical anatomy of the dorsal branch of the ulnar nerve and artery: A cadaver study. *Surgical and Radiologic Anatomy*, 33, 229-233.

- CHAUHAN, P., KALRA, S., JAIN, S. K., MUNJAL, S. & ANURAG, A. 2011. Relationship between palmar skin creases and osseous anatomy-a radiological study identification. *Journal of Morphological Sciences*, 28**,** 184-188.

- CHAYNES, P., BÉCUE, J., VAYSSE, P. & LAUDE, M. 2004. Relationships of the palmar cutaneous branch of the median nerve: A morphometric study. *Surgical and Radiologic Anatomy*, 26**,** 275-280.

- CHEUNG, J. W., SHYU, J. F., TENG, C. C., CHEN, T. H., SU, C. H., SHYR, Y. M., WANG, J. J., WU, C. W., LUI, W. Y. & LIU, J. C. 2004. The anatomical variations of the palmar cutaneous branch of the median nerve in Chinese adults. *Journal of the Chinese Medical Association*, 67**,** 27-31.

- CHOW, J. C. Y. 1989. Endoscopic release of the carpal ligament: A new technique for carpal tunnel syndrome. *Arthroscopy*, 5, 19-24.

- CIRPAR, M., ESMER, A. F., TÜRKER, M. & YALÇINOZAN, M. 2012. Dorsal cutaneous innervation of the hand with respect to anatomical landmarks: Is there a safe zone? *Eklem Hastaliklari ve Cerrahisi*, 23, 161-165.

- CULP, R. W. 1999. Complications of wrist arthroscopy. *Hand Clinics*, 15, 529-535.

- CUMMING, D., MFULA, N. & JONES, J. W. M. 2008. Paediatric forearm fractures: The increasing use of elastic stable intra-medullary nails. *International Orthopaedics*, 32, 421-423.

- CUTTS, A. 1988. Shrinkage of muscle fibres during the fixation of cadaveric tissue. *Journal of Anatomy*, 160**,** 75-78.

- DAS, S. K. & BROWN, H. G. 1976. In search of complications in carpal tunnel decompression. *Hand*, 8**,** 243-249.

- DASILVA, M. F., MOORE, D. C., WEISS, A. P. C., AKELMAN, E. & SIKIRICA, M. 1996. Anatomy of the palmar cutaneous branch of the median nerve: Clinical significance. *Journal of Hand Surgery*, 21**,** 639-643.

- DE LA FUENTE, J., MIGUEL-PEREZ, M. I., BALIUS, R., GUERRERO, V., MICHAUD, J. & BONG, D. 2013. Minimally invasive ultrasound-guided carpal tunnel release: A cadaver study. *Journal of Clinical Ultrasound*, 41**,** 101-107.

- DE SMET, L. 1998. Entrapment of the palmar cutaneous branch of the median nerve. *Journal of Hand Surgery. British volume*, 23**,** 115-116.

- DENTON, T. A., TRENTO, L., COHEN, M., KASS, R. M., BLANCHE, C., RAISSI, S., CHENG, W., FONTANA, G. P. & TRENTO, A. 2001. Radial artery harvesting for coronary bypass operations: Neurologic complications and their potential mechanisms. *Journal of Thoracic and Cardiovascular Surgery*, 121**,** 951-956.

- DIAMOND J. 1981. Modelling and competition in the nervous system: clues from the sensory innervation of skin. *Current topics in developmental biology* 17:147-205.

- DOGAN, N. U., UYSAL, I. I., KARABULUT, A. K., SEKER, M. & ZIYLAN, T. 2010. Communications between the palmar digital branches of the median and ulnar nerves: A study in human fetuses and a review of the literature. *Clinical Anatomy*, 23**,** 234-241.

- DON GRIOT, J. P. W., ZUIDAM, J. M., VAN KOOTEN, E. O., PROSÉ, L. P. & HAGE, J. J. 2000. Anatomic study of the ramus communicans between the ulnar and median nerves. *Journal of Hand Surgery*, 25**,** 948-954.

- DOWDY, P. A., RICHARDS, R. S. & MCFARLANE, R. M. 1994. The palmar cutaneous branch of the median nerve and the palmaris longus tendon: A cadaveric study. *Journal of Hand Surgery*, 19**,** 199-202.

- DOYLE, J. R. & BOTTE, M. J. 2003. *Surgical Anatomy of the Hand and Upper Extremity*, Philadelphia; London, Lippincott, Williams & Wilkins, pages: 185-236, 486-489, 532-535, 568-581, 642-643.

- DRAKE, R. L., VOGL, W., MITCHELL, A. W. M. & GRAY, H. 2010. *Gray's Anatomy for Students*, Philadelphia, Pa, Churchill Livingstone/Elsevier, pages: 751-774.

- DRAKE, R. L., VOGL, W., MITCHELL, A., TIBBITTS, R. & RICHARDSON, P. 2008. *Gray's Atlas of Anatomy*, Philadelphia, Pa, Churchill Livingstone Elsevier, pages: 390-425.

- DUTRA DE OLIVEIRA, A. L. C. R., BARREIRA, A. A. & MARQUES JR, W. 2000. Limitations on the clinical utility of the ulnar dorsal cutaneous sensory nerve action potential. *Clinical Neurophysiology*, 111**,** 1208-1210.

- EIKEN, O., CARSTAM, N. & EDDELAND, A. 1971. Anomalous distal branching of the median nerve. Case reports. *Scandinavian Journal of Plastic and Reconstructive Surgery*, 5**,** 149-152.

- EKEROT, L., HOLMBERG, J. & EIKEN, O. 1983. Denervation of the wrist. *Scandinavian Journal of Plastic and Reconstructive Surgery*, 17, 155-157.

- EMERICK, K. S. & DESCHLER, D. G. 2007. Incidence of donor site skin graft loss requiring surgical intervention with the radial forearm free flap. *Head and Neck*, 29, 573-576.

- ENGBER, W. D. & GMEINER, J. G. 1980. Palmar cutaneous branch of the ulnar nerve. *Journal of Hand Surgery*, 5, 26-29.

- FAWEETT, J. & KEYNES, R. J. 1990. Peripheral nerve regeneration. *Annual review of neuroscience*, 13, 43-60.

- FERNANDEZ, F. F., LANGENDÖRFER, M., WIRTH, T. & EBERHARDT, O. 2010. Failures and complications in intramedullary nailing of children's forearm fractures. *Journal of Children's Orthopaedics*, 4, 159-167.

- FERRARI, G. P. & GILBERT, A. 1991. The superficial anastomosis on the palm of the hand between the ulnar and median nerves. *Journal of Hand Surgery*, 16 B, 511-514.

- FERRERES, A., FOUCHER, G. & SUSO, S. 2002. Extensive denervation of the wrist. *Techniques in Hand and Upper Extremity Surgery*, 6, 36-41.

- FLORES, A. J., LAVEMIA, C. & OWENS, P. W. 2000. Anatomy and physiology of peripheral nerve injury and repair. *AMERICAN JOURNAL OF ORTHOPEDICS-BELLE MEAD-*, 29, 167-178.

- FRIEDMAN, L. 2008. The Wrist and Hand. *In:* O'NEILL, J. M. D. (ed.) *Musculoskeletal Ultrasound.* Springer New York.

- GALAJDA, Z., SZENTKIRÁLYI, I., PÉTERFFY, Á., DENTON, T. A. & TRENTO, A. 2002. Neurologic complications after radial artery harvesting. *Journal of Thoracic and Cardiovascular Surgery*, 123**,** 194-195.

- GARG, N. K., BALLAL, M. S., MALEK, I. A., WEBSTER, R. A. & BRUCE, C. E. 2008. Use of elastic stable intramedullary nailing for treating unstable forearm fractures in children. *The Journal of Trauma*, 65**,** 109-115.

- GARIBALDI, S. G. & NUCCI, A. 2000. Dorsal cutaneous branch of ulnar nerve: An appraisal on the anatomy, injuries and application of conduction velocity studies in diagnosis. *Arquivos de Neuro-Psiquiatria*, 58**,** 637-641.

- GEHWOLF, S. 1921. Ein Fall aussergewohnlicher Nervenverzweigung in der Hohlhand. *Anatomischer Anzeiger*, 54**,** 1-8.

- GERRITSEN, A. A. M., UITDEHAAG, B. M. J., VAN GELDERE, D., SCHOLTEN, R. J. P. M., DE VET, H. C. W. & BOUTER, L. M. 2001. Systematic review of randomized clinical trials of surgical treatment for carpal tunnel syndrome. *British Journal of Surgery*, 88**,** 1285-1295.

- GLUCKMAN, P. D., HANSON, M. A., SPENCER, H. G. & BATESON, P. 2005. Environmental influences during development and their later consequences for health and disease: implications for the interpretation of empirical studies. *Proceedings of the Royal Society B: Biological Sciences*, 272**,** 671-677.

- GOODMAN, C. S. & SHATZ, C. J. 1993. Developmental mechanisms that generate precise patterns of neuronal connectivity. *Cell*, 72**,** 77-98.

- GOTO, A., KUNIHIRO, O., MURASE, T. & MORITOMO, H. 2010. The dorsal cutaneous branch of the ulnar nerve: an anatomical study. *Hand Surgery: An*

International Journal Devoted to Hand and Upper Limb Surgery and Related Research: Journal of the Asia-Pacific Federation of Societies for Surgery of the Hand, 15, 165-168.

- GRANT, G. A., GOODKIN, R. & KLIOT, M. 1999. Evaluation and surgical management of peripheral nerve problems. *Neurosurgery*, 44, 825-839.

- GRECHENIG, W., PEICHA, G., FELLINGER, M., SEIBERT, F. J. & WEIGLEIN, A. H. 1999. Anatomical and safety considerations in establishing portals used for wrist arthroscopy. *Clinical Anatomy*, 12, 179-185.

- GREENE, M. A. & MALIAS, M. A. 2001. Arm complications after radial artery procurement for coronary bypass operation. *Annals of Thoracic Surgery*, 72, 126-128.

- GRINSELL, D. & THEILE, D. 2005. Radial nerve morbidity in radial artery free flaps: Harvest of cephalic vein versus venae comitantes. *ANZ Journal of Surgery*, 75, 542-545.

- GRIOT, J. P. D., VAN KOOTEN, E. O., ZUIDAM, J. M. & HAGE, J. J. 2002. Internal anatomy of the communicating branch between the ulnar and median nerves in the hand and its relevance to volar digital sensibility. *Journal of Hand Surgery*, 27, 143-146.

- GROSS M.S., GELBERMAN R.H. 1985. The anatomy of the distal ulnar tunnel. *Clinical Orthopaedics and Related Research*. 196:238-247.

- GROSSMAN, J. A. I., YEN, L. & RAPAPORT, D. 1998. The dorsal cutaneous branch of the ulnar nerve. An anatomic clarification with six case reports. *Annales de Chirurgie de la Main et du Membre Superieur*, 17, 154-158.

- GUPTA, R., AGGARWAL, A., SAHNI, D., HARJEET, K. & BARNWAL, M. 2012. Anatomical survey of terminal branching patterns of superficial branch of radial nerve in fetuses. *Surgical and Radiologic Anatomy*, 34, 415-420.

- HOBBS, R. A., MAGNUSSEN, P. A. & TONKIN, M. A. 1990. Palmar cutaneous branch of the median nerve. *Journal of Hand Surgery*, 15, 38-43.

- HOCHWALD, N. L., LEVINE, R. & TORNETTA III, P. 1997. The risks of Kirschner wire placement in the distal radius: A comparison of techniques. *Journal of Hand Surgery*, 22, 580-584.

- HOOGBERGEN, M. M. & KAUER, J. M. G. 1992. An unusual ulnar nerve-median nerve communicating branch. *Journal of Anatomy*, 181, 513-516.

- HOPPENFELD, S. 1976. *Physical examination of the spine and extremities*, East Norwalk, CT, Appleton-Centrury-Crofts as cited in STAPPAERTS, K. H., VAN HEES, J. & VAN DEN BROECK, E. A. 1996. Peripheral cutaneous nerve distribution to the fingers. *Physiotherapy Research International*, 1, 41-49.

- HUANMANOP, T., AGTHONG, S., LUENGCHAWAPONG, K., SASIWONGPAKDEE, T., BURAPASOMBOON, P. & CHENTANEZ, V. 2007. Anatomic characteristics and surgical implications of the superficial radial nerve. *Journal of the Medical Association of Thailand*, 90, 1423-1429.

- IKIZ, Z. A. A. & ÜÇERLER, H. 2004. Anatomic characteristics and clinical importance of the superficial branch of the radial nerve. *Surgical and Radiologic Anatomy*, 26, 453-458.

- IMAI, T., WADA, T. & MATSUMOTO, H. 2004. Entrapment neuropathy of the palmar cutaneous branch of the median nerve in carpal tunnel syndrome. *Clinical Neurophysiology*, 115**,** 2514-2517.

- JABALEY, M. E., WALLACE, W. H. & HECKLER, F. R. 1980. Internal topography of major nerves of the forearm and hand: a current view. *The Journal of hand surgery*, 5, 1-18.

- JAIN, A. K., PRABHAKAR, S. & PANKANTI, S. 2002. On the similarity of identical twin fingerprints. *Pattern Recognition*, 35**,** 2653-2663.

- JEON, I. H., KIM, P. T., PARK, I. H., PARK, B. C. & IHN, J. C. 2002. High bifurcation of median nerve at the wrist causing common digital nerve injury in endoscopic carpal tunnel release. *Journal of Hand Surgery*, 27 B**,** 580-582.

- JOLLEY, B. J., STERN, P. J. & STARLING, T. 1997. Patterns of median nerve sensory innervation to the thumb and index finger: An anatomic study. *Journal of Hand Surgery*, 22**,** 228-231.

- KANG, S. N., MANGWANI, J., RAMACHANDRAN, M., PATERSON, J. M. H. & BARRY, M. 2011. Elastic intramedullary nailing of paediatric fractures of the forearm: A decade of experience in a teaching hospital in the United Kingdom. *Journal of Bone and Joint Surgery*, 93 B**,** 262-265.

- KAPLAN, E. B. 1963. Variation of the ulnar nerve at the wrist. *Bulletin of the Hospital for Joint Diseases*, 24**,** 85-88 as cited in BONNEL, F. & VILA, R. M. 1985. Anatomical study of the ulnar nerve in the hand. *Journal of Hand Surgery*, 10, 165-168.

- KAPLAN, E. B. 1968. Guide lines to deep structures and dynamics of intrinsic muscles of the hand. *Surgical Clinics of North America*, 48, 993-1002.

- KAWASHIMA, T., SATO, K. & SASAKI, H. 2004. Stratification of the flexor retinaculum and the course and distribution of the ulnar, median, and palmar digital nerves: An anatomical study. *Clinical Anatomy*, 17, 643-650.

- KIERNAN, J. A. & RAJAKUMAR, N. 2014. *Barr's the human nervous system: an anatomical viewpoint* Philadelphia, Wolters Kluwer Lippincott Williams & Wilkins, pages: 45-47.

- KILIÇ, A., KALE, A., USTA, A., BILGILI, F., KABUKÇUOĞLU, Y. & SÖKÜCÜ, S. 2009. Anatomic course of the superficial branch of the radial nerve in the wrist and its location in relation to wrist arthroscopy portals: A cadaveric study. *Arthroscopy: Journal of Arthroscopic and Related Surgery*, 25, 1261-1264.

- KITSUKAWA, T., SHIMIZU, M., SANBO, M., HIRATA, T., TANIGUCHI, M., BEKKU, Y., YAGI, T. & FUJISAWA, H. 1997. Neuropilin–semaphorin III/D-mediated chemorepulsive signals play a crucial role in peripheral nerve projection in mice. *Neuron*, 19, 995-1005.

- KLITSCHER, D., MÜLLER, L. P. & ROMMENS, P. 2007. Anatomical course of the superficial branch of the radial nerve and clinical significance for surgical approaches in the distal forearm. *European Journal of Trauma and Emergency Surgery*, 33, 69-73.

- KONIG, P. S. A., HAGE, J. J., BLOEM, J. J. A. M. & PROSE, L. P. 1994. Variations of the ulnar nerve and ulnar artery in Guyon's canal: A cadaveric study. *Journal of Hand Surgery*, 19, 617-622.

- KORCEK, L. & WONGWORAWAT, M. 2011. Evaluation of the safe zone for percutaneous Kirschner-wire placement in the distal radius: Cadaveric study. *Clinical Anatomy*, 24, 1005-1009.

- KUHLMANN, N. & MEYER OTETEA, G. 1976. The cutaneous branches of the palm [Nerfs cutanes palmaires et voies d'abord de la face anterieure du poignet et de la paume]. *Annales de Chirurgie*, 30, 859-865 as cited in BEZERRA, A. J., CARVALHO, V. C. & NUCCI, A. 1986. An anatomical study of the palmar cutaneous branch of the median nerve. *Surgical and Radiologic Anatomy*, 8, 183-188.

- KUHLMANN, N., TUBIANA, R. & LISFRANC, R. 1978. An anatomical study of the factors relating to the carpal tunnel syndrome [Apport de l'anatomie dans la comprehension des syndromes de compression du canal carpien et des sequelles des interventions decompressives]. *Revue de Chirurgie Orthopedique et Reparatrice de l'Appareil Moteur*, 64, 59-70 as cited in BEZERRA, A. J., CARVALHO, V. C. & NUCCI, A. 1986. An anatomical study of the palmar cutaneous branch of the median nerve. *Surgical and Radiologic Anatomy*, 8, 183-188.

- KURUVILLA, A., LAAKSONEN, S. & FALCK, B. 2002. Anomalous superficial radial nerve: A patient with probable autosomal dominant inheritance of the anomaly. *Muscle and Nerve*, 26, 716-719.

- KUVAT S.V. & TAGIL S.M. 2009. A rare nerve variation: Duplication of the digital nerves in the index finger [Nadir bir sinir varyasyonu: İşaret parmağı{dotless}ndaki digital sinirlerin duplikasyonu] *Acta Orthopaedica et Traumatologica Turcica*, 43:453-455.

- KUVAT, S. V. 2004. A rare nerve variation: duplication of the digital nerves in the index finger [Nadir bir sinir varyasyonu: İşaret parmağındaki digital sinirlerin duplikasyonu]. *Acta Orthopaedica et Traumatologica Turcica*, 43, 453.

- LAMA, P., POTU, B. K. & BHAT, K. M. R. 2009. High origin of dorsal branch of the ulnar nerve and variations in its branching pattern and distribution: A case report. *Cases Journal*, 2, 9130-9134.

- LANGLEY, J. & HASHIMOTO, M. 1917. On the suture of separate nerve bundles in a nerve trunk and on internal nerve plexuses. *The Journal of physiology*, 51, 318-346.

- LAROY, V., SPAANS, F. & REULEN, J. 1998. The sensory innervation pattern of the fingers. *Journal of Neurology*, 245, 294-298.

- LAROY, V., SPAANS, F. & REULEN, J. 1999. Nerve conduction studies show no exclusive ulnar or median innervation of the ring finger. *Clinical Neurophysiology*, 110, 1492-1497.

- LE CORROLLER, T., BAUONES, S., ACID, S. & CHAMPSAUR, P. 2013. Anatomical study of the dorsal cutaneous branch of the ulnar nerve using ultrasound. *European Radiology*, 23, 2246-2251.

- LEE M, MCPHEE R, STRINGER M. 2008. An evidence-based approach to human dermatomes. *Clinical anatomy* 21:363.

- LEIS, A. A., STETKAROVA, I. & WELLS, K. J. 2010. Martin-Gruber anastomosis with anomalous superficial radial innervation to ulnar dorsum of hand: A pitfall when common variants coexist. *Muscle and Nerve*, 41, 313-317.

- LINDSEY, J. T. & WATUMULL, D. 1996. Anatomic study of the ulnar nerve and related vascular anatomy at Guyon's canal: A practical classification system. *Journal of Hand Surgery*, 21**,** 626-633.

- LINELL, E. A. 1921. The distribution of nerves in the upper limb, with reference to variabilities and their clinical significance. *Journal of Anatomy*, 55**,** 79-112.

- LOUKAS, M., ABEL, N., TUBBS, R. S., MATUSZ, P., ZURADA, A. & COHEN-GADOL, A. A. 2011. Neural interconnections between the nerves of the upper limb and surgical implications: A review. *Journal of Neurosurgery*, 114**,** 225-235.

- LOUKAS, M., LOUIS JR, R. G., STEWART, L., HALLNER, B., DELUCA, T., MORGAN, W., SHAH, R. & MLEJNEK, J. 2007. The surgical anatomy of ulnar and median nerve communications in the palmar surface of the hand. *Journal of Neurosurgery*, 106**,** 887-893.

- LOUKAS, M., LOUIS JR, R. G., WARTMANN, C. T., TUBBS, R. S., TURAN-OZDEMIR, S. & KRAMER, J. 2008. The clinical anatomy of the communications between the radial and ulnar nerves on the dorsal surface of the hand. *Surgical and Radiologic Anatomy*, 30**,** 85-90.

- LUMSDEN, A. & DAVIES, A. 1983. Earliest sensory nerve fibres are guided to peripheral targets by attractants other than nerve growth factor. *Nature*, 306**,** 786.

- LUTZ, B. S., WEI, F. C., CHANG, S. C. N., YANG, K. H. & CHEN, I. 1999. Donor site morbidity after suprafascial elevation of the radial forearm flap: A prospective study in 95 consecutive cases. *Plastic and Reconstructive Surgery*, 103**,** 132-137.

- MACKINNON, S. E. & DELLON, A. L. 1985. The overlap pattern of the lateral antebrachial cutaneous nerve and the superficial branch of the radial nerve. *Journal of Hand Surgery*, 10**,** 522-526.

- MADHAVI, C. & HOLLA, S. J. 2003. Dual sensory innervation of the dorsum of the thumb. *Clinical Anatomy*, 16**,** 344-345.

- MARTÍN INZUNZA, A., GUILLERMO SALGADO, A., ANDREA GONZÁLEZ, S., JUAN CARLOS DE LA CUADRA, F. & OSCAR INZUNZA, H. 2011. Massive communication between the superficial branch of radial nerve and lateral cutaneous nerve of the forearm, anatomical and clinical implications. a case report [Comunicación masiva del ramo superficial del nervio radial con el nervio cutáneo antebraquial lateral, implicancias anatomo-clínicas. reporte de un caso]. *International Journal of Morphology*, 29**,** 681-685.

- MARTIN, C. H., SEILER III, J. G. & LESESNE, J. S. 1996. The cutaneous innervation of the palm: An anatomic study of the ulnar and median nerves. *Journal of Hand Surgery*, 21**,** 634-638.

- MARTIN, P., KHAN, A. & LEWIS, J. 1989. Cutaneous nerves of the embryonic chick wing do not develop in regions denuded of ectoderm. *Development*, 106**,** 335-346.

- MATLOUB, H. S., YAN, J. G., VAN DER MOLEN, A. B. M., ZHANG, L. L. & SANGER, J. R. 1998. The detailed anatomy of the palmar cutaneous nerves and its clinical implications. *Journal of Hand Surgery: European Volume*, 23**,** 373-379.

- MAY JR, J. W. & ROSEN, H. 1981. Division of the sensory ramus communicans between the ulnar and median nerves: A complication following carpal tunnel release. A case report. *Journal of Bone and Joint Surgery - Series A*, 63, 836-838.

- MCADAMS, T. R. & HENTZ, V. R. 2002. Injury to the dorsal sensory branch of the ulnar nerve in the arthroscopic repair of ulnar-sided triangular fibrocartilage tears using an inside-out technique: A cadaver study. *Journal of Hand Surgery*, 27, 840-844.

- MCCARTHY, R. E. & NALEBUFF, E. A. 1980. Anomalous volar branch of the dorsal cutaneous ulnar nerve: A case report. *Journal of Hand Surgery*, 5, 19-20.

- MEALS, R. A. & SHANER, M. 1983. Variations in digital sensory patterns: A study of the ulnar nerve-median nerve palmar communicating branch. *Journal of Hand Surgery*, 8, 411-414.

- MELLOR, S. J. & FERRIS, B. D. 2000. Complications of a simple procedure: De Quervain's disease revisited. *International Journal of Clinical Practice*, 54, 76-77.

- MOK, D., NIKOLIS, A. & HARRIS, P. G. 2006. The cutaneous innervation of the dorsal hand: detailed anatomy with clinical implications. *Journal of Hand Surgery*, 31, 565-574.

- MOORE, K. L., AGUR, A. M. R. & DALLEY, A. F. 2011. *Essential Clinical Anatomy*, Philadelphia, Pa, Lippincott Williams & Wilkins, pages: 31-34, 417-421, 461-469.

- MOORE, K. L., AGUR, A. M. R. & DALLEY, A. F. 2011. *Essential clinical anatomy*, Philadelphia, Pa, Lippincott Williams & Wilkins.

- MOORE, K. L., DALLEY, A. F. & AGUR, A. M. R. 2006. *Clinically Oriented Anatomy*, Philadelphia, Pa.; London, Lippincott Williams & *Wilkins*, pages: 819-844.

- MOORE, K. L., DALLEY, A. F. & AGUR, A. M. R. 2013. *Clinically oriented anatomy*, Philadelphia, Pa, Lippincott Williams & Wilkins, pages: 782-786.

- MURATA, K., TAMAI, M. & GUPTA, A. 2004. Anatomic study of variations of hypothenar muscles and arborization patterns of the ulnar nerve in the hand. *Journal of Hand Surgery*, 29, 500-509.

- NAFF, N., DELLON, A. L. & MACKINNON, S. E. 1993. The anatomical course of the palmar cutaneous branch of the median nerve, including a description of its own unique tunnel. *Journal of Hand Surgery*, 18 B, 316-317.

- NAGLE, D. J. & SANTIAGO, K. J. 2008. Anomalous palmar cutaneous branch of the median nerve in the distal forearm: Case Report. *Journal of Hand Surgery*, 33, 1329-1330.

- NAKAMICHI, K. I. & TACHIBANA, S. 2000. Median nerve compression by a radially inserted palmaris longus tendon after release of the antebrachial fascia: A complication of carpal tunnel release. *Journal of Hand Surgery*, 25, 955-958.

- NGUYEN, M. K., BOURGOUIN, S., GAILLARD, C., BUTIN, C., GUILHEM, K., LEVADOUX, M. & LEGRÉ, R. 2011. Accidental section of the ulnar nerve in the wrist during arthroscopy. *Arthroscopy - Journal of Arthroscopic and Related Surgery*, 27, 1308-1311.

- NOWAK T.J. & HANDFORD A. G. 2003. *Pathophysiology: Concepts and Applications for Health Care Professionals*: McGraw-Hill Education, pages: 598-601.

- O'CONNOR, R. L. 1972. Digital nerve compression secondary to palmar aneurysm. *Clinical Orthopaedics and Related Research*, 83**,** 149-150.
- OLAVE, E., DEL SOL, M., GABRIELLI, C., MANDIOLA, E. & RODRIGUES, C. F. S. 2001. Biometric study of the relationships between palmar neurovascular structures, the flexor retinaculum and the distal wrist crease. *Journal of Anatomy*, 198**,** 737-741.
- OLAVE, E., DEL SOL, M., GABRIELLI, C., PRATES, J. C. & RODRIGUES, C. F. 1997. The ulnar tunnel: a rare disposition of its contents. *Journal of Anatomy*, 191**,** 615-616.
- OZCANLI, H., COSKUN, N. K., CENGIZ, M., OGUZ, N. & SINDEL, M. 2010. Definition of a safe-zone in open carpal tunnel surgery: A cadaver study. *Surgical and Radiologic Anatomy*, 32**,** 203-206.
- PARASKEVAS, G., GEKAS, C. C., TZAVEAS, A., SPYRIDAKIS, I., STOLTIDOU, A. & TSITSOPOULOS, P. P. 2008. Kaplan anastomosis of the ulnar nerve: A case report. *Journal of Medical Case Reports*, 2, 107.
- PARDAL-FERNÁNDEZ, J. M., GRACIA-RODRÍGUEZ, I., INIESTA-LÓPEZ, I. & RODRÍGUEZ-VÁZQUEZ, M. 2011. Posttraumatic neuropathy of the palmar cutaneous branch of the median nerve: Four cases. Laceration or entrapment? *Acta Neurochirurgica*, 153**,** 617-620.
- PHALEN, G. S., GARDNER, W. J. & LA LONDE, A. A. 1950. Neuropathy of the median nerve due to compression beneath the transverse carpal ligament. *Journal of Bone and Joint Surgery; American volume*, 32**,** 109-112.

- POLLAK, L., RABEY, J. M. & KUSHNIR, M. 2013. Clinical and neurophysiological aspects of anatomical variants in dorsomedial hand innervation. *Neurophysiologie Clinique*, 43, 105-108.

- PUNA, R. & POON, P. 2010. The anatomy of the dorsal cutaneous branch of the ulnar nerve. *Journal of Hand Surgery: European Volume*, 35, 583-585.

- REMPEL, D., DAHLIN, L. & LUNDBORG, G. 1999. Pathophysiology of Nerve Compression Syndromes: Response of Peripheral Nerves to Loading. *The Journal of Bone & Joint Surgery*, 81, 1600-10.

- RICHARDSON, D., FISHER, S. E., DAVID VAUGHAN, E. & BROWN, J. S. 1997. Radial forearm flap donor-site complications and morbidity: A prospective study. *Plastic and Reconstructive Surgery*, 99, 109-115.

- ROBINSON, L. R. 2000. Traumatic injury to peripheral nerves. *Muscle & nerve*, 23, 863-873.

- ROBSON, A. J., SEE, M. S. & ELLIS, H. 2008. Applied anatomy of the superficial branch of the radial nerve. *Clinical Anatomy*, 21, 38-45.

- RODEO, S. A., FORSTER, R. A. & WEILAND, A. J. 1993. Current concepts review: Neurological complications due to arthroscopy. *Journal of Bone and Joint Surgery - Series A*, 75, 917-926.

- ROLLINS, J. & MEALS, R. A. 1985. Recognition of acutely lacerated ulnar nerve-median nerve palmar communicating branch. A case report. *Clinical Orthopaedics and Related Research*, 201, 91-93.

- ROPARS, M., FONTAINE, I., MORANDI, X., BERTON, E., KAILA, R. & DARNAULT, P. 2010. Preserving the superficial branch of the radial nerve during carpometacarpal and metacarpophalangeal joint arthroscopy: An anatomical study. *Surgical and Radiologic Anatomy*, 32**,** 271-276.

- SAMARAKOON, L. B., LAKMAL, K. C., THILLAINATHAN, S., BATADUWAARACHCHI, V. R., ANTHONY, D. J. & JAYASEKARA, R. W. 2011. Anatomical relations of the superficial sensory branches of the radial nerve: A cadaveric study with clinical implications. *Patient Safety in Surgery*, 5, 28-34.

- SAWAIZUMI, T., SAKAMOTO, A. & ITO, H. 2003. Injury of superficial radial nerve on the wrist joint induced by intravenous injection. *Journal of Nippon Medical School*, 70**,** 355-359.

- SCOTT, S. 1992. The development of peripheral sensory innervation patterns. *Sensory Neurons: Diversity, Development and Plasticity, Oxford University Press, New York***,** 242-263.

- SCOTT, S. A. 1982. The development of the segmental pattern of skin sensory innervation in embryonic chick hind limb. *The Journal of physiology*, 330**,** 203-220.

- SCOTT, S. A. 1988. Skin sensory innervation patterns in embryonic chick hindlimbs deprived of motoneurons. *Developmental Biology*, 126**,** 362-374.

- SEDDON, H. 1943. Three types of nerve injury. *Brain*, 66**,** 237-288.

- SEMER, N., CRIMMINS, C. & JONES, N. F. 1996. Compression neuropathy of the palmar cutaneous branch of the median nerve by the antebrachial fascia. *Journal of Hand Surgery: European Volume*, 21**,** 666-667.

- SERRA, J. M. R., BENITO, J. R. & MONNER, J. 1997. Carpal tunnel release with short incision. *Plastic and Reconstructive Surgery*, 99**,** 129-135.

- SHAPIRA, O. M., ESKENAZI, B. R., HUNTER, C. T., ANTER, E., BAO, Y., MURPHY, R., LAZAR, H. L. & SHEMIN, R. J. 2006. Endoscopic versus conventional radial artery harvest - Is smaller better? *Journal of Cardiac Surgery*, 21**,** 329-335.

- SHARMA, H., CHERNILO, J. & DREGHORN, C. R. 2006. "Superficial radial nerve damage due to Kirschner wiring of the radius" by Singh et al. [Injury 36 (2005) 330-332]. *Injury*, 37**,** 86-87.

- SHIMIZU, K., IWASAKI, R., HOSHIKAWA, H. & YAMAMURO, T. 1988. Entrapment neuropathy of the palmar cutaneous branch of the median nerve by the fascia of flexor digitorum superficialis. *Journal of Hand Surgery*, 13**,** 581-583.

- SIEGEL, J. L., DAVLIN, L. B. & AULICINO, P. L. 1993. An anatomical variation of the palmar cutaneous branch of the median nerve. *Journal of Hand Surgery*, 18 B**,** 182-183.

- SIERAKOWSKI, A., TARE, M. & MAAN, Z. 2012. Co-existing neuroma of the palmar cutaneous branch of the median nerve and an arterio-venous malformation after open carpal tunnel decompression. *Journal of Plastic, Reconstructive and Aesthetic Surgery*, 65**,** 541-542.

- SIMINELAKIS, S., KARFIS, E., ANAGNOSTOPOULOS, C., TOUMPOULIS, I., KATSARAKI, A. & DROSSOS, G. 2004. Harvesting radial artery and neurologic complications. *Journal of Cardiac Surgery*, 19**,** 505-510.

- SINGH, S., TRIKHA, P. & TWYMAN, R. 2005. Superficial radial nerve damage due to Kirschner wiring of the radius. *Injury*, 36**,** 330-332.

- STANČIĆ, M. F., ESKINJA, N. & STOSIC, A. 1995. Anatomical variations of the median nerve in the carpal tunnel. *International Orthopaedics*, 19**,** 30-34.

- STANČIĆ, M. F., MIĆOVIĆ, V. & POTOČNJAK, M. 1999. The anatomy of the Berrettini branch: Implications for carpal tunnel release. *Journal of Neurosurgery*, 91**,** 1027-1030.

- STAPPAERTS, K. H., VAN HEES, J. & VAN DEN BROECK, E. A. 1996. Peripheral cutaneous nerve distribution to the fingers. *Physiotherapy Research International*, 1**,** 41-49.

- STEINBERG, B. D., PLANCHER, K. D. & IDLER, R. S. 1995. Percutaneous Kirschner wire fixation through the snuff box: An anatomic study. *Journal of Hand Surgery*, 20**,** 57-62.

- STEWART, J. 1987. The variable clinical manifestations of ulnar neuropathies at the elbow. *Journal of Neurology, Neurosurgery & Psychiatry*, 50, 252-258.

- STEWART, J. D. 2003. Peripheral nerve fascicles: Anatomy and clinical relevance. *Muscle and Nerve*, 28, 525-541.

- STOPFORD, J. S. B. 1918. The variation in distribution of the cutaneous nerves of the hand and digits. *Journal of Anatomy*, 53**,** 14-25.

- SUNDARAM, S. M., KUMAR, M. S. J., SETHUPATHI, B. B., NAYAK, S. R. & KRISHNAMURTHY, A. 2008. Split median nerve with variation in its common digital branch - A case report. *Neuroanatomy*, 7**,** 15-16.

- SUNDERLAND, S. 1951. A classification of peripheral nerve injuries producing loss of function. *Brain*, 74, 491-516.

- SUNDERLAND, S. 1965. The connective tissues of peripheral nerves. *Brain*, 88, 841-854.

- TAGIL, S. M., BOZKURT, M. C., ÖZÇAKAR, L., ERSOY, M., TEKDEMIR, I. & ELHAN, A. 2007. Superficial palmar communications between the ulnar and median nerves in Turkish cadavers. *Clinical Anatomy*, 20, 795-798.

- TALEISNIK, J. 1973. The palmar cutaneous branch of the median nerve and the approach to the carpal tunnel: An anatomical study. *Journal of Bone and Joint Surgery*, 55-A, 1212-1217.

- TELLIOĞLU, A. T., TEKDEMIR, I., ERSOY, M. & KARABAĞ, O. 2000. Dorsal branches of superficial radial nerve: An anatomic study with potential clinical applications. *European Journal of Plastic Surgery*, 23, 419-421.

- TINDALL, A., PATEL, M., FROST, A., PARKIN, I., SHETTY, A. & COMPSON, J. 2006. The anatomy of the dorsal cutaneous branch of the ulnar nerve - A safe zone for positioning of the 6R portal in wrist arthroscopy. *Journal of Hand Surgery*, 31, 203-205.

- TIZNADO, G., SOUSA-RODRIGUES, C. & OLAVE, E. 2012. Superficial branch of the radial nerve: Large distribution in the dorsum of hand [Ramo superficial del nervio radial: Amplia distribución en el dorso de la mano]. *International Journal of Morphology*, 30, 374-378.

- TORREZ, J. C. & OLAVE, E. 2008. Biometric and morphometric parameters of the terminal end of the median nerve, superficial branch of the ulnar nerve and common palmar digital nerves in the human hand [Parámetros biométricos y morfometría de la porción terminal del nervio mediano, ramo superficial del nervio ulnar y nervios digitales palmares comunes de la mano humana]. *International Journal of Morphology*, 26**,** 675-679.

- TOSNEY, K. W. & LANDMESSER, L. T. 1985. Growth cone morphology and trajectory in the lumbosacral region of the chick embryo. *The Journal of neuroscience*, 5**,** 2345-2358.

- TOSNEY, K. W. & OAKLEY, R. A. 1990. The perinotochordal mesenchyme acts as a barrier to axon advance in the chick embryo: implications for a general mechanism of axonal guidance. *Experimental neurology*, 109**,** 75-89.

- TRAN, N. Q., PRETTO, J. J. & WORSNOP, C. J. 2002. A randomized controlled trial of the effectiveness of topical amethocaine in reducing pain during arterial puncture. *Chest*, 122**,** 1357-1360.

- TROJABORG, W. 1970. Rate of recovery in motor and sensory fibres of the radial nerve: clinical and electrophysiological aspects. *Journal of Neurology, Neurosurgery & Psychiatry*, 33, 625-638.

- TRYFONIDIS, M., CHARALAMBOUS, C. P., JASS, G. K., JACOB, S., HAYTON, M. J. & STANLEY, J. K. 2009. Anatomic relation of dorsal wrist arthroscopy portals and superficial nerves: a Cadaveric study. *Arthroscopy: Journal of Arthroscopic and Related Surgery*, 25**,** 1387-1390.

- TSAI, T. M., TSURUTA, T., SYED, S. A. & KIMURA, H. 1995. A new technique for endoscopic carpal tunnel decompression. *Journal of Hand Surgery*, 20 B, 465-469.

- TSU-HSIN CHEN, E., WEI, J. D. & HUANG, V. W. S. 2006. Injury of the dorsal sensory branch of the ulnar nerve as a complication of arthroscopic repair of the triangular fibrocartilage. *Journal of Hand Surgery*, 31, 530-532.

- TUBBS, R. S., ROGERS, J. M., LOUKAS, M., CÖMERT, A., SHOJA, M. M. & COHEN-GADOL, A. A. 2011. Anatomy of the palmar branch of the ulnar nerve: Application to ulnar and median nerve decompressive surgery - Laboratory investigation. *Journal of Neurosurgery*, 114**,** 263-267.

- TUBBS, R. S., SALTER, E. G., SHEETZ, J., ZEHREN, S., LEE, D. H., OAKES, J. & OAKES, W. J. 2005. Novel surgical approach to the carpal tunnel: Cadaveric feasibility study. *Clinical Anatomy*, 18**,** 350-356.

- VERGARA-AMADOR, E. & NIETO, J. L. 2010. Superficial branch of radial nerve: An anatomical study and its surgical implications [Estudio anatómico de la rama superficial del nervio radial. implicaciones quirúrgicas]. *Revista Facultad de Medicina (Colombia)*, 58**,** 214-220.

- VIALLE, R., PIETIN-VIALLE, C., CRONIER, P., BRILLU, C., VILLAPADIERNA, F. & MERCIER, P. 2001. Anatomic relations between the cephalic vien and the sensory branches of the radial nerve: How can nerve lesions during vien puncture be prevented? *Anesthesia and Analgesia*, 93**,** 1058-1061.

- VOS, P., STARK, F. & PITTMAN, R. 1991. Merkel cells in vitro: production of nerve growth factor and selective interactions with sensory neurons. *Developmental Biology*, 144, 281-300.

- WADA, T., IMAI, T. & ISHII, S. 2002. Entrapment neuropathy of the palmar cutaneous branch of the median nerve concomitant with carpal tunnel syndrome: A case report. *Journal of Hand Surgery*, 27 B, 583-585.

- WAGHMARE, V. K. R. & SONAR, S. V. 2012. Muscle fibers length changes during fixation: A cadaveric study. *Indian Journal of Forensic Medicine and Toxicology*, 6, 142-143.

- WATCHMAKER, G. P., WEBER, D. & MACKINNON, S. E. 1996. Avoidance of transection of the palmar cutaneous branch of the median nerve in carpal tunnel release. *Journal of Hand Surgery*, 21, 644-650.

- WAXMAN, S. G., KOCSIS, J. D. & STYS, P. K. 1995. *The axon: structure, function and pathophysiology* New York; Oxford, Oxford University Press, pages: 13-22.

- WERNER G, WHITSEL BL. 1967. The topology of dermatomal projection in the medial lemniscal system. *The Journal of physiology* 192:123-144.

- WESSELS, K. D. 2004. Arthroplasty of osteoarthritic triscaphe (distal scaphoid) joint [Arthroplastik bei Arthrose im Triskaphoidgelenk (Synonym: Distales Kahnbeingelenk) nach Koob]. *Operative Orthopädie und Traumatologie*, 16, 48-58.

- WHIPPLE, T. L. & POEHLING, G. G. 1996. Kirschner wire fixation through anatomic snuffbox. *The Journal of Hand Surgery*, 21, 322-323.

- WILKINSON, J. L. 1998. *Neuroanatomy for medical students*, Oxford, Butterworth Heinemann, pages: 28-38.

7. Appendix I

Table 7.1: The chi-square test results for the effect of sex on the branching pattern of the palmar cutaneous branch of the median nerve

Case Processing Summary

	Cases					
	Valid		Missing		Total	
	N	Percent	N	Percent	N	Percent
Sex * Branching pattern	110	68.8%	50	31.3%	160	100.0%

Sex * Branching pattern Cross-tabulation

			Branching pattern				Total
			Type I	Type II	Type III	Variation to Type I	
Sex	Male	Count	20	14	7	6	47
		Expected Count	18.8	17.1	6.8	4.3	47.0
		% within Sex	42.6%	29.8%	14.9%	12.8%	100.0%
		% within Branching pattern	45.5%	35.0%	43.8%	60.0%	42.7%
		% of Total	18.2%	12.7%	6.4%	5.5%	42.7%
	Females	Count	24	26	9	4	63
		Expected Count	25.2	22.9	9.2	5.7	63.0
		% within Sex	38.1%	41.3%	14.3%	6.3%	100.0%
		% within Branching pattern	54.5%	65.0%	56.3%	40.0%	57.3%
		% of Total	21.8%	23.6%	8.2%	3.6%	57.3%

		Branching pattern				Total
		Type I	Type II	Type III	Variation to Type I	
Total	Count	44	40	16	10	110
	Expected Count	44.0	40.0	16.0	10.0	110.0
	% within Sex	40.0%	36.4%	14.5%	9.1%	100.0%
	% within Branching pattern	100.0%	100.0%	100.0%	100.0%	100.0%
	% of Total	40.0%	36.4%	14.5%	9.1%	100.0%

Chi-Square Tests

	Value	df	Asymp. Sig. (2-sided)
Pearson Chi-Square	2.336[a]	3	.506
Likelihood Ratio	2.338	3	.505
Linear-by-Linear Association	.238	1	.626
N of Valid Cases	110		

a. 1 cells (12.5%) have expected count less than 5. The minimum expected count is 4.27.

Table 7.2: The chi-square test results for the effect of body side on the branching pattern of the palmar cutaneous branch of the median nerve

Case Processing Summary

	Cases					
	Valid		Missing		Total	
	N	Percent	N	Percent	N	Percent
Body side * Branching pattern	110	68.8%	50	31.3%	160	100.0%

Body side * Branching pattern Cross-tabulation

			Branching pattern				Total
			Type I	Type II	Type III	Variation to Type I	
Body side	RT	Count	17	24	7	4	52
		Expected Count	20.8	18.9	7.6	4.7	52.0
		% within Body side	32.7%	46.2%	13.5%	7.7%	100.0%
		% within Branching pattern	38.6%	60.0%	43.8%	40.0%	47.3%
		% of Total	15.5%	21.8%	6.4%	3.6%	47.3%
	LT	Count	27	16	9	6	58
		Expected Count	23.2	21.1	8.4	5.3	58.0
		% within Body side	46.6%	27.6%	15.5%	10.3%	100.0%
		% within Branching pattern	61.4%	40.0%	56.3%	60.0%	52.7%
		% of Total	24.5%	14.5%	8.2%	5.5%	52.7%

		Branching pattern				Total
		Type I	Type II	Type III	Variation to Type I	
Total	Count	44	40	16	10	110
	Expected Count	44.0	40.0	16.0	10.0	110.0
	% within Body side	40.0%	36.4%	14.5%	9.1%	100.0%
	% within Branching pattern	100.0%	100.0%	100.0%	100.0%	100.0%
	% of Total	40.0%	36.4%	14.5%	9.1%	100.0%

Chi-Square Tests

	Value	df	Asymp. Sig. (2-sided)
Pearson Chi-Square	4.208[a]	3	.240
Likelihood Ratio	4.229	3	.238
Linear-by-Linear Association	.127	1	.722
N of Valid Cases	110		

a. 1 cells (12.5%) have expected count less than 5. The minimum expected count is 4.73.

Table 7.3: The chi-square test results for the effect of sex on the branching pattern of the first common digital nerve (CDN)

Case Processing Summary

	Cases					
	Valid		Missing		Total	
	N	Percent	N	Percent	N	Percent
Sex * Branching pattern of the first common digital nerve (CDN)	142	88.8%	18	11.3%	160	100.0%

Sex * Branching pattern of the 1st CDN Cross-tabulation

			Branching pattern of the 1st CDN			Total
			Type I	Type II	Type III	
Sex	Male	Count	40	21	2	63
		Expected Count	44.8	16.9	1.3	63.0
		% within Sex	63.5%	33.3%	3.2%	100.0%
		% within Branching pattern of the 1st CDN	39.6%	55.3%	66.7%	44.4%
		% of Total	28.2%	14.8%	1.4%	44.4%
	Females	Count	61	17	1	79
		Expected Count	56.2	21.1	1.7	79.0
		% within Sex	77.2%	21.5%	1.3%	100.0%
		% within Branching pattern of the 1st CDN	60.4%	44.7%	33.3%	55.6%
		% of Total	43.0%	12.0%	0.7%	55.6%

		Branching pattern of the 1st CDN			Total
		Type I	Type II	Type III	
Total	Count	101	38	3	142
	Expected Count	101.0	38.0	3.0	142.0
	% within Sex	71.1%	26.8%	2.1%	100.0%
	% within Branching pattern of the 1st CDN	100.0%	100.0%	100.0%	100.0%
	% of Total	71.1%	26.8%	2.1%	100.0%

Chi-Square Tests

	Value	df	Asymp. Sig. (2-sided)
Pearson Chi-Square	3.361[a]	2	.186
Likelihood Ratio	3.353	2	.187
Linear-by-Linear Association	3.321	1	.068
N of Valid Cases	142		

a. 2 cells (33.3%) have expected count less than 5. The minimum expected count is 1.33.

Table 7.4: The chi-square test results for the effect of body side on the branching pattern of the first common digital nerve (CDN)

Case Processing Summary

	Cases					
	Valid		Missing		Total	
	N	Percent	N	Percent	N	Percent
Body side * Branching pattern of the first common digital nerve (CDN)	142	88.8%	18	11.3%	160	100.0%

Body side * Branching pattern of the 1st CDN Cross-tabulation

			Branching pattern of the 1st CDN			Total
			Type I	Type II	Type III	
Body side	RT	Count	48	25	3	76
		Expected Count	54.1	20.3	1.6	76.0
		% within Body side	63.2%	32.9%	3.9%	100.0%
		% within Branching pattern of the 1st CDN	47.5%	65.8%	100.0%	53.5%
		% of Total	33.8%	17.6%	2.1%	53.5%
	LT	Count	53	13	0	66
		Expected Count	46.9	17.7	1.4	66.0
		% within Body side	80.3%	19.7%	0.0%	100.0%
		% within Branching pattern of the 1st CDN	52.5%	34.2%	0.0%	46.5%
		% of Total	37.3%	9.2%	0.0%	46.5%

		Branching pattern of the 1st CDN			Total
		Type I	Type II	Type III	
Total	Count	101	38	3	142
	Expected Count	101.0	38.0	3.0	142.0
	% within Body side	71.1%	26.8%	2.1%	100.0%
	% within Branching pattern of the 1st CDN	100.0%	100.0%	100.0%	100.0%
	% of Total	71.1%	26.8%	2.1%	100.0%

Chi-Square Tests

	Value	df	Asymp. Sig. (2-sided)
Pearson Chi-Square	6.364[a]	2	.041
Likelihood Ratio	7.557	2	.023
Linear-by-Linear Association	6.093	1	.014
N of Valid Cases	142		

a. 2 cells (33.3%) have expected count less than 5. The minimum expected count is 1.39.

Table 7.5: The chi-square test results for the effect of sex on the branching pattern of the ulnar nerve in Guyon's canal

Case Processing Summary

	Cases					
	Valid		Missing		Total	
	N	Percent	N	Percent	N	Percent
Sex * Branching type for the ulnar nerve	143	89.4%	17	10.6%	160	100.0%

Sex * Branching type for ulnar nerve Cross-tabulation

			Branching type for ulnar nerve		Total
			Type I	Type II	
Sex	Male	Count	48	15	63
		Expected Count	50.7	12.3	63.0
		% within Sex	76.2%	23.8%	100.0%
		% within Branching type for ulnar nerve	41.7%	53.6%	44.1%
		% of Total	33.6%	10.5%	44.1%
	Females	Count	67	13	80
		Expected Count	64.3	15.7	80.0
		% within Sex	83.8%	16.3%	100.0%
		% within Branching type for ulnar nerve	58.3%	46.4%	55.9%
		% of Total	46.9%	9.1%	55.9%

		Branching type for ulnar nerve		Total
		Type I	Type II	
Total	Count	115	28	143
	Expected Count	115.0	28.0	143.0
	% within Sex	80.4%	19.6%	100.0%
	% within Branching type for ulnar nerve	100.0%	100.0%	100.0%
	% of Total	80.4%	19.6%	100.0%

Chi-Square Tests

	Value	df	Asymp. Sig. (2-sided)	Exact Sig. (2-sided)	Exact Sig. (1-sided)
Pearson Chi-Square	1.279[a]	1	.258		
Continuity Correction[b]	.844	1	.358		
Likelihood Ratio	1.271	1	.260		
Fisher's Exact Test				.293	.179
Linear-by-Linear Association	1.270	1	.260		
N of Valid Cases	143				

a. 0 cells (0.0%) have expected count less than 5. The minimum expected count is 12.34.

b. Computed only for a 2x2 table

Table 7.6: The chi-square test results for the effect of body side on the branching pattern of the ulnar nerve in Guyon's canal

Case Processing Summary

	Cases					
	Valid		Missing		Total	
	N	Percent	N	Percent	N	Percent
Body side * Branching type for ulnar nerve	143	89.4%	17	10.6%	160	100.0%

Body side * Branching type for ulnar nerve Cross-tabulation

			Branching type for ulnar nerve		Total
			Type I	Type II	
Body side	RT	Count	58	17	75
		Expected Count	60.3	14.7	75.0
		% within Body side	77.3%	22.7%	100.0%
		% within Branching type for ulnar nerve	50.4%	60.7%	52.4%
		% of Total	40.6%	11.9%	52.4%
	LT	Count	57	11	68
		Expected Count	54.7	13.3	68.0
		% within Body side	83.8%	16.2%	100.0%
		% within Branching type for ulnar nerve	49.6%	39.3%	47.6%
		% of Total	39.9%	7.7%	47.6%

		Branching type for ulnar nerve		Total
		Type I	Type II	
Total	Count	115	28	143
	Expected Count	115.0	28.0	143.0
	% within Body side	80.4%	19.6%	100.0%
	% within Branching type for ulnar nerve	100.0%	100.0%	100.0%
	% of Total	80.4%	19.6%	100.0%

Chi-Square Tests

	Value	df	Asymp. Sig. (2-sided)	Exact Sig. (2-sided)	Exact Sig. (1-sided)
Pearson Chi-Square	.954[a]	1	.329		
Continuity Correction[b]	.586	1	.444		
Likelihood Ratio	.962	1	.327		
Fisher's Exact Test				.401	.222
Linear-by-Linear Association	.947	1	.330		
N of Valid Cases	143				

a. 0 cells (0.0%) have expected count less than 5. The minimum expected count is 13.31.

b. Computed only for a 2x2 table

Table 7.7: The chi-square test results for the effect of sex on the branching pattern of the palmar communicating branch (CB) between the median and ulnar nerve

Case Processing Summary

	Cases					
	Valid		Missing		Total	
	N	Percent	N	Percent	N	Percent
Sex * Palmar CB branching pattern	98	61.3%	62	38.8%	160	100.0%

Sex * Palmar CB branching pattern Cross-tabulation

			Palmar CB branching pattern					Total
			Type I	Type II	Type III	Type IV	Type V	
Sex	Male	Count	37	4	1	1	1	44
		Expected Count	36.4	2.2	2.2	1.8	1.3	44.0
		% within Sex	84.1%	9.1%	2.3%	2.3%	2.3%	100.0%
		% within Palmar CB branching pattern	45.7%	80.0%	20.0%	25.0%	33.3%	44.9%
		% of Total	37.8%	4.1%	1.0%	1.0%	1.0%	44.9%
	Females	Count	44	1	4	3	2	54
		Expected Count	44.6	2.8	2.8	2.2	1.7	54.0
		% within Sex	81.5%	1.9%	7.4%	5.6%	3.7%	100.0%
		% within Palmar CB branching pattern	54.3%	20.0%	80.0%	75.0%	66.7%	55.1%
		% of Total	44.9%	1.0%	4.1%	3.1%	2.0%	55.1%

		Palmar CB branching pattern					Total
		Type I	Type II	Type III	Type IV	Type V	
Total	Count	81	5	5	4	3	98
	Expected Count	81.0	5.0	5.0	4.0	3.0	98.0
	% within Sex	82.7%	5.1%	5.1%	4.1%	3.1%	100.0%
	% within Palmar CB branching pattern	100.0%	100.0%	100.0%	100.0%	100.0%	100.0%
	% of Total	82.7%	5.1%	5.1%	4.1%	3.1%	100.0%

Chi-Square Tests

	Value	df	Asymp. Sig. (2-sided)
Pearson Chi-Square	4.565[a]	4	.335
Likelihood Ratio	4.825	4	.306
Linear-by-Linear Association	.871	1	.351
N of Valid Cases	98		

a. 8 cells (80.0%) have expected count less than 5. The minimum expected count is 1.35.

Table 7.8: The chi-square test results for the effect of body side on the branching pattern of the palmar communicating branch between the median and ulnar nerve

Case Processing Summary

	Cases					
	Valid		Missing		Total	
	N	Percent	N	Percent	N	Percent
Body side * Palmar CB branching pattern	98	61.3%	62	38.8%	160	100.0%

Body side * Palmar CB branching pattern Cross-tabulation

			Palmar CB branching pattern					Total
			Type I	Type II	Type III	Type IV	Type V	
Body side	RT	Count	45	3	2	2	2	54
		Expected Count	44.6	2.8	2.8	2.2	1.7	54.0
		% within Body side	83.3%	5.6%	3.7%	3.7%	3.7%	100.0%
		% within Palmar CB branching pattern	55.6%	60.0%	40.0%	50.0%	66.7%	55.1%
		% of Total	45.9%	3.1%	2.0%	2.0%	2.0%	55.1%
	LT	Count	36	2	3	2	1	44
		Expected Count	36.4	2.2	2.2	1.8	1.3	44.0
		% within Body side	81.8%	4.5%	6.8%	4.5%	2.3%	100.0%
		% within Palmar CB branching pattern	44.4%	40.0%	60.0%	50.0%	33.3%	44.9%
		% of Total	36.7%	2.0%	3.1%	2.0%	1.0%	44.9%

		Palmar CB branching pattern					Total
		Type I	Type II	Type III	Type IV	Type V	
Total	Count	81	5	5	4	3	98
	Expected Count	81.0	5.0	5.0	4.0	3.0	98.0
	% within Body side	82.7%	5.1%	5.1%	4.1%	3.1%	100.0%
	% within Palmar CB branching pattern	100.0%	100.0%	100.0%	100.0%	100.0%	100.0%
	% of Total	82.7%	5.1%	5.1%	4.1%	3.1%	100.0%

Chi-Square Tests

	Value	df	Asymp. Sig. (2-sided)
Pearson Chi-Square	.720[a]	4	.949
Likelihood Ratio	.722	4	.949
Linear-by-Linear Association	.010	1	.919
N of Valid Cases	98		

a. 8 cells (80.0%) have expected count less than 5. The minimum expected count is 1.35.

Table 7.9: The chi-square test results for the effect of sex on the branching pattern of the superficial branch of the radial nerve (SBRN)

Case Processing Summary

	Cases					
	Valid		Missing		Total	
	N	Percent	N	Percent	N	Percent
Sex * SBRN branching pattern according to digits	150	93.8%	10	6.3%	160	100.0%

Sex * SBRN branching pattern according to digits Cross-tabulation

			SBRN branching pattern according to digits						Total
			Type 1	Type 2	Type 3	Type 4	Type 5	Type 6	
Sex	Male	Count	22	16	17	1	1	5	62
		Expected Count	23.1	14.5	18.2	.8	1.2	4.1	62.0
		% within Sex	35.5%	25.8%	27.4%	1.6%	1.6%	8.1%	100.0%
		% within SBRN branching pattern according to digits	39.3%	45.7%	38.6%	50.0%	33.3%	50.0%	41.3%
		% of Total	14.7%	10.7%	11.3%	0.7%	0.7%	3.3%	41.3%
	Females	Count	34	19	27	1	2	5	88
		Expected Count	32.9	20.5	25.8	1.2	1.8	5.9	88.0
		% within Sex	38.6%	21.6%	30.7%	1.1%	2.3%	5.7%	100.0%
		% within SBRN branching pattern according to digits	60.7%	54.3%	61.4%	50.0%	66.7%	50.0%	58.7%
		% of Total	22.7%	12.7%	18.0%	0.7%	1.3%	3.3%	58.7%

		SBRN branching pattern according to digits						Total
		Type 1	Type 2	Type 3	Type 4	Type 5	Type 6	
Total	Count	56	35	44	2	3	10	150
	Expected Count	56.0	35.0	44.0	2.0	3.0	10.0	150.0
	% within Sex	37.3%	23.3%	29.3%	1.3%	2.0%	6.7%	100.0%
	% within SBRN branching pattern according to digits	100.0%	100.0%	100.0%	100.0%	100.0%	100.0%	100.0%
	% of Total	37.3%	23.3%	29.3%	1.3%	2.0%	6.7%	100.0%

Chi-Square Tests

	Value	df	Asymp. Sig. (2-sided)
Pearson Chi-Square	.957[a]	5	.966
Likelihood Ratio	.952	5	.966
Linear-by-Linear Association	.135	1	.714
N of Valid Cases	150		

a. 5 cells (41.7%) have expected count less than 5. The minimum expected count is .83.

Table 7.10: The chi-square test results for the effect of body side on the branching pattern of the superficial branch of the radial nerve (SBRN)

Case Processing Summary

	Cases					
	Valid		Missing		Total	
	N	Percent	N	Percent	N	Percent
Body side * SBRN branching pattern according to digits	150	93.8%	10	6.3%	160	100.0%

Body side * SBRN branching pattern according to digits Cross-tabulation

			SBRN branching pattern according to digits						Total
			Type 1	Type 2	Type 3	Type 4	Type 5	Type 6	
Body side	RT	Count	26	20	23	0	1	4	74
		Expected Count	27.6	17.3	21.7	1.0	1.5	4.9	74.0
		% within Body side	35.1%	27.0%	31.1%	0.0%	1.4%	5.4%	100.0%
		% within SBRN branching pattern according to digits	46.4%	57.1%	52.3%	0.0%	33.3%	40.0%	49.3%
		% of Total	17.3%	13.3%	15.3%	0.0%	0.7%	2.7%	49.3%
	LT	Count	30	15	21	2	2	6	76
		Expected Count	28.4	17.7	22.3	1.0	1.5	5.1	76.0
		% within Body side	39.5%	19.7%	27.6%	2.6%	2.6%	7.9%	100.0%
		% within SBRN branching pattern according to digits	53.6%	42.9%	47.7%	100.0%	66.7%	60.0%	50.7%
		% of Total	20.0%	10.0%	14.0%	1.3%	1.3%	4.0%	50.7%

		SBRN branching pattern according to digits						Total
		Type 1	Type 2	Type 3	Type 4	Type 5	Type 6	
Total	Count	56	35	44	2	3	10	150
	Expected Count	56.0	35.0	44.0	2.0	3.0	10.0	150.0
	% within Body side	37.3%	23.3%	29.3%	1.3%	2.0%	6.7%	100.0%
	% within SBRN branching pattern according to digits	100.0%	100.0%	100.0%	100.0%	100.0%	100.0%	100.0%
	% of Total	37.3%	23.3%	29.3%	1.3%	2.0%	6.7%	100.0%

Chi-Square Tests

	Value	df	Asymp. Sig. (2-sided)
Pearson Chi-Square	3.798[a]	5	.579
Likelihood Ratio	4.582	5	.469
Linear-by-Linear Association	.250	1	.617
N of Valid Cases	150		

a. 5 cells (41.7%) have expected count less than 5. The minimum expected count is .99.

Table 7.11: The chi-square test results for the effect of sex on the branching pattern of the dorsal communicating branch (CB) between the superficial branch of the radial nerve and the dorsal branch of the ulnar nerve

Case Processing Summary

	Cases					
	Valid		Missing		Total	
	N	Percent	N	Percent	N	Percent
Sex * Branching pattern of dorsal CB	37	23.1%	123	76.9%	160	100.0%

Sex * Branching pattern of dorsal CB Cross-tabulation

			Branching pattern of dorsal CB					Total
			Type I A	Type I B	Type I C	Type II	Type III	
Sex	Male	Count	2	2	0	2	7	13
		Expected Count	1.4	2.5	.4	1.4	7.4	13.0
		% within Sex	15.4%	15.4%	0.0%	15.4%	53.8%	100.0%
		% within Branching pattern of dorsal CB	50.0%	28.6%	0.0%	50.0%	33.3%	35.1%
		% of Total	5.4%	5.4%	0.0%	5.4%	18.9%	35.1%
	Females	Count	2	5	1	2	14	24
		Expected Count	2.6	4.5	.6	2.6	13.6	24.0
		% within Sex	8.3%	20.8%	4.2%	8.3%	58.3%	100.0%
		% within Branching pattern of dorsal CB	50.0%	71.4%	100.0%	50.0%	66.7%	64.9%
		% of Total	5.4%	13.5%	2.7%	5.4%	37.8%	64.9%

		Branching pattern of dorsal CB					Total
		Type I A	Type I B	Type I C	Type II	Type III	
Total	Count	4	7	1	4	21	37
	Expected Count	4.0	7.0	1.0	4.0	21.0	37.0
	% within Sex	10.8%	18.9%	2.7%	10.8%	56.8%	100.0%
	% within Branching pattern of dorsal CB	100.0%	100.0%	100.0%	100.0%	100.0%	100.0%
	% of Total	10.8%	18.9%	2.7%	10.8%	56.8%	100.0%

Chi-Square Tests

	Value	df	Asymp. Sig. (2-sided)
Pearson Chi-Square	1.480[a]	4	.830
Likelihood Ratio	1.773	4	.777
Linear-by-Linear Association	.040	1	.842
N of Valid Cases	37		

a. 8 cells (80.0%) have expected count less than 5. The minimum expected count is .35.

Table 7.12: The chi-square test results for the effect of body side on the branching pattern of the dorsal communicating branch (CB) between the superficial branch of the radial nerve and the dorsal branch of the ulnar nerve

Case Processing Summary

	Cases					
	Valid		Missing		Total	
	N	Percent	N	Percent	N	Percent
Body side * Branching pattern of dorsal CB	37	23.1%	123	76.9%	160	100.0%

Body side * Branching pattern of dorsal CB Cross-tabulation

			Branching pattern of dorsal CB					Total
			Type I A	Type I B	Type I C	Type II	Type III	
Body side	RT	Count	2	3	0	2	10	17
		Expected Count	1.8	3.2	.5	1.8	9.6	17.0
		% within Body side	11.8%	17.6%	0.0%	11.8%	58.8%	100.0%
		% within Branching pattern of dorsal CB	50.0%	42.9%	0.0%	50.0%	47.6%	45.9%
		% of Total	5.4%	8.1%	0.0%	5.4%	27.0%	45.9%
	LT	Count	2	4	1	2	11	20
		Expected Count	2.2	3.8	.5	2.2	11.4	20.0
		% within Body side	10.0%	20.0%	5.0%	10.0%	55.0%	100.0%
		% within Branching pattern of dorsal CB	50.0%	57.1%	100.0%	50.0%	52.4%	54.1%
		% of Total	5.4%	10.8%	2.7%	5.4%	29.7%	54.1%

		Branching pattern of dorsal CB					Total
		Type I A	Type I B	Type I C	Type II	Type III	
Total	Count	4	7	1	4	21	37
	Expected Count	4.0	7.0	1.0	4.0	21.0	37.0
	% within Body side	10.8%	18.9%	2.7%	10.8%	56.8%	100.0%
	% within Branching pattern of dorsal CB	100.0%	100.0%	100.0%	100.0%	100.0%	100.0%
	% of Total	10.8%	18.9%	2.7%	10.8%	56.8%	100.0%

Chi-Square Tests

	Value	df	Asymp. Sig. (2-sided)
Pearson Chi-Square	.954[a]	4	.917
Likelihood Ratio	1.334	4	.856
Linear-by-Linear Association	.026	1	.871
N of Valid Cases	37		

a. 8 cells (80.0%) have expected count less than 5. The minimum expected count is .46.

8. Appendix II

Table 8.1: Palmar cutaneous nerve of the median nerve (PCBMN) results expressed as incidence rates:

Measurements	Incidence rate (%)
PCBMN origin side from the main trunk of the median nerve:	
Lateral side	93.5
Posterolateral side	1.6
Medial side	1.6
Anterior side	3.3
Two PCBMNs	**8.9**
PCBMN relationship to other anatomical structures:	
PCBMN passed through the fascia of flexor carpi radialis	8.3
PCBMN passed posterior to the tendon of flexor carpi radialis	4.2
PCBMN passed superficial to the palmar carpal ligament	16.1
PCBMN passed deep to the palmar carpal ligament	12.5
Branching types of the PCBMN:	
Type I	40
Variations to Type I	9.1
Type II	36.4
Type III	14.5
Communications with other nerves in the area:	
With the lateral antebrachial cutaneous nerve	4.1
With the superficial branch of the radial nerve	0.8
With the recurrent motor branch of the median nerve	1.6
With the palmar cutaneous nerve of the ulnar nerve	0.8
With the first common digital nerve	0.8

Table 8.2: Anatomical measurements recorded for the palmar cutaneous branch of the median nerve (PCBMN) (mm)

	Mean	SD	Max	Min
Origin from main trunk	54.1	15.7	138.4	22.1
Detaches from main trunk	41.2	14.0	114.9	16.2
Length of PCBMN tunnel	11.3	3.4	24.5	5.7
Angle (degrees)	43.9	14.7	85.0	15.0
Distance of 1st branch to wrist crease	1.2	8.1	21.5	-18.2
Origin of the proximal branch from main trunk of the median nerve	70.9	20.6	100	42.1
Detachment of the proximal branch from main trunk of the median nerve	55.9	18.9	85.7	29.9
Origin of the distal branch from main trunk of the median nerve	64.8	17.8	92.3	42.1
Detachment of the distal branch from main trunk of the median nerve	46.5	16.7	77.0	27.9

Table 8.3: Common digital nerves (CDNs) results expressed as incidence rates:

Measurements	Incidence rate (%)
First CDN branching pattern	
Type I	70.8
Type II	27.1
Type III	2.1
The second CDN was found to divide at a point located distal to the 70% of the distance between the third MCP[1] joint and the BSL[2]	94.3
The Third CDN was found to divide at a point located distal to the 70% of the distance between the third MCP joint and the BSL	99.2
The Fourth CDN was found to divide at a point located distal to the 70% of the distance between the third MCP joint and the BSL	73.6

[1] Metacarpophalangeal
[2] Bistyloid line

Table 8.4: Absolute measurements for the branching points of the common digital nerves (CDNs) into proper digital nerves in the palm (mm)

		Mean	SD	Max	Min
First common digital nerve (CDN) first division	ST	29.9	5.4	54.3	16.7
	BSL	45.3	6.1	63.5	32.4
First CDN second division	ST	35.5	7.1	63.3	16.9
	BSL	51.7	7.4	71.9	35.4
Second CDN division	ST	59.8	7.9	81.1	42.9
	BSL	74.1	9.1	94.7	42.3
Third CDN division	ST	66.1	7.38	86.2	49.1
	BSL	78.9	7.7	99.5	60.1
Fourth CDN division	Pisiform	65.2	7.4	83.9	49.3
	BSL	72.6	7.7	92.2	55.0

Table 8.5: Branching points of the common digital nerves (CDNs) into the proper digital nerves to the distance between the third metacarpophalangeal joint and the bistyloid line (%)

	Mean	SD	Max	Min
First common digital nerve (CDN) first division	51.2	5.3	63.3	40.2
First CDN second division	58.7	7.2	76.9	41.6
Second CDN division	83.8	8.6	101.5	39.4
Third CDN division	89.3	6.3	108.1	65.3
Fourth CDN division	74.2	7.6	93.7	55.4

Table 8.6: Ulnar nerve (UN) results expressed as incidence rates:

Measurements	Incidence rate (%)
UN branching pattern based on the number of branches at the division point as suggested by Bonnel and Vila (1985)	
Type I	80.4
Type II	19.6
UN branching pattern based on the branches contributing to the innervation of the little and medial side of the ring finger	
Type I A	75.5
Type I B	18.2
Type II A	3.5
Type II B	2.1
Communications on the medial side of the hand:	
The fourth CDN[1] can communicate with the PDN[2] crossing the hypothenar eminence	7.7
the deep motor branch sent a communicating branch through the hypothenar muscles to connect with the PDN to the medial side of the little finger	4.9

[1] Common digital nerve
[2] Proper digital nerve to the medial side of the little finger

Table 8.7: The first and second division points of Type I and the point of trifurcation of Type II to the proximal edge of the pisiform (mm)

	Mean	SD	Max	Min
Ulnar nerve division into deep & superficial (Type I first division point)	13.6	4.0	22.1	1.8
Superficial branch division into the 4th CDN[1] & PDN[2] (Type I second division point)	25.2	4.6	37.2	13.1
Ulnar nerve trifurcation into deep, 4th CDN & PDN (Type II trifurcation point)	14.9	4.1	22.42	7.7

[1] Common digital nerve
[2] Proper digital nerve to the medial side of the little finger

Table 8.8: Palmar communicating branch (CB) between median nerve and the ulnar nerve results expressed as incidence rates:

Measurements	Incidence rate (%)
Palmar CB branching pattern based on the proximal and distal attachment points	
Type I A	61.2
Type I B	21.4
Type II A	4.1
Type II B	1.0
Type III A	2.0
Type III B	3.1
Type IV	4.1
Type V	3.1

Table 8.9: Distances measured for the proximal and distal attachments of the palmar communicating branch (CB) to different anatomical landmarks (mm)

Distance between:	Mean	SD	Max	Min
Proximal attachment of CB to TCL[1]	5.3	5.2	19.4	-10.6
Distal attachment of CB to TCL	16.4	6.4	39.5	1.3
Proximal attachment of CB to WC[2]	32.3	5.8	46.6	20.5
Distal attachment of CB to WC	43.9	6.6	60.6	27.8
Proximal attachment of CB to BSL[3]	43.6	7.1	64.5	30.8
Distal attachment of CB to BSL	52.6	7.4	69.2	38.1

[1] Transverse carpal ligament
[2] Wrist crease
[3] Bistyloid line

Table 8.10: Distances measured for the proximal and distal attachments of the palmar communicating branch (CB) to the distance between the third metacarpophalangeal (MCP) joint and the wrist crease (WC) or the bistyloid line (BSL) (%)

Distance between:	Mean	SD	Max	Min
Proximal attachment of CB to the distance between the third MCP joint and the WC	40.7	7.1	60.3	25.9
Distal attachment of CB to the distance between the third MCP joint and the WC	55.0	8.5	79.3	36.6
Proximal attachment of CB to the distance between the third MCP joint and the middle of the BSL	49.1	5.9	60.5	34.5
Distal attachment of CB to the distance between the third MCP joint and the middle of the BSL	59.1	6.3	75.4	41.8

Table 8.11: Superficial branch of the radial nerve (SBRN) results expressed as incidence rates:

Measurements	Incidence rate (%)
SBRN originated proximal to the lateral epicondyle	13.7
SBRN pierced the tendon of brachioradialis to become subcutaneous	2
SBRN divided for the first time after it became subcutaneous into three branches	2.7
The SBRN communicated with the lateral antebrachial cutaneous nerve	30.7
Branching pattern of the SBRN	
Type I	37.3
Type I A	5.3
Type I B	30.7
Type I C	1.3
Type II	23.3
Type II A	2
Type II B	2
Type II C	16.7
Type II D	2
Type II E	0.7
Type III	29.3
Type III A	4
Type III B	18.7
Type III C	3.3
Type III D	3.3
Type IV	1.3
Type V	2
Type VI	6.7
Type VI A	0.7
Type VI B	1.3
Type VI C	3.3
Type VI D	1.3

Table 8.12: Measurements of the closest branches of the superficial branch of the radial nerve (SBRN) to various anatomical points (mm)

	Mean	SD	Max	Min
Closest palmar branch at the level of the RSP[1]	8.5	4.1	17.8	0.7
Closest dorsal branch at the level of the RSP	4.9	3.0	14.7	1.1
Closest palmar branch to a point 25 mm proximal to the RSP	5.6	3.4	15.1	0
Closest dorsal branch to a point 25 mm proximal to the RSP	4.1	2.6	10.9	0
Closest branch to Lister's tubercle	14.1	3.8	23.1	4.6
First intersection between the SBRN and the cephalic vein	47.9	19.3	93.6	6.7
SBRN diameter prior to its first division	3.2	0.8	5.8	1.94

[1] Radial styloid process

Table 8.13: The major division points of the superficial branch of the radial nerve to the radial styloid process (mm)

	Mean	SD	Max	Min
First division point into palmar and dorsal branches	-51.4	14.9	-14.5	-85.0
Palmar branch: Second major division point	-4.9	21.7	48.5	-54.0
Dorsal branch: Second major division point	-4.6	14.4	26.8	-48.2
Palmar branch: Third major division point	22.2	24.0	73.2	-30.7
Dorsal branch: Third major division point	22.3	13.1	62.2	-31.6

Table 8.14: Anatomical measurements recorded for the dorsal branch of the ulnar nerve (mm)

	Mean	SD	Max	Min
Origin from the ulnar nerve to the proximal edge of the pisiform	63.3	14.8	110	26.7
Origin from the ulnar nerve to the USP[1]	61.3	21.0	140	18.5
Pierced the fascia	18.1	7.1	33.1	1.74
Closest branch to USP	6.8	3.1	14.0	0.4
First major branching point	-3.4[2]	17.4	53.4	-38.7
Second major branching point	39.2	13.2	73.6	-8.8

[1] Ulnar styloid process
[2] Minus signs indicate that the point were located below the level of the respective landmark

Table 8.15: Sensory innervation in the dorsum of the hand with reference to digits

		SBRN[1]		DBUN[2]		UD[3]		Total
		n	%	n	%	N	%	
Index	lateral	150	100.0	0	0.0	0	0.0	150
	medial	147	98.0	0	0.0	3	2.0	150
Middle	lateral	146	97.3	0	0.0	4	2.7	150
	medial	57	38.0	57	38.0	36	24.0	150
Ring	lateral	28	18.7	89	59. 3	33	22.0	150
	medial	15	10.0	135	90.0	0	0.0	150
Little	lateral	14	9.3	136	90.7	0	0.0	150
	medial	10	6.7	140	93.3	0	0.0	150

[1] Superficial branch of the radial nerve
[2] Dorsal branch of the ulnar nerve
[3] Undetermined regions where one nerve could not be assigned due to SBRN and DBUN communication or dual innervation

Table 8.16: Sensory innervation in the dorsum of the hand communications expressed as incidence rates:

Measurements	Incidence rate (%)
SBRN[1] communicated with the LABCN[2]	30.0
LABCN contributed to the innervation on the lateral side of the thumb by connecting to the palmar branch of the SBRN	24.7
LABCN contributed to the innervation of the entire territory innervated by the SBRN by communicating with the main SBRN trunk	5.3
The DBUN[3] and the SBRN communicated in the dorsum surface of the hand	26.4
The dorsal communicating branch affected branches supplying	
The lateral side of the ring finger and medial side of the middle finger	20.7
The lateral side of the middle finger and medial side of the index finger	2
The medial side of the middle finger	1.3
The lateral side of the middle finger	0.7
Dual innervation where both nerves overlap and contribute to the innervation of the same area with no communications	2.7
Branching pattern in the dorsum of the hand symmetry	43.2

[1] Superficial branch of the radial nerve
[2] Lateral antebrachial cutaneous nerve
[3] Dorsal branch of the ulnar nerve

Table 8.17: Dorsal communicating branch (CB) between the superficial branch of the radial nerve (SBRN) and the dorsal branch of the ulnar nerve (DBUN) results expressed as incidence rates (%)

Measurements	Incidence rate (%)
Dorsal CB branching pattern	
Type I	32.4
Type I A	10.8
Type I B	18.9
Type I C	2.7
Type II	10.8
Type III	56.8

Table 8.18: Anatomical measurements for the dorsal communicating branch between the superficial branch of the radial nerve and the dorsal branch of the ulnar nerve (mm)

	Mean	SD	Max	Min
Proximal attachment to the BSL[1] in Type I	18.5	22.0	62.9	-6.2
Distal attachment to the BSL in Type I	51.0	21.1	93.4	25.3
Communicating branch length in Type I	54.6	19.5	86.3	30.6
Angle of origin in Type I	139	29.3	168	60
The merging point recorded in Type III	71.3	9.8	85.2	55.4

[1] Bistyloid line

Table 8.19: Distances measured for the dorsal communicating branch (CB) to the distance between the third metacarpophalangeal (MCP) joint and the bistyloid line (BSL) (%)

	Mean	SD	Max	Min
Proximal attachment to the BSL in Type I	25.4	30.6	85.6	-7.6
Distal attachment to the BSL in Type I	65.4	24.5	98.4	32.9
The merging point recorded in Type III	87.0	6.9	100.2	74.1[1]

[1] Minus signs indicate that the point were located proximal to the level of the respective landmark